

Fachbereich Biologie/Chemie
Institut für Chemie

Dissertation

zur Erlangung des Grades eines Doktors der Naturwissenschaften
Dr. rer. nat.

**Synthesis of redox units and modification of mesoporous
surfaces by covalent cascade reactions**

von

Carmen Simona Asaftei
aus Bacau, Rumänien

Osnabrück 2005

This work is dedicated to the memory of my beloved late father

Ein Tropfen Liebe gilt mehr denn ein Ozean an Wille und Verstand

Blaise Pascal

Promotionskommission:

Hauptberichterstatter: Prof. Dr. L. Walder

Berichterstatter: Prof. Dr. Gh. Surpateanu

weitere Mitglieder: Prof. Dr. M.D. Lechner

Prof. Dr. M. Haase

PD. Dr. H. Rosemeyer

Datum der Abgabe: 10.06.2005

Datum der Prüfung: 06.07.2005

I would like to express my sincere gratitude to my supervisor *Prof. Dr. Lorenz Walder* for the interesting subject and for his never ending personal support and guidance throughout the years. He has always been extremely generous with his time, knowledge and ideas, and allowed me great freedom in this research. His enthusiastic approach to research, his excitement for organic electrochemistry and material science has made this experience all the more enjoyable, and I am greatly appreciative.

I would like to express my appreciation to *Prof. Dr. Gheorghe Surpateanu*, Dunkerque who kindly agreed to report on my thesis. I also thank *Prof. Dr. M. Haase*, *Prof. Dr. M. D. Lechner* and *PD Dr. H. Rosemeyer* for being members of my commission.

I am thankful to my colleague *Martin Möller* for the kind cooperation on the topic of this thesis over the years.

Moreover, I highly appreciate the valuable help and friendship of my co-workers *Marianne Gather*, *Christine Schulz-Köbel*, *Simona Webersinn*, *Wolfdietrich Meyer*, *Dr. Peter Schön*, *Tesfaye Degefa*, *Dirk Bongart*, *Burghart Lutter*, *Holger Oelrich*, *Ralph Michalek*. They have indeed done a great job in supporting me every day in the laboratory and to endure the typical temperament of a Romanian woman.

The extraordinarily helpful friendship of *Dr. Cristoph Hess*, *Dipl.-Biol. Arno Rodenbusch* and all the other friends of the Department of Physical Chemistry is particularly acknowledged.

I am very thankful to *Doris Brink*, *Claudia Ratermann*, *Monika Dubiel* and *Bertraud Riepenhausen*, who helped me with numerous administrative problems.

Thanks to *Dr. Richard Smith*, Verlag Helvetica Chimica Acta, Zürich, for helps concerning the nomenclature of new compounds.

I would like to express my gratitudes to *Dr. Karsten Kömpe*, *Dr. Dietrich Steinmeier*, and *Dr. Helmut Rosemeyer* for many helps, supports, understandings, and for their friendship.

Particularly, in the beginning of my stay in Germany I got an overwhelming support by *Prof. W. Frühling*, *Siegfried Meyer*, and especially by *Maria Dorniak*. I am so grateful to them. Thank you all.

I would like to thank my teachers *Prof. Dr. Ion Brad*, Bucuresti, *Prof. Dr. Doru Miron*, Bacau, *Prof. Dr. Abdelkrim Azzouz*, Montreal, *Prof. Dr. Emil Dumitriu*, Cagliari, as well as my "special friend" *Dr. Dumitru Radu*, Bacau.

Thanks to Dr. Jörg Mucha who kept me healthy over the years, and who always had an open ear for me.

Last, but not least, thanks to my dear mother and to dear Irinel for their understanding and for their faith in me.

I appreciate financial support by Ntera Ltd., Dublin, Ireland, between 2001 and 2003.

Die experimentellen Arbeiten wurden in Zeit von März 2001 bis Januar 2005 in der Abteilung Organische Chemie II des Instituts für Chemie der Universität Osnabrück unter der Anleitung von Prof. Dr. Lorenz Walder durchgeführt.

CONTENTS

Chapter 1	Introduction	17
1.1.	Background	17
1.2.	Concept and objectives	18
1.2.1.	Concept	18
1.2.2.	Objectives	20
1.3.	Chemically modified electrodes by cascade reaction	20
1.3.1.	Ways to obtain covalently attached multilayer assemblies	20
Chapter 2	Electrochromics and electrochromic device	24
2.1.	What is electrochromics?	24
2.2.	Electrochromics of viologens	25
2.3.	Existing electrochromic devices without high resolution	26
2.4.	How to build an electrochromic device with persistent high resolution	27
2.5.	How electrochromic systems work	28
2.6.	Electrochromic device with surface confined chromophores	28
Chapter 3	Methodology of modification and irreversible stabilization of electrochromic materials on mesoporous electrode surfaces	30
3.1.	Titanium dioxide (TiO ₂) as mesoporous electrodes	30
3.1.1.	Why titanium dioxide (TiO ₂)?	30
3.2.	Why cross-linking?	33
3.3.	Types of cascade reactions on the nanostructured TiO ₂ film	39
3.3.1.	Multi-step cross-linking by an S _N 2- mechanism and accelerated aging tests	39
3.3.1.1.	Application of the cascade reaction to ink-jet produced electrochromic images	49
3.3.1.2.	Adsorption-Desorption on TiO ₂ of the different viologens without anchoring groups	51
3.3.1.3.	Why repellents?	56
3.3.1.4.	Masking experiments on ink-jetted electrochromic pictures	60

3.3.2.	Cross-linking by condensation of a carboxylic halide and an amine via amide bond formation	62
3.3.3.	Cross-linking by electropolymerization of pending vinyl groups in redox active species after monolayer formation	66
3.4.	Application: Ink-jetted switchable electrochromic image	69
3.4.1.	TiO ₂ coating glass	69
3.4.2.	Ink-jetted electrochromic pictures	70
3.4.3.	Procedure for the preparation of electrochromic pictures	70
3.4.4.	Optimization of the solvent electrolyte system	72
3.4.4.1.	Square voltage excitation of three- and two-electrode systems	72
3.4.4.2.	Effects of electrolyte and solvent on the working- and counter electrodes	76
Chapter 4	Modifications of mesoporous electrode surfaces with ferrocen derivatives	79
4.1.	Poly-ferrocene modification by surface cascade reactions	79
4.2.	Procedure for the preparation of poly-ferrocene on oxide electrodes	81
4.2.1.	The preparation of poly CC14-30, 33-CC3, and 34-CC3 on oxide electrode	81
4.2.2.	Electrode surface modification	82
4.2.3.	The electrochemistry of the modified electrode	83
4.3.	Effects of electrolyte and solvent on poly-ferrocene counter electrodes	87
4.4.	Closed cells with E-33 counter electrodes	90
Chapter 5	Electrocatalytic application of the layer-by-layer technique: TiO₂ - electrode with cross-linkable B₁₂ - derivatives	91
5.1.	Background. The modified surface electrodes with B ₁₂ - Derivatives	91
5.2.	Modification of TiO ₂ – electrodes with cross-linkable B ₁₂ - derivatives	92
5.2.1.	Synthesis of vitamin B ₁₂ derivatives	92
5.2.2.	Procedure for the preparation of vitamin B ₁₂ modified TiO ₂ film electrodes	93
5.2.3.	Electrode surface modification	95
5.3.	The catalytic reduction of organic halides with E-1-(CC7-CC4) _n and E-CC3-(CC6-CC3) _n electrodes	98

Chapter 6	Synthesis and characterization of redoxactive subunits for the preparation of multilayer-modified electrodes	101
6.1.	Redoxactive subunit-groups	101
6.1.1.	Synthesis of anchoring compounds	102
6.1.2.	Synthesis of cross-linker	105
6.1.3.	Synthesis of the end group compounds	108
6.1.4.	Synthesis of vinyl monomers	108
6.1.5.	Synthesis of substituted ferrocenes	111
6.2.	Synthesis of monomers	113
6.2.1.	Synthesis of 1-(2-phosphonoethyl)-4-pyridin-4-ylpyridinium bromide	113
6.2.2.	Synthesis of 1-(3-aminopropyl)-1'-(phosphono-2-ethyl)-4,4'-bipyridinium dibromide hydrobromide	113
6.2.3.	Synthesis of 1-(2-phosphonoethyl)-4-(2-pyridin-4-ylethyl) pyridinium bromide	114
6.2.4.	Synthesis of 4-amino-1-(phosphono-2-ethyl) pyridinium bromide hydrobromide	115
6.2.5.	Synthesis of 1-(4-aminophenyl)-1'-(3-hydroxy-4-carboxyphenyl)-4,4'-bipyridinium dihexafluorophosphate	115
6.2.6.	Synthesis of 1-(phosphono-2-ethyl)-1'-toluoyl-4,4'-bipyridinium dibromide	116
6.2.7.	Synthesis of 1-[4-(bromomethyl)benzyl]-1'-(2-phosphonoethyl)-4,4'-bipyridinium dibromide	117
6.2.8.	Synthesis of 1-[3,5-bis(bromomethyl)benzyl]-1'-(2-phosphonoethyl)-4,4'-bipyridinium dibromide	118
6.2.9.	Synthesis of 1-[3,5-bis(bromomethyl)phenyl]-1'-(2-phosphonoethyl)-4,4'-bipyridinium hexafluorophosphate	118
6.2.10.	Synthesis of 1,1'-bis[(4-carboxyphenyl)-4,4'-bipyridinium dichloride	120
6.2.11.	Synthesis of 1,1'-bis(2-ammoniopropyl)-4,4'-bipyridinium tetrabromide	121
6.2.12.	Synthesis of 1,1'-bis(4-aminophenyl)-4,4'-bipyridinium dihexafluorophosphate	121
6.2.13.	Synthesis of 1,1'-bis[3,5-bis(hydroxymethyl)phenyl]-4,4'-bipyridinium dihexafluorophosphate	122

6.2.14.	Synthesis of 1,1',1''- [benzene-1,3,5-triyltris(methylene)tris](4-pyridin-4-ylpyridinium trihexafluorophosphate	123
6.2.15.	Synthesis of 1,1',1''- [benzene-1,3,5-triyltris(methylene)]tris(1'-hydroxyethyl- 4,4'-bipyridinium) hexabromide	124
6.2.16.	Synthesis of 1,3,5-tris-(bromomethyl) benzene	124
6.2.17.	Synthesis of 1,1'-bis[3,5-bis(bromomethyl)benzyl]-4,4'-bipyridinium dihexafluorophosphate	125
6.2.18.	Synthesis of 1,1'-bis[3,5-bis(bromomethyl)phenyl]-4,4'bipyridinium dihexafluorophosphate	126
6.2.19.	Synthesis of 1-methyl-4-pyridin-4ylpyridinium hexafluorophosphate	126
6.2.20.	Synthesis of 1-ethyl-4-pyridin-4-ylpyridinium hexafluorophosphate	127
6.2.21.	Synthesis of 1-propyl-4-pyridin-4ylpyridinium hexafluorophosphate	128
6.2.22.	Synthesis of 1-[4-(bromometyl)benzyl]-1'-ethyl-4,4'-bipyridinium dihexafluorophosphate	129
6.2.23.	Synthesis of 1-(2-phosphonoethyl)pyridinium bromide	129
6.2.24.	Synthesis of 1-(2-phosphonoethyl)-1'-vinyl-4,4'-bipyridinium dibromide	130
6.2.25.	'In-situ' synthesis of 1,1'-[(5-{[1'-(2-phosphonoethyl)-4,4'-bipyridinium-1-yl]methyl}-1,3-phenylene)bis(methylene)]bis(1'-vinyl-4,4'-bipyridinium) hexabromide	131
6.2.26.	Synthesis of 4-pyridin-4-yl-1-vinylpyridinium bromide	132
6.2.27.	Synthesis of 1,1',1''- [benzene-1,3,5-triyltris(methylene)]tris(1'-vinyl 4,4'-bipyridinium) hexafluorophosphate	133
6.2.28.	Synthesis of 1,1'-bis(vinyl)-4,4'-bipyridinium dibromide	134
6.2.29.	Synthesis of 1-methyl-1'-vinyl -4,4'-bipyridinium dihexafluorophosphat	135
6.2.30.	Synthesis of ferrocenyl-1,1'-diacid fluoride	136
6.2.31.	Synthesis of 1-(2-mercaptoethyl)-1-(ferrocenylmethyl) amine	136
6.2.32.	Synthesis of 1-(2-mercaptoethyl) ferrocene carboxamide	137
6.2.33.	Synthesis of 1,1'-bis(2-aminoethyl)-1-{2-[(ferrocenylmethyl)amino]ethyl} amine	138
6.2.34.	Synthesis of 1-{2-[bis(2-aminoethyl)amino]ethyl}ferrocene-carboxamide	138
6.2.35.	Synthesis of 1,1'-bis[[bis(aminoethyl)amino]ethyl]ferrocene-dicarboxamide	139
6.2.36.	Synthesis of fluorocarbonylferrocene	140
6.2.37.	Synthesis of fluorocarbonylferrocene-dimethylester	140

Chapter 7		
	Summary	142
	Zusammenfassung	144
	Abbreviations	147
	Literature	149

Chapter 1

Introduction

1.1. Background

The creation of nanostructured composite molecular films with tailored functionalities is an area of intense interest in current material research. Nanostructured materials, including monolayer and multilayer films on inorganic solids, are a branch of supramolecular systems with specific interactions between the solid surfaces and the adsorbed organic species. The surface - based devices, created by the organization of organic species on the surfaces of inorganic solids, have been well investigated in order to use thin films as chemically modified electrodes. The surface of metal or metal oxide can be used for the direct deposition of layer-by-layer thin films from a solution by covalent or ionic bonds. This concept of absorption and direct reaction on the surface is universal and can be used to assemble multicomponent 2D lateral and 3D film microstructures using cheap and easy processing techniques. The same technique can be used with different components as smart organic or inorganic molecules [1-5], colloids [6-8], macromolecules [9-12] and biological components such as proteins or DNA [13-22].

The monolayer film could be formed by exploiting the chemisorption of an active surfactant-containing material on a solid surface, e.g., the formation of gold thiolate resulting in self-assembled monolayers (SAMs) of organosulfur compounds [23] and the in situ formation of polysiloxane-directing SAMs of organosilicon derivatives [22].

The molecularly controlled creation of nanostructured films has been dominated by Langmuir-Blodgett (LB) deposition since about 70 years, in which monolayers are formed from a gas-liquid interface to a solid planar substrate [24]. In 1960 *Kuhn et al.* have carried out controlled synthetic multicomposite films of organic molecules by using the LB technique with donor and acceptor dyes [25]. The LB technique is limited, because noncovalently attached films are not very robust; the molecules are often not firmly trapped and can be lost in solvents.

A layer-by-layer assembly technique with alternating physisorption of opposite charge at liquid/solid interfaces was first introduced by *Decher et al* in 1991 [13, 26-29] giving access to multilayer films.

The multilayer film could be also formed using layer-by-layer assembly techniques including: electrostatic interaction π - π^* stacking [30, 31], hydrogen bonding [32, 33],

coordination bonding [15, 34, 35], charge transfer [36, 37], molecular recognition [13, 38, 39], adsorption/drying cycles [40, 41], stereocomplex formation [42, 43], covalent bonds [44-46], etc. The sequence of deposition of different materials defines the multilayer architecture and thus the device properties. Each deposited monolayer is able to enhance the deposition of the next layer.

Also in 1991, *Grätzel* decided to copy a nature's trick and to project the '*Grätzel cell*' [47, 48]. The cell uses organic dye molecules to capture light energy to inject an electron from a dye into a semiconductor. As semiconductor he introduced mesoporous TiO₂, a scaffold for photo- and electroactive compounds on electrodes [47, 49]. The TiO₂ structure consists of nanocrystals which build the mesoporous structure of thin films (thickness 100 nm - 5 μm). If electro- or photo- active monolayers are coordinated to the porous structure, amplification of the surface concentrations of 100 per μm is achieved [50-54].

Similar phenomena are observed by antimony tin oxide (ATO) [55, 56], fluoro tin oxide (FTO) [57] and indium tin oxide (ITO) [58, 59] layers, but the highest surface concentrations are achieved with TiO₂. A number of promising applications for these materials are in the area of nonlinear optical materials [60, 61], conductive film [62], light emitting device [47, 63], sensor and biosensor [64, 65], display [66-69], solar cell [64, 65] etc.

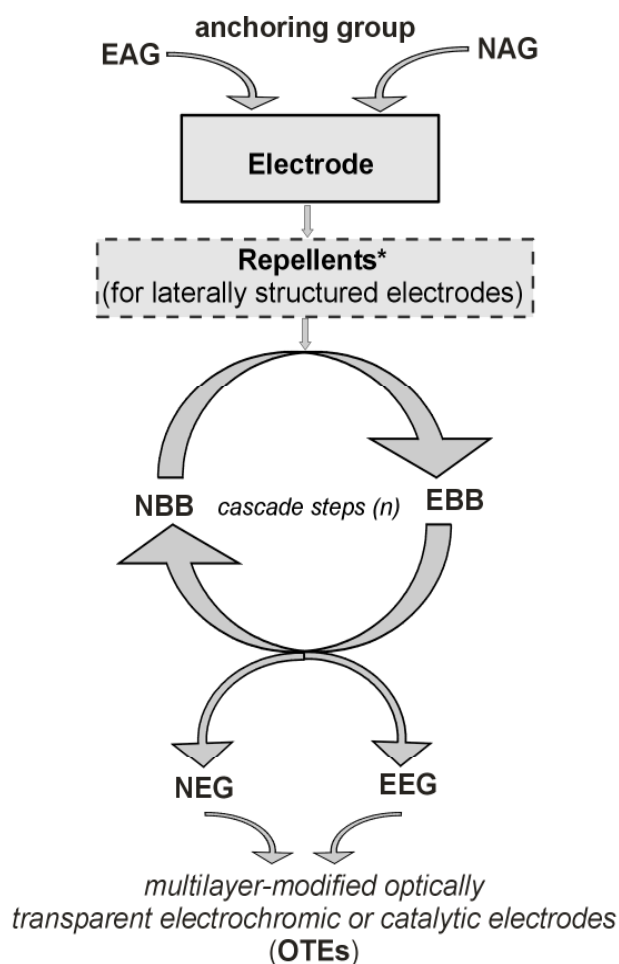
1.2. Concept and objectives

1.2.1. Concept

The principal idea behind this work consists in the modification of different mesoporous electrode materials (TiO₂, ATO, FTO and ITO) with various interesting organic and electroactive compounds. The materials include electrochromic and electrocatalytic compounds, as well as simple reversible redox systems. The main goals concern

- (i) the methodology of the modification and irreversible stabilization of the compounds on the mesoporous support, and
- (ii) the optimization of different applications in the fields of electrochromic cells (working and counter electrodes) and electrocatalysis of the reduction of alkyl bromides.

In all cases the method consists in the coordination of a bifunctional anchoring group onto the inner walls of the mesoporous system. One functionality is a TiO₂ chelating phosphonate (carboxylate, salicylate etc.). The other is either an electrophilic or nucleophilic group. The name of the compounds reflects the two ends of the compound: electrophilic (EAG) and nucleophilic anchoring groups (NAG) (scheme 1).



*N: nucleophilic, E: electrophilic, AG: anchoring group, BB: building block, EG: end group; * it was used only in the Viologens case;*

Scheme 1. Cascade type preparation of modified electrodes

According to the scheme, these compounds will be cross-linked and grown using the following techniques:

- S_N2-type bond formation between a benzyl bromide and the free nitrogen of a bipyridine;
- Condensation between a free carboxylic acid and an amine via an activated ester;
- Condensation of a carboxylic halide and an amine via amide bond formation;

- Condensation of a carboxylic halide and an alcohol via ester bond formation;
- Electropolymerisation of pending vinyl groups in redox active species after monolayer formation.

1.2.2. Objectives

With the above mentioned techniques we plan to achieve the following goals:

- Improvement of the stability of the image information in electrochromic cells with ink-jetted images;
- Improvement of the contrast ratio of ink-jetted electrochromic images:
 - a) using repellent monolayers for “white regions”;
 - b) using molecular amplification techniques.
- Optimization of the oxidation kinetics of viologen modified TiO₂ electrodes
- Preparation of a high capacity colourless counter electrode.
- Application of B₁₂-electrocatalysis to the mesoporous TiO₂ system

1.3. Chemically modified electrodes by cascade reaction

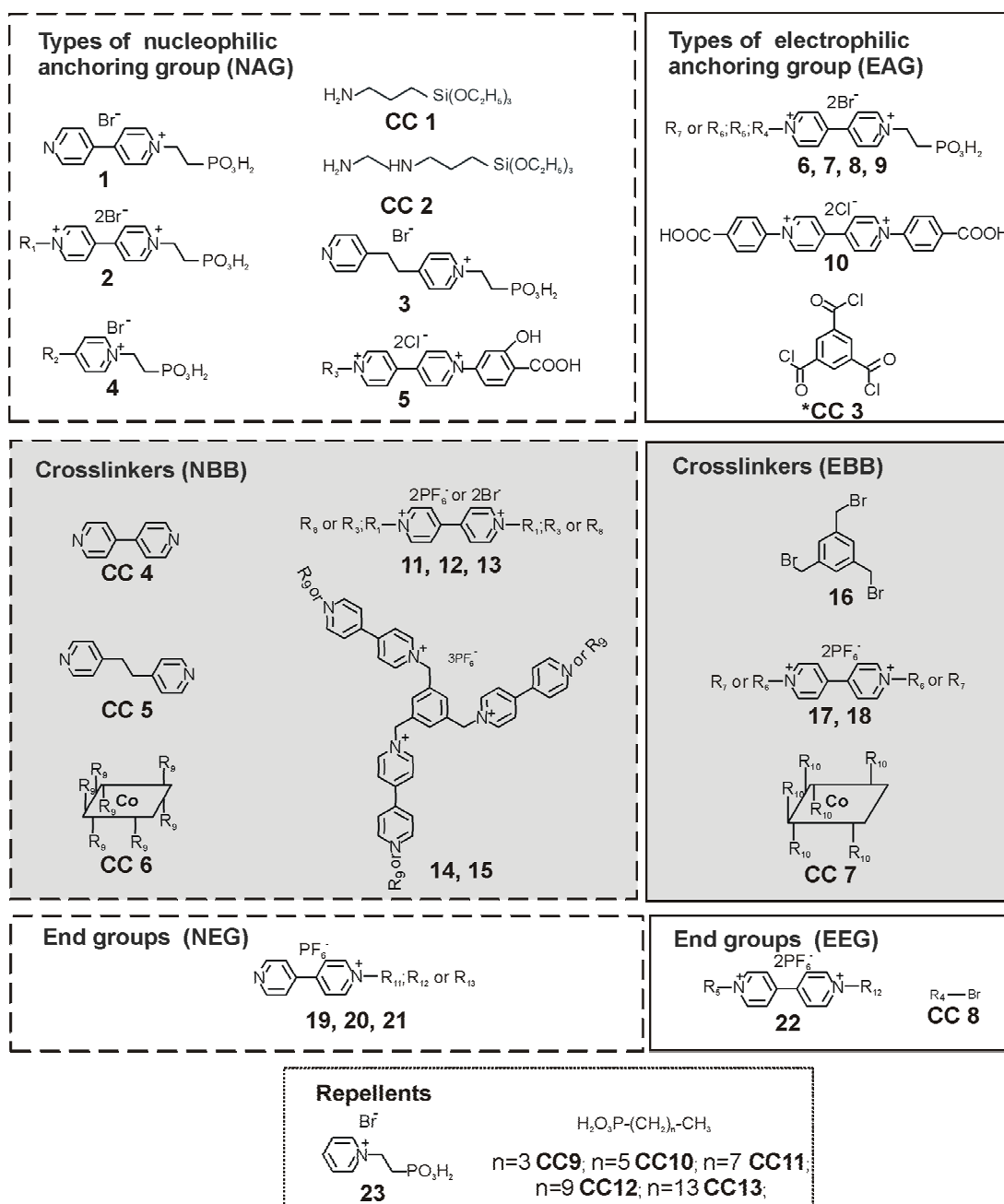
1.3.1. Ways to obtain covalently attached multilayer assemblies

The principle of the chemically modified electrodes by cascade reaction is easy and involves ionic self-assembly technique and chemical reactions in situ. Depending on the nucleophilic or electrophilic nature of the anchoring group attached on the surface (EAG and NAG in figure 1.1), the next steps consist in the sequential exposure of the electrodes to a counter part solution containing electrophilic (EBB) and nucleophilic (NBB) building blocks, respectively. The building blocks are multifunctional. There are two, three or even six or seven identical nucleophilic or electrophilic groups in the NBB or EBB present, allowing for cross-linking and/or exposition to further unreacted groups. In the following reaction step, the electrode is exposed to a solution of the counter part building block with opposite reactivity.

The reaction can be repeated again and again, and the redox units cross-link and grow layer by layer from the pore walls into the solution. The general reaction

scheme is shown in scheme 1. The amplification (growth of the number of electroactive subunits) and cross-linking is granted in this procedure.

The final step consists in the exposure of the electrode to a solution of a compound with a single electrophilic or nucleophilic group (EEG or NEG, figure 1.1). The single functional group with opposite reactivity (as compared to the exposed electrode) terminates the cycle and leaves the surface non-reactive.



(2,11) $\text{R}_1 = (\text{CH}_2)_3\text{NH}_2$; (4) $\text{R}_2 = \text{NH}_2$; (5,12) $\text{R}_3 = (\text{C}_6\text{H}_4)\text{NH}_2$; (6, CC8) $\text{R}_4 = \text{CH}_2(\text{C}_6\text{H}_5)$; (7, 22) $\text{R}_5 = \text{CH}_2(\text{C}_6\text{H}_4)\text{CH}_2\text{Br}$; (8, 17) $\text{R}_6 = \text{CH}_2(\text{C}_6\text{H}_3)(\text{CH}_2)_2\text{Br}$; (9, 18) $\text{R}_7 = (\text{C}_6\text{H}_3)(\text{CH}_2)_2\text{Br}$; (13) $\text{R}_8 = (\text{C}_6\text{H}_3)(\text{CH}_2)_2(\text{OH})_2$; (CC6, 15) $\text{R}_9 = (\text{CH}_2)_2\text{OH}$; (CC7) $\text{R}_{10} = (\text{CH}_2)_2\text{I}$; (19) $\text{R}_{11} = \text{CH}_3$; (20, 22) $\text{R}_{12} = \text{C}_2\text{H}_5$; (21) $\text{R}_{13} = \text{C}_3\text{H}_7$;
 *CC3 = EAG and EEB

Figure 1.1. Synthetic scheme of the viologen monomers used for reaction type cascade on mesoporous electrodes (TiO_2)

Another type of layer growth is represented in figure 1.2. In this case the first layer consists of an anchoring of the building block or the end groups are electropolymerizable. In contrast to the reaction in figures 1.1 and 1.3, this reaction executed with building blocks is not of the cascade type, but an electropolymerization which is more difficult to control.

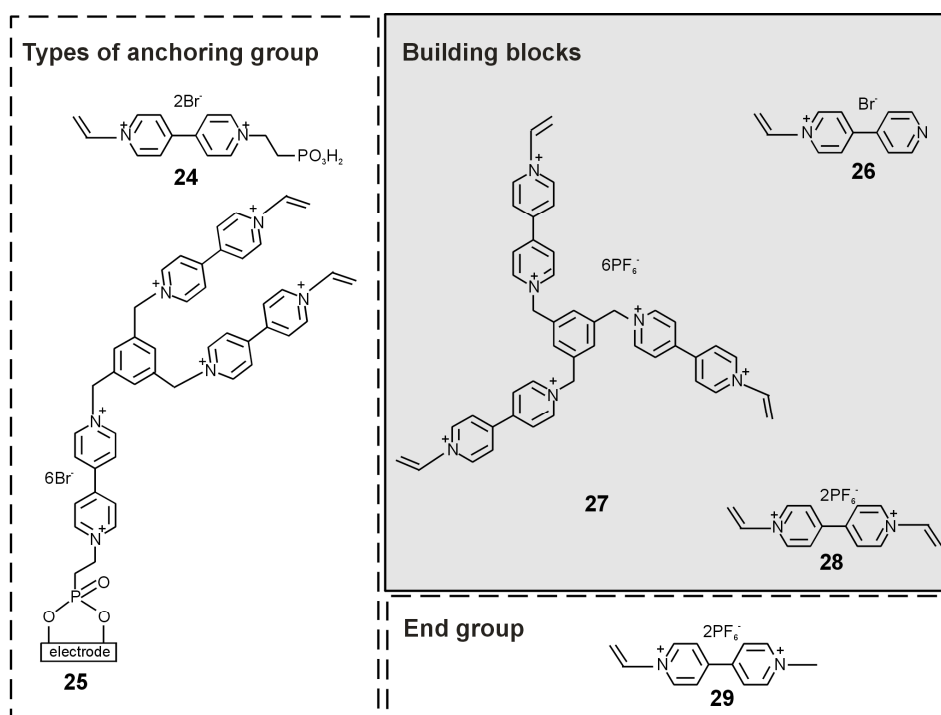


Figure 1.2. Synthetic scheme of the vinyl-viologen monomers surface cross-linking and growth on mesoporous electrodes (TiO_2)

In the figure 1.3 are shown other electrophilic or nucleophilic redox active subunits such as ferrocene derivatives used by reaction type cascade to other mesoporous materials, such as ATO and ITO.

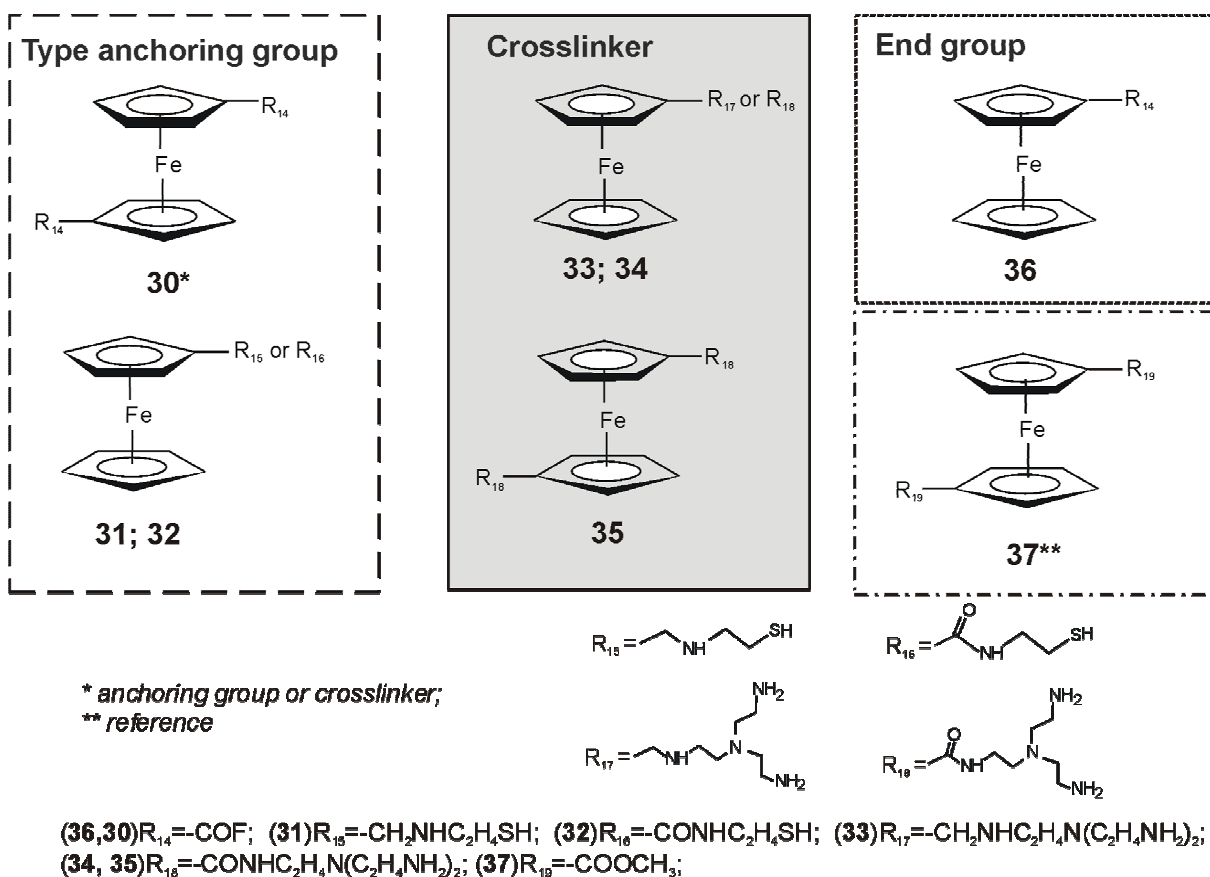


Figure 1.3. Synthetic scheme of the ferrocen monomers used for reaction type cascade on mesoporous electrodes (ATO, ITO, FTO, Au)

The bond forming reactions in figures 1.1 and 1.3 are based on substitution reactions between (multifunctional) pyridine N and (multifunctional) benzylic bromides, alcohols with carboxylic acid chlorides, as well as the condensation between carbonyl compounds or carboxylic fluorides with amines.

In conclusion, a synergy effect between incorporating electroactive species into multilayer and solid-phase supported is obtained. These materials will endow the resulting assemblies with novel properties. This technique to create a covalently attached multilayer film can be used to produce chemically modified electrodes with high stability, which guarantees the application of these electrodes under severe conditions.

Chapter 2

Electrochromics and electrochromic device

2.1. What is electrochromics?

The history of chromogenics dates back to 1704, when *Diesbach* discovered the chemical coloration of Prussian Blue (PB). In the 1930s, electrochemical coloration was noted in bulk tungsten oxide. Twenty years later, in 1953 *Kraus* observed electrochemical coloration in thin films of WO_3 , deposited on a semitransparent metal layer [70]. The first electrochromic devices (ECD) were made in 1969 by *Deb* [71, 72]. In 1973, *Philips* laboratories took up the idea that diheptyl viologen could be used in a display device called “*Schoot’s ECD device*” [73]. Electrochromics phenomena, based on viologens and tungsten oxide had found an application in the 1980s as switchable mirrors in cars [74]. *Wrighton et al.* prepared derivatized electrodes with bipyrylium species, which bind to the oxide lattice on the surface of an OTE [75-77]. In the 1990s, several companies began to develop devices for glazing applications, and the work continues. For example, companies such as *Donnelly* and *Gentex* produce currently and market successfully the automotive rear-view mirrors.

The species, which are involved in electrochromism phenomena (i.e. electron donor or acceptor), exhibit a change of colour, resulting from an electron-transfer reaction at an electrode either at an electroactive surface film or in an electroactive solution [78].

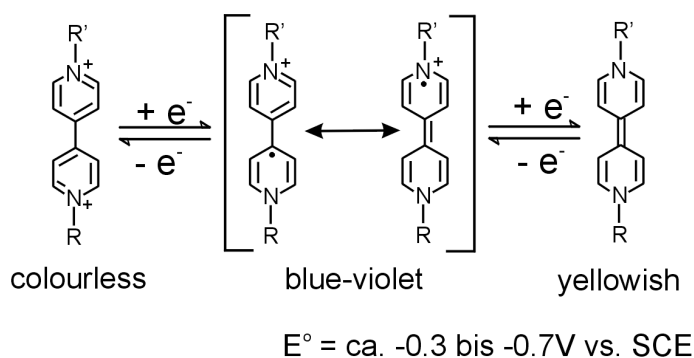
Electrochromic materials, which change their optical properties in response to an electric field and can be returned to their original state by a field reversal, are divided at least into five major families:

- metal oxide systems (WO_3 , MoO_3 , NiO_2 , IrO_2 or Co_2O_3),
- Prussian Blue systems,
- conducting polymers (polyaniline, polypyrrole, or polythiophene),
- metallopolymers and phthalocyanines
- 1,1'-disubstituted-4,4'-bipyridylium salts (the viologens) [61].

These materials have major advantages such as: a small switching voltage, a high contrast between their two coloured states, high colour purity in those states, reversibly coloured or bleached.

2.2. Electrochromics of viologens

1,1'-Disubstituted-4,4'-bipyridyls, so called viologens, are of great electrochemical interest because of their three oxidation states and the high reversibility of the redox reactions especially of the first one [79]. Fields of applications are: solar energy storage devices [50], preparation of chemically modified electrodes [80], catalytic reduction of a substrate [81]; studies of the rates of electron transfer at electrode substrate-film interface [82]; their potential electrochromic applications [73, 83], their use in electrochromic writing paper [84], bioelectronic devices [85], electron-transfer mediation to various biological molecules [86, 87], etc.



Scheme 2. Redox states of viologen

The viologens have three common redox states. The most stable is the dication state which is colourless (scheme 2) when pure unless optical charge transfer with the counter anion occurs. Reductive electron transfer to viologen dications forms coloured radical cations, the stability of which is attributable to the delocalization of the radical electron throughout the π -framework of the bipyridyl nucleus, the R and R' substituents commonly bearing some of the charge [61].

The electrochromism occurs in viologens because, in contrast to the viologen dications, the radical cations have delocalized positive charge, colouration arising from an intramolecular electron transition. Suitable choice of nitrogen substituents to attain the appropriate molecular orbital energy levels can, in principle, allow a colour choice of the radical cation. The alkyl group, for example, promotes a blue-violet colour whereas aryl groups generally impart a green hue to the radical cation. The intensity of the colour exhibited by di-reduced viologens is low since no optical charge transfer or internal transition corresponding to visible wavelengths is accessible.

A system based on substituted viologens with all compounds in solution may be operating as follows: the substituted (cationic) viologen serves as the cathodic colouring electrochromic material with a negative charge, whereas ferrocen derivatives (in this case) acting on as the anodic colourless electrochromic materials. When the system is switched on, the species will move by electrical migration to their respective electrodes. After the dual electrochromic colouration process is initiated, the products will diffuse off from their respective electrodes and meet in the intervening solution where mutual reactions regenerating the original uncoloured species take place. Bleaching occurs at short or open circuit by homogeneous electron transfer in the solution.

2.3. Existing electrochromic devices without high resolution

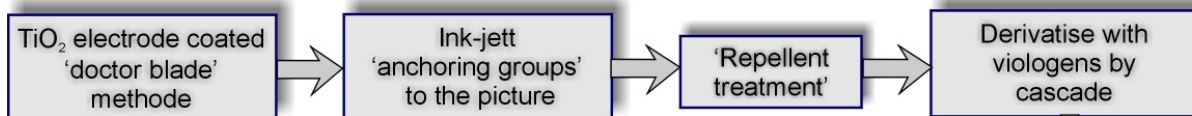
The currently used electrochromic devices belong to two categories.

In the first type of system the electrodes made of conducting glass are covered with an organic or inorganic polymer the colour which is different in the reduced and in the oxidized state. The colour change that occurs by oxidation on the first electrode must be the same that occurs by reduction of the second electrode. This type of assembly is used in electrochromic windows. It is bi-stable, which means that once the colour has been switched, the state of the device remains even if in the absence of applied voltage. Limitation of these types of systems is the slowness of the colour change, due to the low migration rate of the counter ions in the bulk polymer.

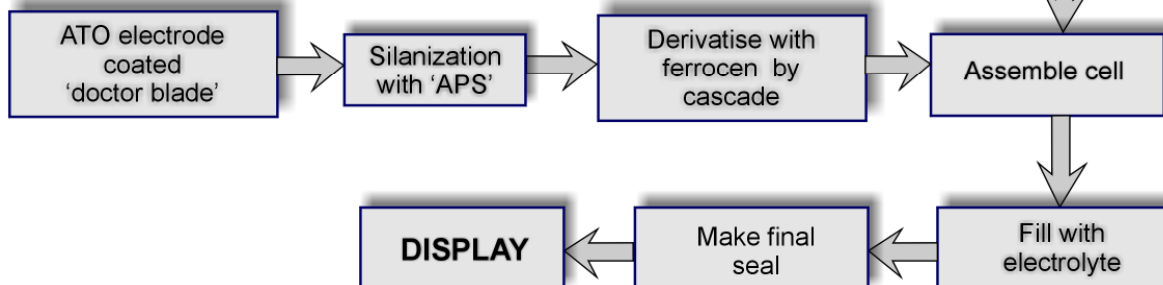
In the second type of systems, two complementary electrochromic molecules are dissolved in a solvent. One becomes coloured by oxidation and the second one by reduction. This type of system is very simple to build, reacts very fast and allows the production of dark or bright colours. However it has the strong drawback that an electrical current is needed to maintain the coloured state, because the two types of coloured molecules diffuse through the system and react with each other to restore the bleached states. Therefore, it cannot be used for large area devices or for battery-powered displays.

2.4. How to build an electrochromic device with persistent high resolution

Working electrode



Counter electrode



2.5. How electrochromic systems work

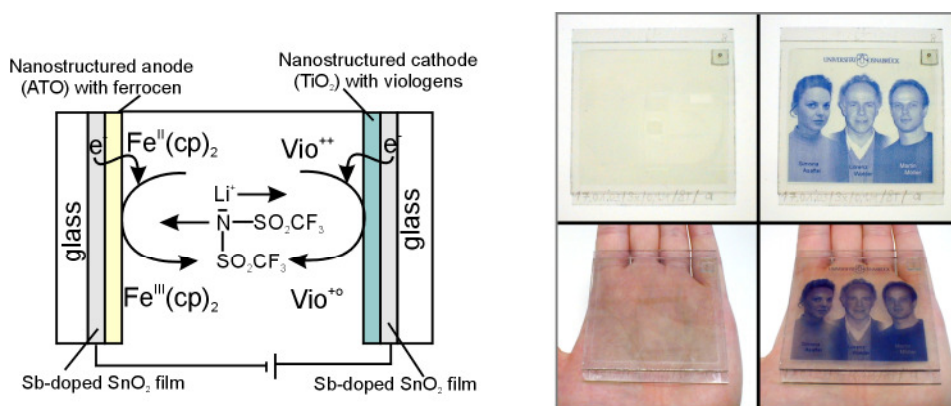


Figure 2.1. Electrochromic systems

To colour the pictures, a voltage is applied across the two transparent conducting oxide layers. This voltage drives electrons into the counter electrode, through the electrode and into the electrochromic layer. The presence of the electrons in the electrochromic layer changes its optical properties.

To reverse the process, the polarity is reversed driving the ions in the opposite direction, out of the electrochromic layer, and the pictures become transparent again.

2.6. Electrochromic device with surface confined chromophores

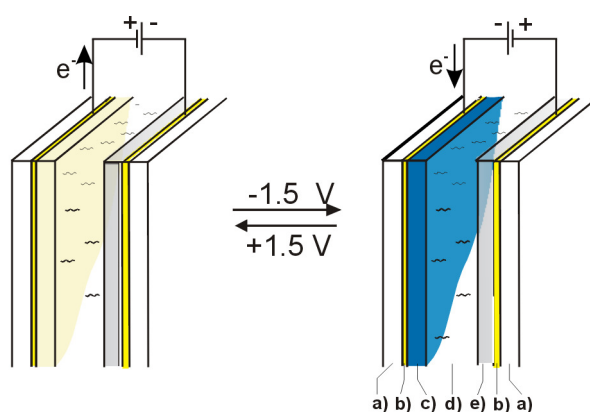


Figure 2.2. Principle of an electrochromic cell

The conventional method of fabricating electrochromic devices utilizes a 'sandwich' configuration of electrodes. The electrochromic devices consist of up to five layers of

materials; they are further sandwiched between two layers of glass (a). The central three layers are: electrochromic layer: inorganic (WO_3) or organic compounds (viologens) (c), electrolyte (d), ion storage (e) are sandwiched between two transparent conducting oxide layers as i.e. indium-doped tin oxide (ITO) (b). All layers are of course transparent to visible light. The electrochromic device is able to change its colour reversibly upon a voltage pulse.

The principle procedure was known at beginning of my work. Furthermore, it was recently shown that laterally resolved high resolution images become accessible by an ink jet technique [88].

However, the stability was a problem because such pictures tend to diffuse over prolonged times. Further it was not known how to amplify the contrast ration of such electrochromic pictures.

Here, studies have been performed for the development of an electrochromic display using nanostructured films of semiconducting metal oxides in which two electrochromic molecules are fixed on the solid surfaces. The working electrode- TiO_2 nanostructured films have a large surface area which means that up to 1000 times as many electrochromic molecules can be attached to the film. The viologens are bound to the surface and can be switched from "colourless" to "coloured" and vice versa very fast. The high number of viologen molecules attached gives strong colouration and a high rate of electron transfer. The charge to colour the viologen molecules is supplied by a second, nanostructured counter electrode. The electrode is comprised of a doped semiconductor ATO with CeO_2 layer (parallel development) or with a self assembled multilayer of the ferrocen derivatives (my contribution). It can store the charge due to its high capacity. The display is endowed with memory, resulting bistability and low power consumption.

Chapter 3

Methodology of modification and irreversible stabilization of electrochromic materials on mesoporous electrode surfaces

3.1. Titanium dioxide (TiO_2) as mesoporous electrodes

3.1.1. Why titanium dioxide (TiO_2)?

Titanium dioxide, TiO_2 , is a material that appears in a number of common substances such as white paint, toothpaste, sun lotion, soap, coloured food and medical implants. It is a low cost material, easy to produce in large quantities, chemically inert, non-toxic and biocompatible. Titanium dioxide (TiO_2) exists in three different crystal structures: brookite, anatase and rutile, is a high band gap semiconductor with an indirect gap of 3-3.2 eV (i.e., 3.05 eV rutile and 3.2 eV anatase). It is transparent to visible light (down to 370 nm) and has excellent optical transmittance. TiO_2 shows good electronic conductivity under doping conditions, charge separating properties, a high refractive index and good insulating properties, and, as a result, it is widely used as protective layer for very large scale integrated circuits (VLSI) as well as for the manufacture of optical elements.

In this thesis two aspects of TiO_2 have been exploited:

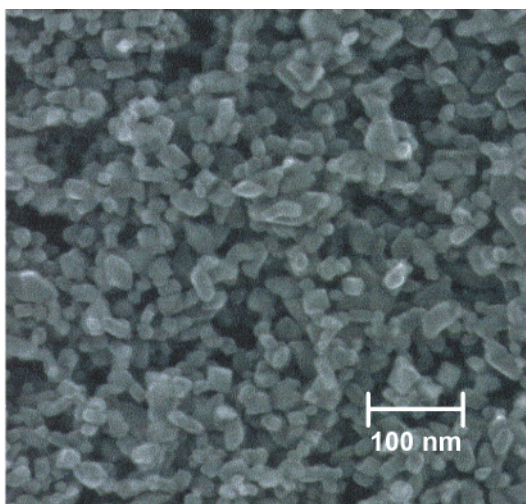


Figure 3.1. SEM - picture of sintered TiO_2

- i) the electrochromic properties of a ca. 5 μm thick layer of nanostructured TiO_2 , dyed with viologens are of specific interest for display applications;
- ii) the electrocatalytic properties of TiO_2 electrodes, modified with vitamin B_{12} derivatives.

Nanocrystalline films consist of particles with typical diameters in the size range from ~10 nm to ~100 nm, which are loosely packed, thereby forming highly porous materials that provide strong enlargement of the surface area (~1000 times). The TiO₂ films show high affinity towards many molecules (e.g. dyes), that makes possible surface modifications with carboxylates, salicilates and phosphonates. Very interesting devices have been achieved by molecular derivatization of the surface of nanocrystalline TiO₂ thin film electrodes. TiO₂ film electrodes have a potential use for a number of electronic device applications such as dye-sensitized photovoltaic cells [89], as well as antireflective (AR) coating [90], planar waveguides [91], electrocatalytic electrodes and sensors [53], electroluminescent devices [47], photochromic [54], and electrochromic displays [66, 88]. The common principle in some of these devices relies on fast electron transfer between a surface-bound molecular modifier and the nanocrystalline TiO₂ electrode.

In figure 3.2 a schematic representation of the energy level diagram of the FTO/TiO₂/Viologens interface in an aprotic electrolyte is presented, showing the electron transfer during colouration. In the TiO₂ film, used as transparent wide band-gap semiconductor, the valence band (VB) is filled with electrons (HOMO level) and the conduction band (CB) is empty (LUMO level). Between the CB and VB the so-called band-gap is located, an energetically forbidden region, meaning, that charged species (electron or holes) cannot exist in this energy range.

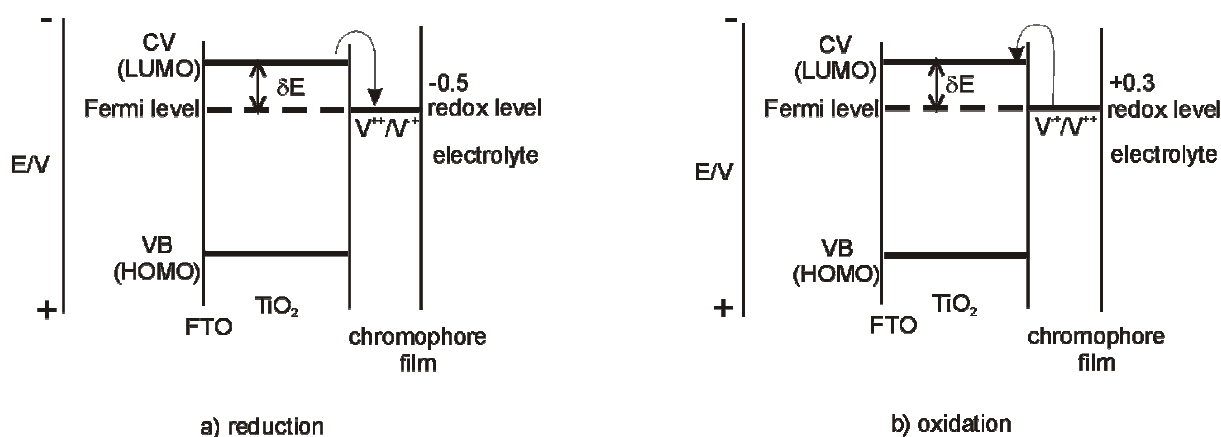


Figure 3.2. Energy diagram of a nanoporous electrode with attached viologen molecules in an aprotic electrolyte showing electron transfer in reduction-oxidation processes

When an electrochemical potential, negative enough to reach the conduction band of the metal oxide, is applied to the electrode, electrons flow from the power source to the TiO₂ into the conducting band. These electrons are transferred to the viologen

molecule confined on the surfaces, switching it from the uncoloured state to the coloured state by a reduction process (figure 3.2 a).

The electron transfer between the TiO_2 and the viologen is energetically favorable. When this transfer is nearly reversible with respect to interfacial charge transfer, the redox level of the viologen will be close to equilibrium with the Fermi level of the semiconductor $E_{\text{redox}}=E_{\text{Fn}}$ [92].

The reverse process is shown in figure 3.2 b. These electrons of the reduced chromophore jump back to the conduction band of TiO_2 . The energetic configuration is less favorable since the electrons have to move uphill in order to be extracted from the film. The difference between the conduction band edge and the chromophore's redox level (δE) constitutes a potential energy barrier that is responsible for the slower or incomplete observed bleaching.

Figure 3.3 is a schematic representation of an energy level diagram of the FTO/ TiO_2 /Viologen interface in a protic electrolyte and the influence of acid or base on the position of the conduction band edge. The position of the conduction band edge of TiO_2 is mainly governed by the solvent-electrolyte system and must be optimized for electrochromics or solar cells.

The presence of the proton in an electrolyte system moves the conduction band edge of the TiO_2 into a positive direction (figure 3.3 a), and a complete oxidation (bleaching) is observed. This behavior is attributed to charge trapping due to the movement of the relative location of the conduction band of the semiconductor and the viologen reduction potential. The semiconductor conduction band is too negative for efficient oxidation.

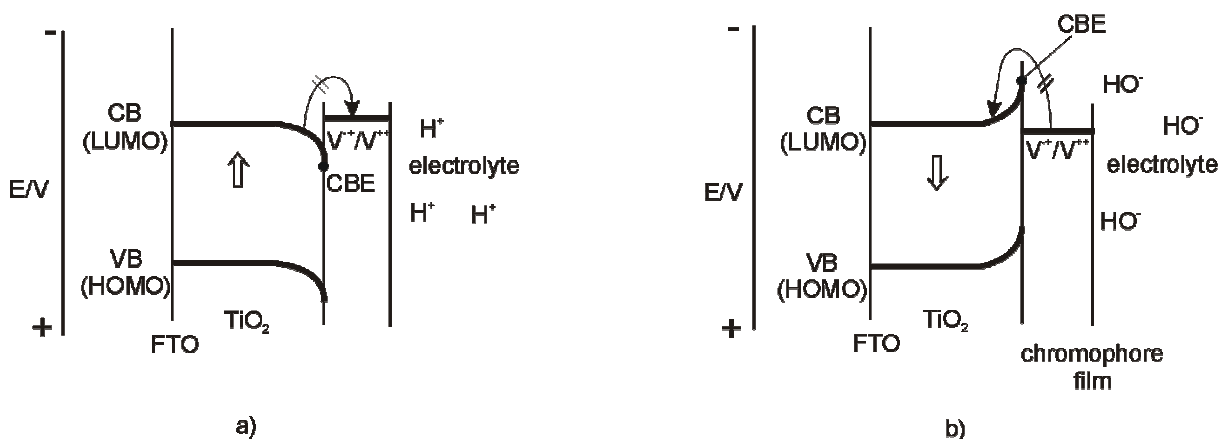


Figure 3.3. The influence of acid or base on the position of the conduction band edge (CBE) of a nanoporous electrode with attached viologen molecules in a protic electrolyte

When in an electrolyte system a base is added (figure 3.3 b), the proton effect is suppressed, and the conducting band is driven into negative direction. This leads to a typical charge trapping situation that prevents electrochemical reoxidation of the reduced chromophore and thus inhibits reversible phenomena.

To combine both, the advantage of the nanostructured TiO₂ film and the advantage of rapidity and colouration efficiency of the molecular electrochromism, I developed a method to produce a device using on molecular multilayers anchored to the semiconductor surface of TiO₂.

A suitable molecule that is colourless in the oxidized state and coloured in the reduced state is linked to the surface of the colourless semiconductor (5 μm TiO₂ film in this case) on conducting glass.

3.2. Why cross-linking?

Most studies started with nanostructured TiO₂ films and a monolayer of viologen, similar to those prepared by *O'Regan* and *Grätzel* for the corresponding solar cell [47]. The electrochromic properties of a TiO₂ electrode modified with a viologen monolayer was first reported by *Marguerettaz et al.* in a study about the electron transfer to viologens [93]. *Cinnsealach et al.* described an electrochromic (EC) window with a working electrode consisting of viologens chemisorbed on the surface of a nanostructured TiO₂ film [68]. The preparation of homogeneously colouring working electrodes consisting of a TiO₂ film with a monomolecular layer of viologens equipped with TiO₂-coordinating groups such as phosphonic, salicylic or benzoate acid functionality, have been described by *Campus et al.* [50]. The chemical modification is achieved by immersing the mesoporous nanocrystalline electrode into a solution of the modifying material for times ranging from approximately 10 minutes to approximately 24 hours. It was not clear if electrochromic materials can be deposited without reversible diffusion of the material into the solution. In the case of laterally patterned structures of viologens, as in case of ink-jetted images, this phenomenon reduces the resolution of the pattern.

Since data are not available in literature, I have checked the stability of the derivatized TiO₂ electrodes with monolayer and cross-linked viologens under accelerated aging conditions.

For the prevention of the lateral diffusion I developed a technique to fix the image via a molecular cross-linking reaction. The cross-linking takes place in a single or multi-step reaction. The process i.e. involves a cascade reaction and takes place in a solvent, where migration of the anchoring material is suppressed. This procedure has the following advantages:

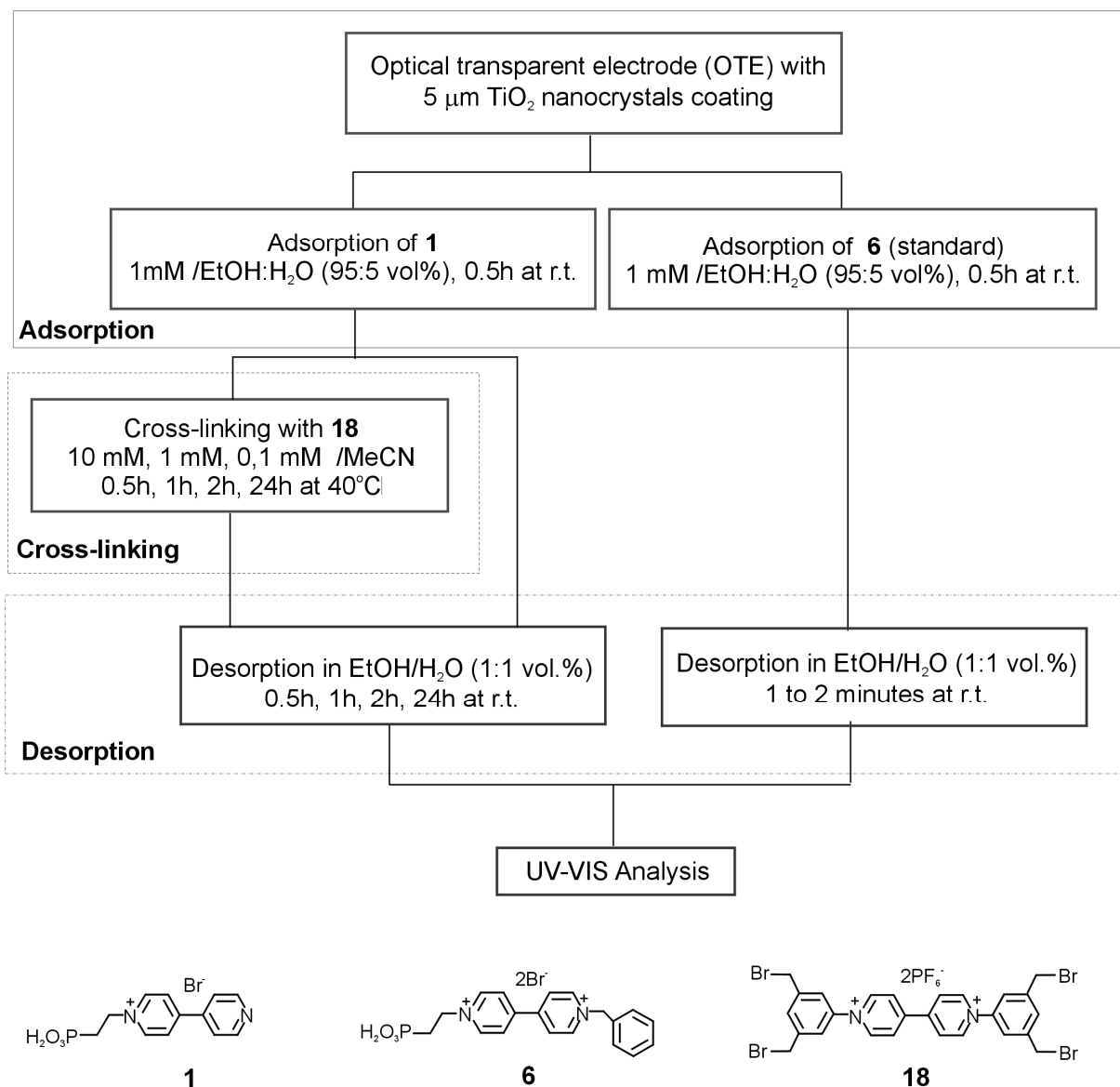
- dual effect: limited lateral diffusion of the materials and amplified color by introducing further viologen centers;
- the creation of branched structures between the electrochromic material;
- improvement of the fixation of the compounds, applied on the surface.

In general, the term “cross-linking” includes reactions where either chains or individual molecules are linked together. The cross-linking process may be a cascade type process, particularly a stepwise cascade reaction as described in chapter 1 (scheme 1).

In a first series of experiments cascade-reaction-modified TiO₂ electrodes have been prepared using compounds **1** as anchor, **18** as cross-linker and **6** as a standard (see scheme 3.1).

The study shown in scheme 3.1 contains three sections describing the precursor adsorption (**adsorption**), the cross-linking reaction (**cross-linking**) and the stability test under accelerated aging conditions (**desorption**). Each reaction step was checked by spectroelectrochemical techniques.

The following parameters were varied in a systematic way: time of cross-linking reaction, concentration of the precursor **1**, concentration of cross-linker **18** and standard **6** as well as the time of desorption.



Scheme 3.1. Solid phase synthesis and stability of cross-linked viologens on TiO_2

In figures 3.4 to 3.6 selected results are presented (spectroelectrochemical absorptions at 510 nm in $\text{LiClO}_4/\text{MeCN}$). Figure 3.4 shows the fast loss of the non-cross-linked electrochromophore E-**6** in EtOH/H₂O (1:1) ($t_{1/2} < 1$ min).

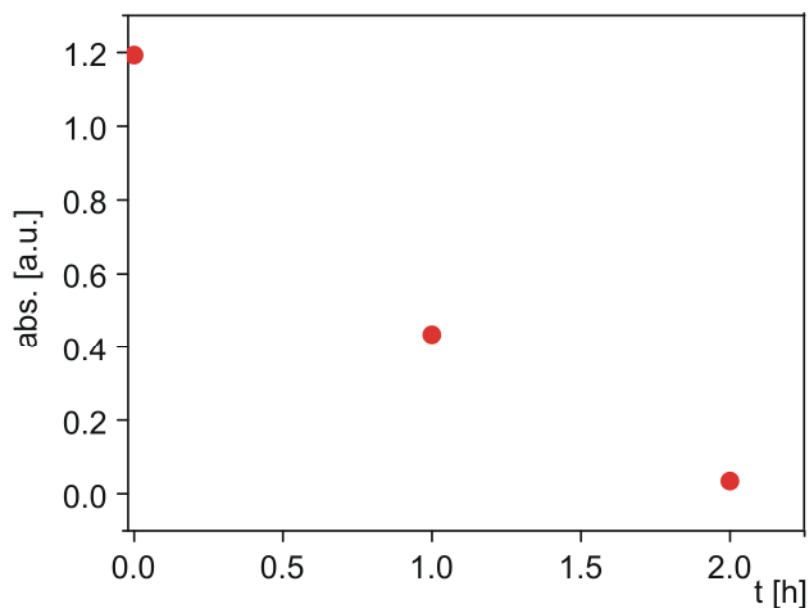


Figure 3.4. Desorption kinetic of standard ● E-6 in EtOH/H₂O

In figure 3.5 the same traces can be found in combination with those of the cross-linked viologens. Obviously, the cross-linked compounds exhibit a higher initial absorption as well as an enhanced half-life time (ca. two orders of magnitude) as compared to the non-cross-linked standard E-6. The other parameter in figure 3.5 is the time of cross-linking.

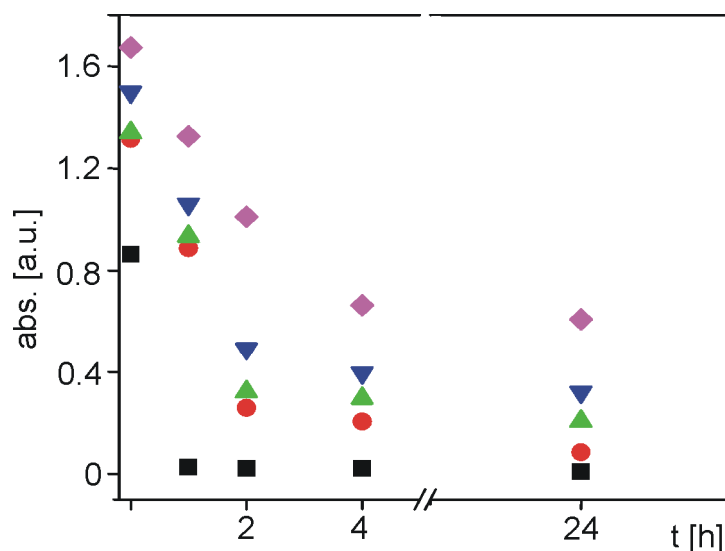


Figure 3.5. Influence of cross-linking time on desorption kinetics E-1, E-1-18 TiO₂ in EtOH/H₂O,
 ■ E-1, E-1-18; t_{synthesis}: ● 0.5 h; ▲ 1 h; ▼ 2 h; ◆ 24 h

The longer the reaction time, the higher is the absorption, as expected. However, decay rates do not seem to depend strongly on the cross-linking time. All desorption experiments were performed at room temperature.

In figure 3.6 the influence of the concentration of the cross-linker **18** is demonstrated. Absorbance is increased with increasing concentration of **18** present during the synthesis.

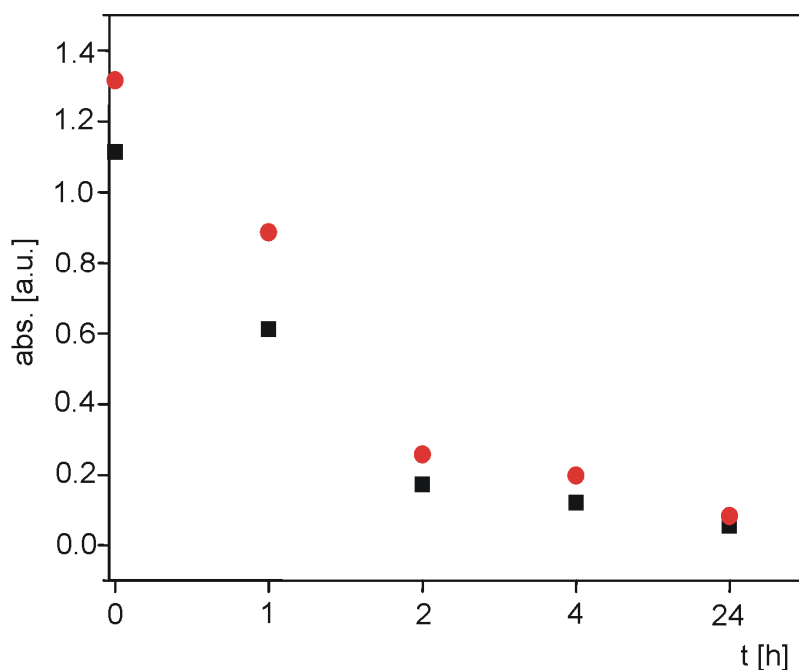


Figure 3.6. Desorption of E-1, E-1-18 from TiO₂ electrodes in EtOH/H₂O prepared from different concentration of **18**: ■ 0.1 mM and ● 100 mM, $t_{\text{synthesis}} = 2$ h

In a second series of experiments with cascade reactions, TiO₂ electrodes (E) have been prepared using compounds **1** and **8**, as anchoring compounds, **14** and **16** as cross-linkers and **20**, **22** and **CC8** as end groups. The effect of the number (1-3) of the cascade reaction steps on the surface concentration Γ is shown in table 3.1. In addition to this increased stability the amplification of the coloud areas towards forced desorption is observed with the number of cascade cycles.

Monomer sequence in cascade reaction	Surface concentration (without and after forced desorption)			
	Γ [mol·cm ⁻²] x 10 ⁻⁷			
E-1	0.4 [a]	0.26 [a]	0.08 [a]	0.02 [a]
E-1-(16-14) ₁ -22-20	1.97 [a]	1.63 [b]	1.26 [c]	1.13 [d]
E-1-(16-14) ₂ -22-20	2.57 [a]	2.28 [b]	1.97 [c]	1.96 [d]
E-8-14-CC8	9.3 [e]			

[a] without desorption, [b] 1 day in MeCN, [c] 1 h in EtOH/H₂O (1:1), [d] 1 day in EtOH/H₂O (1:1), [e] 2 min. n EtOH/H₂O (1:1)

Table 3.1. Single step and cross-linking, i.e. stabilization. Γ [mol·cm⁻²] calculated from UV-VIS absorption and desorption measurements at 740 nm (using $\epsilon=3.20 \cdot 10^3$) and 560 nm (using $\epsilon=1.82 \cdot 10^4$), respectively.

It can be concluded that in a monolayer TiO₂ device, when applied and kept at negative potential in two or three cell electrode systems (vs. Ag/AgCl), the affinity of the coloured viologens towards the TiO₂ drops substantially and some viologen is lost into the electrolyte by diffusion. In an electrochromic filter device this phenomenon is no problem because the dissolved viologen molecules get back to the TiO₂-coordinating sites. In an electronic picture consisting of TiO₂-anchoring viologen pixels, such diffusion may result in continuous loss of the pictorial information by lateral diffusion of the viologen from occupied to unoccupied sites via the solution figure 3.7 [88].

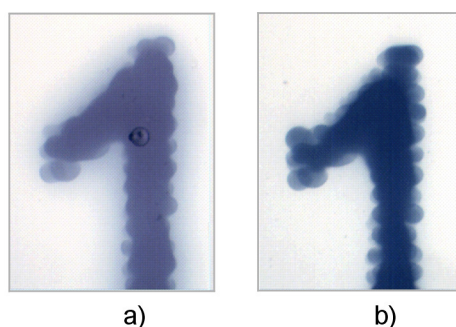


Figure 3.7. Effect of cross-linking on the long-term behaviour of the dissolution quality in an electrochromic display
a) without cross-linking and b) with cross-linking 6 months old

3.3. Types of cascade reactions on the nanostructured TiO₂ film

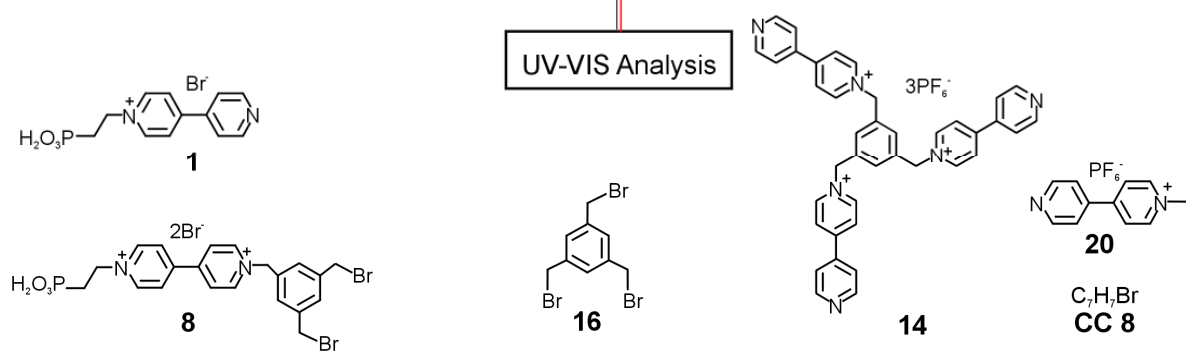
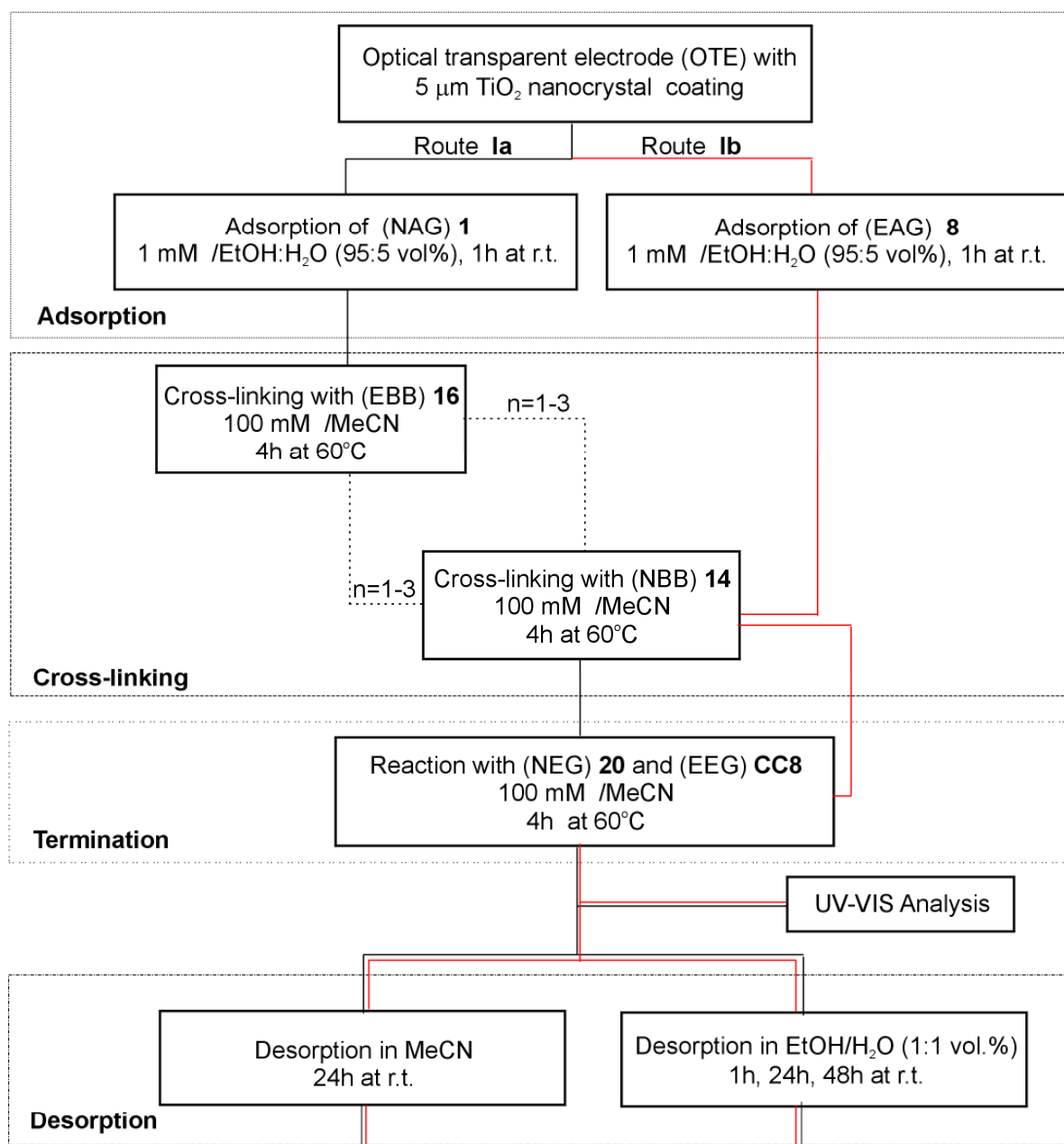
Depending on the nature of anchoring groups (nucleophilic NAG or electrophilic EAG) coordinated on TiO₂ electrodes, there are different types of **solid-phase-supported reactions**:

- S_N2-type bond formation between a benzyl bromide and the free nitrogen of a bipyridine;
- Condensation of a carboxylic halide and an amine via amide bond;
- Electropolymerisation of pending vinyl groups in redox active species after monolayer formation

3.3.1. Multi-step cross-linking by an S_N2- mechanism and accelerated aging tests

From the preliminary results in chapter 3.2 I decided to study multi step cross-linking reactions. In schema 3.2 a typical cross-linking experiment on mesoporous TiO₂ with two different anchoring groups NAG **1** route **1a** and EGA **8** route **1b** is shown.

After exposure of the TiO₂ electrodes to the anchoring mono-alkylated bipyridine **1** (plate E-1, figure 3.8) at millimolar concentration, the electrodes are treated with the electrophilic triple cross-linker **16** at 0.1 M to induce the surface-confined substitution reaction, followed by treatment with the nucleophilic triple cross-linker **14** (compare E-1-**16-14** in figure 3.8). Further treatment of the electrodes with **16**, or **16** followed by **14**, yields cross-linked modified electrodes E-1-**16-14-16** or E-1-(**16-14**)₂, respectively. In order to saturate all open reactive sites, the electrodes were treated sequentially with compound **CC8** and **20** to yield electrode E-1-(**16-14**)₃-**20-CC8**.



Scheme 3.2. Cascade reaction on TiO_2 with anchoring compounds

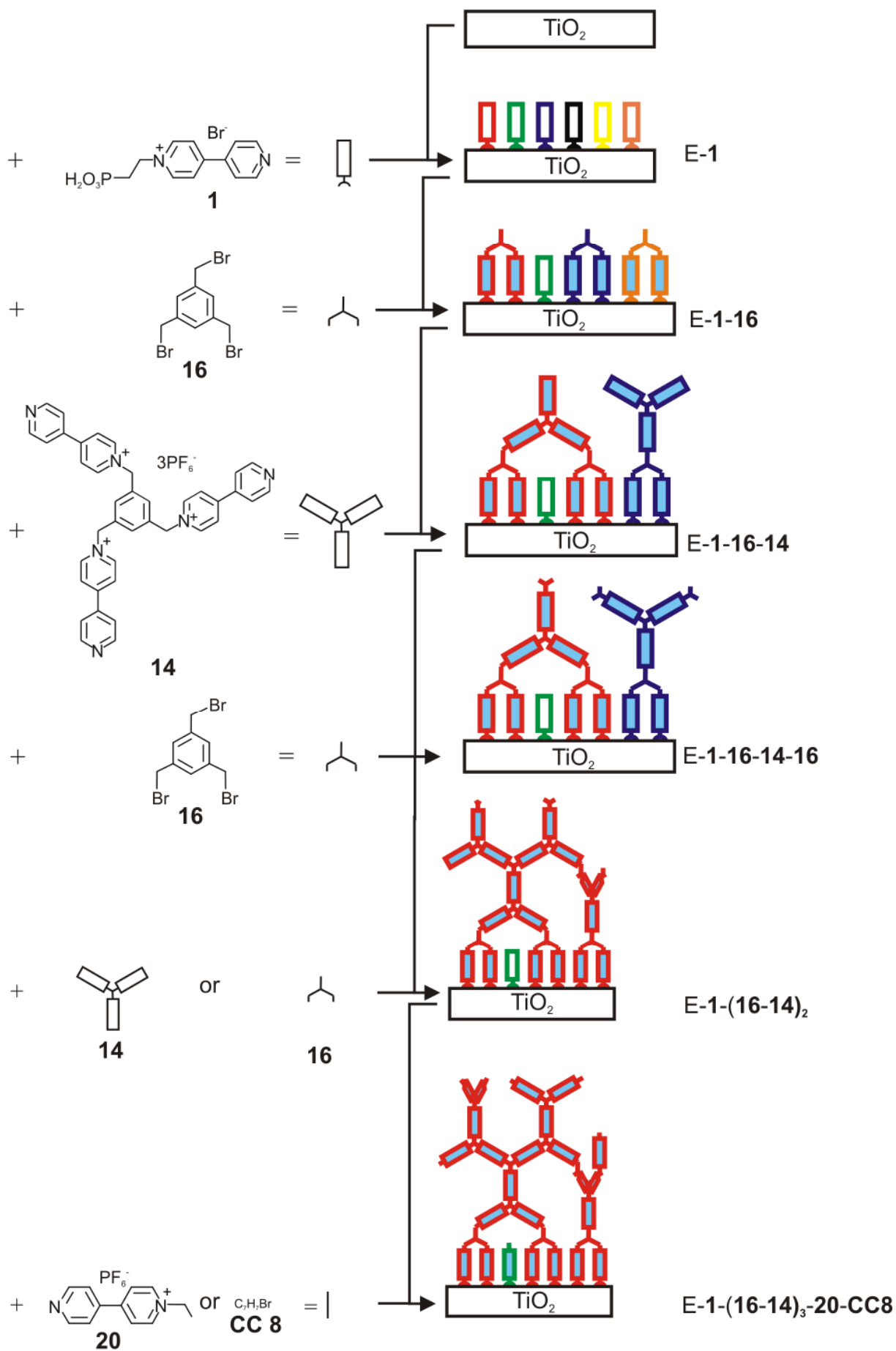


Figure 3.8. Cascade reaction on TiO_2

The UV-VIS results of plates E-1, E-1-16-14, E-1-16-14-16 and E-1-(16-14)₃-20-CC8 are shown in figure 3.9. Obviously, increased cross-linking leads to increased surface concentration of electrochromic sub-units (in LiClO₄/MeCN using $\epsilon = 3200$, $\tilde{\Gamma} = A_{740 \text{ nm}} / \epsilon \cdot 1000$ with abs. = absorbance, ϵ = extinction coefficient [$\text{dm}^3 \text{mol}^{-1} \text{cm}^{-1}$] and Γ = surface concentration [$\text{mol} \cdot \text{cm}^{-2}$]). From the coulometric analysis of the cyclic voltammograms respectively at 20 mV/s, $\tilde{\Gamma} = Q / nF A_{\text{electrode}}$ [$\text{mol} \cdot \text{cm}^{-2}$], Q =charge [C], F =Faraday constant, $A_{\text{electrode}}$ =electrode surface [cm^2]). As a matter of fact the absorbance at 540 nm is beyond the limits if the spectrometer used.

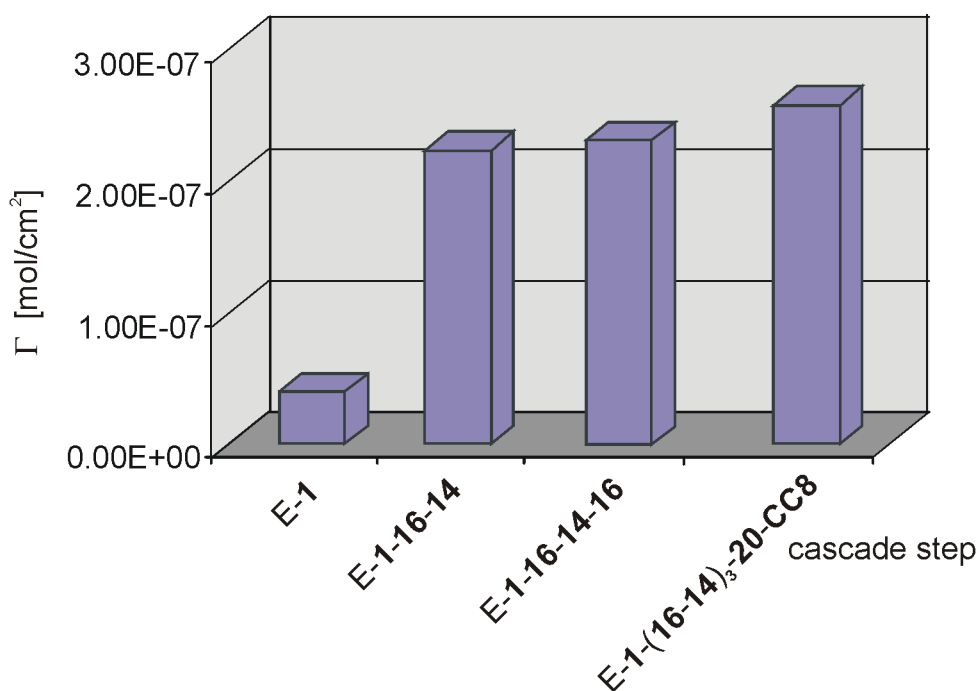


Figure 3.9. Influence of cascade step on the surface concentration

The same plates have been subjected to an accelerated aging test. The plates have been sequentially rinsed in acetonitrile and water-ethanol for several hours up to days. Such a treatment releases most of the dye if it is only present as an anchored monolayer.

Figure 3.10 shows the results. I used normalized surface concentrations for case E-1, E-1-16-14, E-1-16-14-16 and E-1-(16-14)₃-20-CC8. The simple anchored modifier decays to approximately 2 percent of its initial surface concentration during this treatment, but the cross-linked electrodes withstand the accelerated aging showing

generally more than 50 % of the activity at the end. The persistence is much better in the cross-linked state.

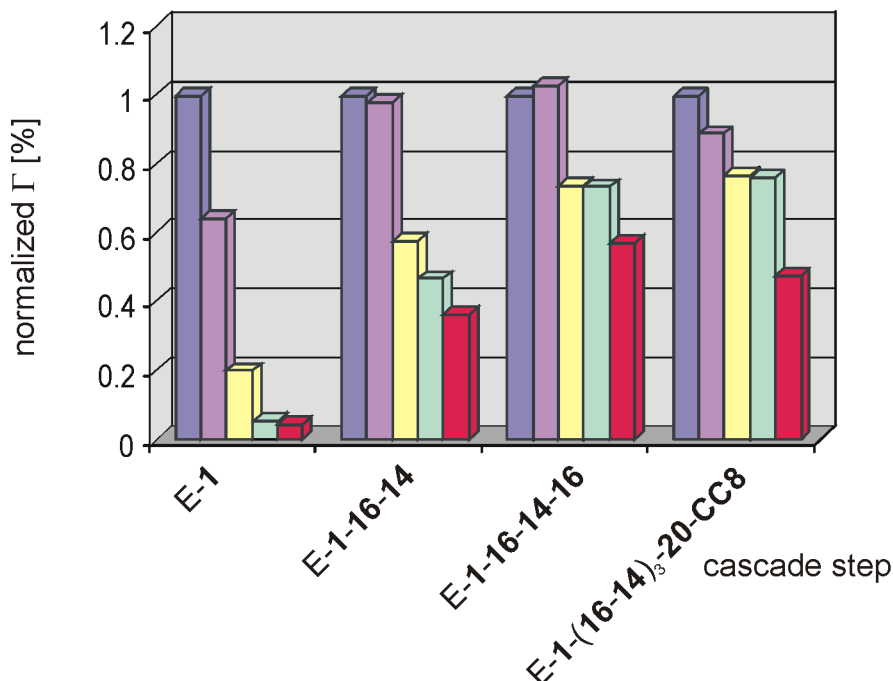


Figure 3.10. Influence of cross-linking on relative stability towards forced desorption:

■ after synthesis, ■ 1 d in MeCN, ■ 1 d in MeCN + 1 h in EtOH/H₂O, ■ 1 d in MeCN + 1 d in EtOH/H₂O, ■ 1 d in MeCN + 2 d in EtOH/H₂O,

In scheme 3.2 route **1b** a comparative cross-linking experiment is shown using the electrophilic anchor (EAG) **8** for monolayer surface modification with a monolayer (electrode E-**8**), in contrast to route **1a** where the nucleophilic anchor (NGA) **1** was used. Such an electrode was treated with the electrophilic triple cross-linker **14** at 0.1 M concentration to induce the surface-confined substitution reaction (electrode E-**8-14**) and then treated with benzyl bromide **CC8** (electrode E-**8-14-CC8**).

The corresponding surface concentrations after the synthesis are shown in figure 3.11 (as calculated from the absorbance at 560 nm in LiClO₄/MeCN using $\epsilon = 17670$). Again, a multiple exposition increases the surface concentration.

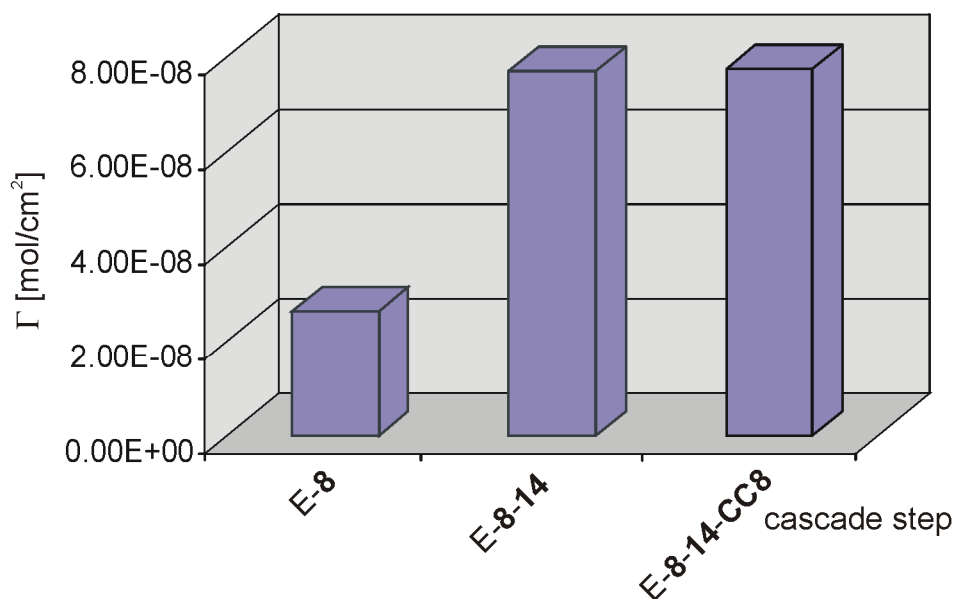


Figure 3.11. Influence of cascade step on the surface concentration using anchoring group **8**

Figure 3.12 shows the aging test of the three plates. The influence of cross-linking is obvious but less pronounced than in the sequence described in scheme 3.2 route **1a**. This may be related to the fact that only one cross-linking step was used in this sequence.

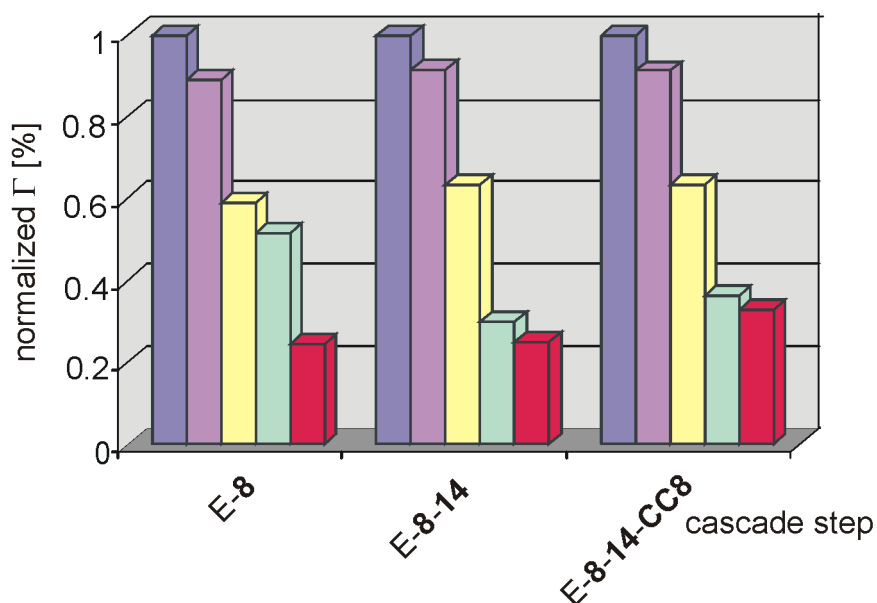
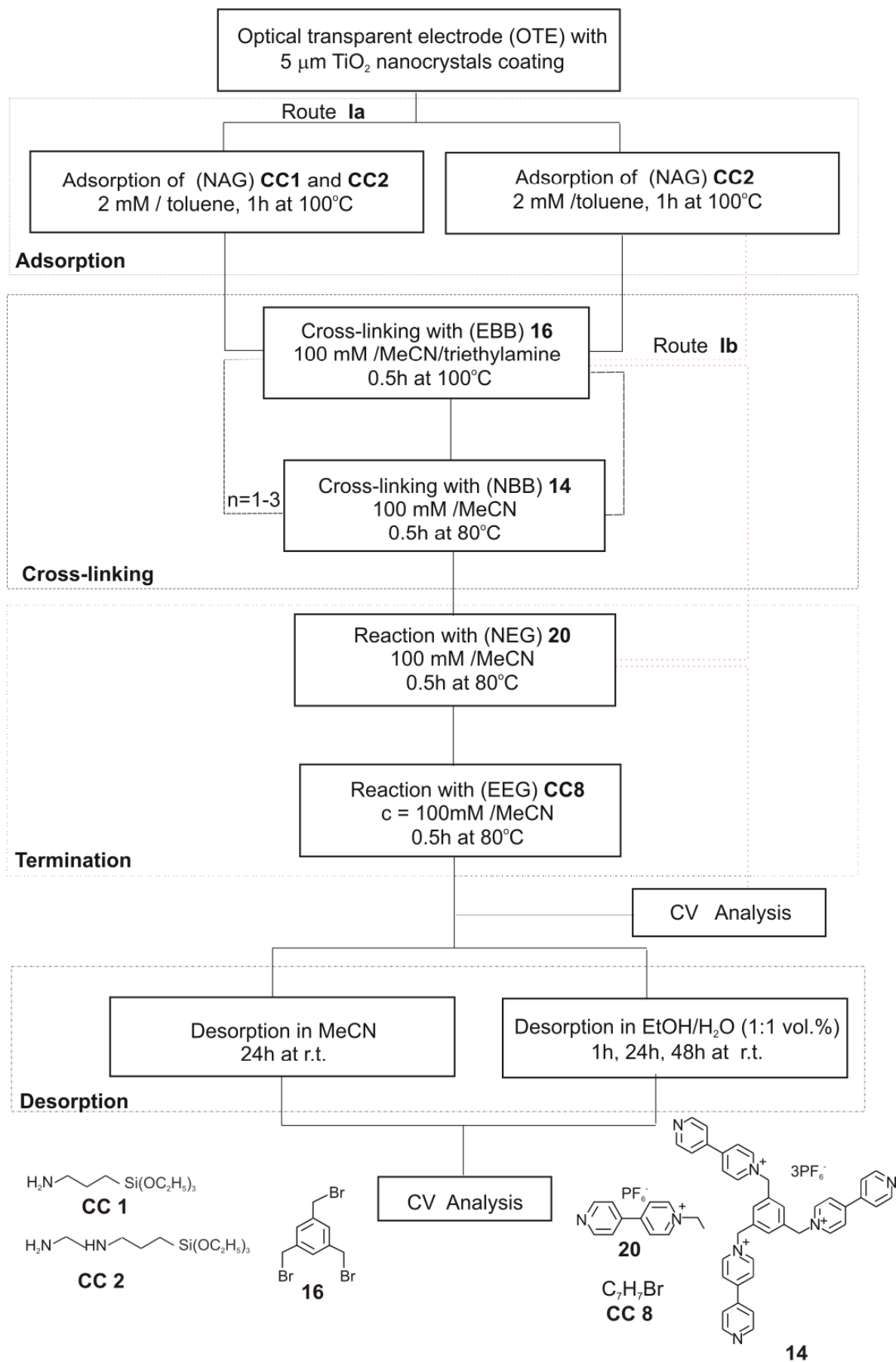


Figure 3.12. Influence of cross-linking on the relative stability towards forced desorption using anchoring group **8**:
 ■ after synthesis, ■ 1 d in MeCN, ■ 1 d in MeCN + 1 h in EtOH/H₂O, ■ 1 d in MeCN + 1 d in EtOH/H₂O, ■ 1 d in MeCN + 2 d in EtOH/H₂O,

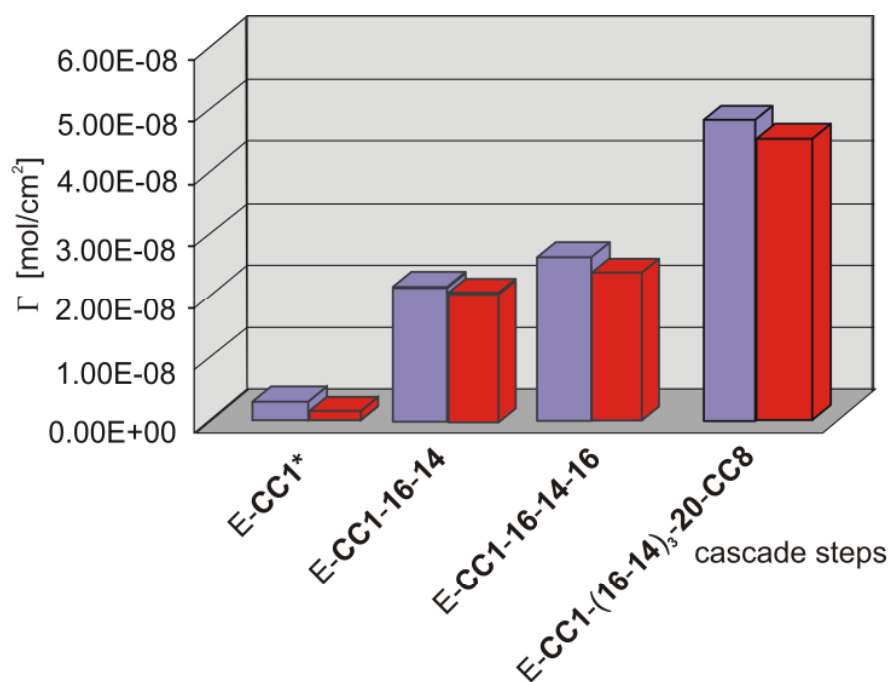
In conclusion, high stability can be achieved for the electrochromic layer on mesoporous TiO₂ by S_N2 cross-linking reactions directly on the surfaces. The absorbance increase almost by a factor of 10 and the stability towards accelerated aging (washing with organic and/or aqueous solutions over hours) is much higher than traditionally anchored electrochromophore monolayers (cfm. scheme 3.2). This means that principally the TiO₂ layer could be reduced by the same factor in order to reach traditional absorbance. This could improve the optical quality of the plates (reduction of haze).

In scheme 3.3 a preliminary experiment is shown using two different amino-silane derivatives as anchoring groups followed by a reaction under formation of secondary amines in the first reaction step. This type of reaction may replace the S_N2-type reaction between benzylic bromides and pyridine nitrogen.

The new anchoring compounds are easily adsorbed on TiO₂, but the reaction takes generally more time and needs higher temperature as compared to alkylphosphonates. It is not yet known if they can be used in the ink jet mode (ongoing research). However, as the amino alkyl moiety can easily be reacted with benzylic bromides. I used either the monoamino- compound 3-amino-propyl triethoxysilan **CC1** or the diamino- compound N-[3-(trimethoxy silanyl) propyl] ethane 1,2-diamine **CC2** route **1a** (scheme 3.3, figure 3.13). The monoamino compound **CC1** yields TiO₂-plates of better optical quality than the diamino compound (slight haze). The coloration of the reduced plates shows similar intensities as those observed with phosphonates for the same amount of cascade steps.



Scheme 3.3. Cascade reaction on TiO_2 using anchoring compounds such as 3-(aminopropyl)-triethoxysilane (**CC1**) and N-[3-(trimethoxy silanyl) propyl] ethane-1,2 diamine (**CC2**)



*CC1 and CC2 anchoring groups with ferrocene

Figure 3.13. Influence of cascade step on surface concentration using the anchoring compounds : ■ 3-amino triethoxysilan (CC1) and ■ N-[3-(trimethoxy silanyl) propyl] ethane 1,2-diamine (CC2)

The stability upon washing is also enhanced after cross-linking, as with the phosphonates (figure 3.14).

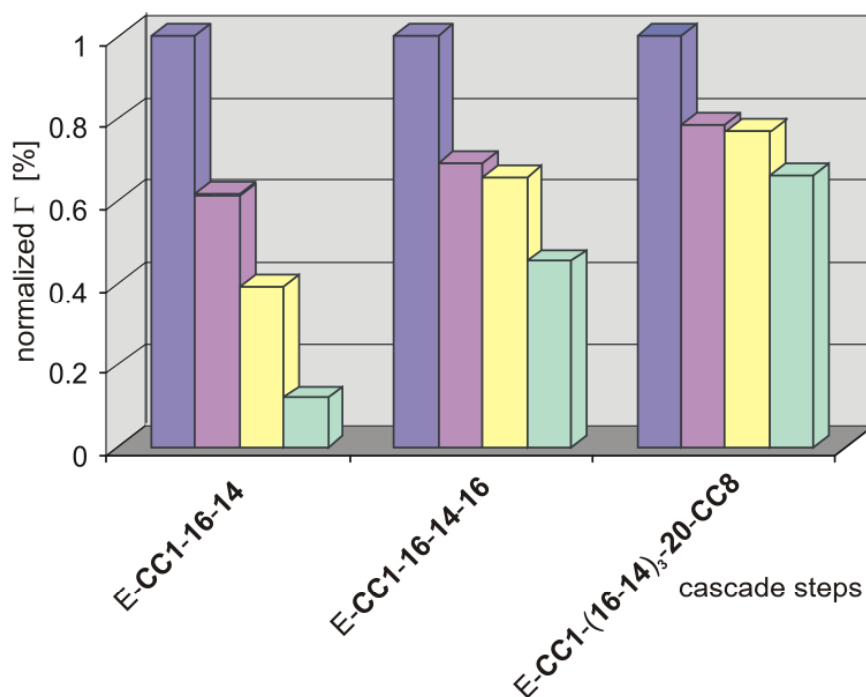


Figure 3.14. Influence of cross-linking on the relative stability towards forced desorption using anchoring groups: 3-amino-propyltriethoxysilan or N-[3-(trimethoxy silanyl) propyl] ethane 1,2-diamine
 ■ after synthesis, ■ 1 d in MeCN, ■ 1 d in MeCN + 1 h in EtOH/H₂O, ■ 1 d in MeCN + 1 d in EtOH/H₂O

Experimental conditions for the preparation were similar as described for phosphonates anchoring, but the cross-linking temperature was higher and the reaction time shorter. The analysis was partly done by coulometry in a 3-electrode system in 0.2 LiClO₄/MeCN, vs. Ag/AgCl, 20 mV·s⁻¹, besides spectroelectrochemistry. In a parallel experiment, following route Ib (see scheme 3.3), the plates were treated with N-[3-(trimethoxy silanyl) propyl] ethane 1,2-diamine **CC2** as anchoring group, crosslinked with compound **16**, and finally treated with end group compound **20**. Thus, a TiO₂ electrode, containing a viologen monolayer was obtained. The surface concentration for the monolayer viologen is shown in figure 3.15 (as determined by cyclovoltammetry in the 3-electrode system in 0.2 LiClO₄/MeCN, vs. Ag/AgCl, 20 mV·s⁻¹) with corresponding forced desorption in figure 3.16.

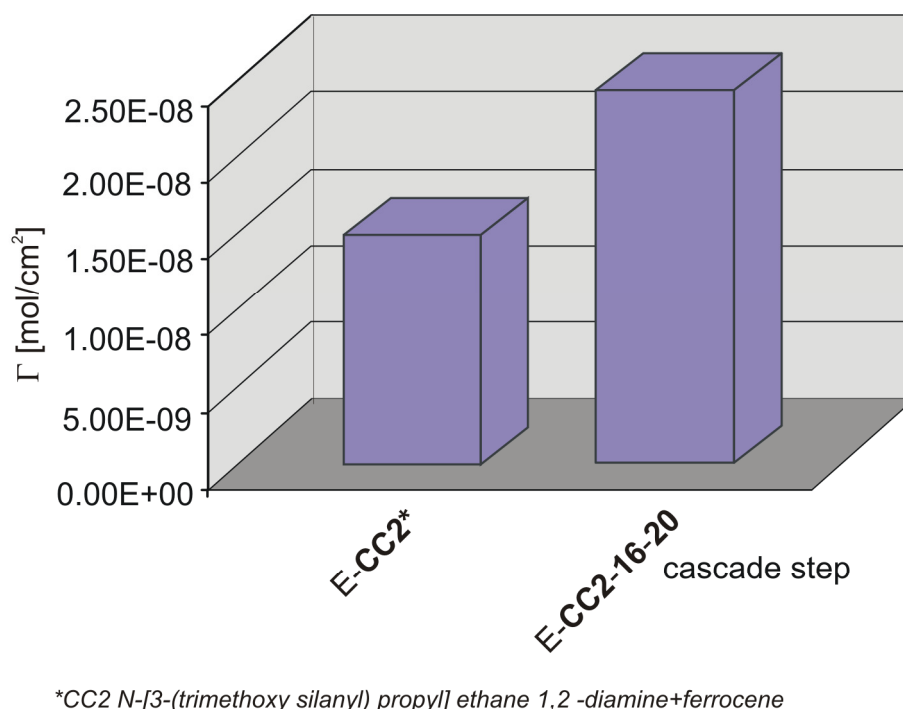
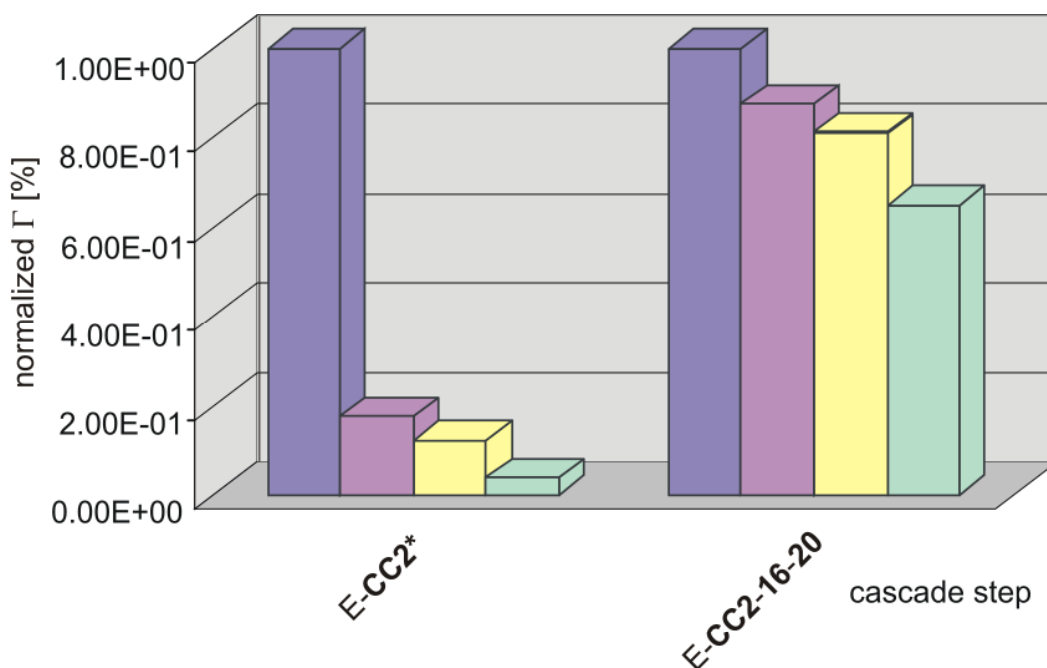


Figure 3.15. Influence of cross-linking on the surface concentration using N-[3-(trimethoxy silanyl) propyl] ethane 1,2 -diamine (**CC2**)



*CC2 N-[3-(trimethoxy silanyl) propyl] ethane 1,2 -diamine + ferrocene

Figure 3.16. Influence of cross-linking on the relative stability towards forced desorption using anchoring group: N-[3-(trimethoxy silanyl) propyl] ethane 1,2-diamine (**CC2**)
 ■ after synthesis, ■ 1 d in MeCN, ■ 1 d in MeCN + 1 h in EtOH/H₂O,
 ■ 1 d in MeCN + 1 d in EtOH/H₂O

The new anchoring compounds 3-amino-propyl triethoxysilane **CC1** or the diamino-compound N-[3-(trimethoxy silanyl) propyl] ethane 1,2-diamine **CC2** with additional functional groups offer the possibility for solid phase cascade reactions, either by substitution or by condensation.

3.3.1.1 Application of the cascade reaction to ink-jet produced electrochromic images

360 ppi (points per inch) electrochromic images can be cross-linked according scheme 3.2 route **la** or **lb**.

Functionalized anchoring groups were printed on a TiO₂-coated glass plate to obtain stabilized electrochromic images after cross-linking. A suitable test-pattern was created (figure 3.17) to evaluate the results.

Synthesis:

Step 1: The test-pattern (figure 3.17) was printed on a TiO₂ coated ITO-electrode using a 0.1 M solution of compound **8** (electrochromic anchoring group).

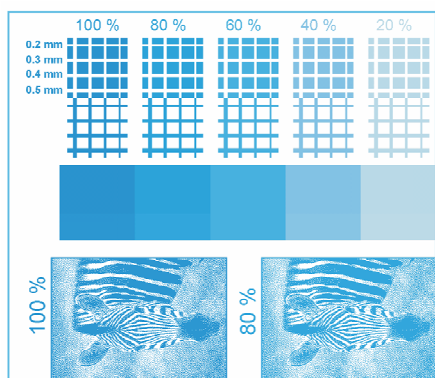


Figure 3.17. Test pattern for cross-linked images with the coloration intensity of one pure colour (cyan) in % (original size). The two pictures at the bottom have a resolution of 360 ppi.

Step 2: The electrode was then treated with a 0.02 M solution of **14** in MeCN at 60 °C for 1 h and thereafter rinsed with pure MeCN.

Step 3: The remaining N-groups of compound **14** on the electrode surface were saturated with compound **CC8**. For this step the electrode was treated with a 0.1 M solution of **CC8** for 4 h at 60 °C and rinsed with pure MeCN at the end.

Treatment with a polar solvent:

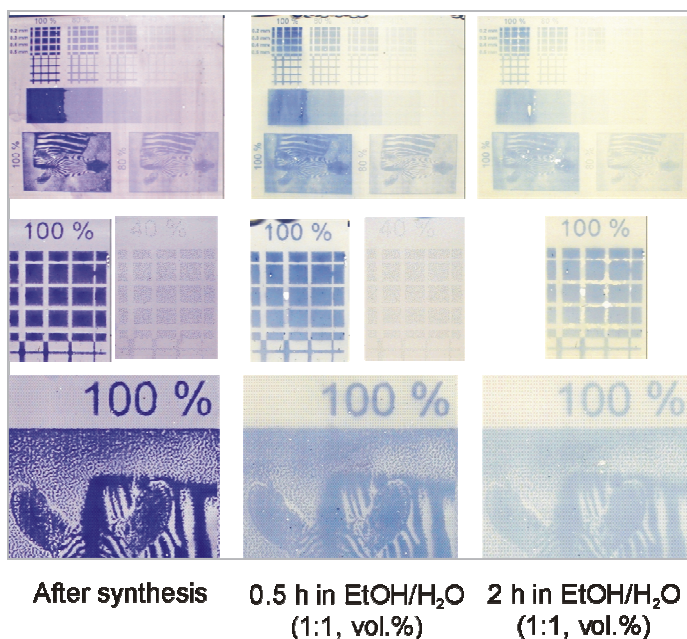


Figure 3.18. Electrode after synthesis and after the accelerated aging process

To simulate an accelerated aging process the electrode was treated with EtOH/H₂O (1:1 vol. %) at r.t. Figure 3.18 shows the electrode direct after synthesis and after the accelerated aging process.

The resolution of the image and intensities of the dots are comparable to the results of a printed electrochromic image without cross-linking. The wash-cycles caused a decrease of the colour intensity and a

slightly diffusion of the dots. Have in mind that under the same conditions an electrochromophore without cross-linking is washed out within 2 min.

The picture is as rich in details and as well resolved as one which has not been cross-linked and that is checked prior to force aging. The picture obtained after

cross-linking gains much in stability as compared to the non-crosslinked case. If, for example, an image-jetted plate, which is not cross-linked, is treated with ethanol/water for a few minutes, all the information is lost. Unfortunately, the cross-linking step with **14** occurs in a slight coloration of the "white" areas (ca. 15% of intensity), because of the direct adsorption on the TiO₂.

However, as seen from figure 3.18, a 30 min. exposition to ethanol/water does not abolish the image because of completely cross-linking, but leads to a decrease of the absorption to ca. 0.5 of its original value.

3.3.1.2. Adsorption-desorption on TiO₂ of the different viologens without anchoring groups

Adsorption-desorption is an undesirable side reaction in electrochromic prints, because it leads to bluish tint in 'white regions'.

From 3.3.1.1 it was evident that viologens without anchoring group can coordinate on the TiO₂ surface. Using the procedure in scheme 3.4 this phenomenon was studied in more detail. In route **1a** is shown additionally an experiment in which no anchoring compound was used (i.e. the triple viologen **14** is depicted).

After treatment with benzyl bromide **CC8** the plate shows considerable absorbance (figure 3.19 as calculated from absorbance at 540 nm in LiClO₄/MeCN using $\epsilon = 5930$), but washing leads to loss of most of the electrochromophore.

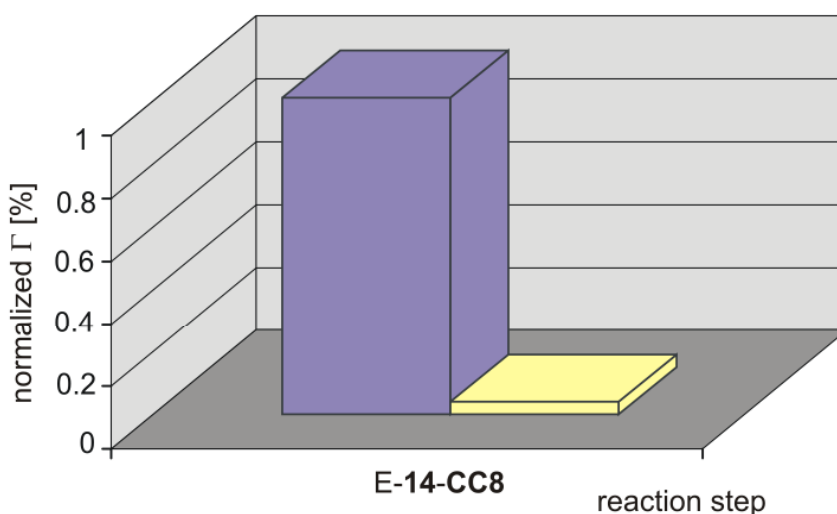
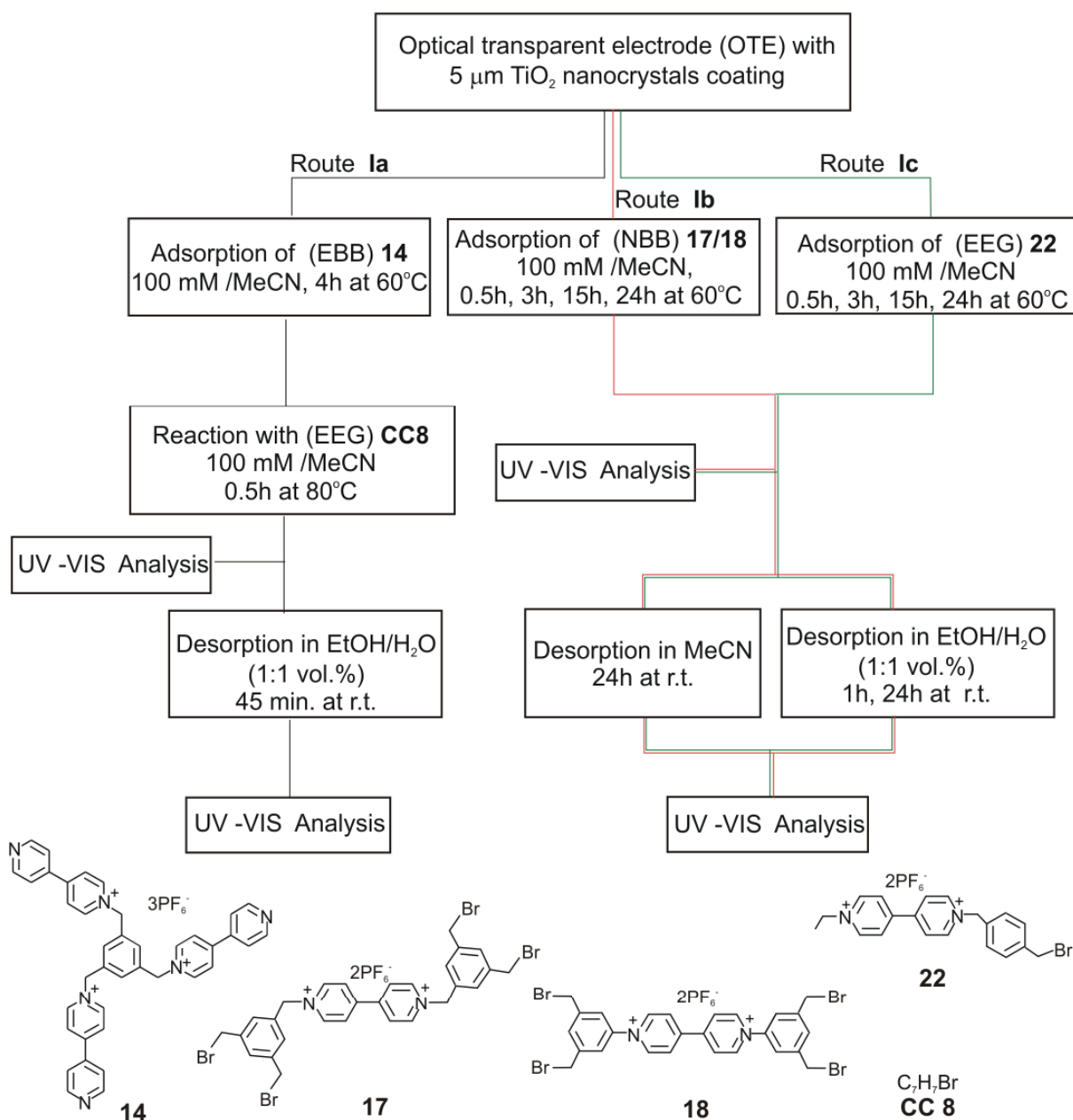


Figure 3.19. Influence of the cross-linking on the relative stability towards forced desorption
 ■ after synthesis, ■ 45 min. EtOH H₂O (1:1 vol. %)



Scheme 3.4. Absorption desorption on TiO_2 with different viologens

The experiments shown in scheme 3.4 route **Ib** and **Ic**, respectively, (and figures 3.20 to 3.25) describe a surprising phenomenon: benzylic bromides react with the TiO_2 surface or polymerize under the condition of surface substitution. The TiO_2 electrodes were treated with the tetrabromides **17** and **18**, route **Ib**, as well as with the monobromide **22**, route **Ic**, for different times at elevated temperature.

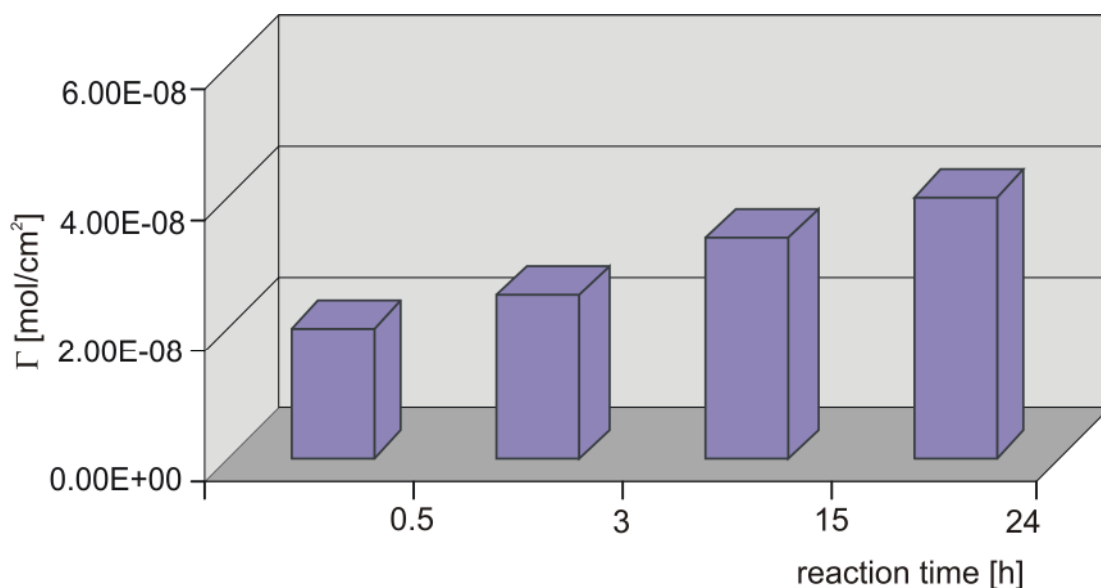


Figure 3.20. Influence of the surface reaction time of compound **17** on the surface concentration

Figure 3.20 shows the surface reaction of the tetrabromide **17** (benzyl type viologen) after synthesis (as calculated from absorbance at 440 nm in LiClO₄/MeCN using $\epsilon = 5018$), and diagram 3.21 shows the corresponding forced desorption. Obviously, this compound is either surface confined by a direct link or it has been polymerized as seen from its slow surface concentration decay.

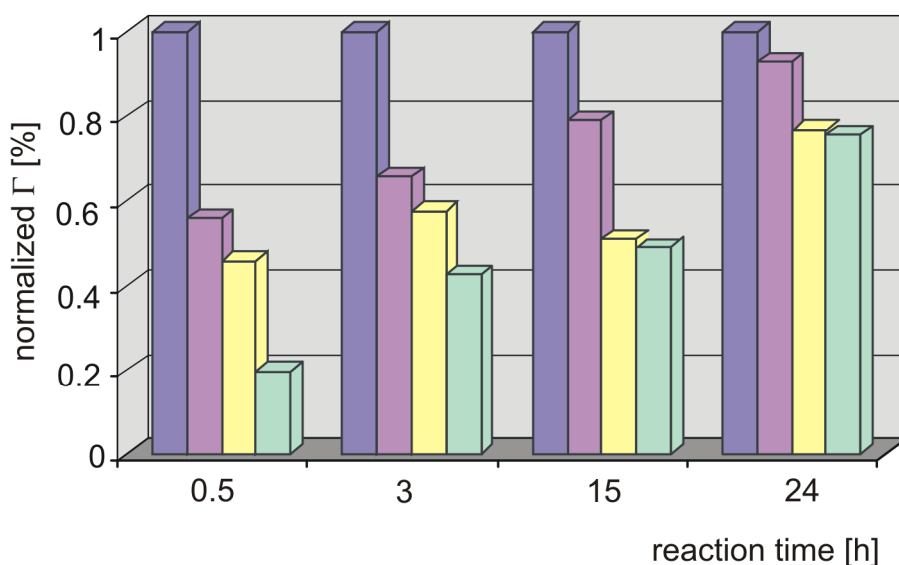


Figure 3.21. Influence of the surface reaction time on the relative stability towards forced desorption using compound **17**:

■ after synthesis, ■ 1 d in MeCN, ■ 1 d in MeCN + 1 h in EtOH/H₂O, ■ 1 d in MeCN + 1 d in EtOH/H₂O,

In figure 3.22 the tetrabromide **18** (phenyl-type viologen) is shown that was used as modifier. This sequence shows the growth of the surface concentration as a function of the reaction time (calculated from absorbance at 440 nm in LiClO₄/MeCN using $\epsilon = 29000$). The electrodes show a fast loss upon accelerated aging experiments (figure 3.23).

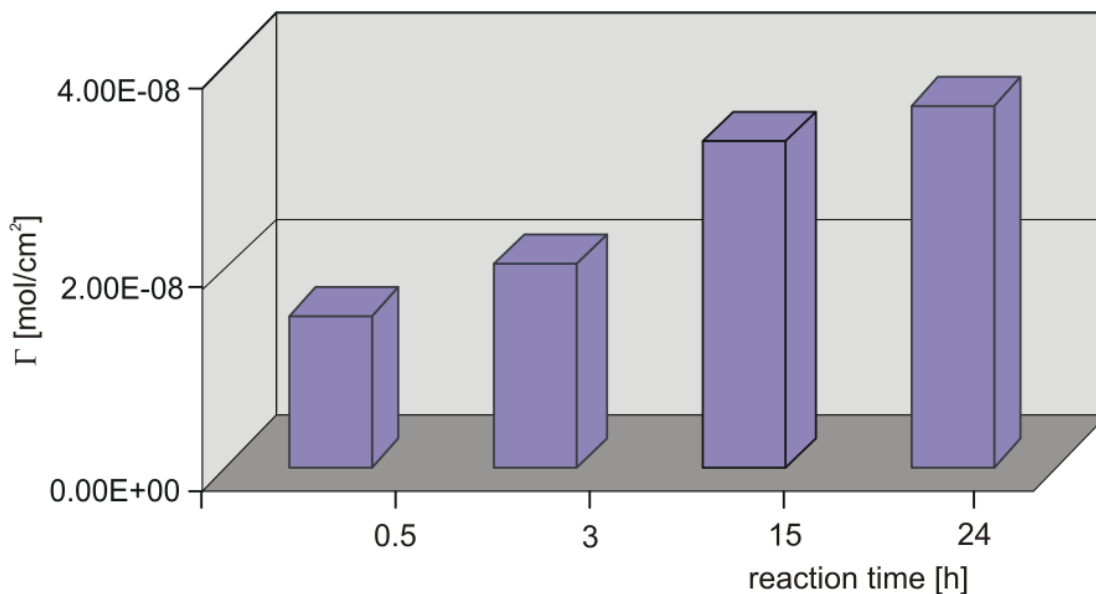


Figure 3.22. Influence of the surface reaction time of compound **18** on the surface concentration

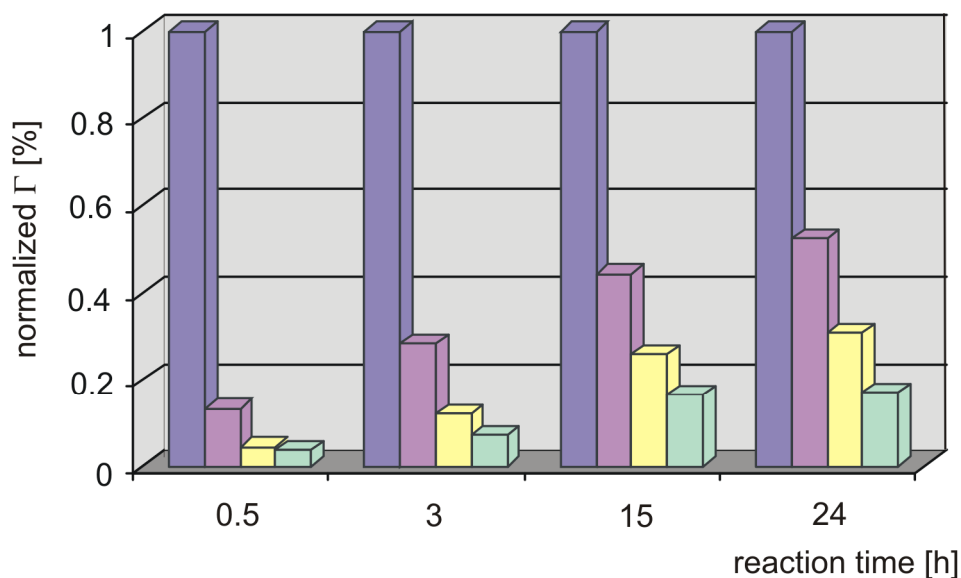


Figure 3.23. Influence of the surface reaction time on the relative stability towards forced desorption using compound **18**:

■ after synthesis, ■ 1 d in MeCN, ■ 1 d in MeCN + 1 h in EtOH/H₂O, ■ 1 d in MeCN + 1 d in EtOH/H₂O,

Finally, the resulting surface concentrations for the mono-bromide **22** treatment are shown in figure 3.24 (as calculated from absorbance at 735 nm in LiClO₄/MeCN using $\epsilon = 4122$) with the corresponding forced desorption in figure 3.25. Almost complete loss is observed.

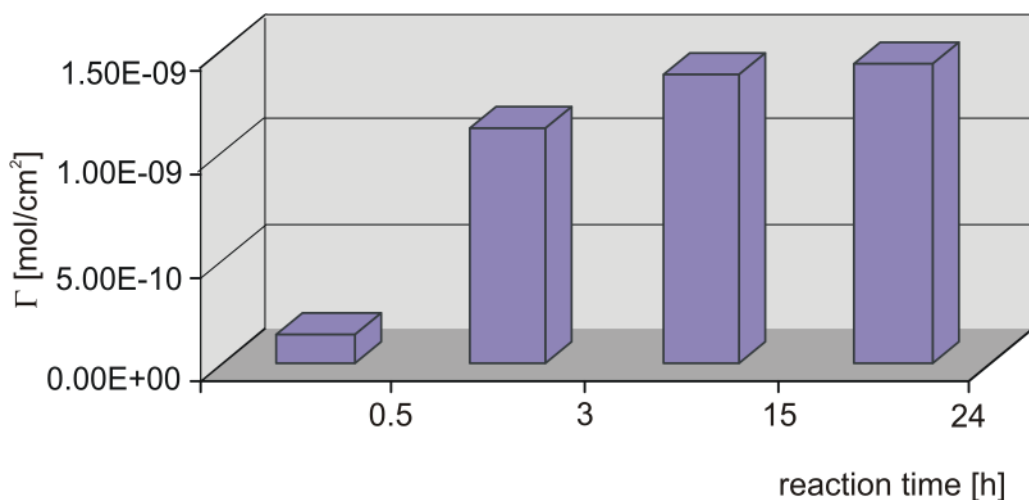


Figure 3.24. Influence of the reaction time of compound **22** on the surface concentration

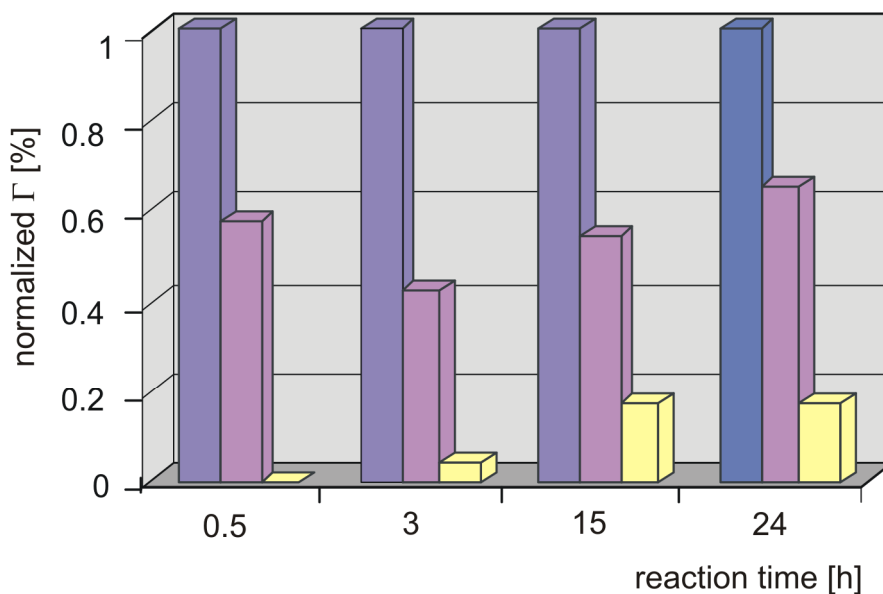


Figure 3.25. Influence of the surface reaction time on the relative stability towards forced desorption using compound **22**:
 ■ after synthesis, ■ 1 d in MeCN, ■ 1 d in MeCN + 1 h in EtOH/H₂O,

Thus, the undesirable side reaction of some of the benzylic or phenylic viologen bromides consists either of a reaction with the surface or of a polymerization reaction. This reaction needs to be controlled in a better way, because they tend to reduce the contrast ratio of printed images. The “white” regions are also collared (ca. 15% intensity). An effective method of suppression is described in the following chapters.

3.3.1.3. Why repellents?

Above I mentioned the problem that the white surfaces resulting from an ink-jetted electrochromic picture (using e.g. **8** in figure 3.26), that is cross-linked with a viologen compound such as **14** (figure 3.26), are slightly bluish (see also the pictures of the zebra test image chapter 3.3.1.2). This phenomenon is probably due to an unknown type of adsorption of **14** (or other viologen precursors) to the naked TiO_2 surface. It is graphically shown in figure 3.26 (inset 1 and 3). Therefore, I have tried to cover the white surfaces with different repellent compounds. The repellent compounds are printed parallel with the viologen as shown in figure 3.26, inset 2 and 4. Their task is to prevent adsorption of **14** onto the surface and we expected a better contrast as schematically shown in figure 3.26 (inset 4) as compared to (inset 3).

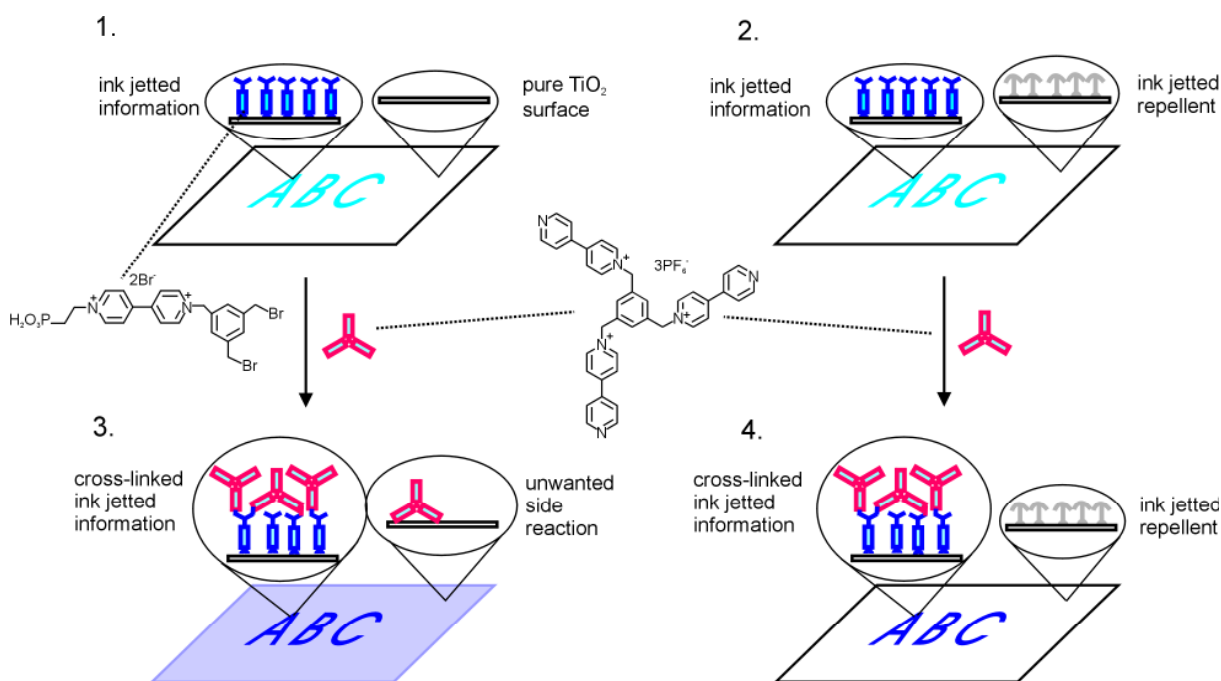
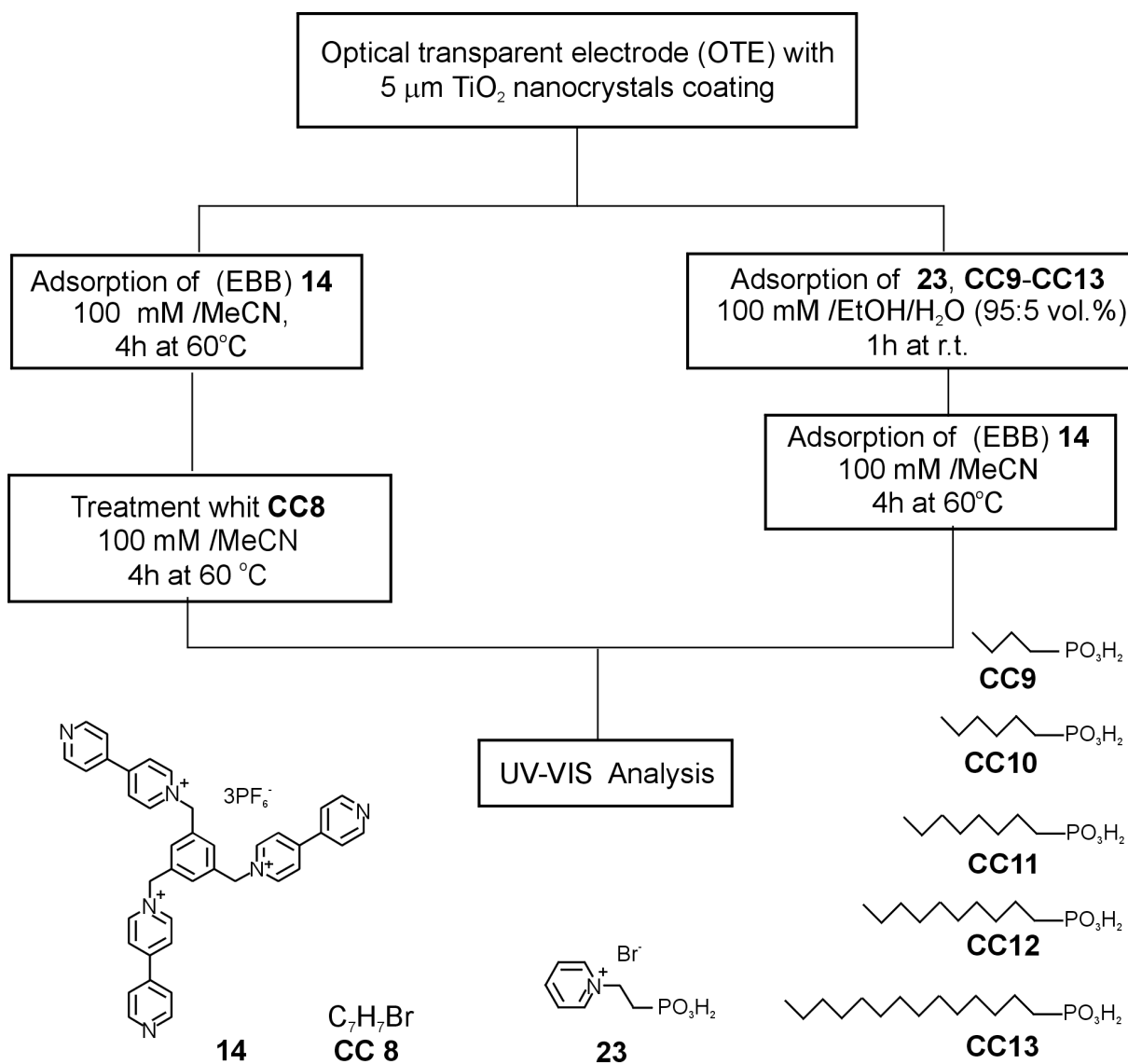


Figure 3.26. Suppression of viologen attachment on "white" areas

The influence of six potential repellent compounds was studied. TiO₂ electrodes have been prepared according to the protocol in scheme 3.5.



Scheme 3.5. Reaction sequence TiO₂ with using six different masks **23**, **CC9-CC13**

The structure of the repellents is shown in figure 3.27. One type consists of alkane phosphonates with different alkyl chain length. These compounds are supposed to build up a self assembled monolayer (SAM) on the jetted areas. If the SAM is tight for a charged compound such as **14** (used in the cascade reaction) I may get none of the undesired colouration within the white areas. Another approach is performed by the use of compound **23**, a cationic pyridinium compound equipped with an

anchoring functionality. This compound should repel the cationic cross-linking compound **14** due to unfavorable electrostatic interactions.

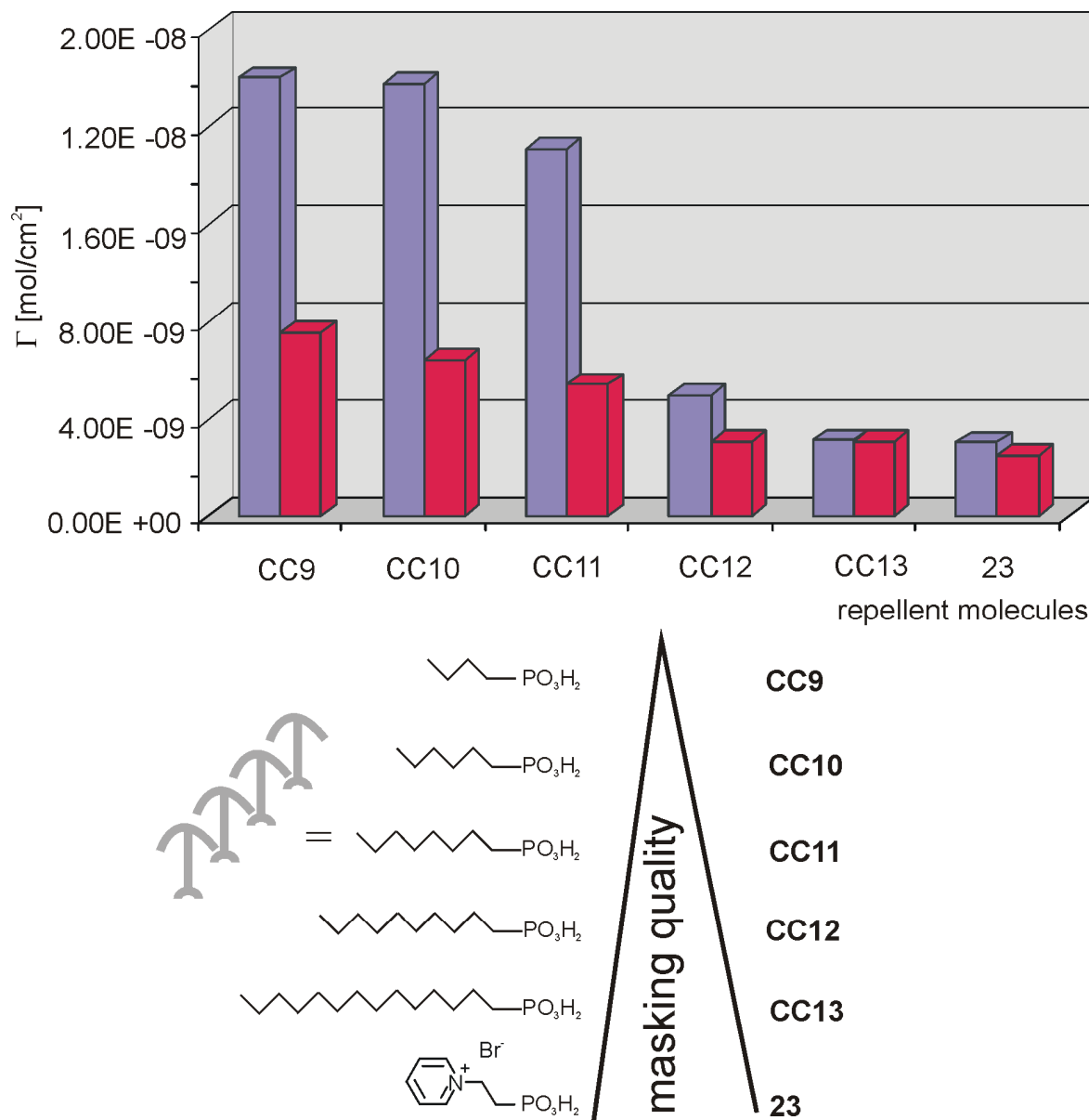


Figure 3.27. Influence of six repellent molecules a reaction sequence (**14-CC8**) on TiO₂
■ after synthesis, ■ 2' minutes in EtOH/H₂O (1:1 vol.%)

The results of these studies are presented in figure 3.28. Here, we compare the surface concentration of viologen chromophores anchored traditionally on compound **8** (E-**8-14-CC8**), with the un-masked (and unwanted) surface concentration of a plate without **8** (E-**14-CC8**) and those obtained with different repellents. Definitely, the unwanted absorption is drastically reduced in all masked cases.

The efficiency of masking can be correlated with the molecular structure of the masking compound as shown in figure 3.28. With the straight chain alkyl phosphonates the masking efficiency (= low surface concentration) grows with the length of the alkyl chain. However, the “short” anchored pyridinium compound is as efficient as the C₁₄-alkyl phosphonate probably because of the build-in repulsion of cations. Interestingly a much higher part of “loosely”-hold chromophores can be washed off in case of short alkyl phosphonates.

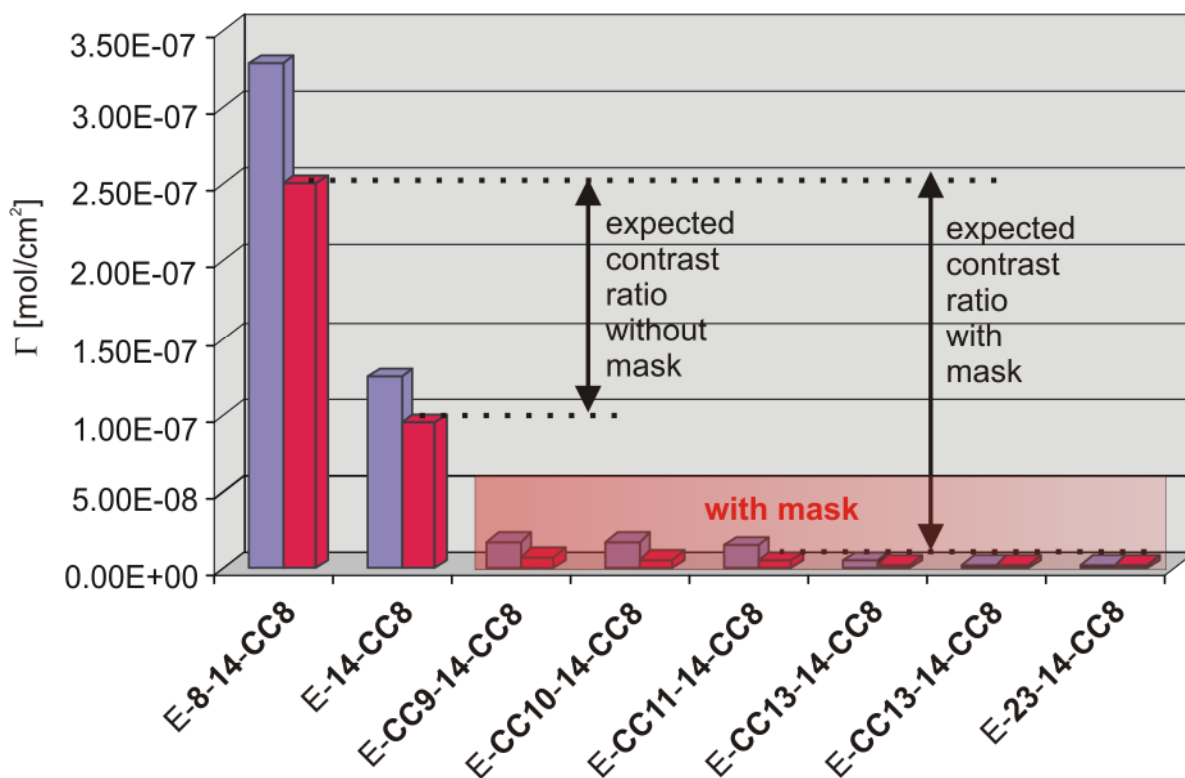


Figure 3.28. Quality of masking using different repellents under cascade synthesis conditions
 ■ after synthesis, ■ 2' minutes in EtOH/H₂O (1:1 vol.%)

In conclusion, good repellents are long-chain alkyl phosphonic acids **CC9-CC13** or pyridinium ethyl phosphonic acid **23**. The beneficial effect of such a treatment is documented in table 3.2.

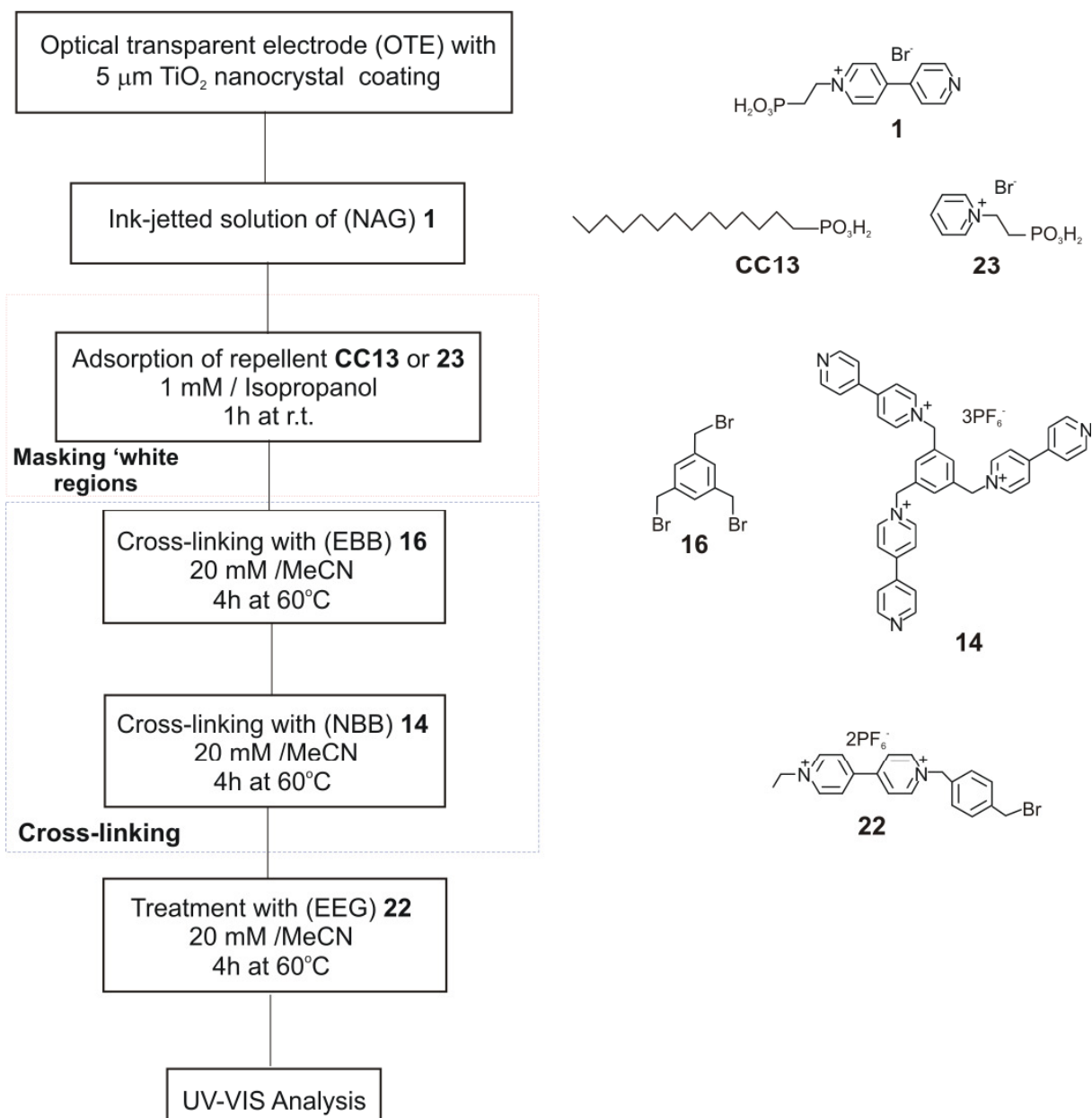
Monomer sequence in cascade reaction	Surface concentration Γ [mol·cm ⁻²] x 10 ⁻⁷
E-14-CC8	2.9 [e]
E-23-14-CC8	0.10 [e]
E-CC9-14-CC8	0.30 [e]
E-CC12-14-CC8	0.13 [e]
E-CC13-14-CC8	0.13 [e]

[e] 2 min. in EtOH/H₂O (1:1)

Table 3.2 Repellents and adsorption of the viologens in cascade reaction. Γ [mol·cm⁻²] calculated from UV-VIS absorption and desorption measurements at 740 nm using $\epsilon=3.20 \cdot 10^3$ and at 560 nm using $\epsilon=1.82 \cdot 10^4$.

3.3.1.4. Masking experiments on ink-jetted electrochromic pictures

Cross-linking an electrochromic print by cascade reactions stabilizes the picture towards lateral diffusion and loss of information. In previous chapters (3.3.1.1 and 3.3.1.2) I have mentioned problems that arise when one is using a reaction cascade on an ink-jetted anchored precursor viologen. The problem is that the “white regions”, i.e. those without jetted viologen anchor still turn violet when a cascade reaction is performed on the plate. In the last chapter (3.3.1.3), a study to circumvent that problem was presented, using different 'repellent compounds' like alkyl phosphonates and cationic pyridinium salts equipped with anchoring groups. I have now applied this technique on ink-jetted pictures.



The electrode was washed in MeCN for 10 minutes, prior to the next reaction step

Scheme 3.6. Procedure for the preparation of electrochromic pictures with chromophores using the repellent technique

TiO_2 electrodes were treated according to the procedure shown in scheme 3.6. I have applied “the best conditions” that have been worked out and presented in preliminary experiment. The results are shown in figure 3.29.

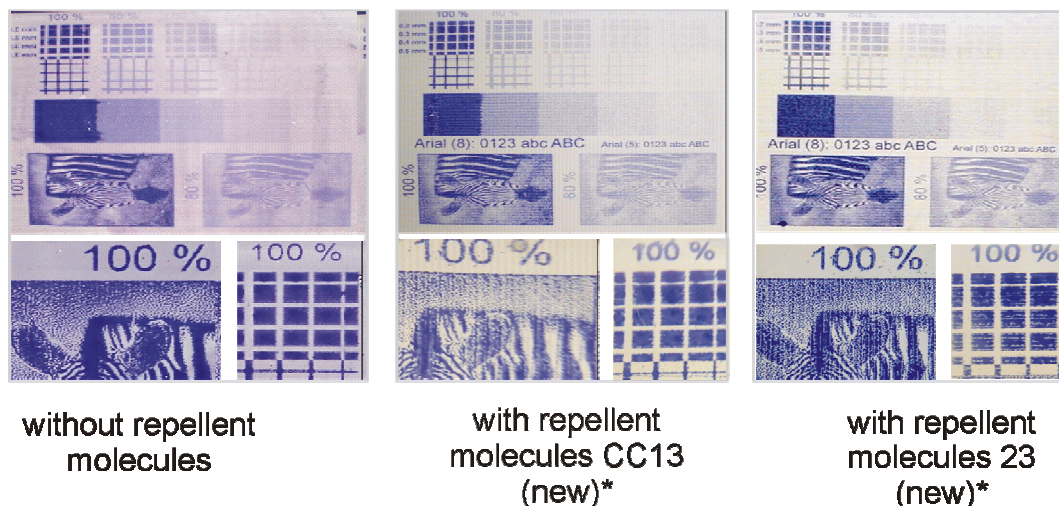


Figure 3.29. Electrochromic picture prepared by cascade reactions with and without repellent molecules
** printed with partials clogged nozzles*

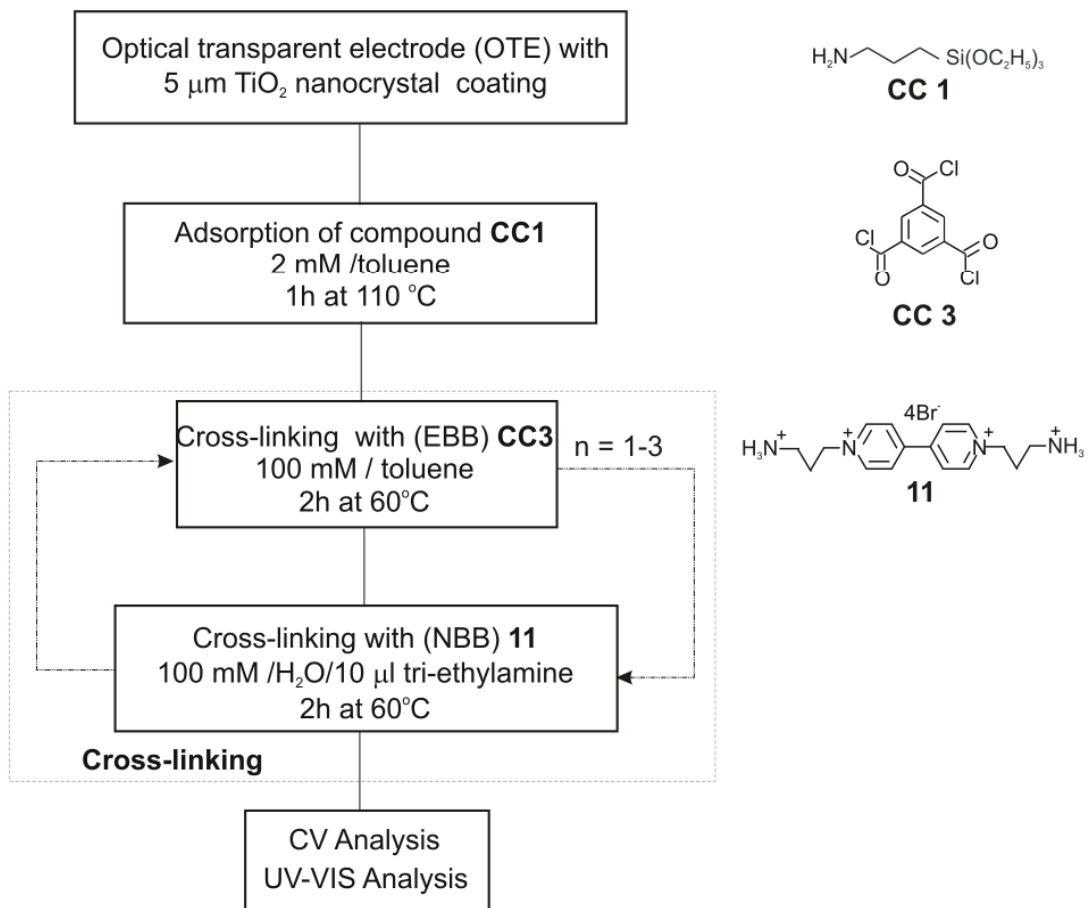
On the left is presented the state of the art of the cross-linked electrode without repellent (figure 3.29 a). One can easily see the violet color touch in the “white regions” in the middle (figure 3.39 b). On the right (c) the electrochromic pictures are presented, obtained if a repellent is used for the white regions, either an alkyl phosphonate or the pyridinium phosphonate. Significantly less colored white regions are obtained. It should be pointed out that the print quality of pictures b) and c) is bad because some nozzles of the printer did not work. However, this is usually not a problem.

In conclusion, “white regions” come out much better in ink-jetted electrochromic prints after cross-linking the electrochromophore by cascade reactions if a repellent compound is used. This can be either a mono-pyridinium phosphonate or an alkyl phosphonate.

3.3.2. Cross-linking by condensation of a carboxylic halide and an amine via amide bond formation

In chapter 3.3.1 I have introduced triethoxy-amino alkyl silyl (**CC1** and **CC2**) compounds as new anchors for the TiO_2 surface. The bond formation occurred between the viologen compound **14** and tris bromomethyl benzene **16**. Now the formation of an amide bond formation between the amino alkyl silyl compounds **CC1**

and bis- amino- alkyl viologen **11** using trimesic acid chlorides **CC3** was studied. The reaction sequence is shown in figure 3.30 and in the protocol in scheme 3.7.



The electrode was washed with pure solvent (toluene and water, respectively) and drying in argon, prior to the next reaction step

Scheme 3.7. Cascade reaction on TiO_2 using a new amide type bond formation

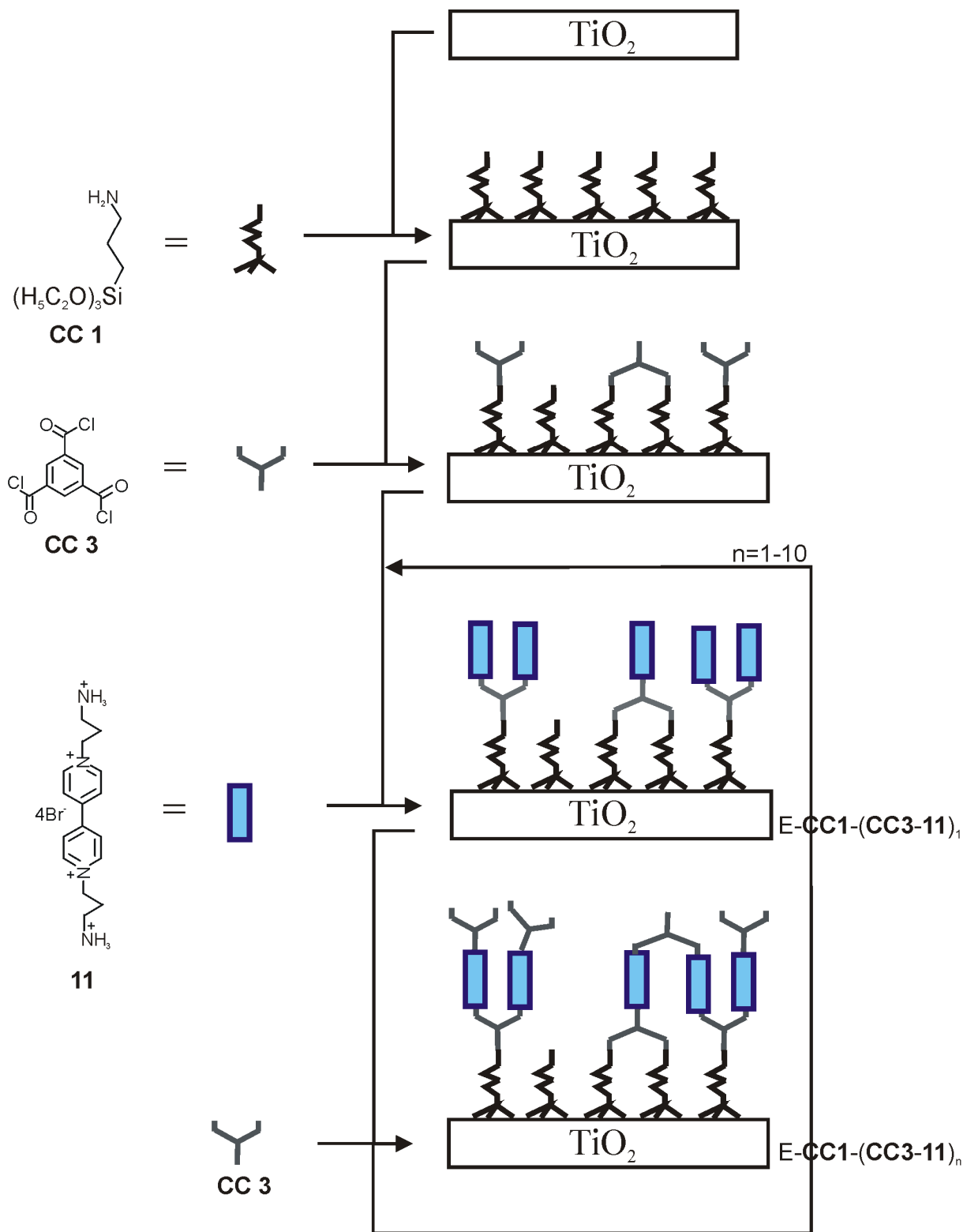
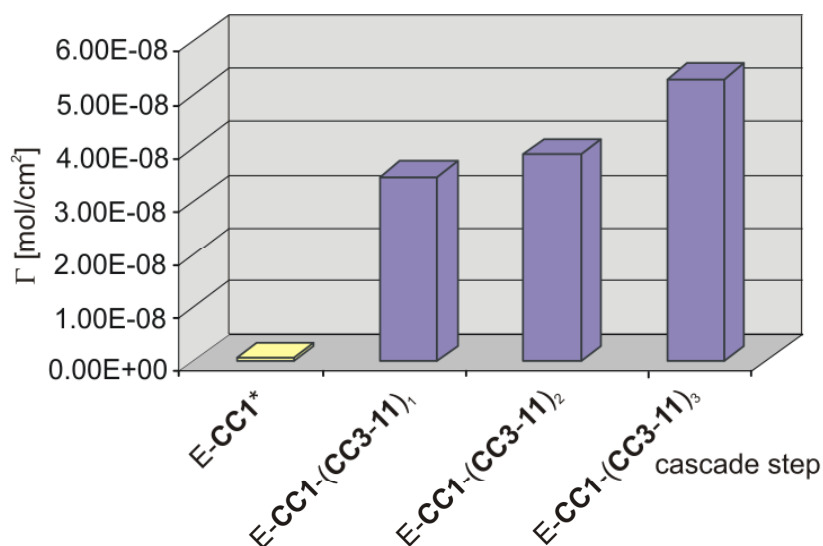


Figure 3.30. Cascade reactions on TiO_2 using a new amide type bond formation



*CC1 3-amino-propyltriethoxysilan with ferrocenyl carboxylic acid fluoride

Figure 3.31. Influence of cascade step on surface concentration using a new amide type bond formation

The results of the cascade reactions are shown in figure 3.32. The amount of absorption or surface concentrations are comparable with those reported in the case using tris- bromomethyl benzene **16** and an S_N2 type substitution reaction with the same O-Si-anchor. The switching kinetics of these electrodes is extremely slow (minutes to hours), especially with many cascade steps. One may improve this unfavourable kinetics by quarternization of non-alkylated amino functions with alkylating agent. Absorbance grows linearly with the cascade steps up to ca. 5 steps, and then it flattens out (figure 3.32).

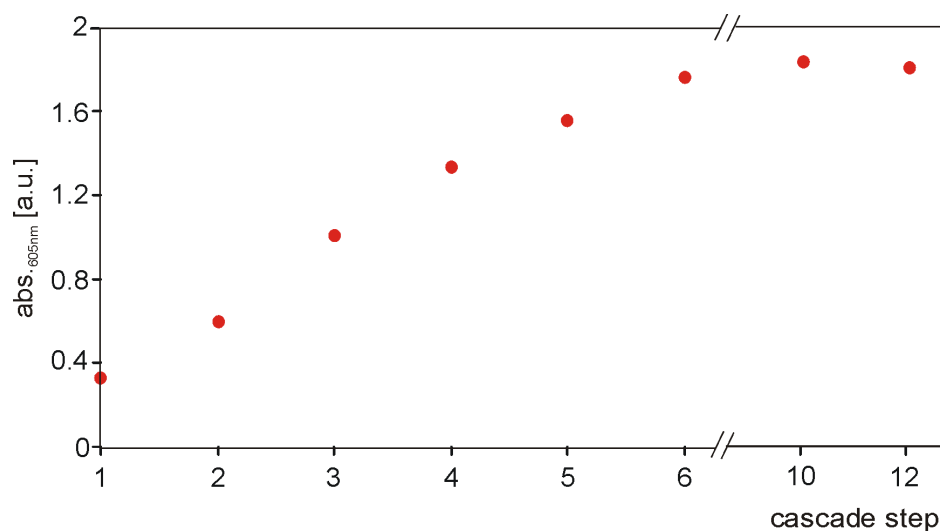
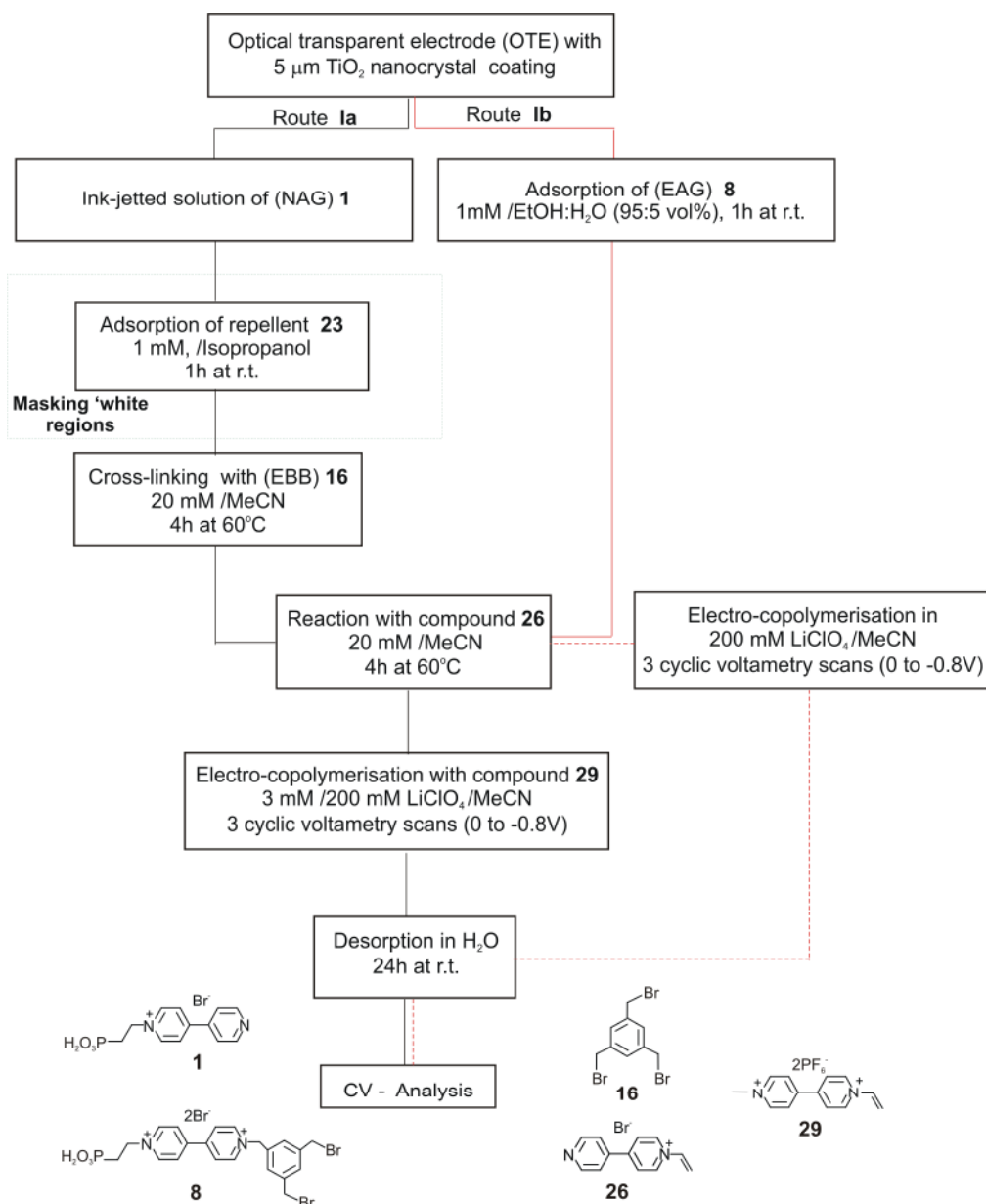


Figure 3.32. Influence of the cascade reaction number's on the absorbance using a new amide type bond formation, $t_{\text{synthesis}} = 2$ minutes

Amide-type bond formation can be used instead of a substitution reaction in the cascade reaction; however, the resulting electrochromic response is slow.

3.3.3. Cross-linking by electropolymerization of pending vinyl groups in redox active species after monolayer formation

Using a printable ink containing an electrochromic compound with a TiO₂ anchor (i.e. **8**) and a reductively polymerizable end group, it is possible to stabilize the monomolecular electrochromic layer after printing by reductive cathodically-induced electrocopolymerization.



Scheme 3.8. Two ways of the preparation of the surface polymerisable viologens

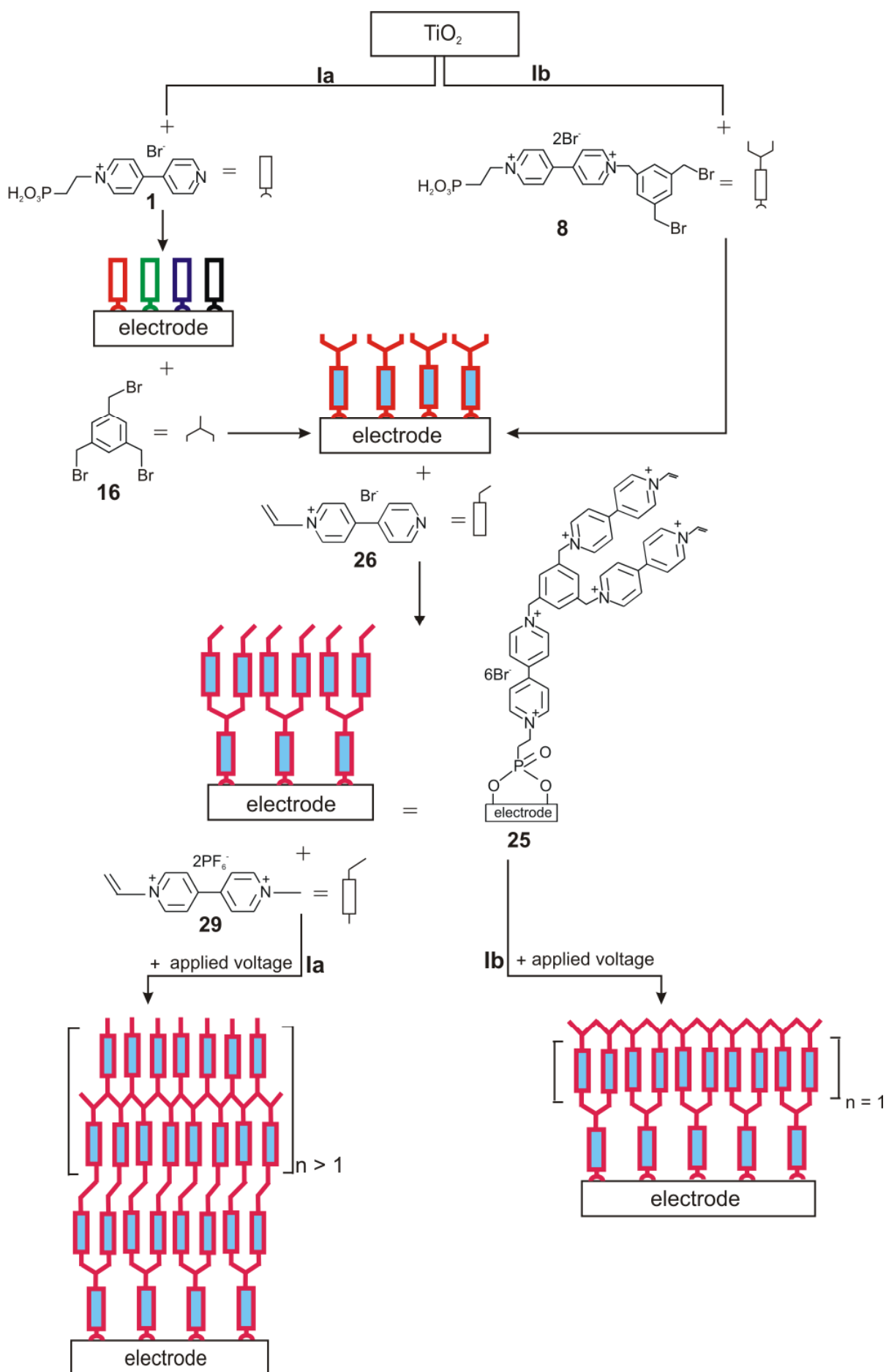


Figure 3.33. Two ways of the preparation of the surface - polymerizable viologens

Figure 3.33 shows a schematic representation of a typical electrocopolymerization reaction of pending vinyl group of the monolayer vinyl electrochromophore thereof on an electrode and vinyl end groups into an electrolyte by applied voltage. The TiO₂ electrodes were printed with the anchoring electrophilic compound **8** at 1 mM and treated with vinyl-bipyridine **26** at 0.02M to produce the surface-confined compound E-**25** (scheme 3.8). The surface confined compound was polymerized by application of a negative electrode potential in acetonitrile / 0.2 M LiClO₄ (route I) in figure 3.33) using ca. 3 cyclic voltammetry scans (0 to – 0.8 V vs. AgAgCl).

Another approach (figure 3.34, route II) comprises the cyclisation of the E-**25** electrode in the same potential range, but now in presence of methylvinyl viologen **29** (3 mM in acetonitrile (0.2M LiClO₄)). It is expected that **29** is co-polymerizing with E-**25** when the radical anion on E-**25** has developed, thus leading to an anchored multi-layer (figure 3.33), similar to our earlier described cascade crosslinking reaction. In preliminary experiments we have studied the new procedure on plane TiO₂ electrodes as well as on ink-jetted structures. We found an increased stability for both approaches (route I and II), i.e. we found the Zebra picture after accelerated aging (one day in water) being still present (figure 3.34).

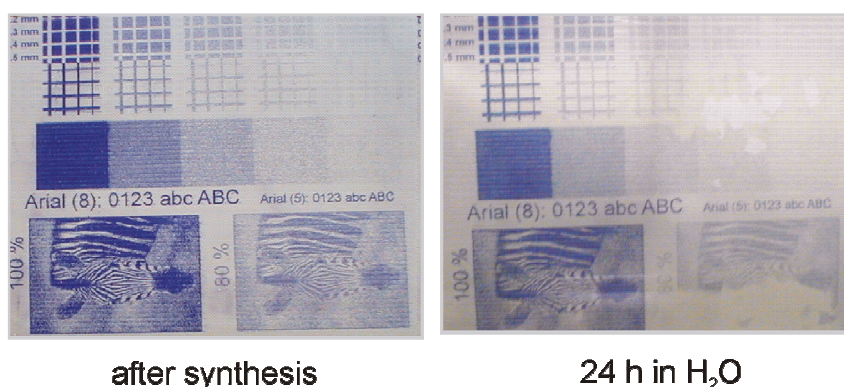


Figure 3.34. Electrode directly after synthesis and after an accelerated aging process. Graphical information prepared according route Ia scheme 3.8

The new electro-polymerization of vinyl-terminated viologens on TiO₂ may be an interesting way to stabilize the compounds. Preliminary results indicate that the stabilization towards accelerated aging (i.e. washing) is similar to cascade-type cross-linked viologens, however, electrocopolymerization occurs in ink-jetted as well as in 'white regions' if a vinyl viologen is present in solution (copolymerization).

3.4. Application: Ink-jetted switchable electrochromic image

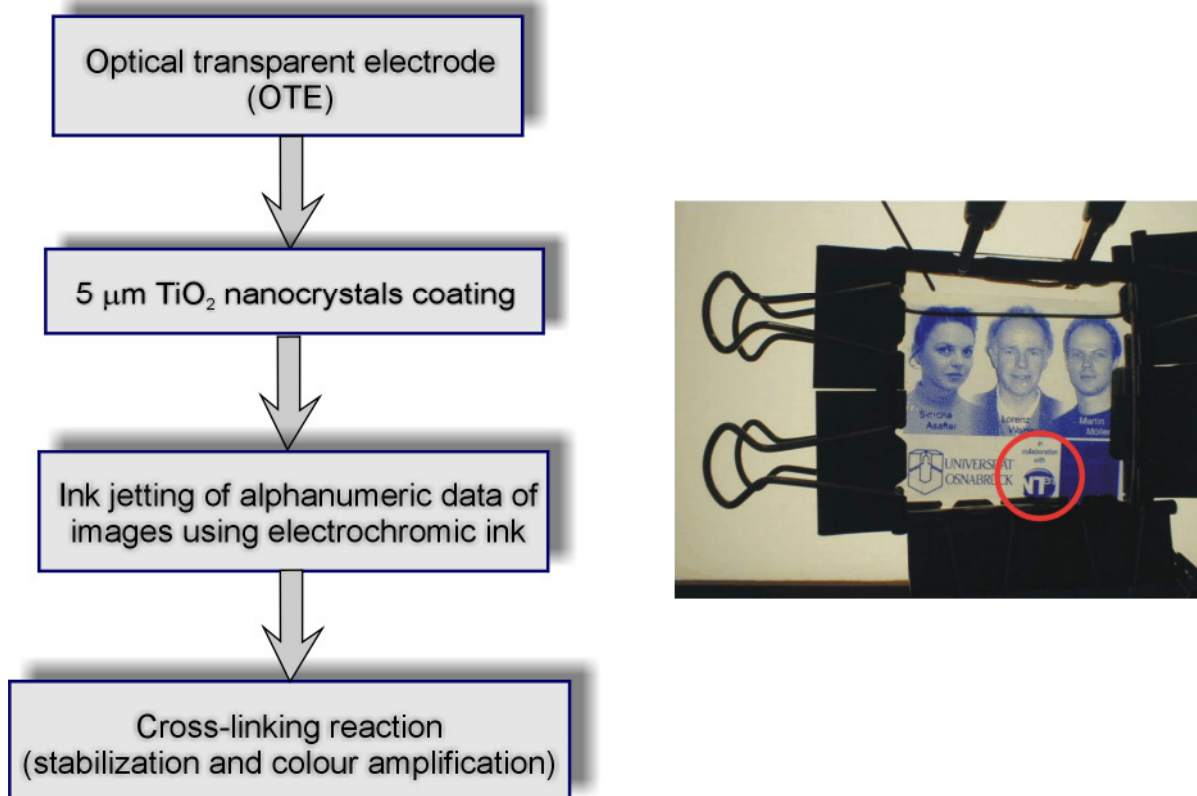


Figure 3.35. 5 x 5 cm working electrode

3.4.1. TiO_2 coating glass

The nanostructured TiO_2 film is obtained by the doctor blade method on conducting glass. The colloidal suspension of TiO_2 was spread onto a piece of conducting glass (FTO) with scotch tape on the edges to shield the conducting layer in a narrow area from the non-conducting TiO_2 and to set the height between the FTO substrate and the glass rod used to spread the suspension. After approximately three minutes of drying, the electrodes were heated at $450^\circ C$ for 30 minutes leading to well-crystallized porous anatase TiO_2 film of about $5 \mu m$ of thickness.

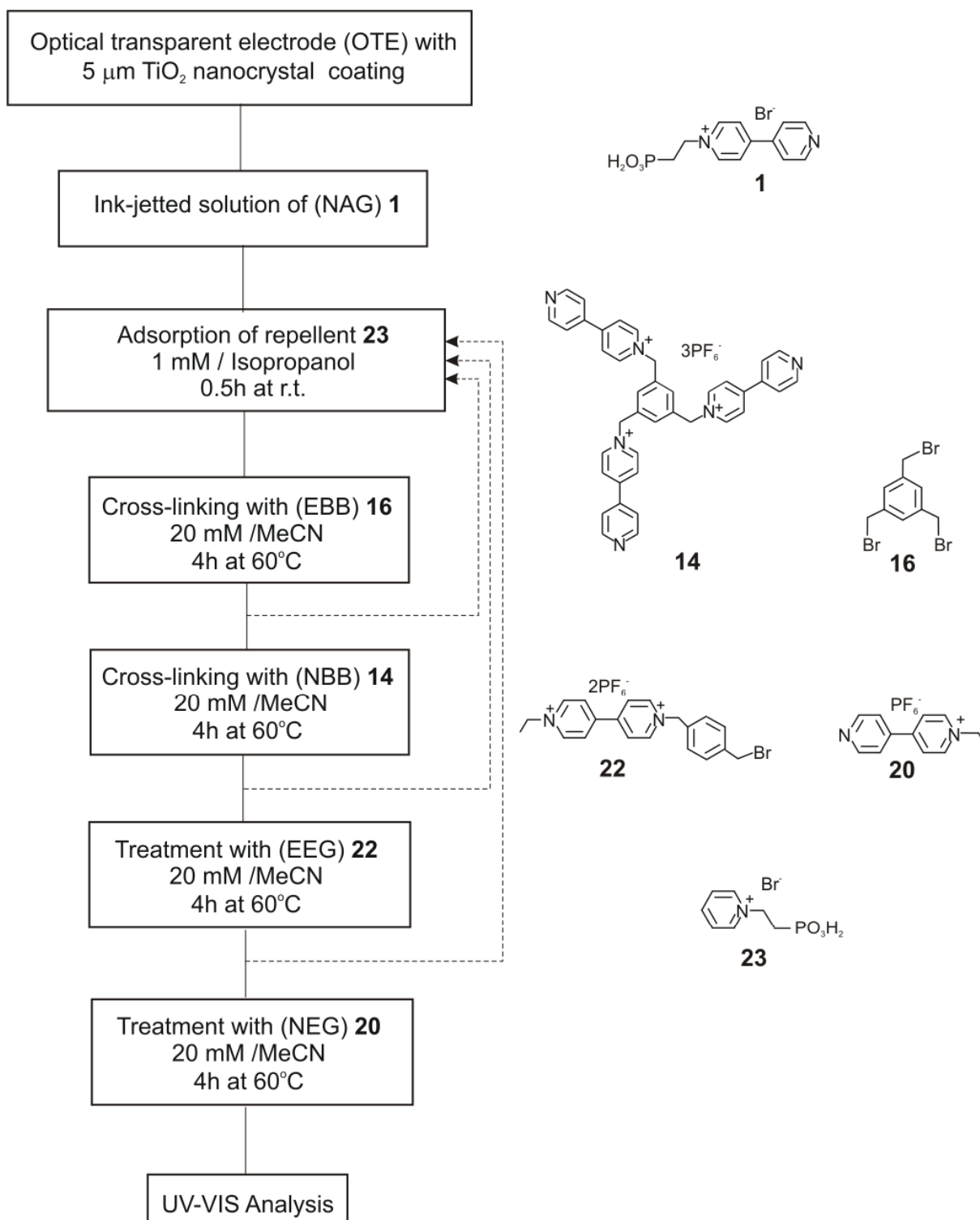
3.4.2. Ink-jetted electrochromic pictures

The electrochromic picture was prepared using a personal computer (PC) and a commercial ink jet CD printer [88]. The caddy and the spacing of the printer were adapted to handle the TiO₂/OTE/glass substrate, and the ink nozzles of the printer head were equipped with vessels for electrochromic ink instead of the original cartridges. The electrochromic ink consists of a viologen or a precursor equipped with a phosphonic acid anchoring group and a further nucleophile (**1**) or electrophile (**8**) as functional group (NAG, EAG see chapter 1, figure 1.1). The concentration of the ink is 100 mM resulting in 1.3×10^{-7} mol/cm² of anchoring viologen; provided that the volume jetted for a 100 % coloured area is 1.3 μl / cm². The solvent and its ingredients are optimized for fine droplet formation. The images received directly after ink jetting were checked for their quality (absorbance, switching time and stability) [88].

3.4.3. Procedure for the preparation of electrochromic pictures

The electrochromic picture on the nanostructured TiO₂ film was obtained according to a literature procedure [88].

The electrochromophore for example may be provided with a nucleophilic anchoring (NAG) or an electrophilic anchoring group (EAG). In the case of an NAG electrochromophore once applied, it may be treated alternatively with electrophilic building blocks (EBB) and nucleophilic building blocks (NBB). Washing may take place between the steps. The treatment is terminated by a nucleophilic end group (NEG). In the case where an EAG is employed, the cross-linking may be built firstly treating the deposited electrochromophore with NBB and alternatively with EBB. In this case the cross-linking reaction can be terminated with an electrophilic end group (EEG) (scheme 3.9).



The electrode was washed in MeCN for 10 minutes, prior to the next reaction step

Scheme 3.9. Procedure for the preparation of electrochromic pictures

3.4.4. Optimization of the solvent electrolyte system

3.4.4.1. Square voltage excitation of three- and two-electrode systems

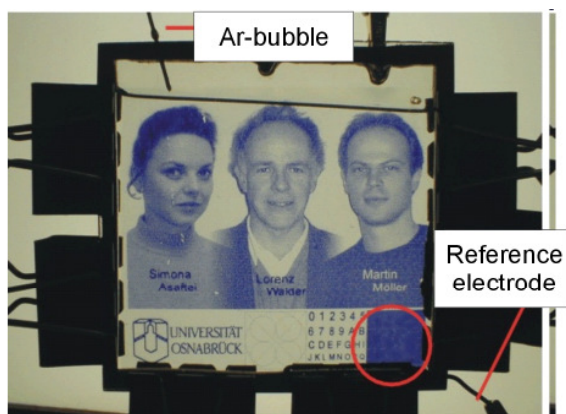


Figure 3.36. Clamp-closed cell 7 x 7 cm (three electrode arrangement, 1M LiClO₄ /ethylen glycol) *the square (red circle) was used for spectroscopic control of the absorption, as the blank was used the electrode in oxidized state*

Figure 3.37 shows the absorption of the working electrode (figure 3.36) in the 3-electrode system using an ITO-glass as counter electrode and a silver wire as reference electrode as a function of the applied potential. The working electrode was prepared according to the cross-linking procedure in scheme 3.9.

The absorbance vs. voltage, figure 3.37, shows a typical Nernstian behavior and a maximum of absorbance at 560 nm of ca. 1.35, i.e. a good dynamic behavior. The absorbance at 607 nm is that showing a little contribution of pymerization, whereas that at 940 nm shows exclusively pymerization.

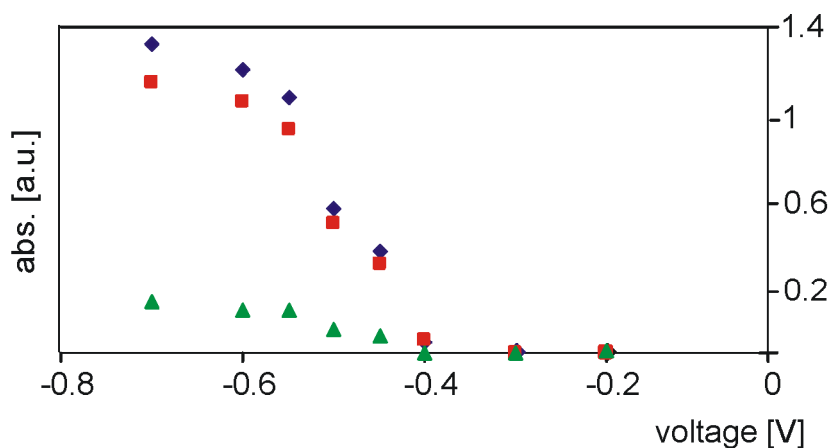


Figure 3.37. Absorption in the three electrode system after equilibration
◆ abs. 560 nm, ■ abs. 607 nm, ▲ abs. 940 nm

Figure 3.38 show the absorbance responses of the three electrode system with 2, 5, 10 and 20-second square voltage steps. As seen from the absorbance vs. time plots, the system is too slow to follow the 2-second excitation. With 5-second excitation the absorbance changes are almost doubled as compared to the 2-second excitation.

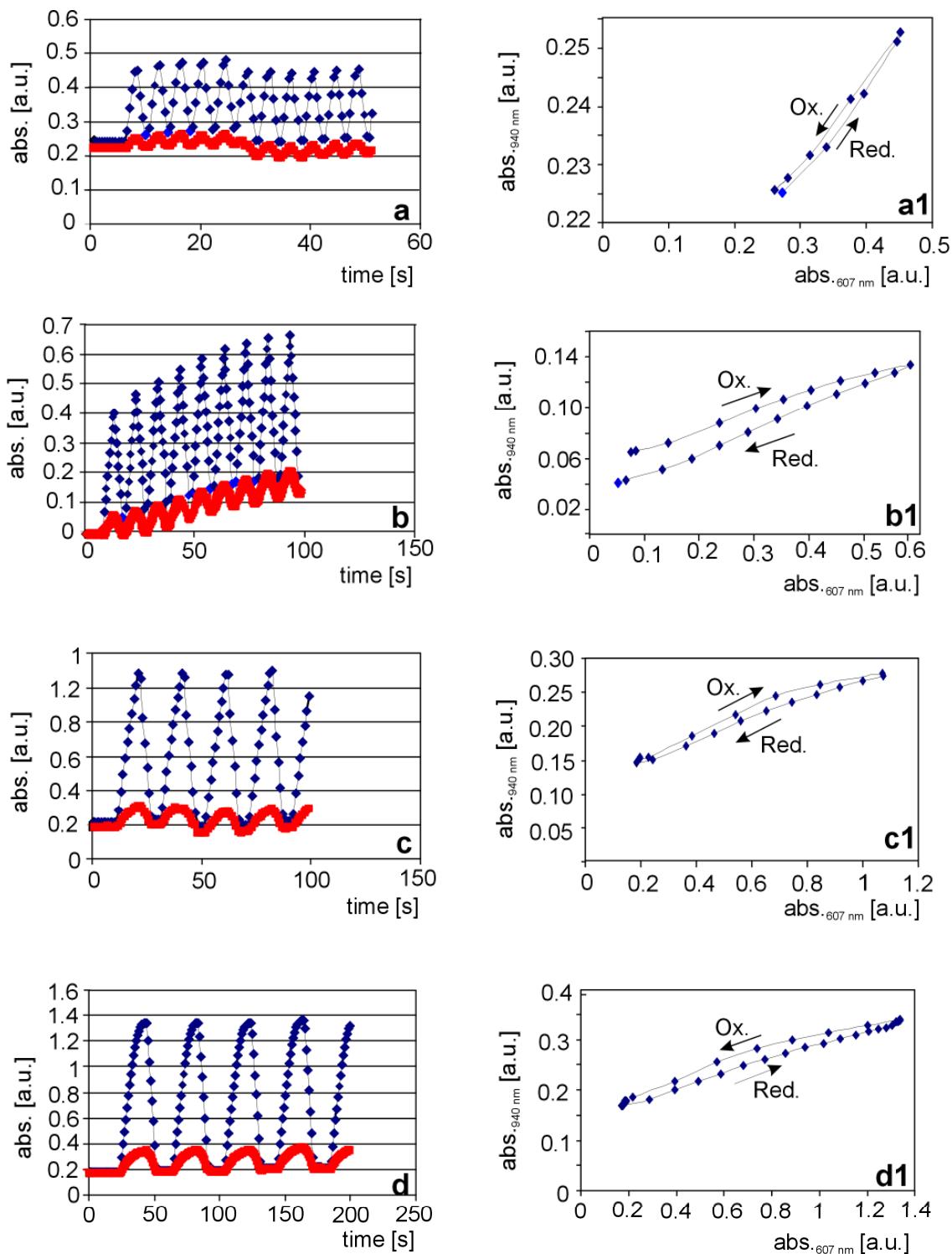


Figure 3.38. Absorbance responses of a three-electrode system with 2 (a), 5(b), 10 (c) and 20 (d) seconds square voltage steps (0 to -0.7V), \blacklozenge 607 nm and \blacksquare 940 nm
a1, b1, c1, d1 reduction-oxidation hysteresis

With a 10-second excitation (figure 3.38 c) the absorbance changes grow to approx. 1 at 607 nm and with 20-seconds excitation (figure 3.38 d) an absorbance change of ca. 1.2 is reached.

It is interesting to observe a time-dependent change in the pymerization that results in a hysteresis when the absorbance at 607 nm (slightly influenced by pymerization) is plotted vs. the absorbance at 940 nm (exclusively pymerization). In practice this results in a fast change to blue when the electrode is reduced followed by a slow build-up of the violet tint due to pymerization. When oxidized, first the blue tint disappears and later the violet tint disappears.

Figures 3.39 and 3.40 shows the results of the same measurements but in the closed cell two-electrode system using a CeO_2 counter electrode as described according to literature [88]. In figure 3.39 the absorbance (square) on the right scale of the figure is drawn as a function of the cell voltage. An almost linear increase of the absorbance over approximately one volt under equilibrating conditions is observed. The maximum absorbance is the same as in the three-electrode system (ca. 1.4).

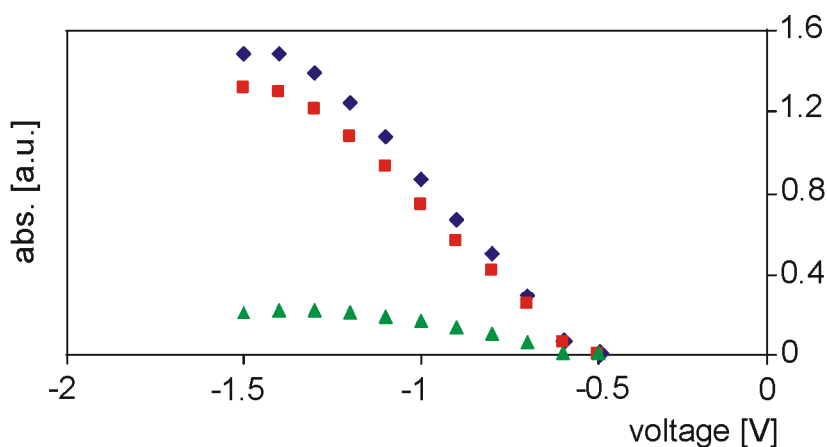


Figure 3.40. Absorption in the two electrode system after equilibration
 ◆ abs. 560 nm, ■ abs. 607 nm, ▲ abs. 940 nm

Figure 3.40 shows again square-voltage excitation responses of the absorbance. Considering the starting absorbances which are not always zero, the dynamic behavior of the two and three electrode systems is very similar. The same hysteresis is observed, i.e. first reduction of the blue part followed by pymerization upon reduction, and the first oxidation of the blue part followed by oxidation of the pymerized part.

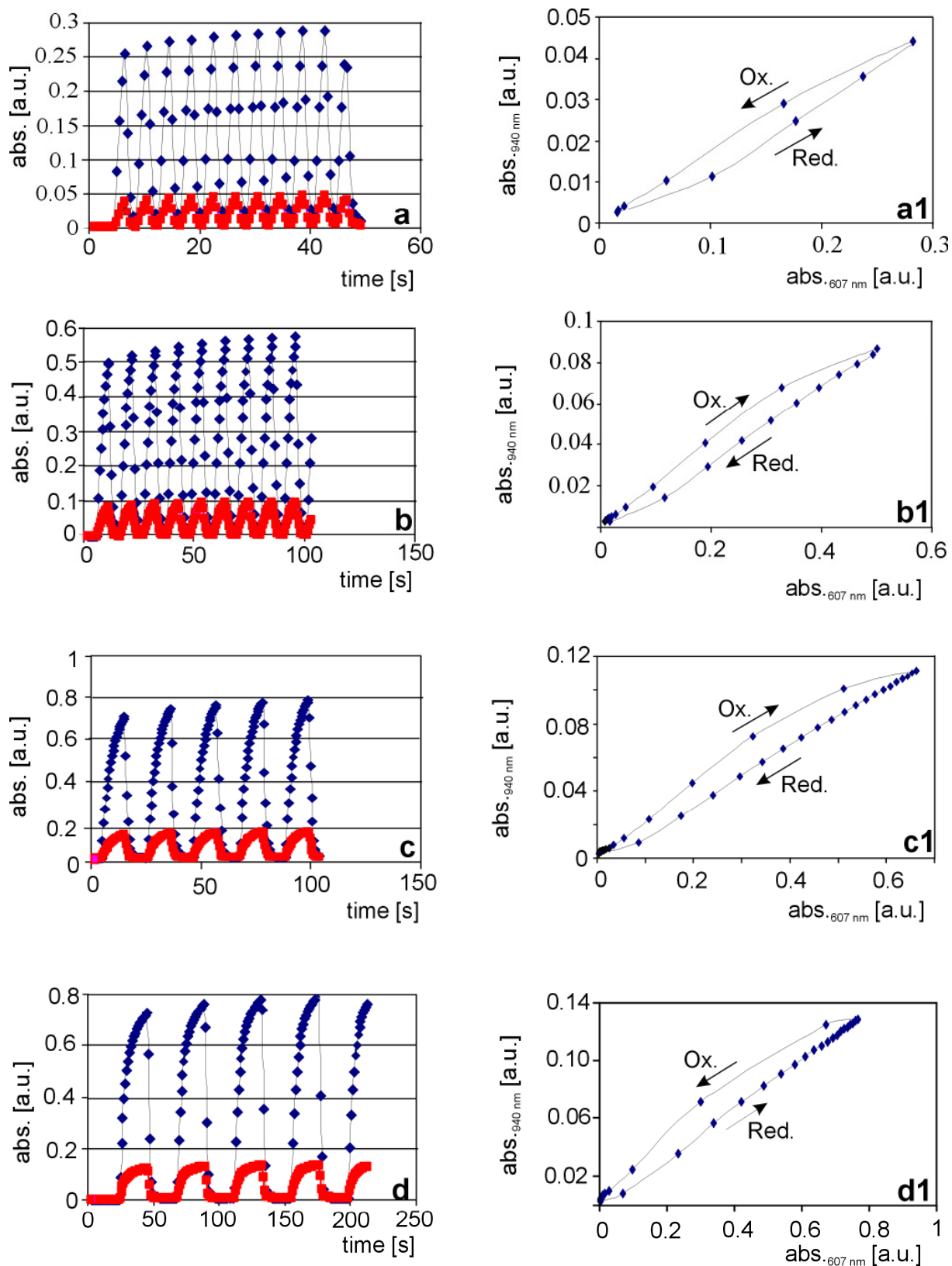
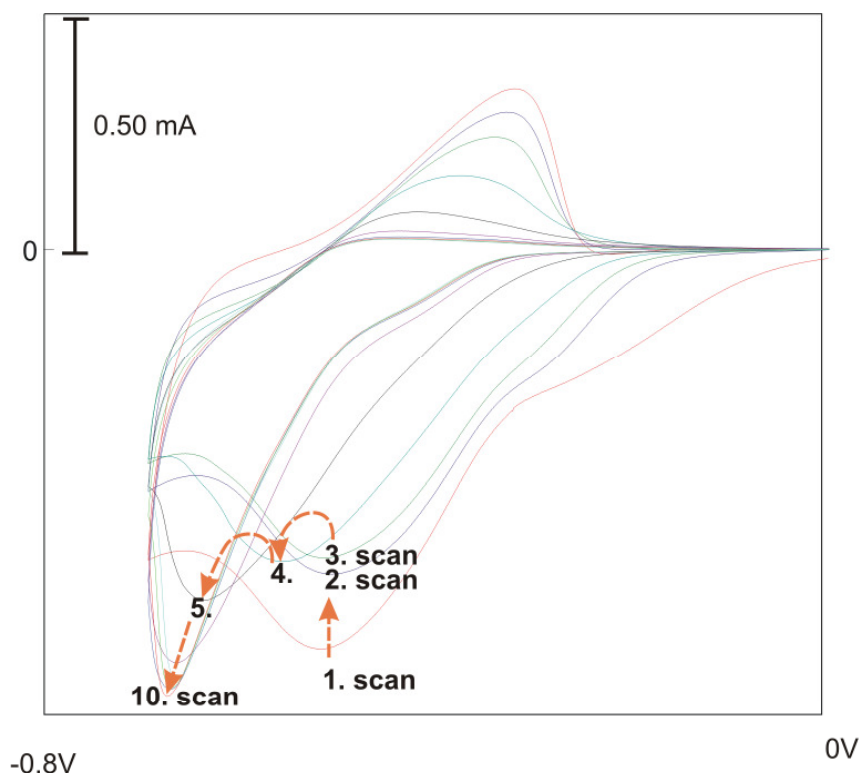


Figure 3.41. Absorbance responses of a two-electrode system with 2 (a), 5(b), 10 (c) and 20 (d) seconds square voltage steps (0 to -1.4V), \blacklozenge 607 nm and \blacksquare 940 nm
a1, b1, c1, d1 reduction-oxidation hysteresis

From the identical behavior of the switching experiment and the equilibration experiment It can be concluded that the amount of the charge present on the counter electrode was sufficient for the experiment as well as that the kinetics are not influenced by the counter electrode.

3.4.4.2. Effects of electrolyte and solvent on the working- and counter electrodes

A series of electrolyte/solvent systems has been studied to find the optimal kinetics. Again we used cross-linked viologens on TiO_2 according to scheme 3.9. Earlier studies have shown the beneficial effect of protons on the reversibility of the electrochromic images. I have studied this phenomenon more intensively now. If a viologen-modified electrode is pretreated by dipping it into a 1 M HCl solution, dried, and then measured in 0.2 M LiClO_4 / MeCN I find reversibility (first scan in the CV of figure 3.41).



**The electrode was dipped in 1 M HCl, dried and then in 0.2M $\text{LiClO}_4/\text{MeCN}$, vs. Ag/AgCl, 20 mV/s measured*

Figure 3.41. Cyclic voltammograms demonstrating the transition from reversibility to irreversibility due to loss of protons at the TiO_2 -surfaces of their cross-linked working electrode* pretreated in 1M HCl

However, after the 3rd scan the cathodic peak moves into the negative direction and after the 10th scan oxidation is no more observed. I attribute this behavior to charge trapping. The relative location of the conduction band edge of the semi-conductor and the viologen reduction potential becomes unfavorable, i.e. the semi-conductor band CB is too negative for an efficient oxidation. This may be due to the fact that benzylic viologens are more positive than alkyl viologens. With HCl pretreatment I obviously protonate the surface but then I loose the protons on the semi-conductor after a few scans, and the viologen oxidation becomes very slow.

In table 3.3 we present a series of experiments using electrolyte solvent systems with different amounts of water or in the presence of different acids in the electrolyte-solvent. Polyethylene glycol proved to be a reasonable solvent only if ca. 50 % water is present. Further addition of HCl improves the kinetics. In pure water the system is reversible, but, of course, there is the danger of H₂ evolution. Water cannot be used for traditional phosphonate monolayers. One would loose the electrochromophore after the first scan in water. Only cross-linked viologens withstand such conditions.

Electrolyte/ solvent	Proton source μl(mg) in 5ml solvent	1x cross-linked				Obs.
		E _{pc} /V	E _{pa} /V	E° /V	Γ mol/cm ² x10 ⁻⁷	
0,2M LP /H ₂ O	H ₂ O	-0.52	-0.40	-0.46	0.74	reversible
0,3 M LiN(SO ₂ CF ₃) ₂ / Glutaronitrile	10 mg toluol p-sulfon acid	-0.49	-0.17	-0.33	1.17	irreversible
0,5M LP/ PEG 200	1% H ₂ O (50μl)	-	-0.29	-	-	irreversible
	2% H ₂ O (100μl)	-	-0.27	-	-	irreversible
	5% H ₂ O (250μl)	-	-0.30	-	-	irreversible
	50% H ₂ O (2500μl)	-0.67	-0.54	-0.60	0.12	irreversible
0,5M LP/PEG 200	37%HCl (25 μl)	-	-	-	-	irreversible
	16% HCl (in 100μl H ₂ O)	-	-0.12	-	-	irreversible
	10% HCl (in 250μl H ₂ O)	-	-0.20	-	-	irreversible
	0.4% HCl (in 2500μl H ₂ O)	-0.59	-0.46	-0.52	0.64	reversible
0,1M LP/TEG- DiMe	1M HCl (500μl)	-0.58	-0.30	-0.44	0.66	reversible

- LP: LiClO₄;
- PEG 200: polyethylene glycol 200;
- TEG-DiMe: tetraethylene glycol dimethyl ether;

Table 3.3. Effects of water or of a proton source in the solvent/electrolyte, scan rate 20 mV/s vs. Ag/AgCl

In table 3.4 we present a series of experiments using different organic, water-free solvents/electrolytes and the cross-linked viologen-modified TiO₂-electrode. Reversibility increases in all solvents with increasing salt concentration. Good results are achieved with: 1M LiClO₄ in ethylene glycol, 0.2 M LiClO₄ in γ -butyrolactone and methoxy propionitrile (1:3), 0.2 M LiClO₄ in γ -butyrolactone and glutaronitrile (1:3).

Electrolyte/solvent	1x cross-linked				Observations
	E _{pc} /V	E _{pa} /V	E° /V	Γ mol/cm ² x10 ⁻⁷	
0,2M LP /MeCN	-0.50	-0.35	-0.42	1.00	slow oxidation
0,3 M LiN(SO ₂ CF ₃) ₂ /Glutaronitrile**	-0.51	-0.16	-0.34	0.77	slow oxidation
0,5M LP/PEG 200*	-	-0.22	-	-	slow oxidation and reuction
1M LP /EG	-0.58	-0.32	-0.45	1.08	very reverible
0,5M LP /EG*	-	-0.19	-	-	slow reduction
0,25M LP /EG*	-	-0.16	-	-	slow reduction
1M LP /TEG-DiMe*	-0.63	-0.24	-0.44	0.69	slow reduction
0,5M LP /TEG-DiMe*	-	-0.25	-	-	slow reduction
0,25M LP /TEG-DiMe*	-	-0.18	-	-	slow reduction
0,2 M LP/ γ BL+G (1:3vol.%)	-0.65	-0.19	-0.42	0.97	reversible
0,2 M LP / γ BL+3MeOPN (1:3vol.%)	-0.55	-0.29	-0.42	1.03	very reversible
0.2LiCl /EG	-0.61	-0.12	-0.35	0.72	reversible

- LP: LiClO₄;
- PEG 200: polyethylene glycol 200
- EG: ethylene glycol;
- TEG-DiMe: tetraethylene glycol dimethyl ether;
- γ -BL+G: γ -butyrolactone and glutaronitrile
- γ -BL+G : γ -butyrolactone and 3- methoxypropyionitrile

* values differ because of partial oxidation – reduction at 20 mV/s or values are small because of charge trapping

Table 3.4. Effects of electrolyte/solvent on the working electrode, scan rate 20 mV/s

Conclusion:



Figure 3.42. Closed electrochromic cell
(CeO₂, counter electrode, 1 M LiClO₄,/ethylen glycol)

We have achieved excellent long-term stability of the high resolution working electrodes using cross linking techniques as described in report 1 to 10. In connection with the ferrocene derivatives-counter electrode we reached convincing dynamics between the bleached and colored state. However, we are not sure if we got the best results with

respect to the electrolyte/solvent system. The stability of the picture is excellent. Figure 3.42 at the bottom of the electrode was checked with a microscope after 6 months for lateral diffusion. No indication of such diffusion was found at this time (see chapter 3.2, figure 3.7).

Chapter 4

Modifications of mesoporous electrode surfaces with ferrocen derivatives

4.1 Poly-ferrocene modification by surface cascade reactions

Ferrocenes have found broad applications as outer sphere redox mediators in solution because of their fast electron transfer rate, their broad range of E° , which is adjusted via substituents attached to the cyclopentadienyl ring system [94, 95] and due to the ease of their synthesis [96].

Attempts to prepare electrode surface confined ferrocenes are numerous and based on SAM and Langmuir Blodgett techniques [97, 98] or on surface confined polymers. The latter comprise polysiloxane-ferrocenes [99], or hydrophobic Nafion gels loaded with ferrocenes [100], or polymers prepared by electropolymerization [93, 101].

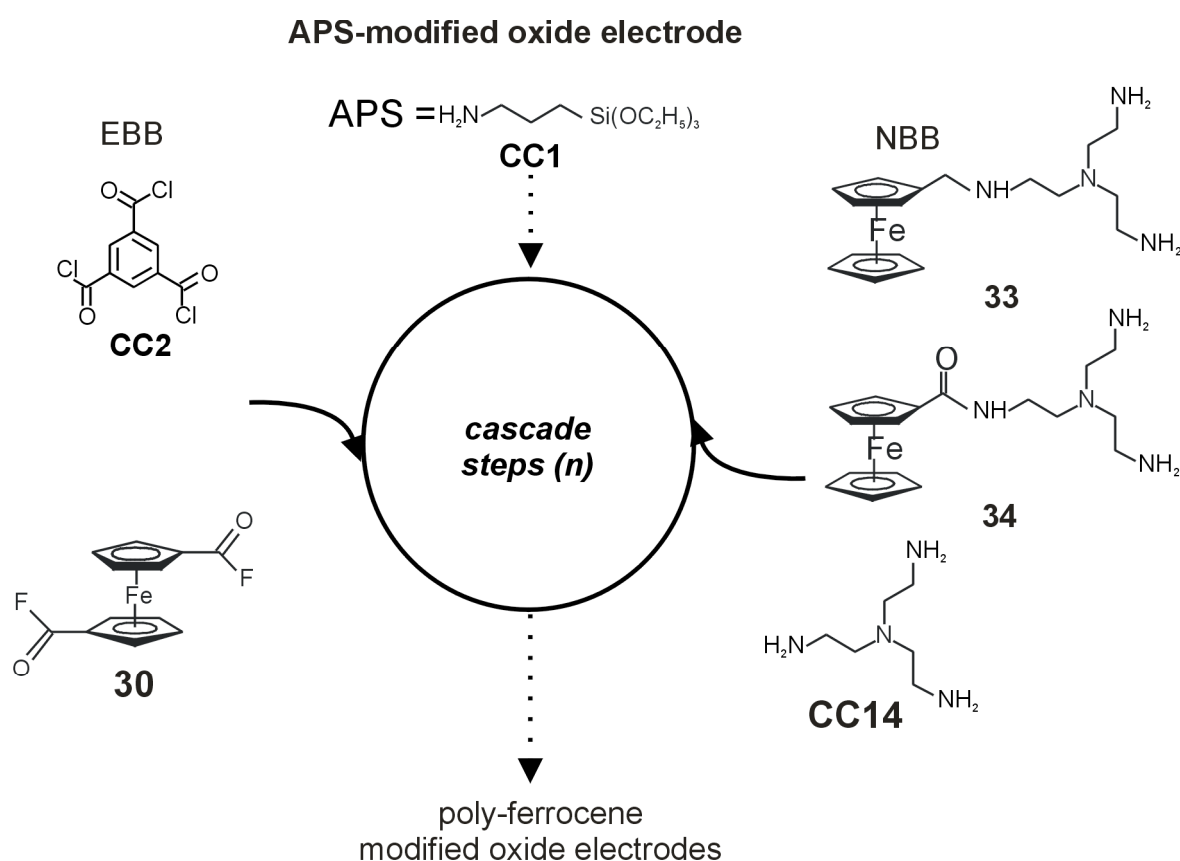
More recently, the so called layer-by-layer surface modifications known to work with oppositely charged polyelectrolytes [102] have been applied to ferrocenyl organometallic polyelectrolytes [103].

Notably, the layer-by-layer technique allows to control easily the surface concentration by the number of deposition steps [55]. A drawback of this technique is that the multilayer structure is rather fragile. It is often sufficiently stable in an aqueous system, and the stability is crucially dependent on the ionic strength and pH. Related are attempts to build up electroactive layers on electrodes using the sequential exposition of the electrode to ferrocenyl-modified streptavidin and biotin [104] i.e. layer fixation based on strong antigen antibody interactions.

In chapter 3, I have described the layer-by-layer technique using covalent bond forming reactions [104]. I have shown how to grow and cross-link ink-jetted viologens

anchored to nanocrystalline TiO_2 . The electrode modification was based on substitution reactions between electrode surfaces confined species and sequentially exposed di- or tri-functional benzylic bromides and bipyridines in solution. Thus, a layer of viologens from a three-dimensional network of covalent bonds, the layer thickness of which was fabricated with the layer thickness controlled by the number of reaction steps (n).

On the basis of these results, I have extended now the principle of the solid phase-supported electrode modification to fast amide-forming reactions. For this purpose the OTE was first modified with a layer of the anchoring amine **CC1** and then sequentially exposed to the multifunctional electrophilic and nucleophilic building blocks, EBB and NBB, respectively, in scheme 4.1.



Scheme 4.1. Cascade modification of electrode surfaces with poly-ferrocenes

Typically, the molar extinction coefficients of ferrocenes in both oxidation states are negligible in the visible range ($\epsilon_{\text{max}} < 1000$) as compared to strongly colouring

electrochromophores such as viologens with $\epsilon_{\max} > 15000$. Thus, ferrocenes have been used in transparent or reflective electrochromic cells as non-colouring charge storing system, mainly in solution under self-erasing conditions [88, 105, 106].

4.2. Procedure for the preparation of poly-ferrocene on oxide electrodes

4.2.1 The preparation of poly CC14-30, 33-CC3, and 34-CC3 on oxide electrode

The monomeric ferrocenes **30** to **37** were synthesized according to scheme 6.5 in Chapter 6.

Glass slides (69 mm x 69 mm), coated with ITO (In-doped SnO₂, 20Ω/cm²) from BTE Bedampfungstechnik (Elsoff, Germany) or FTO glass (F-doped SnO₂, 15Ω/cm²) from LOF were used as received. The glasses were cleaned according to the method reported by *Hillebrandt et al.* [107] prior to silanization.

Colloidal ATO paste [69] was coated on 69 mm x 69 mm FTO glass electrode using the doctor blade method to yield after firing 4 μm thick films [50].

Silanization. The ITO, FTO and ATO electrodes were functionalized with (3-aminopropyl) triethoxysilane (APS) **CC1** according to the method reported by *Lee et al* [108]. The silanization of FTO and ITO was checked electrochemically by reaction of the amine-terminated surface with ferrocenyl carboxylic acid fluoride **36** yielding surface concentrations of $\Gamma = 4.2 \cdot 10^{-10}$ mol cm⁻² and $\Gamma = 3.3 \cdot 10^{-10}$, respectively, from CV at 0.1 V/s in 0.2 M LiClO₄/MeCN.

Cross-linking. Freshly prepared APS-coated ITO and FTO plates (NAG, see scheme 4.1) were exposed sequentially to a solution of the electrophilic trimesic acid chloride (Fluka) **CC3** (c = 5 mM in toluene) or to a solution of ferrocenyl-1,1'-diacid fluoride **30** (5 mM in CH₂Cl₂) for 15 min. at 20 °C (EBB in scheme 4.1). Thereafter, the electrodes were treated with the nucleophilic compounds **34** or **CC14**, 5 mM in CH₂Cl₂ containing 2% pyridine, 15 min., at 20 °C, (NBB in scheme 4.1). The procedure was repeated using the sequence EBB-NBB-EBB-NBB and so on for up to 20 cascade steps (n=20) to yield the modified electrodes E-(**34-CC3**)_n-(ITO or FTO)

and E-(**CC14-30**)_n-(**ITO** or **FTO**). Between each reaction step the plate was rinsed with the pure solvent of the precedent step. APS-coated ATO plates (NAG) were modified in the same way but for 30 min and at 40 °C using EBB **CC3** (5 mM in toluene) in combination with the NBB compounds **33** or **34** (3 mM in CH₂Cl₂, in presence of 2% pyridine) to yield (after up to three cascade steps (n=3)) the modified electrodes E-(**33-CC3**)_n-**ATO** and E-(**34-CC3**)_n-**ATO**, respectively.

4.2.2. Electrode surface modification

A general procedure for the surface modification of different oxide electrodes (nanocrystalline antimony tin oxide = ATO, fluorine doped tin oxide = FTO, and indium tin oxide = ITO) is presented in scheme 4.1. First, the electrodes are activated with aminopropyl triethoxy silane (APS **CC1**) yielding a monolayer of the compound with amino functionalities exposed to the solution side. The quality of these monolayers on FTO and ITO was checked by quenching the amino functions with the mono functional redox tag ferrocene carboxylic acid fluoride **36**; surface concentrations of $\Gamma = 4.2 \cdot 10^{-10}$ and $\Gamma = 3.3 \cdot 10^{-10}$ mol cm⁻² was achieved. These are larger values than expected for an ideally flat surface but similar to values reported in the literature [55, 98, 109, 110]. Two reasons account for the increased surface concentrations:

- (i) surface roughness of the sputtered oxide and
- (ii) the tendency of APS to polymerize in the presence of moisture [109].

On freshly prepared APS-modified electrode ferrocene multilayer, were produced by entering the cascade cycle (scheme 4.1). Here, the surface is exposed to a high concentration of one of the electrophilic building block (EBB) compounds, i.e. a di- or tri-functional carboxylic acid halide, resulting in a fast and irreversible N-acylation. Reaction conditions are chosen for complete quenching of all surface functionalities and, simultaneously, for the survival of the second (third) acyl halide group on the surface, pointing towards the solution side. In the next step the electrode is exposed to a solution of one of the multifunctional amines, i.e. one of the representatives from the nucleophilic building blocks (NBB). The cascade can be further continued *ad libitum* yielding surface-EBB-NBB-EBB-NBB etc. With each cascade cycle (n) additional electroactive material is bound to the surface, and with each step the

character of the outermost layer is switched between electrophilic and nucleophilic. Notably, sequences involving the electrophilic monomer **30**, e.g. E-(**30-34**)_n, E-(**30-33**)_n and E-(**30-CC14**)_n, yield polymers with ferrocenes build into the backbone, whereas cascade sequences based on the electrophilic monomer **CC3** lead to polymers with pending ferrocenes.

4.2.3. The electrochemistry of the modified electrode

The effect of the cascade cycles on the electrochemistry is shown in figure 4.1, figure 4.2, and table 4.1. When APS-activated ITO or FTO is used as a substrate, the electrochemical response of the surface bound ferrocene grows linearly with the number of cascade cycles up to n = 20 (figure 4.1).

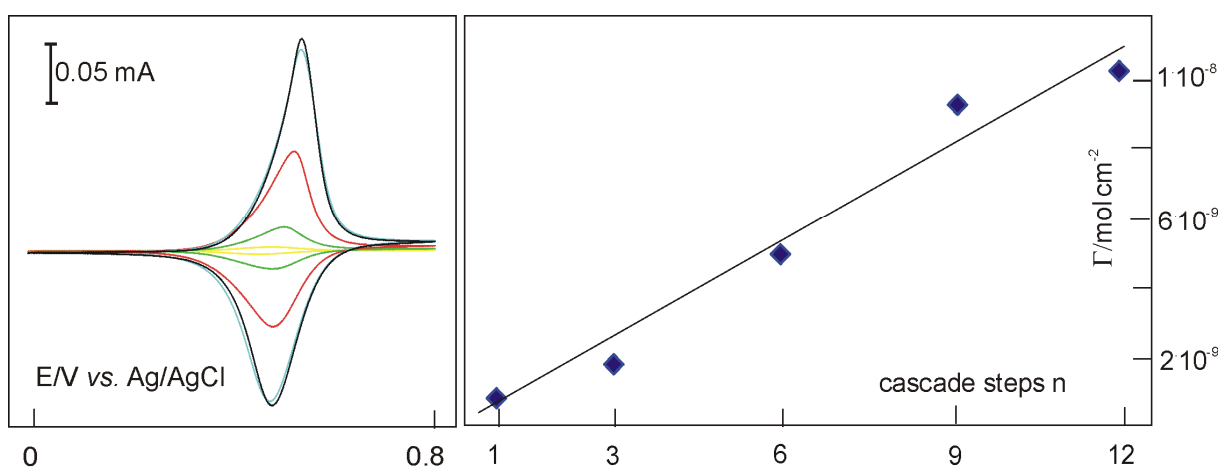


Figure 4.1. CV of E-(**34-CC3**)_n-ITO as a function of cascade steps (n); surface concentration of E-(**34-CC3**)_n on a 0.8 cm² ITO electrode with n = 1,3,6,9,12; v = 0.02 Vs⁻¹ in MeCN/0.2 M LiClO₄ vs. Ag/AgCl. The electrode was pretreated in 1M HCl.

Notably, it is necessary to dip the modified electrode in aq.HCl or to add a drop of aq. HCl to the organic solvent/electrolyte in order to observe the fully developed electroactivity. Protonation of the tertiary amine and/or of unreacted primary amino functions seems to enhance the charge propagation in the polymer. I have, therefore, tried to quaternize the amines by alkylation. However, it was not possible to achieve the same effect by treating the modified electrodes with methyl iodide at 40 °C for up to 24 h.

The effect of the electrode material and of the monomers used in the cascade reaction on the electrochemistry is shown in figure 4.2, table 4.1 and table 4.2.

Cascade Steps (n)	ATO		ITO*		FTO*	
	E-(33-CC3) _n	E-(34-CC3) _n	E-(CC14-30) _n	E-(34-CC3) _n	E-(CC14-30) _n	E-(34-CC3) _n
Γ [mol·cm ⁻²] × 10 ⁻⁷						
n=1	0.11	0.10	0.0078	0.0025	0.012	0.0027
n=2	1.05	1.41	0.0085	0.0083	0.016	0.012
n=3	2.16	2.20	0.011	0.014	0.020	0.025
n=10	-	-	0.026	0.11	0.028	0.14
n=20	-	-	0.052	-	0.04	-

Measured by coulometry from CV at $v = 0.02 \text{ Vs}^{-1}$ in 0.2 LiClO₄/MeCN, vs. Ag/AgCl. *electrode pretreated with aq. HCl

Table 4.1. Surface concentrations observed using the reactive “layer by layer” technique

After one cascade step, corresponding to the formation of a monolayer of ferrocene on the electrode, the surface concentrations on ATO, ITO and FTO are $0.21 \cdot 10^{-7}$, $0.0025 \cdot 10^{-7}$, and $0.0027 \cdot 10^{-7} \text{ mol} \cdot \text{cm}^{-2}$, respectively. Thus, the 4 μm thick mesoporous ATO electrode exhibits a ca. 100 times higher Γ than the flat ITO and FTO electrodes. This ratio is related to the roughness factors of ATO (approx. 20 per μm thickness) and to the tendency of the anchoring silane **CC1** to increase the apparent surface concentration by moisture- induced oligomerization.

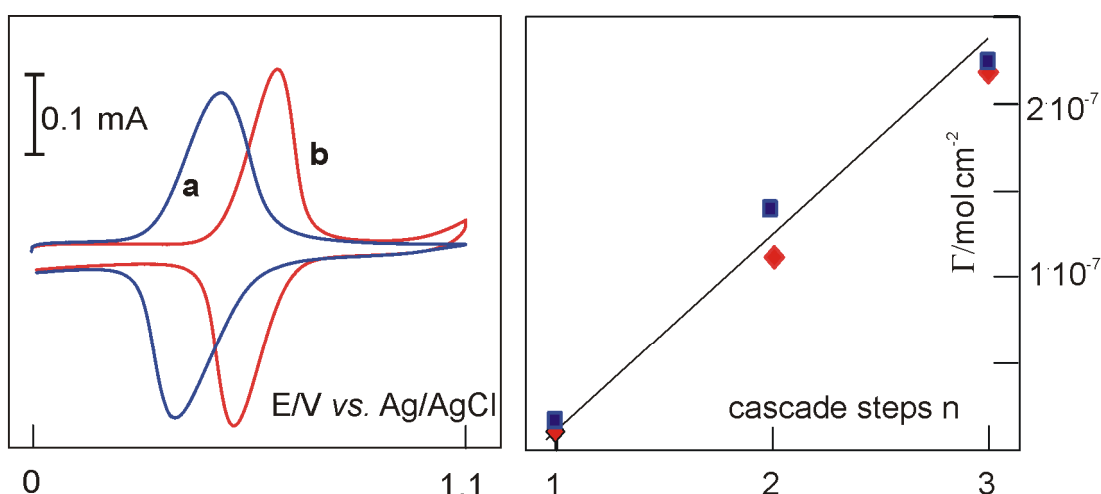


Figure 4.2. CV of a) E-(**33-CC3**)₂-ATO and b) E-(**34-CC3**)₂-ATO as a function of cascade steps (n); \blacklozenge surface concentration of E-(**33-CC3**)_n; and \blacksquare E-(**34-CC3**)_n on a 0.5 cm² ATO electrode, $v = 0.01 \text{ Vs}^{-1}$ in MeCN/0.2 M LiClO₄ vs. Ag/AgCl.

The observable surface-confined electroactivity increases linearly with the increasing number of cascade steps on the large area ATO electrode over three cascade steps (figure 4.2, tabel 4.1).

Up to this polymer thickness it is not necessary to protonate the surface amines in order to observe electroactivity. The response of ferrocene on ATO is fast. We observe ca. 120 mV peak separation at 20 mV s⁻¹ and 500 mV at 100 mV s⁻¹ without loss of coulometry (without IR-compensation). Notably, the peak current density is 3 mA cm⁻² at 100 mV s⁻¹ leading to a significant potential drop in the conducting layer.

When comparing the E^o values of E-(**33-CC3**)_n, E-(**34-CC3**)_n, and E-(**CC14-30**)_n with those of the related monomers, it becomes obvious that E^o mainly reflects the trends yet observed in the monomers (table 4.2). For the E^o values of the monomers it is well known that they are dictated by substituents [94, 95].

E ^o [V]	Fecp ₂ -R	Fecp ₂ -R ₁₇ 33	Fe(cp-R ₁₈) ₂ 35	Fecp ₂ -R ₁₈ 34	Fecp ₂ -R ₁₄ 36	Fe(cp-R ₁₉) ₂ 37	Fe(cp-R ₁₄) ₂ 30
E ^o	0.32	0.41ca. 0.37* [111, 112]	0.53**	0.59 0.409*	0.76	0.82	1.13
poly-ferrocene							
	E-(33-CC3) _n		E-(34-CC3) _n		E-(CC14-30) _n		
E ^o	0.42		0.52 < E ^o < 0.57		0.75		

*in phosphate buffer or aqueous KCl, ** 3mM in 0.2 LiClO₄/H₂O + 1% HCl

R = -H; R₁₄ = -COF; R₁₇ = -CH₂NHCH₂N(C₂H₄NH₂)₂; R₁₈ = -CONHCH₂N(C₂H₄NH₂)₂;
R₁₉=-COOCH₃

Table 4.2. Reduction potentials of ferrocene monomers and polymers

The E^o of the polymer E-(**34-CC3**)_n with one amide function (0.51 < E^o < 0.57 V) is similar to that of monomer **34** in organic solvents (E^o = 0.59 V), just as E^o of the monomer **33** (E^o = 0.41 V) with one amine bound side chain persists in E-(**CC14-30**)_n (E^o = 0.41 V). E-(**CC14-30**) with two amide functions (E^o = 0.75 V) was measured in MeCN. The corresponding monomer **35** was only measureable in water and shows a value of E^o = 0.53 V, the difference in E^o being related to a water induced shift (see below). All monomers exhibit reversible electrochemistry at $\nu = 10 \text{ Vs}^{-1}$, except of **30** and Fe(cp-R₁₉)₂, i.e. those with the most positive oxidation potential. With these compounds ($i_{pc}/i_{pa} \ll 1$) is much smaller than 1 at $\nu = 20 \text{ mV s}^{-1}$ probably because of

solvent attack. E° in water is generally less positive because the product cation of the oxidation process is better stabilized by water than by organic solvents. Thus, addition of trifluoroacetic acid to the amides **34** and **35** in MeCN does not affect E° , whereas addition of aqueous HCl shifts E° to positive potentials by 0.06 V and 0.15 V, respectively, because the effect of water solvation dominates. On the other hand, addition of trifluoroacetic acid to the amine **33** in MeCN shifts E° to more a positive potential by 0.072 V (reflecting the protonated amino function α to the cp ring), whereas addition of aqueous HCl does not affect E° (reflecting the two competing effects protonation (positive shift) and solvation (negative shift)). The same trends are generally observed for the polymer- modified electrodes.

So far I have shown that the poly-ferrocene electrodes show fast response, a high capacity and a high stability. In order to use the electrode as a transparent counter electrode in electrochromic displays, a low absorption in both oxidation states is needed. For this purpose the extinction coefficients of the relevant monomeric ferrocenes were measured in MeCN / LiClO₄ (0.2 M). The dates are reported in table 4.3. Principally, the same absorption maxima are observed for the polymers on ATO as for the monomers in solution. Notably, the ferrocene-related absorptions of the polymers are below 0.15 in the whole visible range using surface concentrations up to 3 to 4x10⁻⁷ mol·cm⁻². Due to the ATO layer, only the absorption peak of the oxidized form at 630 to 635 nm could be evaluated quantitatively. From this analysis and using the corresponding extinction coefficients of the monomers the surface concentrations were calculated. These are identical with those determined by coulometry (table 4.1).

Because of its relatively small extinction coefficients in the visible wavelength range in oxidation states, its high capacity and its fast kinetic behaviour, the poly-ferrocene-modified ATO-electrode is definitely a candidate for a transparent counter electrode in electrochromic devices. In such systems the cathodic material (such as a surface confined viologen) exhibits an extinction coefficient of 15·10³ and a colouration efficiency of 160 cm²·C⁻¹, respectively. Thus, using viologen surface concentrations of 5·10⁻⁸ mol·cm⁻² absorption changes of 0.8 can be reached. The corresponding charge of 5·10⁻³ cm²·C⁻¹ has to be balanced at the counter electrode. In order to ensure sufficient capacity on the counter electrode, even when the system gets off the equilibrium ca. 15·10⁻³ cm²·C⁻¹ or 15·10⁻⁸ mol·cm⁻² is needed on the counter electrode. As shown in table 4.1 and 4.3 these conditions are by far fulfilled using two or three cascade steps to prepare a ferrocene-modified ATO-electrode.

Ferrocene monomers	$\lambda / \text{nm} (\epsilon / \text{dm}^3 \text{mol}^{-1} \text{cm}^{-1})$	
	Red.	Ox.
Fecp ₂ -R	325 (75.5) 437 (64.4)	373 (271.1) 474 (100.0) 617 (264.4)
Fe(cp-R ₁₉) ₂	349 (582.2) 450 (384.4)	641 (384.4)
Fecp ₂ -R ₁₇ 33	320 (811.1) 431 (351.1)	631 (371.1)
Fecp ₂ -R ₁₈ 34	315 (813.3) 420 (353.3)	630 (360.0) 634 (355.5) *
<i>ferrocene polymers (oxidized)</i>		
	$\lambda / \text{nm} (\text{A})$	$\Gamma / \text{mol} / \text{cm}^2$
E-(33-CC3) ₃ -ATO	631 (0.11)	3×10^{-7}
E-(34-CC3) ₂ -ATO	634 (0.13)	3.6×10^{-7}

* used for polymer measured in MeCN/LiClO₄ (0.2 M) polarized at 0 V and 1V vs. Ag/AgCl for the reduced and oxidized state, respectively.

R = -H; R₁₄ = -CO; R₁₇ = -CH₂NHCH₂N(C₂H₄NH₂)₂; R₁₈ = -CONHCH₂N(C₂H₄NH₂)₂,
R₁₉ = -COOCH₃

Table 4.3. UV-VIS absorption maxima and extinction coefficients of reduced and oxidized ferrocenyl monomers and polymers

4.3. Effects of electrolyte and solvent on poly-ferrocene counter electrodes

The modified glasses were studied under “real” conditions (glutaronitrile/LiClO₄) and optimized for high capacity, fast response and good optical quality.

Figure 4.3 shows the surface concentration (available from coulometric measurements) of the electrode as a function of the HCl-content of the glutaronitrile. The presence of aq. HCl was found crucial for a fast electrochemical response. We achieved ca. $1.6 \cdot 10^{-8} \text{ mol} / \text{cm}^2$ under optimized conditions. Moreover, such values are only observed when the electrode is scanned slowly.

I think that residual N-functions within the polymer are protonated by the acid. Thus, higher mobility of ions in the polymer is achieved in the presence of the acid.

I have tried to use alkylating reagents such ethyl iodide and methyl iodide instead of HCl, however, the alkylating agent did not improve the current response. I also have used p-toluene sulfonic acid or trifluoroacetic acid instead of HCl. However, these are not of comparable influence compared to HCl.

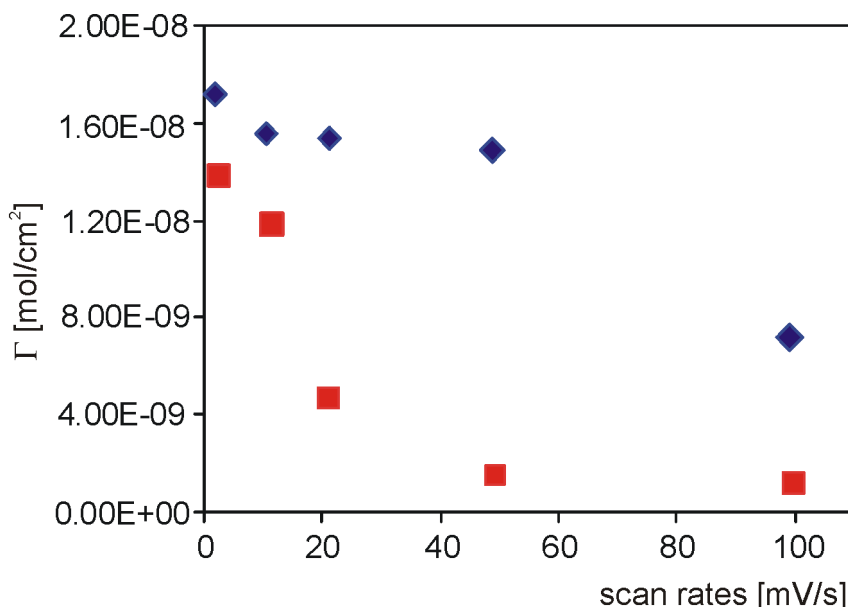


Figure 4.3. Capacity of ferrocene modified counters electrodes
 ◆ 2% HCl in glutaronitrile; ■ counter electrode pretrated in HCl, dried and measured in glutaronitrile

Besides the glutaronitrile-LiClO₄ combination we have tried glutaronitrile-LiN(SO₂CF₃)₂ or glutaronitrile- TBAPF₆⁻ as well as TEG-DiME with LiClO₄. None of these combinations were as good as the glutaronitrile-LiClO₄ (+HCl) electrolyte.

The poly-ferrocene counter electrode reaches surface concentrations of ca. 2·10⁻⁸ mol/cm² but only in the presence of some HCl.

The electrolyte with HCl or water cannot be used because of problems with the mechanical stability of the ATO layer on FTO after heating. Especially, if contacted with water the ATO tends to peel off.

In table 4.4 a series of experiments performed is presented with the same type of solvent electrolytes but with the ferrocene counter electrode (as described in chapter 4.2). Faster responses are observed with MeCN and glutaronitrile in contrast to the working electrode behavior.

Electrolyte/solvent	2x cross-linked E-33 -ATO				3x cross-linked E-34 -ATO			
	E_{pa}/V	E_{pc}/V	E°/V	Γ mol/ $cm^2 \times 10^{-7}$	E_{pa}/V	E_{pc}/V	E°/V	Γ mol/ $cm^2 \times 10^{-7}$
0,2M LP /MeCN	0.62	0.23	0.43	1.94	0.67	0.41	0.544	4.53
0,3 M LiN(SO ₂ CF ₃) ₂ / Glutaronitrile	0.92	0.07	0.50	1.87	0.97	0.31	0.644	2.31
1M LP /EG	0.53	0.22	0.37	1.09	0.66	0.37	0.519	1.16
1M LP /TEG-DiMe	0.54	0.29	0.41	0.79	0.72	0.39	0.559	1.02
0,2 M LP/ γ BL+G (1:3vol.%)	0.56	0.26	0.41	0.94	0.73	0.34	0.538	0.87
0,2 M LP γ BL+3MeOPN (1:3vol.%)	0.50	0.31	0.41	0.82	0.61	0.47	0.541	0.22

LP: LiClO₄; EG: ethylene glycol; TEG-DiMe: tetraethylene glycol dimethyl ether;

γ -BL+G: γ -butyrolactone and glutaronitrile; γ -BL+G : γ -butyrolactone and 3- methoxypropionitril

Table 4.4. Effects of electrolyte/solvent on the ferrocene counter electrode E-33-ATO and E-34-ATO, scan rate 20 mV/s, vs. Ag/AgCl

Both cross-linked ferrocene electrodes show on the new ATO substrate much higher capacity (**10 times more**) than earlier on the FTO glass without ATO. Thus, E-34 on ATO shows $1.51 \cdot 10^{-7}$ mol/cm² and E-33 on ATO shows $1.89 \cdot 10^{-7}$ mol/cm² even using only 2 cascade steps. This is the reason why the kinetics of the poly-ferrocene on ATO in MeCN is very good. In glutaronitrile the kinetics are of course slower but still acceptable.

4.4. Closed cells with E-33 counter electrodes



In order to judge the kinetic and optical quality of the counter electrode under almost real conditions, I used a 2-electrode systems with a ca. 0.5 mm gasket hold together by clamps. A cell with E-33 on ATO counter electrode is shown in figure 4.4. Compared with a cell with a CeO_2 counter electrode (see chapter 3) I preferred definitely the optical impression of the CeO_2 counter electrode.

Figure 4.4. Closed cell with E-33 on the ATO counter electrode and $\text{LiN}(\text{SO}_2\text{CF}_3)_2$ /glutaronitrile

Moreover glued closed systems with E-33 on ATO the counter electrode and glutaronitrile/ $\text{LiN}(\text{SO}_3\text{CF}_3)_2$ have been prepared. The system is optically good but the kinetics is only satisfactory.

Conclusion:

The ATO colloid is an excellent surface electrode on an FTO electrode support. I was able to improve the capacity of our cross-linked ferrocene electrode by a factor of 10 as compared to the FTO support without any loss in kinetics.

Based on the comparative analysis of a counter electrode with phenothiazine on ATO and a CeO_2 counter electrode, poly ferrocene counter electrode can be interesting for closed cells. A minor colouration grey-green is expected, but this is definitely less than the pink colouration resulting from phenothiazine.

Chapter 5

Electrocatalytic application of the layer-by-layer technique: TiO₂ - electrode with cross-linkable B₁₂ - derivatives

5.1. Background. The modified surface electrodes with B₁₂ - derivatives

Vitamin B₁₂ and related macrocyclic Co complexes, that mimic the vitamins reactivity, are used as electrocatalysts in organic synthesis [113-117], in waste water treatment [118, 119] and in sensing applications [120-124].

Originally, vitamin B₁₂ was used as a homogeneous electrocatalyst but more recently much effort has been directed towards the immobilization of vitamin B₁₂ or of one of its derivatives on an electrode surface.

Monolayer or polymeric multilayer on flat electrodes, as well as mono and multilayer on three dimensional electrodes have been reported.

Thus, a mixed long chain cobester derivative combined with an organoalkyl silane monolayer with a very low apparent surface concentration (Γ) was prepared on an ITO (indium tin oxide) electrode, and its physico-chemical properties were described [125]. A tri-alkoxysilyl B₁₂ derivative was covalently linked to an oxidized Pt surface showing $\Gamma = 1.6 \cdot 10^{-10}$ mol/cm² [126]. The electrode was used for the preparative electrosynthesis of styrene with turnover number rates of 6260 per h. Modifications of electrodes with a polymeric epoxy resin formed from a B₁₂ diamine derivative and a di- epoxy component on flat pyrolytic carbon [120], or on carbon felt [127] have been reported, showing a loading of $1 \cdot 10^{-11}$ to $1 \cdot 10^{-9}$ mol/cm² depending on the conditions of preparation and representing sub-mono to 10 vitamin B₁₂ layers. Polypyrrole derivatives of B₁₂ on flat gold or glassy carbon electrodes have also been reported [128] Hydrophobic hepta-propyl cobesters were trapped in a silica sol gel layer on an ITO electrode but only surface concentrations in the range of a monolayer ($6 \cdot 10^{-11}$ mol/cm²) were observed [129]. However, turnover numbers > 1000 for electrocatalytic applications were reported [129].

In a preliminary study I have shown, that the inner surface of mesoporous TiO₂ electrodes can be modified with an EDTA derivative of cobester c-acid that coordinates via three carboxylic groups to TiO₂ [53]. These three-dimensional electrodes exhibit surface concentrations in the range of 0.5 to $3 \cdot 10^{-8}$ mol/cm²,

depending on the TiO₂ film thickness and a reasonable stability allowing preparative scale electrocatalysis, e.g. the photo-assisted radical- type intramolecular cyclization [53]. *Rusling* has extended these studies using 8-aminocob (III)yrinic acid c-lactam (vitamin B₁₂ hexacarboxylate) on TiO₂; he reported $\Gamma = 1.1 \cdot 10^{-8}$ mol/cm² and demonstrated electrocatalytic applications, i.e. another radical- type intramolecular cyclization and reductive eliminations. Both research groups observed a loss of the electrocatalyst from the semiconductor, especially during electrocatalysis.

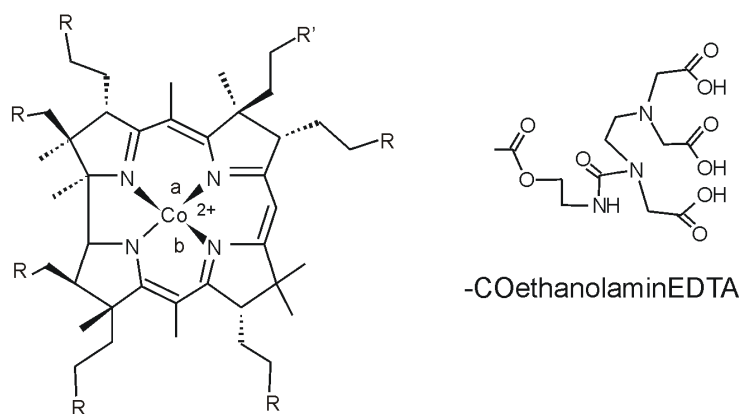
I have developed the cross-linking technique described in chapters 3 and 4 for the modification of TiO₂ electrodes with electrochromic materials and for the modification of antimony- doped tin oxide (ATO) with ferrocene derivatives [55, 88]. This technique was applied for stabilization of vitamin B₁₂ on TiO₂ electrodes.

5.2. Modification of TiO₂ – electrodes with cross-linkable B₁₂ - derivatives

5.2.1. Synthesis of vitamin B12 derivatives

The vitamin B₁₂ or cob(II)ester derivatives **CC15** to **CC17** (see scheme 5.1) have been prepared according to procedures taken from the literature.

The vitamin B12 derivatives were prepared by *Steiger*. The monoacid Cob(II)ester-c-acid **CC15** was prepared according to a literature procedure [130] as aquo-cyano perchlorate, the triacid cob(III)ester-c-EDTA-amide **CC16** according to the method reported by *Mayor et al.* [131] as the dicyano compound, and the heptaacid cob(III)yrin-hepta acid **CC17** according to the method reported by *Stepanek et al.* [132] as the dicyano compound. The heptol **CC6** and the hepta iodide **CC7** were both prepared by *Steiger et al.* [133] as the corresponding dicyano compounds.



CC15 : R = -COOME, R' = -COOH, a = H₂O; b = -CN

CC16 : R = -COOME, R' = -COethanolaminEDTA, a = b = -CN

CC17 : R = -COOH, R' = -COOH, a = b = -CN

CC6 : R = R' = R₉ = -(CH₂)₂OH, a = b = -CN

CC7 : R = R' = R₁₀ = -(CH₂)₂I, a = b = -CN

type and number
of coordinating
groups

1 * COOH

3 * COOH

7 * COOH

number of cross-
linkable groups

7 * CH₂OH

6 * CH₂I

Scheme 5.1. Vitamin B₁₂ derivatives

5.2.2. Procedure for the preparation of vitamin B₁₂- modified TiO₂ film electrodes

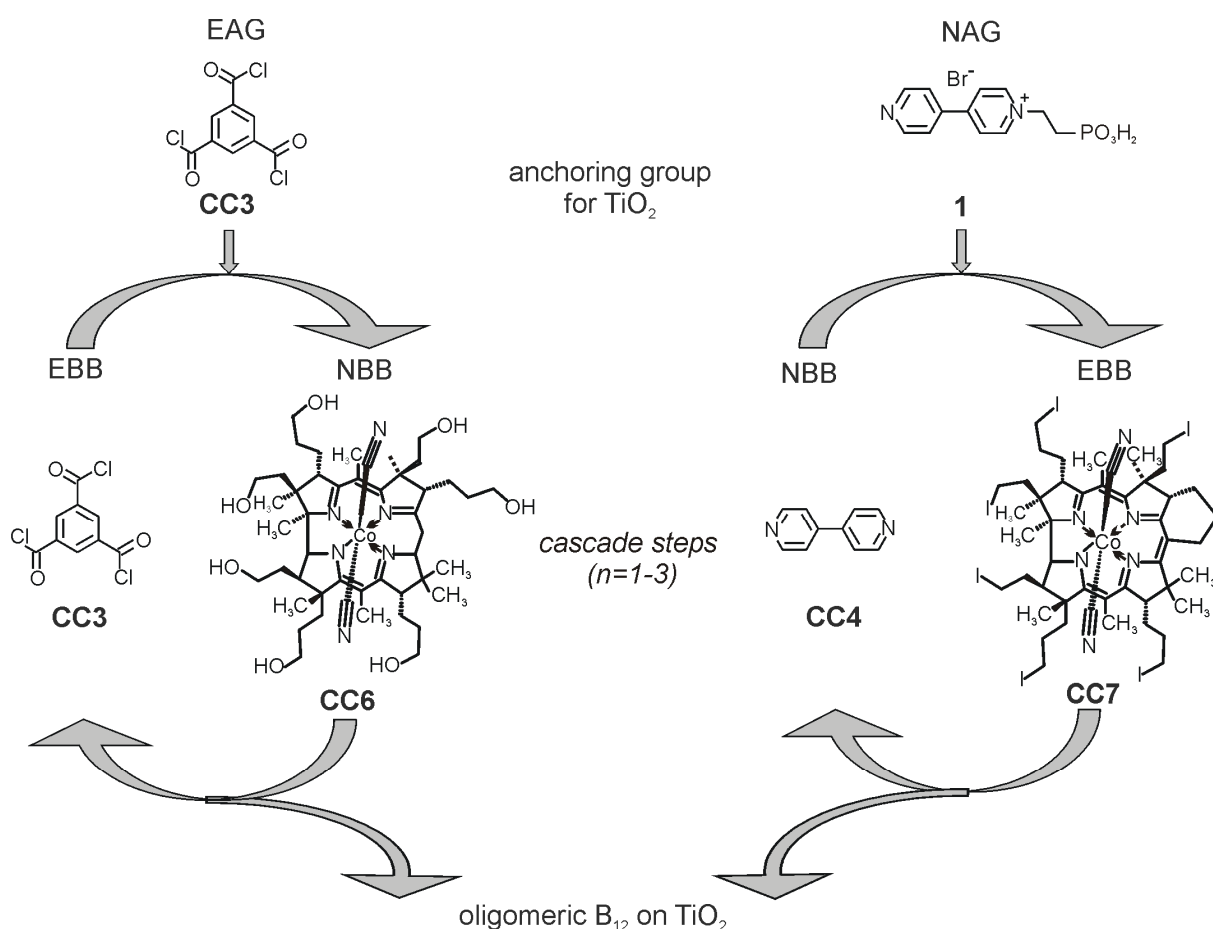
Colloidal TiO₂ [69] paste was coated on 10 mm x 10 mm FTO glass electrodes (F-doped SnO₂, 15 Ω/cm²) from LOF using the *doctor-blade* method to yield 5 μm thick films [50]. The glasses were cleaned according to the method reported by *Hillebrandt et al* [107] prior to coating.

E-**CC15**, E-**CC16** and E-**CC17**: 2 mg of **CC15**, **CC16** or **CC17** per ml were dissolved each in a solution of EtOH / H₂O (95:5 v/v). TiO₂ electrodes were exposed to these solutions for 1 h at r.t. The electrodes were then rinsed with the EtOH/H₂O. E-**CC6**: TiO₂ electrodes were exposed to a solution of trimesic acid chloride (**CC3**, Fluka, c = 20 mM) in toluene for 60 min at 60 °C, and rinsed with toluene. E-**CC7**: The TiO₂ electrodes were then functionalized with the phosphonic acid **1** as described by *Felderhoff et al.*[51].

E-**CC3**-(**CC6-CC3**)_n: E-**CC3** was exposed to a solution of the dicyano-cob(III)yrin-heptole **CC6** 2mg/ml in MeCN for 1h at 60 °C and then treated with **CC3** (c = 20 mM) in toluene for 60 min at 60 °C (see scheme 5.2) to yield E-**CC3**-(**CC6-CC3**)₁.

This electrode was then treated with a solution of **CC6** (2mg/ml) in MeCN for 1h at 60 °C, followed by a treatment with **CC3** (c = 20 mM) in toluene for 60 min at 60 °C to yield E-**CC3**-(**CC6-CC3**)₂. This reaction sequence was repeated more to yield E-**CC3**-(**CC6-CC3**)₃. Between each reaction step the electrode was rinsed with the pure solvent of the precedent step.

E-1-(**CC7-CC4**)_n: E-1 was exposed to a solution of dicyano-cob(III)yrin-hexaiodide **CC7** 4mg/ml in MeCN for 6h at 60 °C (see scheme 5.2), followed by a treatment of the electrode in 50 mM bipyridine **CC4** for 6h at 60 °C in MeCN to yield E-1-(**CC7-CC4**)₁ (at this reaction time the yield was achieved). The procedure was repeated once and twice to yield E-1-(**CC7-CC4**)₂ and E-1-(**CC7-CC4**)₃, respectively. Between each reaction step the electrode was rinsed with the pure solvent of the precedent step.



Scheme 5.2. Vitamin B₁₂-derivatives on TiO₂ electrodes

5.2.3 Electrode surface modification

Two new types of vitamin B₁₂- modified TiO₂ film electrodes were prepared according to the general reaction scheme 5.2, and the electrochemical and catalytic properties were compared with vitamin B₁₂ mono-, three-, or seven carboxylic acid functions coordinated on TiO₂. After immersion of the TiO₂ electrode in a millimolar solution of the vitamin B₁₂ with one-, three-, or seven- carboxylic acid groups for 1 hour, all electrodes showed an intense orange-red colour. This means, that the 3 components were strongly adsorbed at the surface. Then, the electroactivity of the electrodes was checked in propylene carbonate with 0.5M TBAP between 0 and -0.9V vs. Ag/AgCl. Only the Co(II)/Co(I) wave can be observed on TiO₂ because this material behaves as a semiconductor at potentials more positive than -0.3V. The best response is observed using the tri- acid E-**CC16**, much smaller responses are obtained for mono- **E-CC15** and hepta- **E-CC17** acid (figure 5.1). The surface concentrations calculated from visible absorbance spectroscopy of the electrodes E-**CC15**, E-**CC16** and E-**CC17** at 525 nm, yielded initially $1.49 \cdot 10^{-7} \text{ mol}\cdot\text{cm}^{-2}$ (geometric area) for E-**CC16** (see table 5.1); the values are about 2 times smaller for the E-**CC17** and E-**CC15**. It is believed that the mono acid is a very bad coordinator and that the hepta- acid is occupying too much space, thus diminishing the surface concentration. Measuring the same samples in CV yielded values which are much smaller. The decrease of the surface concentration is 99% for E-**CC15** and about 90% for the other samples in comparison to the UV/VIS values. Since these values which were obtained without electrolyte, I conclude that the coordination is not very stable and the catalyst has been desorbed and is dissolved. This desorption can be prevented by cross-linking the modifiers using cascade type surface reactions (see figure 5.1b, 5.1c).

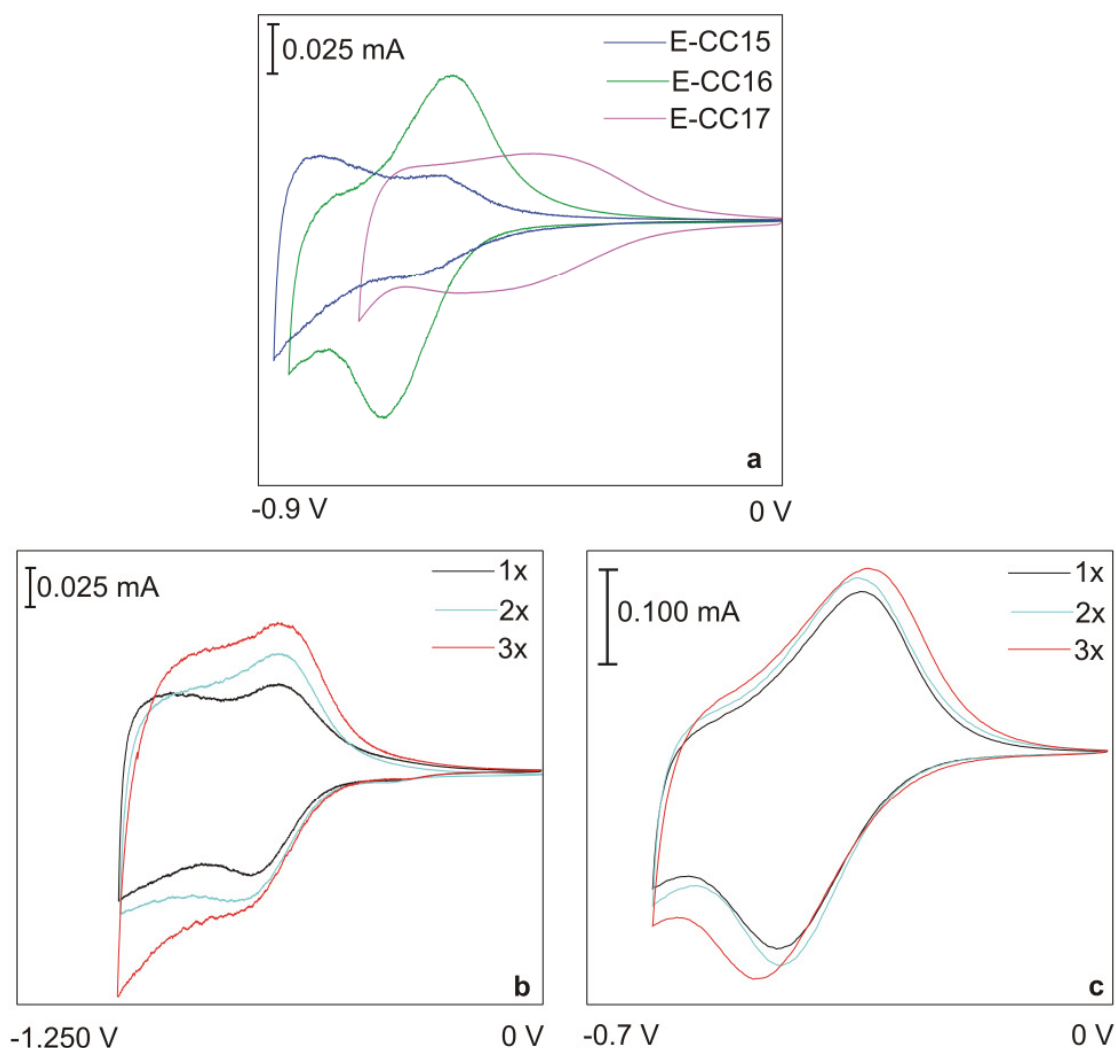


Figure 5.1. Cyclic voltammograms of B_{12} -modified TiO_2 electrodes, a) coordinative modification E-CC15, E-CC16 and E-CC17; b) and c) cross-linking electrode E-CC3-(CC6-CC3) $_n$ and E-1-(CC7-CC4) $_n$ respectively ($n= 1-3$). The electrodes E-CC15, E-CC16; E-CC17 and E-CC3-(CC6-CC3) $_n$ were measured in PC/0.5 M TBAP + 1% HAc, at $v=20\text{ mV s}^{-1}$; and electrode E-1-(CC7-CC4) $_n$ in MeCN/0.5 M LP + 1% HAc, at $v=5\text{ mV s}^{-1}$.

Generally, the preparation of cross linked samples can be done by sequential exposition of the TiO_2 surface to multifunctional electrophilic (EBB) and nucleophilic (NBB) compounds according to scheme 5.2. An oligomeric B_{12} film is irreversibly formed on the TiO_2 surface. With the reaction E-CC3-(CC6-CC3) $_n$ the yield increases with the time of reaction, whereas at E-1-(CC7-CC4) $_n$ a maximum is obtained for a reaction time of 6h (figure 5.2). For extended times the yield decreases i.e. to 75% after 12 h (figure 5.2 inset). It can be seen, that the thickness of the film is determined by the number of cascade steps (figure 5.3. inset).

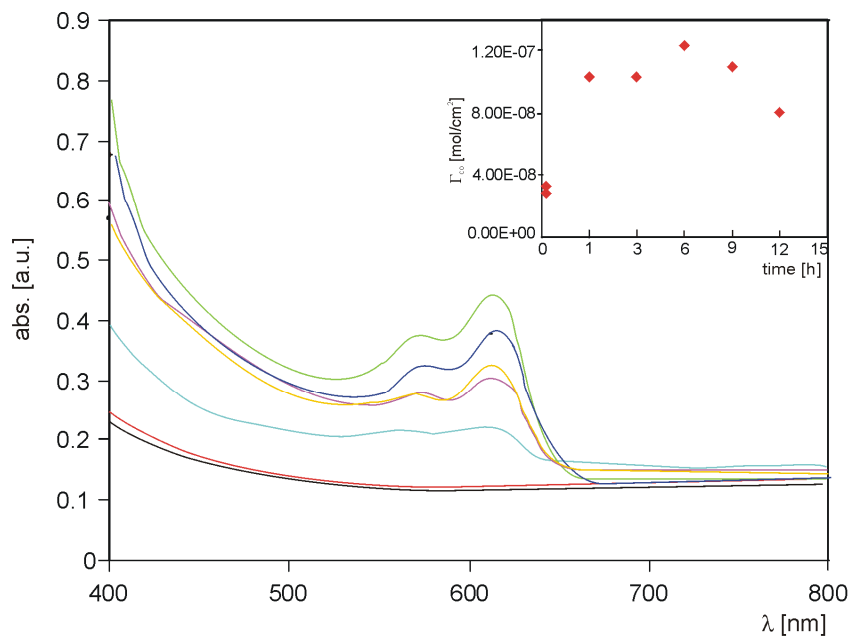


Figure 5.2. Cascade reaction times and absorption of vitamin B₁₂ modified electrodes E-1-(CC7-CC4)₁ after —E_{T02} — E-1 — 1h, — 3h, — 6h, — 9h and — 12h; inset : Γ_{∞} versus reaction time; 525 nm $\epsilon = 2512$; electrodes pretreated with KCN 1h, r.t.

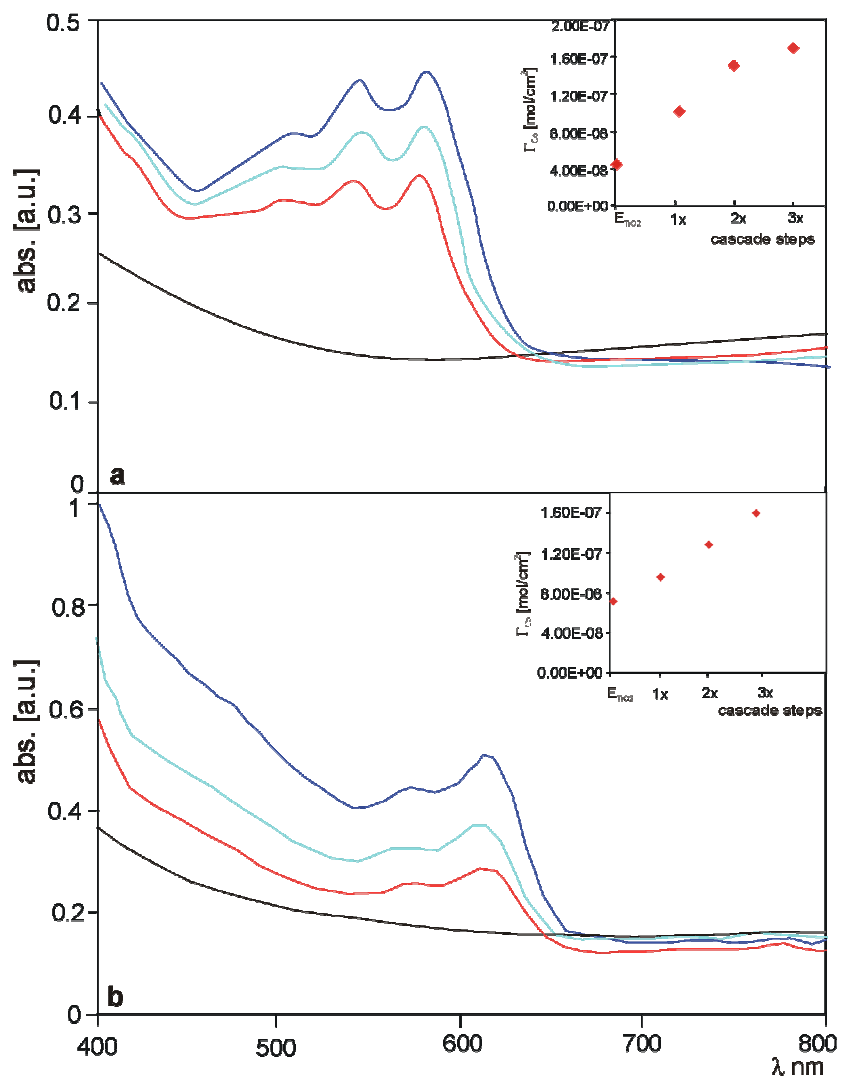


Figure 5.3. Cascade reaction steps and absorption of vitamin B₁₂ modified electrodes a) E-CC3-(CC6-CC3)_n and b) E-1-(CC7-CC4)_n (—E_{T02}, — one, — two and — three cascade steps) inset : Γ_{∞} versus cascade reaction steps, 525 nm $\epsilon = 2512$, electrodes pretreated with KCN 1h, r.t.

The calculated values for the surface concentrations of the oligomeric vitamin B₁₂ film are shown in table 5.1. For CV-measurements the influence of bipyridine must be eliminated. From figure 5.1 (5.1b, and 5.1c) the amount at bipyridine can be obtained by subtraction of the areas in figure 5.1c ($A_{Co} + A_{Bipyridine}$) and in figure 5.1b (A_{Co} alone) (the corrected values (E-1-(**CC7-CC4**)_n) are shown in parentheses, table 5.1). In comparison to the UV measurements the values for CV are about 10 times less because the UV measurements were made in air (without the additional absorption of bipyridine).

$\Gamma \times 10^{-7}$ [mol/cm ²] at $\lambda=525$ nm, $\varepsilon =2512$								
E- CC15	E- CC16	E- CC17	E-1-(CC7-CC4) _n			E- CC3 -(CC6-CC3) _n		
			n=1	n=2	n=3	n=1	n=2	n=3
0,73	1,49	0,83	1,0	1,31	1,6	1,0	1,56	1,7
$\Gamma \times 10^{-7}$ [mol/cm ²] vs. Ag/AgCl, $v=5$ mV								
0,008*	0,11*	0,09*	1,07 (0,07)**	1,22 (0,12)**	1,33 (0,19)**	0,09*	0,16*	0,21*

* Modified electrodes were measured in 0,5M TBAP/PC with 1‰ HAc, $v=20$ mV, vs. Ag/AgCl;

**Corrected values without bipyridine values, modified electrodes were measured in 0,5M LP/PC with 1‰ HAc, $v=5$ mV, vs. Ag/AgCl

Table 5.1. Surface concentration [mol/cm²] of vitamine B₁₂ on TiO₂

5.3. The catalytic reduction of organic halide with E-1-(**CC7-CC4**)_n and E-**CC3**-(**CC6-CC3**)_n electrodes

The modified- electrodes were also tested with respect to the catalytic reduction of organic halides. The catalytic reduction of DBEt (232 μ mol) (Figure 5.4) with E-1-(**CC7-CC4**)₃ showed a characteristic catalytic current (III) at about -0.9V and the oxidation peak disappeared.

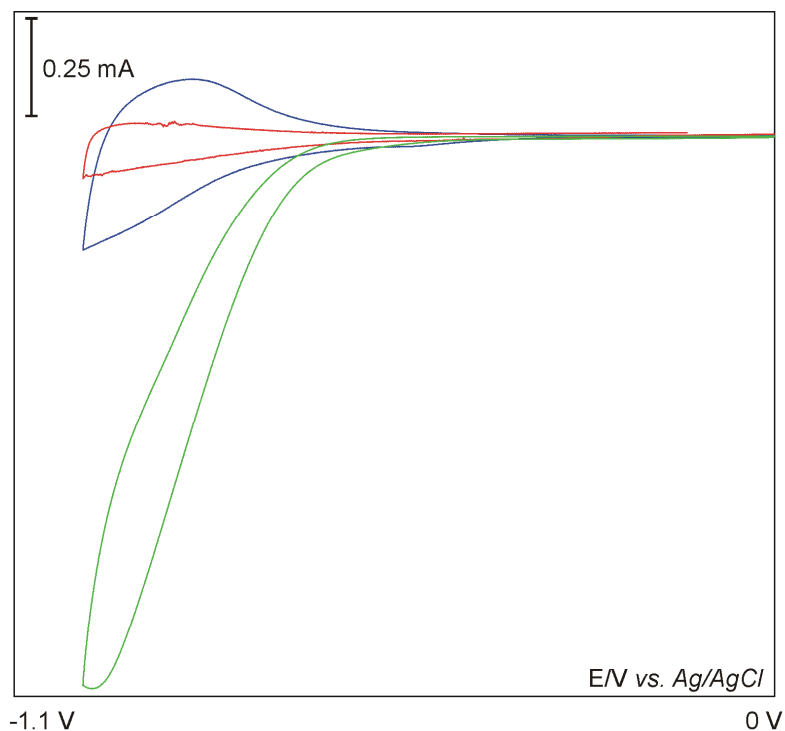


Figure 5.4. Electrocatalytic reduction of 1,2 - dibromoethane with E-1-(**CC7-CC4**)₃, $v = 20$ mV/s, 0.5 M TBAP/PC, C₂H₂Br₂ 0.023 mol/l, — E-TiO₂, — E-1, — E-1-(**CC7-CC4**)₃.

The calculated turnover number and turnover frequencies are presented in table 5.2

Electrode	Substrate	n substrate [μmol]	Q [C]	n catalyst [μmol]	TON*	TOF**
E- CC3 -(CC7-CC3) ₁	DBEt	232	2,7	0,05	260	787
E-1-(CC6-CC4) ₁	DBCH	146	25,2	0,05	2600	156
E-1-(CC6-CC4) ₂	DBCH	146	26,4	0,065	2104	191
E-1-(CC6-CC4) ₃	DBCH	146	24,6	0,08	1586	106
		73	12	0,08	750	374

DBCH = dibromocyclohexane, DBEt = 1,2 dibromoethane in Propylen carbonate/0,5 M Tetrabutylamonium perchlorate at -1,1V vs. Ag/AgCl.

*TON = (Q/2F)/n(cat), *TOF = TON/t(h⁻¹)

Table 5.2. Preparative reductive elimination on 0.5 cm² B₁₂ on TiO₂

In figure 5.5 a typical electrocatalytic curve is shown, as substrate using DBEt with E-**CC3**-(**CC6-CC3**)₁. It can be seen, that the catalytic activity of the electrode is abolished after 20 min; no residual current is observed. The reason could be the formation of an irreversibly polymeric layer on the electrode. The same results are obtained using multilayer electrodes of E-**CC3**-(**CC6-CC3**)₁₋₃ and also for E-1-(**CC7-CC4**)₁₋₃ electrodes. The catalytic reduction of DBCH at E-1-(**CC7-CC4**)_n electrodes work much better (see table 5.2).

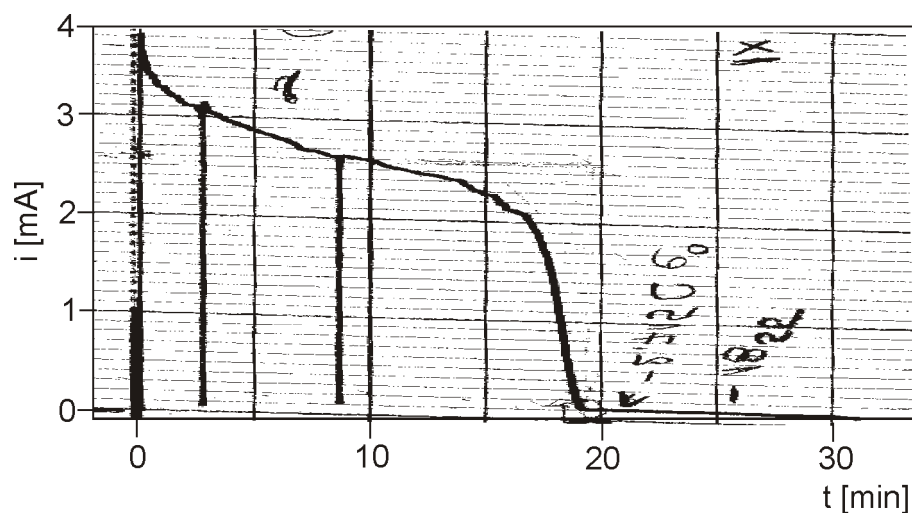


Figure 5.5. Catalytic activity of E-CC3-(CC6-CC3)_n current versus time
 $v = 20 \text{ mV/s}$, 0.5 M TBAP/PC , $\text{C}_2\text{H}_2\text{Br}_2$ 0.023 mol/l , vs. Ag/AgCl

Since the charge is higher than expected for the complete reduction of the substrate I suppose, that the bromide is oxidized at the anode and a small amount of Br_2 diffuses back into the cathode compartment, (in agreement with the weak yellow colour). *Rusling et al.* [134] found for coordinated $\text{B}_{12}/\text{TiO}_2$ a turnover frequency (TOF) of 100 h^{-1} . For my crosslinked electrodes E-1-(CC7-CC4)_n I obtain a turnover frequency (TOF) that is better, although the substrate was consumed and the electrodes showed still catalytic activity. This suggests that our cross-linked vitamin B_{12} derivatives on TiO_2 are even more efficient catalysts than only coordinated vitamin B_{12} on TiO_2 .

It should be mentioned, that these experiments could be further optimized for increased stability and turnover numbers.

In conclusion, cross-linking the vitamin B_{12} derivative can improve efficiency and stability of the electrodes.

Chapter 6

Synthesis and characterization of redoxactive subunits for the preparation of multilayer-modified electrodes

6.1. Redoxactive subunit-groups

As referred above, the main goal of this work was the creation of multilayered electrodes with electrochromic properties. The synthesis of the monomers, which are needed for the crosslinking cascade reaction on mesoporous surfaces, is described in the following.

Generally the synthesis of phenyl substituted bipyridines is in this work always done starting with dinitrobenzene, whereas those with a benzylic or alkyl residue are prepared from aliphatic and benzylic bromides.

In the first part three major groups of compounds were synthesised:

- 1) anchoring compounds
- 2) crosslinkers
- 3) terminal compounds

each of them with either electrophilic or nucleophilic properties.

In the second part of this work the synthesis of vinyl monomers, which can be used for electro-copolymerisation directly at the surface and a couple of monosubstituted ferrocenes are described. The ferrocenes were and crosslinked grown layer by layer (3 up to 20) on metaloxide electrodes. They were later used as transparent counter electrodes in electrochromic devices.

6.1.1. Synthesis of anchoring compounds

The first series of experiments consisted in the synthesis of mono viologen subunits, the electrophilic and nucleophilic compounds **1** to **10**, **23** and **24** equipped with different TiO₂ surface anchoring groups such as benzoate, salicylate and phosphonate (scheme 6.1).

Route **I** shows the preparation of the compounds **1**, **2**, and **6** to **9** according to a literature procedure [50, 51]. The intermediately formed compound N-(diethylphosphono-2-ethyl)-4,4'-bipyridinium bromide **0.1** is the starting point for the subsequent synthesis of different symmetrical and asymmetrical anchoring molecules. The intermediate **0.1** has been prepared in moderate yield (55%) from 4,4'-bipyridine and 2-bromoethane-diethyl phosphonate via an S_N2 mechanism in a Menschutkin- type reaction. Under these conditions double alkylation was excluded. The monomeric viologen **2,6,7,8** was obtained by treatment of the intermediate **0.1** with alkyl- and aryl bromides in MeCN (route **Ib**). All intermediate dicationic products **0.1** to **0.5** were precipitated from MeCN as the dibromides in good yield.

Synthesis of **24** was not successful using the sequence of route **Ic**. The first step consisting in quaternization of **0.1** applying an excess of 1,2-dibromoethane to intermediate **0.6**. Finally, elimination of HBr was initiated in N-ethyldiisopropylamine with good yield (83%). The hydrolysis in 1 M HBr of the corresponding vinyl diethyl phosphonates **0.7** was not easy, because polymerisation could not be prevented completely during the reaction.

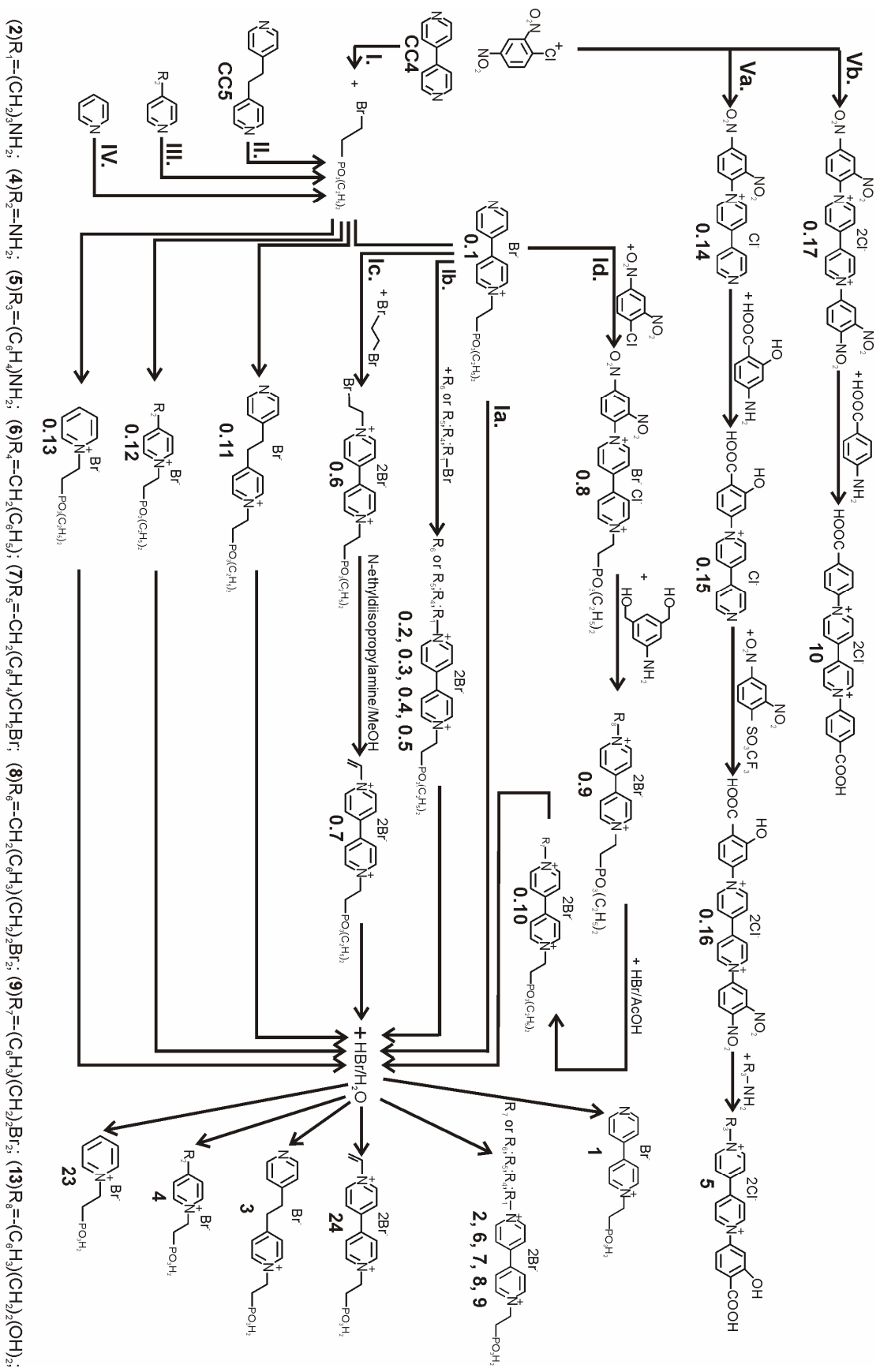
2-Bromoethane-diethyl phosphonate, pyridine or substituted pyridines (route **II** to **IV**) can also react to the uncoloured anchoring molecules (**3**, **4**) or to the repellent (**23**) using a similar procedure as described above.

Solvolysis of all resulting diethylphosphonate derivatives **0.1** to **0.7**, **0.10** to **0.13** was achieved by refluxing the compounds for 48 h in 1 M HBr to yield the corresponding phosphonic acids **1**, **2**, **6** to **9**, **23** and **24** as hygroscopic bromides.

The monomeric benzoate and salicylate viologens **5** and **10** were obtained following a similar reported synthesis [50]. 4,4'-Bipyridin was converted with 1-chloro-2,4-dinitrobenzene by a nucleophile substitution reaction to the intermediately formed compound **0.14** by route **Va**, and **0.17** by route **Vb** according to [135]. The reaction is known as *Sanger method* for the determination of the N terminal amino acids in a peptid rest. The chlorine atom of the 2,4- dinitrobenzene is activated as a lewis group by the two nitro groups. The aniline derivatives are created by opening ring.

This type of reaction is known since approximately 100 years [136] but the mechanism was examined in detail only 70 years later [137]. The resulting dinitro-intermediate is a well known starting material for the synthesis of diphenylbipyridinium salts. Route **Va** shows the preparation of the asymmetrically compound **5**. The first step consists in the mono-quaternization of 4,4'-bipyridyl resulting in the mono-substituted compound **0.14**. This is converted with 4-amino salicylic acid in EtOH to intermediate **0.15** followed by a second quaternization (step two) with 1-trifluoromethanesulfonyl-2,4-dinitrobenzene (triflat) to dinitro-derivate **0.16**. Finally intermediate **0.16** was treated with phenylendiamine in MeOH to yield the product **5**. The preparation of **10** involved the intermediate **0.17** followed by the substitution with 4-amino benzoic acid in good yield.

The detailed steps for synthesis of all compounds are described in chapter 6.2.



Scheme 6.1. Synthesis of the viologen anchoring groups

6.1.2. Synthesis of crosslinkers

In the second series 2-, 3- and 4-fold crosslinker viologen monomers were synthesised (scheme 6.2).

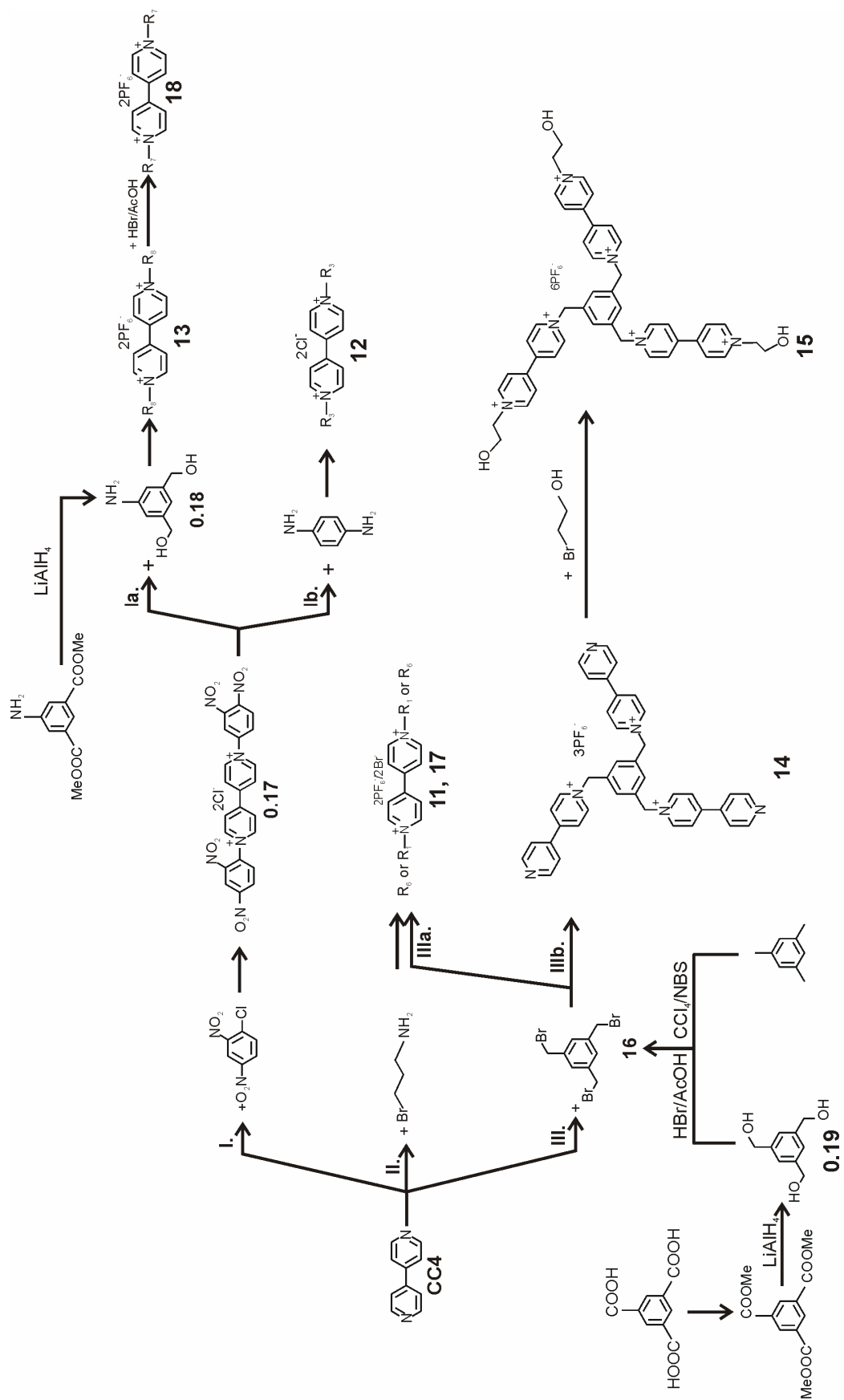
The conjugated 4-fold electrophilic **13**, respectively nucleophilic phenyl crosslinkers **18** have been prepared according to route **la**. The starting material **0.17** (synthesised according to a literature [135, 138, 139], has reacted with 3,5-di(hydroxymethyl) aniline **0.18** synthesized according to literature [140-143] by the reaction of 5-amino-isophthalacid-dimethylester and lithium-aluminium hydride. The electroactive counter anions of compound **0.17** were exchanged to hexafluorophosphate in aqueous solution of NH_4PF_6 before reaction with **0.18**. This was necessary after each reaction step, because the products can be isolated without difficulty as hexafluorophosphate salts. The compound **13** as PF_6^- -salts is good soluble in hydrobromic acid/acetic acid and further can be converted to tetra- bromide **14** PF_6^- - salt in good yield (78%).

The conjugated 2-fold electrophilic crosslinker **12** was prepared according to route **lb**. by the reaction of **0.17** as Cl^- salt and p-phenylenediamine in 80% ethanol. The reaction of 1-(2,4-dinitrophenyl)pyridinium chloride with aniline forming a intermediate pentamethine salt `Zincke salts` and 2,4-dinitroaniline is known as the Zincke reaction. This process is now the standard route to N-arylpyridinium salts which cannot be formed by direct reaction of electrophilics and pyridine [144]. The mechanism consists in two stages ring opening-ring closing and the excess amine does play an important role in assisting proton transfer in conversion of Zincke salts to Zincke product.

Route **II** yields the nucleophilic 2-fold crosslinker by alkylating 4,4'-bipyridine with γ -bromopropylamine hydrobromide in anhydrous ethanol in acceptable yield and a high degree of purity [145]. Formation of the monoalkylation works readily while the second alkylation is slower because of the lower nucleophilicity of the unalkylated pyridine. Therefore the ethanol is a good solvent for the monoalkylation product, allowing the reaction to proceed to the dialkylated stage.

According to route **III** one can obtain the electrophilic 3-fold crosslinker **16** by nucleophyl aryl substitution with LiAlH_4 in dry ether of 1,3,5-trimethoxybenzene to 1,3,5-tris(hydroxymethyl)benzene, followed by treatment with HBr/AcOH to 1,3,5-tris(bromomethyl)benzene [146-148] or by a radical allylic bromination from mesitylen

with N-bromosuccinimide and dibenzoylperoxid/light as catalyst in CCl_4 (low yield 11%) [149]. The compound **16** plays the role of the 'performed branching unit' in the divergent synthesis of dendrimers and is further used for the synthesis of electrophilic 4-fold crosslinker **17** (routes **IIIa**) or the 3-fold nucleophilic **14** and **15** respectively crosslinker (route **IIIb**). The symmetrically substituted 1,1'-[di-3'',5''-bis-(bromomethyl) benzyl]-4,4'-bipyridinium di-hexafluorophosphat **17** was synthesised according to a literature procedure [88] by the alkylation of 4,4'-bipyridine with an excess of 1,3,5-tris(bromomethyl)benzene **16** followed by ion exchange with NH_4PF_6 . Similarly, the well-known trifunctional crosslinker 1,3,5-tris[(-4,4'-bipyridinium)methyl]benzene trihexafluorophosphat **14** consisting of a mesityl derivative, linked to three 4,4'-bipyridine units, was prepared by reaction of compound **16** with an excess of 4,4'-bipyridine in MeCN. For the purpose of crosslinking directly at the electrode surface, the electroactive counter anions were exchanged to hexafluorophosphate in an aqueous solution of NH_4PF_6 [150]. Compound **14** as bromide salt react with the three peripheral nitrogens quantitatively with bromethanol to 1,3,5-tris[(N-hydroxyethyl-4,4'-bipyridinium)methyl]benzene hexabromide **15** [23]. The detailed steps for synthesis of all compounds are described in chapter 6.2.



(11)R₃=(CH₂)₃NH₂; (12)R₃=(C₆H₄)NH₂; (17)R₆=CH₂(C₆H₃)(CH₂)₂Br₂; (18)R₇=(C₆H₃)(CH₂)₂Br₂; (13)R₈=(C₆H₃)(CH₂)₂(OH)₂; (15)R₈=(CH₂)₂OH;

Scheme 6.2. Synthesis of 2-, 3-, and 4-fold crosslinking viologen monomers

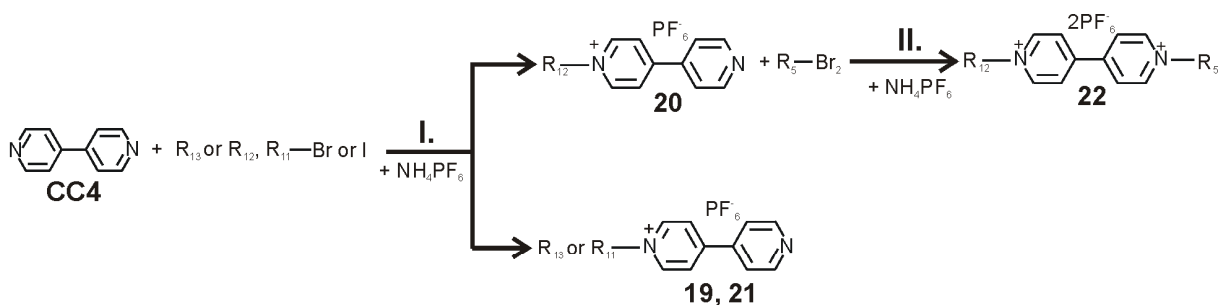
6.1.3. Synthesis of the end group compounds

As shown in scheme 6.3, in the third series of experiments viologen monomers as end groups were synthesised.

Following route **I** nucleophilic end groups were prepared according to a literature procedure [50] by the nucleophilic substitution of 4,4' bipyridinium using a ten-fold excess of aliphatic bromide or iodide to N-methyl-, N-ethyl- and N-propyl-4,4' bipyridinium bromide/iodide respectively (**19**, **20**, **21**).

Route **II** shows the corresponding procedure for the synthesis of electrophilic end groups. 1-[4-(Bromomethyl)benzyl] 1'-ethyl 4,4' bipyridinium dibromide **22** was prepared by a similar synthesis [50] from compound **20** using an excess of α,α' -dibromo-p-xylene in MeCN. For the purpose of crosslinking directly at the surface electrode, the electroactive counter anions of all compounds were finally exchanged to hexafluorophosphate in an aqueous solution of NH_4PF_6 .

The detailed steps for synthesis of all compounds are described in chapter 6.2.



(**19**) $\text{R}_{11} = \text{-CH}_3$; (**20**) $\text{R}_{12} = \text{-C}_2\text{H}_5$; (**21**) $\text{R}_{13} = \text{-C}_3\text{H}_7$;

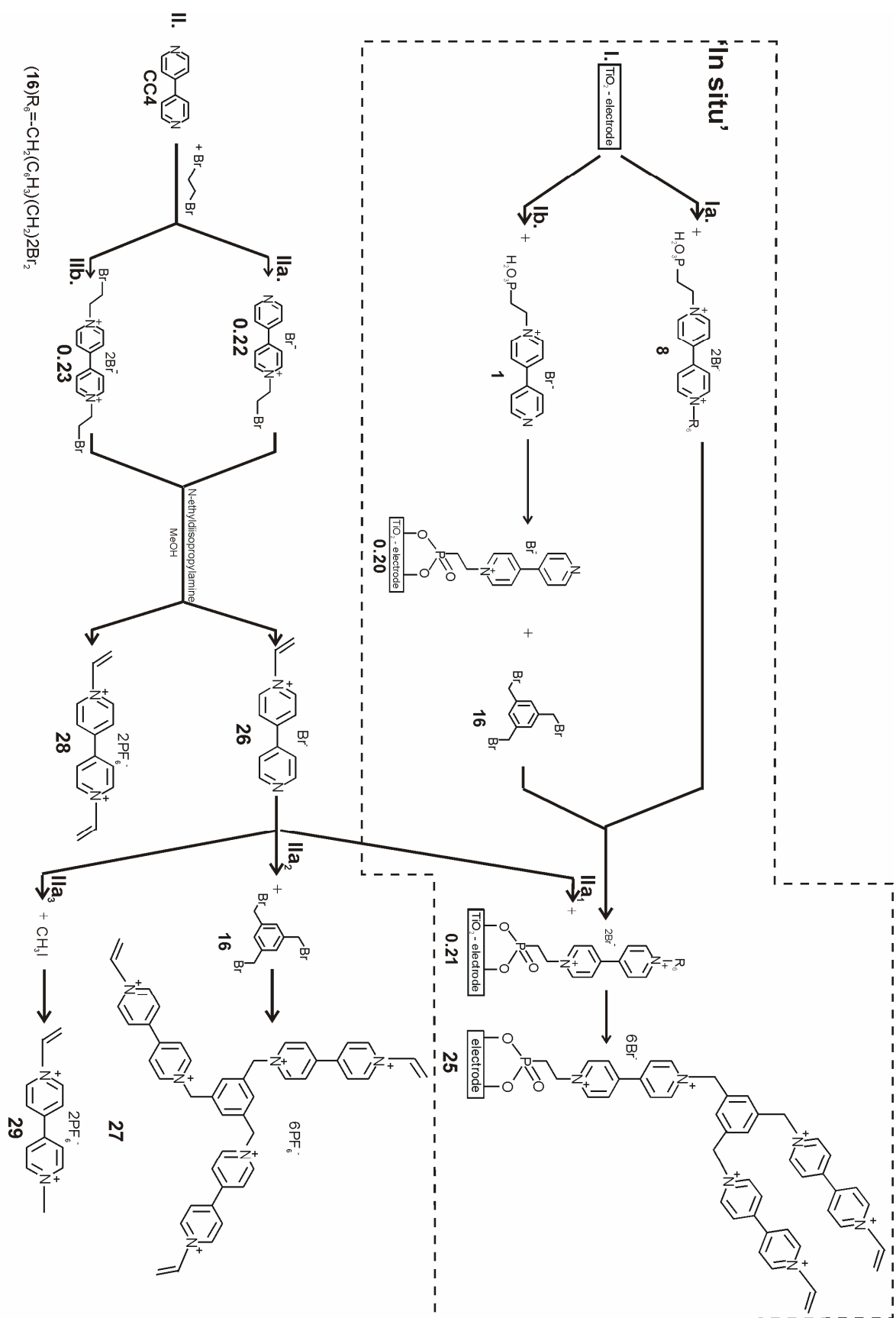
Scheme 6.3. Synthesis of the end group viologen monomers

6.1.4. Synthesis of vinyl monomers

Scheme 6.4 shows, how the vinyl monomers were synthesised. These compounds were electro(co)polymerisation directly at the surface. Route **I** shows an „in situ“ synthesis of vinyl viologen 2 {1'-[3,5- bis- (1' vinyl- 4,4' bipyridinyl-1-ylmethyl)-benzyl]-4,4' bipyridinyl-1-yl}-N-(phosphono-2-ethyl)-hexa-bromide **25** directly at the surface, because the synthesis of the anchoring group **24** was not successful. The polymerisation of anchoring group **24** could not be completely prevented during the

final eliminations step of the synthesis. When the elimination is made directly at the surface of the electrode, the polymerisation could be avoided. The „in situ“ synthesis can be made in one or two reaction steps according to scheme 6.4 route **la** and **lb** respectively. After exposing the TiO₂-plates to the anchoring electrophilic solution **17** at 1mM concentration in EtOH:H₂O (95:5% vol.), 1h at 20°C, the plates are treated with vinyl-bipyridine **26** at 20 mM concentration in MeCN, 4h at 60°C, to produce the surface confined compound TiO₂-**25** (route **la**). The structure elucidation is based on spectroscopic and electrochemistry techniques. Similarly, the compound **25** can be obtained in two reactions steps (route **lb**). The ink-jetted TiO₂-plates were exposed to the anchoring nucleophilic solution **1** at 1 mM concentration in EtOH:H₂O (95:5% vol.) for 1h at 20°C followed by alkylation of the compound **16** at 20 mM concentration in MeCN, 4h at 60°C. The surface confined compound TiO₂-**25** can further be used in an electrocopolymerisation reaction directly at the surface with the vinyl containing compound **29**. The monomers **26** and **28**, used further in electrocopolymerisation reaction were obtained in two reactions steps according to scheme 6.4. (route **IIa** and **IIb** respectively). The first step consisted in the quaternization of 4,4' bipyridine using an excess of 1,2-dibromethane via the intermediate **0.22** and **0.23**, respectively. The elimination of HBr occurred smoothly under base condition (N-ethyl-diisopropylamine/methanol) to form the N-vinyl bipyridinium monocation **26** or N,N'-vinyl bipyridinium dication **28** in high yield [83, 151, 152]. The compound **27**, a trifunctional crosslinker with three peripheral vinyl groups, is obtained by reaction of compound **16** with an excess of vinyl- bipyridine **26** in MeCN following a procedure similar to the reported one [151].

The detailed steps for synthesis of all compounds are described in chapter 6.2.



Scheme 6.4. Synthesis of the vinyl-viologen monomers

6.1.5. Synthesis of substituted ferrocenes

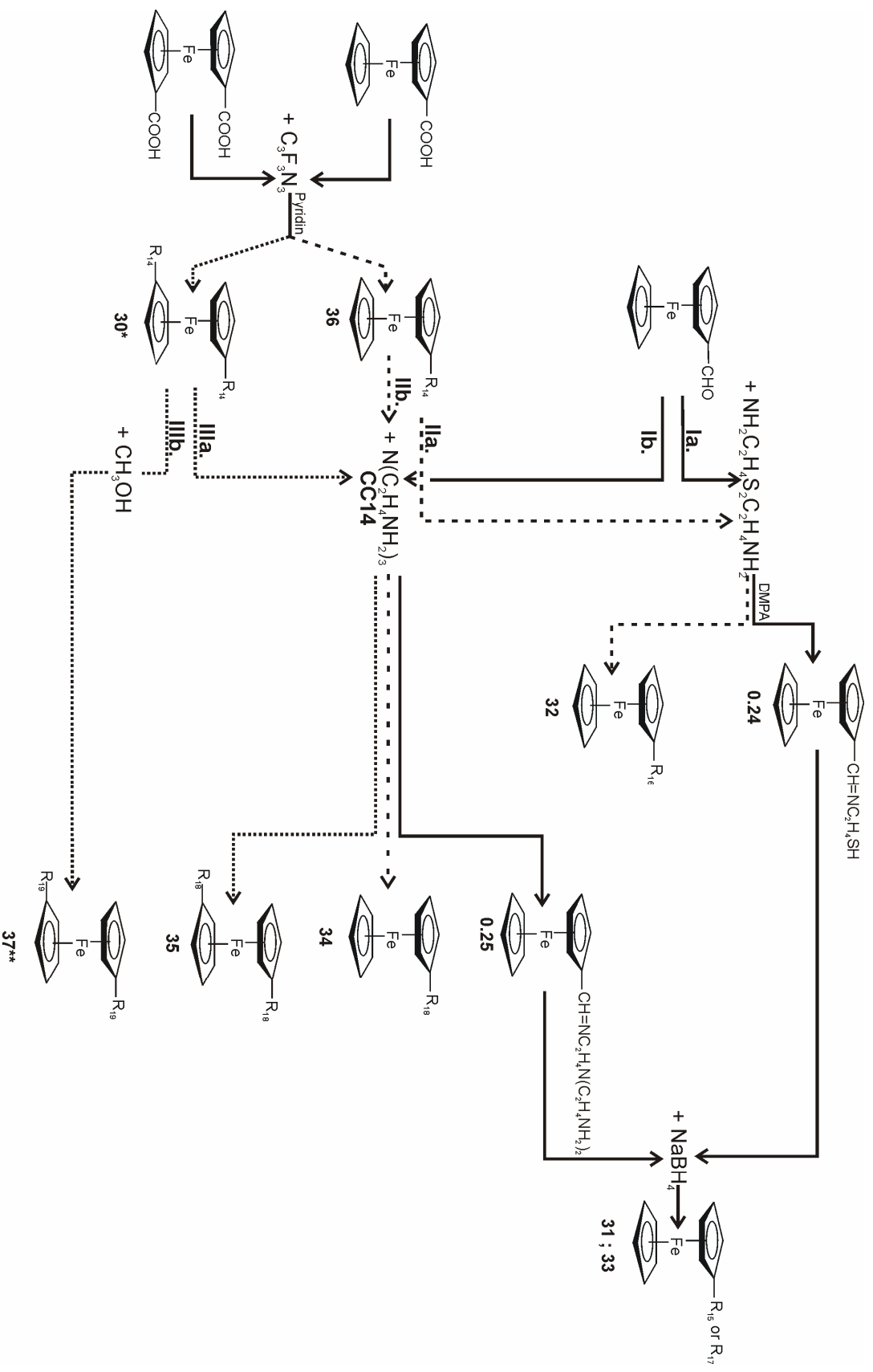
The monomeric ferrocenes **30-37** were synthesized according to scheme 6.5. The compound **33** was prepared according to a literature procedure [55] and **31** was obtained by similar synthesis from ferrocene aldehyde by reductive amination using the same amine, tris- N,N,N- (2-aminoethyl)amine and cystamine respectively via an intermediate Schiff base (route **la.** and **lb.**).

The fluorocarbonylferrocene and di-fluorocarbonylferrocene respectively (**30**, **36**) were prepared according to the method by *Galowd et al.* [153] from mono- and diferrocenecarboxylic with cyanuric fluoride and pyridine in dichlormethane as orange solid in 80% yield. The acid fluorides can be used with success in the synthesis of esters and amides because they are very reactive, stable, no aqueous workup is necessary and they react rapidly and efficiently with alcohols, primary and secondary amines to provide the corresponding esters and amides in good yield.

The monomers **32** and **34** respectively were synthesised according to a literature procedure [55] by reaction of the fluorocarbonylferrocene **36** and cystamine (route **Ila.**) or tris- N,N,N- (2-aminoethyl)amine (route **Ilb.**) respectively in one reaction step. Similar conditions were used to synthesise the monomer **35** by reaction of di-fluorocarbonylferrocene and tris- N,N,N- (2-aminoethyl)amine (route **IIla**). The product is soluble only in acidified water and therefore it cannot be used in the crosslinking reaction.

The monomer **37** was prepared according to the method by *Galowd et al.* by the reaction of di-fluorocarbonylferrocene in methanol in excellent yield (route **IIlb**).

The detailed steps for synthesis of all compounds are described in chapter 6.2.

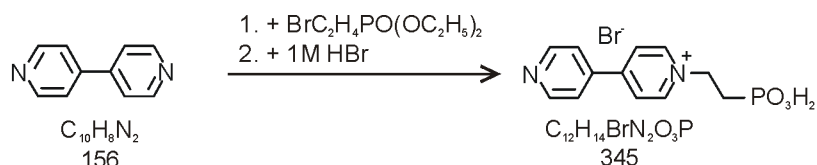


(36,30)R₁₄=COF; (31)R₁₆=CH₂NHC₂H₄SH; (32)R₁₆=CONHC₂H₄SH; (33)R₁₇=CH₂NHC₂H₄N(C₂H₄NH₂)₂; (34)R₁₈=CONHC₂H₄N(C₂H₄NH₂)₂; (37)R₁₈=COO⁻CH₃;

Scheme 6.5. Synthesis of the ferrocen monomers

6.2. Synthesis of monomers

6.2.1. Synthesis of 1-(2-phosphonoethyl)-4-pyridin-4-ylpyridinium bromide (1)

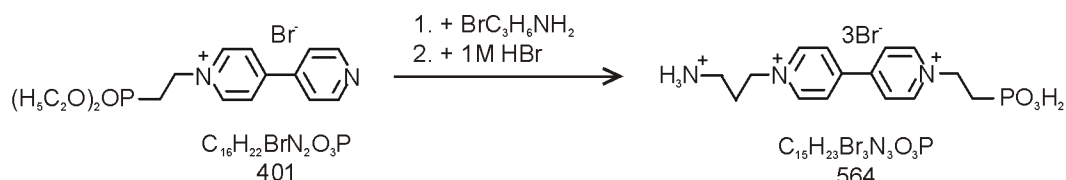


This synthesis follows a known procedure [146]. A suspension of 4 g (25.64 mmol) of 4,4'-bipyridyl with 14 g (57.14 mmol) diethyl 2-bromo-ethylphosphonate and in dibutyl ether (10 ml) was stirred at 50°C for 23 h under reflux. After approximately 30 minutes a white precipitate was obtained. The product was thoroughly washed with dry diethyl ether. The resulting yellow powder was dried for 12h in high *vacuo* (HV) (14.08 mmol, 55 % yields).

1-[2-(Diethoxyphosphoryl)ethyl]-4-pyridin-4-ylpyridinium salt (5.65 g, 14.08 mmol) was heated with 170 ml of HBr (1M, 72 h, 130°C) under reflux. The cold mother liquor was evaporated. The yellow powder was isolated and dried for 24h in HV (13.33 mmol 94.7% yield).

¹H-NMR: (250 MHz, D₂O): 9.04 (m, 4H), 8.54 (m, 4H), 4.94 (d, ³J[H,P] = 12.6Hz, ³J[H,H] = 7.6Hz, 2H), 2.50 (dt, ²J[P,H] = 12.9Hz, ²J[H,H] = 7.6 2H).

6.2.2. Synthesis of 1-(3-aminopropyl)-1' (phosphono-2-ethyl)- 4,4'-bipyridinium dibromide hydrobromide (2)



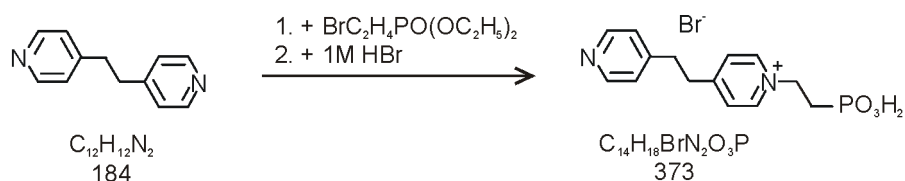
To a solution of 520 mg (1.29 mmol) of 1-[2-(diethoxyphosphoryl)ethyl]-4-pyridin-4-ylpyridinium bromide and 560 mg (2.55 mmol) of 1-bromo 3-aminopropyl hydrobromide in ethanol (20 ml) was stirred at 80°C for 72 h under reflux. After approximately 48 h a pale yellow precipitate was obtained. The warm mixture was

filtered, washed 3 times with dry diethyl ether and dried for 12h in HV (0.75 mmol, 58 % yield).

1-(3-Aminopropyl)-1'-[(diethoxyphosphory)ethyl] 4,4'-bipyridinium-salt (400 mg 0.64 mmol) was heated with 80 ml of HBr (1M, 72 h, 130°C) under reflux. The cold mother liquor was evaporated. The yellow powder was isolated and dried 24h in HV (0.61 mmol 95%, yield).

¹H-NMR: (250 MHz, D₂O): 9.0 (m, 4H), 8.44 (m, 4H), 4.86 (t, ³J[H,H] = 6.2 Hz, 2H), 4.75 (d, ³J[H,H] = 7.6 Hz, 2H), 3.08 (qu, ³J[H,H] = 6.2 Hz, 2H), 2.78 (m, 2H) 2.38 (dt, ²J[H,H] = 7.6 ²J[P,H] = 12.9 Hz, 2H).

6.2.3. Synthesis of 1-(2-phosphonoethyl)-4-(2-pyridin-4-ylethyl) pyridinium bromide (3)

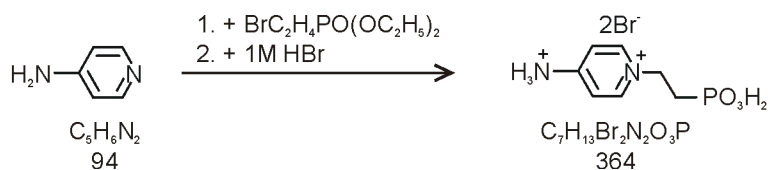


A suspension of 750 mg (4.07 mmol) of 1,2-bis(4-pyridyl) ethane in 3 g (12.24 mmol) of diethyl 2-bromo ethylphosphonate was stirred at 50°C for 24 h under reflux. After approximately 10 h a white precipitate was obtained. The mixture was filtered, washed three times with dry diethyl, and dried for 16 h in HV to obtain 1-[2-(diethoxyphosphory)ethyl]-4-(2-pyridin-4-ylethyl) pyridinium bromide (2.36 mmol, 58 % yields) as white powder was obtained.

1-[2-(Diethoxyphosphory)ethyl]-4-(2-pyridin-4-ylethyl) pyridinium salt (500 mg, 1.16 mmol) was heated with 80 ml of HBr (1M, 48h, 130°C) under reflux. The cold mother liquor was evaporated. The pale yellow powder was isolated and dried for 48h in HV (1.07 mmol 92%, yield).

¹H-NMR (250 MHz, D₂O): 8.64 (d, ³J[H,H] = 7.5 Hz, 2H), 8.54 (dd, ³J[H,H] = 17.5 Hz, ³J[H,H] = 10 Hz, 2H), 7.79 (m, 4H), 4.46 (dt, ³J[H,P] = 17.5 Hz, ³J[H,H] = 7.5 Hz, 2H), 3.30 (s, 4H), 2.50 (dt, ²J[H,H] = 7.6 Hz, ²J[P,H] = 12.9 Hz, 2H).

6.2.4. Synthesis of 4-amino-1-(phosphono-2-ethyl) pyridinium bromide hydrobromide (4)

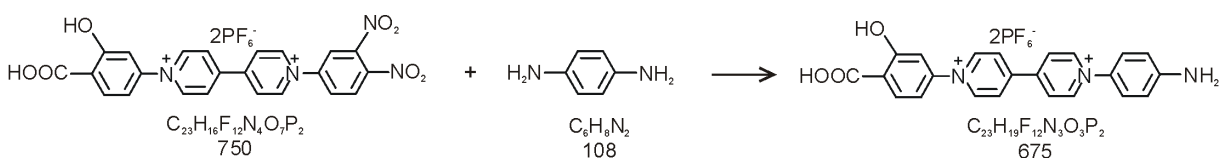


A mixture of 1 g (10 mmol) of 4-amino pyridine and 7.5 g (30.61 mmol) of diethyl 2-bromo-ethylphosphonate was stirred at 50°C for 23 h under reflux. The resulting precipitate was filtered and thoroughly washed with dry diethyl ether. The yellow powder was dried for 12h in HV (6.8 mmol, 68 % yields).

4-Amino-1-[2-(diethoxyphosphoryl)ethyl] pyridinium-salt (2 g, 5.8 mmol) was heated with 170 ml of HBr (1M, 72 h, 130°C) under reflux. The cold mother liquor was evaporated. The yellow powder was isolated and dried 24h in HV (5.1 mmol, 88%, yield).

¹H-NMR (250 MHz, D₂O): 7.90 (t, ³J[H,H] = 5.0 Hz, 2H), 6.78 (t, ³J[H,H] = 7.5Hz, 2H), 4.29 (t, ³J[H,H] = 5.5Hz, 2H), 2.45 (m, 2H).

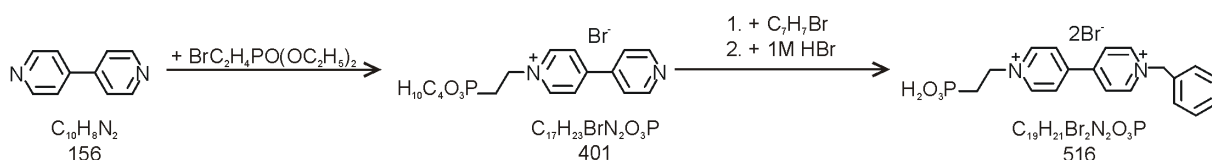
6.2.5. Synthesis of 1-(4-aminophenyl)-1'-(3-hydroxy-4-carboxyphenyl)-4,4'-bipyridinium dihexafluorophosphate (5)



80 mg (0.74 mmol) of phenyldiamine was dissolved in MeOH (20 ml) under argon, and 150 mg (0.192 mmol) of 1-(3-hydroxy-4-carboxyphenyl)-1'-(dinitrophenyl)-4,4'-bipyridinium dihexafluorophosphat were added in MeOH (30 ml) within 1.5 h (1 ml/3 minute) drop wise. The resulting red mixture was stirred for 24 h at 85°C under reflux. The mother liquor was evaporated, and the resulting dark residue was dissolved in MeOH (10 ml). The solution was dropped into 100 ml of diethyl ether; the resulting precipitate was filtered and washed with ether. After drying in *vacuo* (r.t. 24 h), 66 mg (0.098 mmol, 51%, yield) of a 1-(4-aminophenyl)-1'-(3-hydroxy-4-carboxyphenyl)-4,4'-bipyridinium dihexafluorophosphat as red powder was obtained.

¹H-NMR (250 MHz, CD₃CN): 9.22 (d, ³J[H,H] = 7.1Hz, 4H), 8.56(d, ³J[H,H] = 7.2Hz, 4H), 7.52 (d, ³J[H,H] = 2.5 Hz, 1H), 7.25 (m, 2H), 6.8 (s, 2H), 6.55 (d, ³J[H,H] = 12.5Hz, 2H).

6.2.6. Synthesis of 1-(phosphono-2-ethyl)-1'-toluoyl-4,4'-bipyridinium dibromide (6)

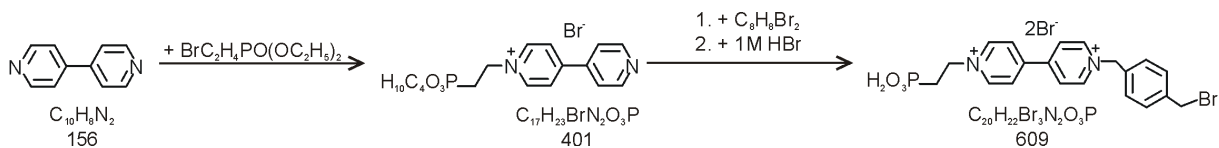


This synthesis follows a known procedure [146]. A suspension of 4 g (25.64 mmol) of bipyridine with 14 g (57.14 mmol) of diethyl 2-bromo-ethylphosphonate in dibutyl ether (10 ml) was stirred at 50°C for 23 h under reflux. After approximately 30 minutes a white precipitate was obtained. The product was thoroughly washed with dry diethyl ether. The resulting yellow powder was dried for 12h in HV (14.08 mmol, 55 % yield).

1-[2-(Diethoxyphosphory)ethyl]-4,4'-bipyridinium-salt (800 mg, 2 mmol) was dissolved in MeCN (10 ml) and 36 μ l (3 mmol) benzylbromide was stirred at 70°C for 7 h under reflux. After approximately 20 minutes a yellow precipitate was obtained. The precipitate was filtered and washed 2 times with MeCN (8 ml) and 2 times with dry CH₂Cl₂ (10 ml). The yellow powder was dried for 24h in HV (1.681 mmol, 84 % yield). 1-[2-(diethoxyphosphory)ethyl]-1'-toluoyl-4,4'-bipyridinium-salt (500 mg, 0.08 mmol) was heated with 170 ml of HBr (1M, 72 h, 130°C) under reflux. The cold mother liquor was evaporated and dried for 24h in HV. Yellow hygroscopic oil was isolated.

¹H-NMR (250 MHz, D₂O): 8.92 - 8.87 (m, 4H), 8.30 - 8.25 (m, 4H), 7.25 (s, 5H), 5.66 (s, 2H), 4.70 (m, 2H), 2.30 (dt, ²J[P,H] = 17.7 Hz, ²J[H,H] = 7.3Hz, 2H).

6.2.7. Synthesis of 1-[4-(bromomethyl)benzyl]-1'-(2-phosphonoethyl)4,4'-bipyridinium dibromide (7)



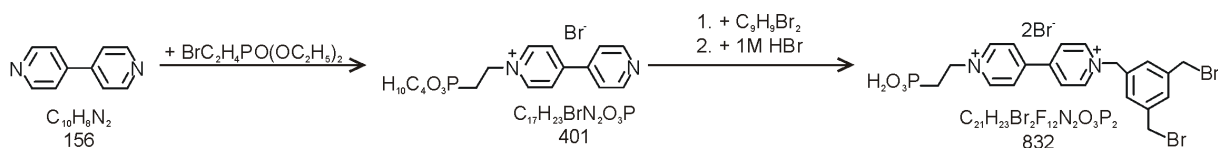
The synthesis was performed according to a literature procedure [50]. 4 g (25.64 mmol) of bipyridine with 14 g (57.14 mmol) of diethyl 2-bromo-ethylphosphonate and 10 ml of dibutyl ether was stirred at 50°C for 23 h under reflux. After approximately 30 minutes a white precipitate was obtained. The product was thoroughly washed with dry diethyl ether. The yellow powder was dried for 12h in HV (14.08 mmol, 55 % yield).

1-[2-(Diethoxyphosphory)ethyl]-4,4'-bipyridinium-salt (3 g, 7.4 mmol) was dissolved in MeCN (30 ml), and 2.9 g (11 mmol) of α,α' -dibromo-p-xylyl in MeCN (20 ml) was added drop wise. Immediately, a yellow precipitate was obtained. The mixture was stirred at 57°C for 6 h under reflux. The resulting precipitate was filtered and washed 2 times with MeCN and 2 times with dry diethyl ether. The yellow powder was dried for 24h in HV (6.6 mmol, 89 % yield).

1-[2-(diethoxyphosphory)ethyl]-1'-[(1-bromo p-xylyl - 4,4'-bipyridinium-salt (1,2 g, 1,8 mmol) was heated with 170 ml of HBr (1M, 72 h, 130°C) under reflux. The cold mother liquor was evaporated, and the orange powder was dried for 48h in HV (1.57 mmol, 87 % yields). The product is very hygroscopic.

¹H-NMR: (250 MHz, D₂O): 9.07 (d, ³J = 5 Hz, 2H), 9.05 (d, ³J = 5 Hz, 2H), 8.44 (d, ³J = 7,5 Hz, 2H), 8.43 (d, ³J = 2.5 Hz, 2H), 7.50 (d, ³J = 15 Hz, 2H), 7.39 (d, ³J = 10 Hz, 2H), 5.83 (s, 2H), 4.88 (dt, ³J[H,P] = 12.5 Hz, ³J[H,H] = 7.6 Hz, 2H), 4.70 (s, 2H), 2.41 (dt, ³J[H,P] = 18.5 Hz, ³J[H,H] = 7.5 Hz, 2H).

6.2.8. Synthesis of 1-[3,5-bis(bromomethyl)benzyl]-1'-(2-phosphonoethyl)-4,4'-bipyridinium dibromide (8)



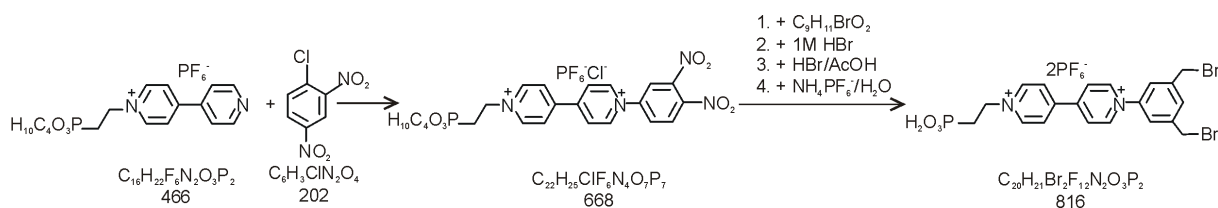
A solution of 1.5 g (3.7 mmol) of 1-[2-(diethoxyphosphoryl)ethyl]-4,4'-bipyridinium-salt (also prepared according to a literature procedure [146] and 2g (5.6 mmol) of 1,3,5-tris(bromomethyl)benzene in MeCN (30 ml) was stirred at 80°C for 7 h under reflux. From the beginning an intensive yellow precipitate were obtained. The yellow suspension was filtered; the filtrate was washed once with MeCN and four times with ether and dried for 16h in HV (3.0 mmol, 81 % yield).

1-[3,5-Bis(bromomethyl)benzyl]-1'-[2-(diethoxyphosphoryl)ethyl]-4,4'-bipyridinium salt (1g, 1,3 mmol) was dissolved in 170 ml of 1M HBr and heated for 48 h at 130°C under reflux. The cold mother liquor was evaporated, and the orange powder was dried for 48h in HV (1.06 mmol, 82 % yield). The product is very hygroscopic.

MS (25 °C, API-S positive): 540.8 (100, M⁺), 265 (80)

¹H-NMR(250 MHz, D₂O): 9.06 (m, 4H), 8.49-8.43 (m, 4H), 7.47 (s, 2H), 7.34 (s, 1H), 5.84 (d, ³J[H,H] = 12.4 Hz, 2H), 4.82 (dt, ³J[H,P] = 12.9 Hz, ³J[H,H] = 7.6 Hz, 2H), 4.49 (s, 4H), 2.40 (dt, ³J[H,P] = 18.1 Hz, ³J[H,H] = 7.4 Hz, 2H).

6.2.9 Synthesis of 1-[3,5-bis(bromomethyl)phenyl]-1'-(2-phosphonoethyl)-4,4'-bipyridinium hexafluorophosphate (9)



A solution of 4 g (8.5 mmol) of 1-[2-(diethoxyphosphoryl)ethyl]-4,4'-bipyridinium-salt (also prepared according to a literature procedure [146] and 13g (64 mmol) of 2,4-dinitro-chlorobenzene in MeCN (150 ml) was stirred at 90°C for 120 h under reflux. After approximately 4h first crystals were obtained. The mother liquor was evaporated; the residue was dissolved in MeCN. The mixture was kept at 6°C for 24 h. The precipitate was filtered and washed with cold water. The aqueous phase was evaporated, and a yellow precipitate was thoroughly washed with MeCN. A white powder was obtained and dried for 24h in HV (2.0 mmol, 23 % yield). The product is very hygroscopic.

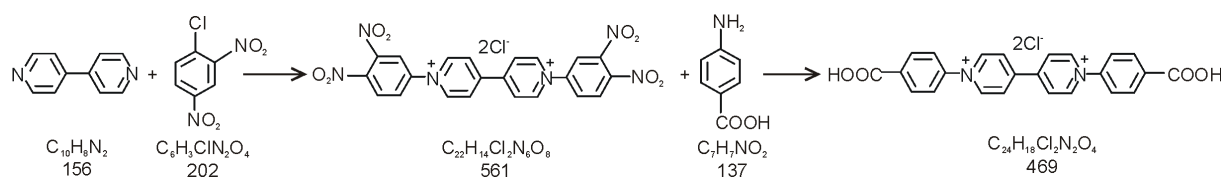
A solution of 250 mg (0.37 mmol) of 1-[2-(diethoxyphosphoryl)ethyl]-1'-(2,4-dinitrophenyl)-4,4'-bipyridinium salt and 132 mg (0.86 mmol) of (5-amino-1,3-phenylene)dimethynol in MeOH (50 ml) was stirred 7d at 70°C under reflux. The cold mixture was poured and brined into 100 ml of diethyl ether. The brown precipitate was filtered, the mother liquor was evaporated, and the resulting residue was dissolved in 15 ml of MeOH and dropped into 250 ml of diethyl ether. The mixture was kept at 6°C for 24 h. The brown precipitate was filtered, washed with diethyl ether and dried for 6 h in HV (0.28 mmol, 75% yield).

1-[3,5-Bis[hydroxymethyl]phenyl]-1'-[2-(diethoxyphosphoryl)ethyl]-4,4'-bipyridinium-salt (150 mg, 0.23 mmol) was dissolved in 170 ml 1M HBr and heated for 48 h at 130°C under reflux. The cold mother liquor was evaporated, and the light yellow powder was dried for 24 h in HV (0.22 mmol, 95 % yield).

The product was then dissolved in 100 ml of HBr/AcOH and stirred for 96 h at 24 °C under argon. The reaction mixture was treated, with 10 ml of water and 5 ml of a 10% NH₄PF₆ solution. The brown precipitate was filtered, washed with water and ether. A light brown powder was isolated which was dried for 24 h in HV (0.15 mmol, 68 % yield).

¹H-NMR: (250 MHz, D₂O): 9.29 (d, ³J[H,H] = 6,9 Hz, 2H), 9.14 (d, ³J[H,H] = 7,0 Hz, 2H), 8.65 - 8.58 (m, 4H), 7.64 (s, 3H), 4.99 - 4.92 (m, 2H) 4.53 (s, 4H), 2.49 (dt, ³J[H,P] = 18.4 Hz, ³J[H,H] = 7.4 Hz, 2H).

6.2.10. Synthesis of 1,1'-bis[(4-carboxyphenyl)-4,4'-bipyridinium dichloride (10)

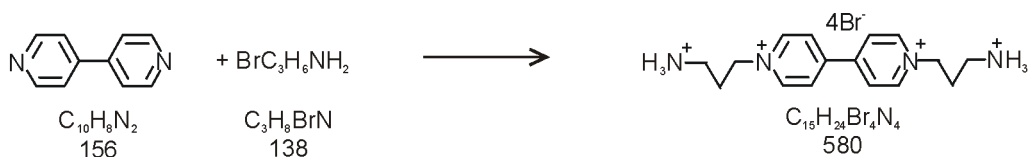


The synthesis follows a known procedure [139]. 4 g (25.6 mmol) of 4,4'-bipyridine and 26 g (89,6 mmol) of 2,4-dinitro-chlorobenzene in MeCN (150 ml) was stirred at 90°C for 24 h under reflux. At the beginning, the solution was clear brown, after 4 h first yellow crystals were obtained. The yellow suspension was filtered. The filtrate was washed once with MeCN (50 ml) and four times with diethyl ether (40 ml), and dried for 16 h in HV (19 mmol, 74% yield).

To a solution of 841 mg (1,5 mmol) of 1,1'-(2,4- dinitrophenyl)-bipyridinium salt in 30 ml of ethanol, 904 mg (6.6 mmol) of 4-amino benzoic acid in ethanol (70 ml) was dropped slowly. After 1.5 h the mixture was colored to dark red. The mixture was stirred at 90°C for 3h. The solvent was evaporated, the resulting residue was dissolved in 30 ml of water, and the reaction was continued for 24h at 100°C. The mother liquor was evaporated. The resulting residue was dissolved in MeOH (40 ml) and dropped into 250 ml of diethyl ether. The brown precipitate was filtered, washed three times with 40 ml of ethylacetate, three times with 40 ml of diethylether and dried for 16 h in HV (1.1 mmol, 73% yield).

¹H-NMR: (250 MHz, MeOH): 9.67 (d, ³J[H,H] = 7.0Hz, 4H), 8.99 (d, ³J[H,H] = 7,0 Hz, 4H), 8.44 (d, ³J[H,H] = 7.5Hz, 4H), 8.07 (d, ³J[H,H] = 7.5Hz, 4H).

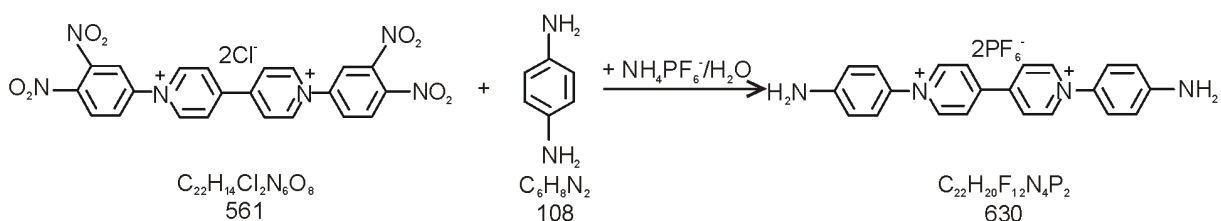
6.2.11. Synthesis of 1,1'-bis(2-ammoniopropyl)-4,4'-bipyridinium tetrabromide (11)



The procedure follows a reported synthesis [145]. To a solution of 25 g (118 mmol) of 3-bromopropylamine hydrobromide in 125 ml of anhydrous ethanol at 45 °C was added 8.3 g (53 mmol) of 4,4' bipyridine dissolved in 100 ml of ethanol. The mixture was refluxed at 80°C for 45 h. After 2 h a pale yellow solid was obtained. The warm mixture was filtered, washed with ethanol and acetone and then reprecipitated from an aqueous solution with ethanol. The pale yellow powder was dried for 12 h in HV (24 mmol, 45 % yield).

¹H-NMR: (250 MHz, D₂O): 9.16 (d, ³J[H,H] = 7.5 Hz, 4H), 8.57 (d, ³J[H,H] = 7,5 Hz, 4H), 5.05 (t, ³J[H,H] = 6.2 Hz, 4H), 3.70 (t, ³J[H,H] = 6.3 Hz, 4H).

6.2.12. Synthesis of 1,1'-bis(4-aminophenyl)-4,4'-bipyridinium dihexafluorophosphate (12)

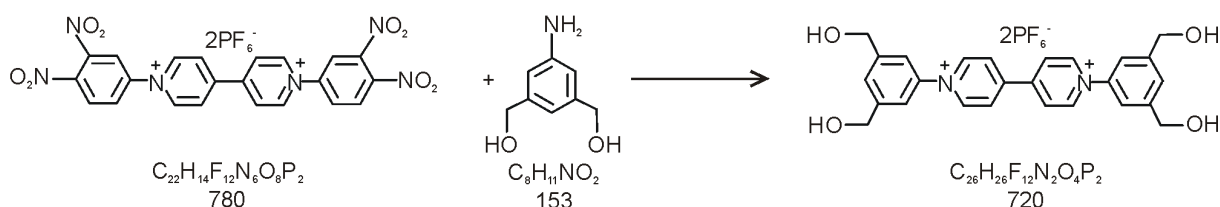


Phenyldiamine (186 g, 1.73 mmol) was dissolved in MeOH (20 ml) under argon, and a solution of 150 mg (0.192 mmol) of 1,1'-(2,4- dinitrophenyl)-bipyridinium salt (also prepared according to a literature procedure [139]) in MeOH (30 ml) was added dropwise within one hour. At the beginning the mixture was colored to dark red. The mixture was stirred at 90°C for 24 h under reflux and argon atmosphere. The solvent was evaporated, and the resulting residue was dissolved in 30 ml of

water and treated with 10 ml of a 10% NH_4PF_6 solution. The red precipitate was filtered off, washed with water and ether. A red powder was isolated which was for dried for 24h in HV (0.101 mmol, 52% yield). The product is hygroscopic.

$^1\text{H-NMR}$: (250 MHz, CD_3CN): 8.94 (d, $^3\text{J}[\text{H},\text{H}] = 7.0$ Hz, 4H), 8.42 (d, $^3\text{J}[\text{H},\text{H}] = 7.0$ Hz, 4H), 7.38 (d, $^3\text{J}[\text{H},\text{H}] = 7.5$ Hz, 4H), 6.81 (d, $^3\text{J}[\text{H},\text{H}] = 7.5$ Hz, 4H).

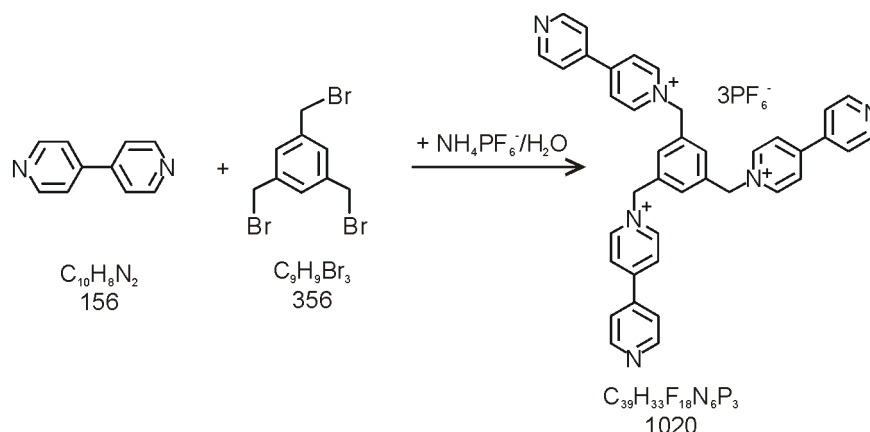
6.2.13. Synthesis of 1,1'-bis [3,5-bis(hydroxymethyl)phenyl]-4,4'-bipyridinium dihexafluorophosphate (13)



The synthesis was performed according to a literature procedure [146]. A mixture of 1 g (1.28 mmol) of 1,1'-bis [3,5-bis(hydroxymethyl)phenyl]-4,4'-bipyridinium dihexafluorophosphate and 460 mg (3.1 mmol) of (5-amino-1,3-phenylene)dimethanol in 50 ml MeOH was stirred at 70°C for 23 h under reflux. The cold mixture was poured into 100 ml of brined diethyl ether. The brown precipitate was filtered off and washed three times with ether; a brown powder was obtained and dried for 6 h in HV (1.14 mmol, 89 % yield).

$^1\text{H-NMR}$: (250 MHz, DMSO-d_6): 9.68 (d, $^3\text{J}[\text{H},\text{H}] = 6.1$ Hz, 4H), 9.03 (d, $^3\text{J}[\text{H},\text{H}] = 6.2$ Hz, 4H), 7.74 (s, 4H), 7.68 (s, 2H), 5.58 (b, 4H), 4.70 (s, 8H).

6.2.1.4. Synthesis of 1,1',1''-[benzene-1,3,5-triyltris(methylene)tris](4-pyridin-4-ylpyridinium trihexafluorophosphate (14)

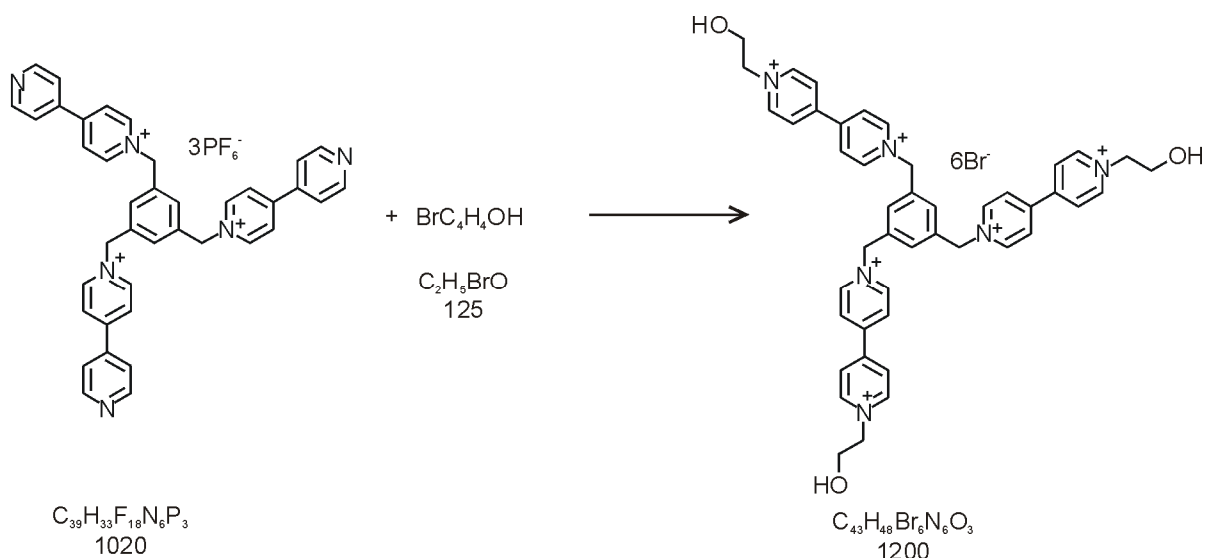


The synthesis was performed according to a literature procedure [146]. 4,4'-Bipyridine (14 g, 89 mmol) was dissolved in warm MeCN (80 ml), and 5 g (5.8 mmol) of 1,3,5 tris (bromomethyl) benzene was added in 50 ml MeCN within 7 h (1 ml/8,5 minute). The mixture was stirred at 70°C for 30 h under reflux. The cold mixture was filtered and washed three times with CH₂Cl₂. The filter cake was dissolved in water and extracted four times with CH₂Cl₂. Methanol was added dropwise to initiate the precipitation. A yellow powder was obtained and dried in HV (4.4 mmol, 74% yield as bromide salt).

The bromide -salt (3.2 g, 3.88 mmol) was dissolved in 80 ml of water, and 15 ml of a NH₄PF₆ 10% was added dropwise. The precipitate was filtered and washed with cold water; a white powder was obtained and dried for 24 h in HV (2.7 mmol, 78% yields).

¹H-NMR: (250 MHz, CD₃CN): 8.88 (d, ³J[H,H] = 6.3 Hz, 6H), 8.82 (d, ³J[H,H] = 7,0 Hz, 6H), 8.37 (d, ³J[H,H] = 7.0 Hz, 6H), 7.83 (d, ³J[H,H] = 6,3 Hz, 6H), 7.60 (s, 3H), 5.80 (s, 6H).

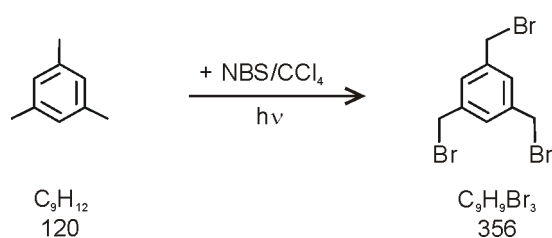
6.2.15. Synthesis of 1,1',1''- [benzene-1,3,5-triyltris(methylene)]tris(1'-hydroxyethyl- 4,4'-bipyridinium) hexabromide (15)



1,1',1''-[Benzene-1,3,5-triyltris(methylene)]tris(4-pyridin-4-ylpyridinium) trihexafluorophosphate (320 mg, 0.38 mmol) (prepared according to a published procedure [154]) was reacted in 2.5 ml of bromoethanol/10 ml methanol at 80 °C for 7 days. The mother liquor was evaporated, and the resulting red oil was dissolved in 50 ml of methanol and precipitated with 30 ml ether. The solid was isolated and washed with ether several times to remove excessive bromoethanol. After drying in vacuo (r.t., 24h), 320 mg (0.26 mmol, 70%) 1,3,5-tris-[(N-hydroxyethyl-4,4'-bipyridinium) methyl] benzol-hexabromide was obtained as yellow solid.

¹H-NMR (250 MHz, D₂O): 9.08 (s, 10H), 8.87 (s, 2H), 8.48 (s, 10H), 8.26 (s, 2H), 7.68 (s, 3H), 5.90 (s, 6H), 4.51 (superimposed by water, 6H), 4.03 (s, 4H), 3.46 (s, 2H).

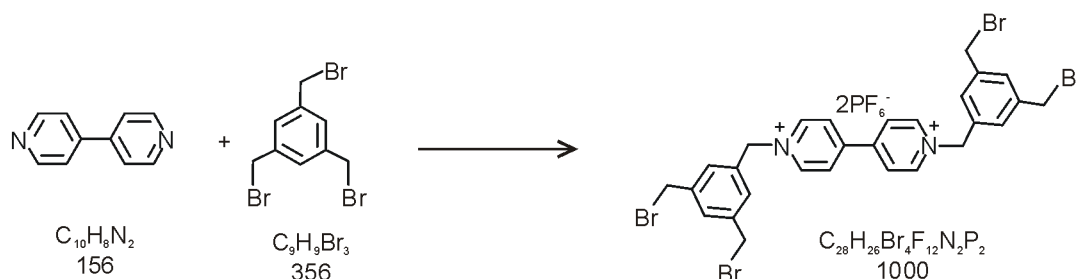
6.2.16. Synthesis of 1,3,5-tris-(bromomethyl) benzene (16)



The synthesis follows a known procedure [149]. Mesitylene (20 g, 166 mmol) and 95 g (530 mmol) N-bromo succinimide (NBS) dissolved in 500 CCl₄ (dried 24 h over CaCl₂ and distilled) was irradiated with a 500 W-lamp for 24 h and stirred at 70 °C for 30 h under reflux. The mixture was kept at 6 °C for 24 h. The succinimide was filtered off, and the solvent was evaporated. The residue was dissolved in CHCl₃, and washed once with an aq. NaHCO₃ solution and two times with H₂O. The organic layer was then dried (Na₂SO₄), filtered and CHCl₃ was evaporated. The oily residue was dried in HV, and then dissolved in CHCl₃, and petrol ether was added. Under these conditions the crystallization starts. The mixture was kept for 3 days at 6 °C. Light yellow crystals were obtained, isolated and dried for 24 h in HV (19 mmol, 12% yield).

¹H-NMR: (250 MHz, CDCl₃): 7.38 (s, 3H), 4.48 (s, 6H)

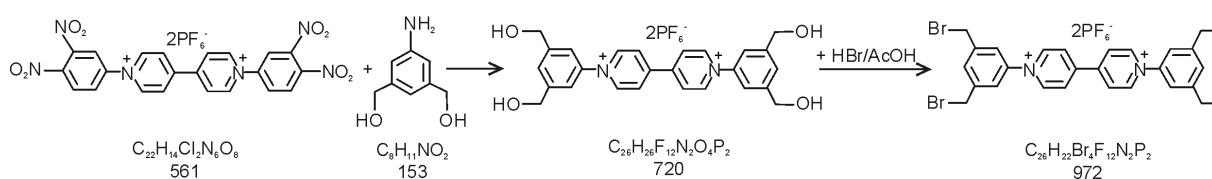
6.2.17. Synthesis of 1,1'-bis[3,5-bis(bromomethyl)benzyl]-4,4'-bipyridinium dihexafluorophosphate (17)



The synthesis was performed according to a literature procedure [88]. A solution of 1,3,5-tris-(bromomethyl)benzene (1.07 g, 2.9 mmol) in MeCN (10 ml) was reacted at 70 °C with a dropwise added solution of 150 mg (0.96 mmol) 4,4'-bipyridine in 8 ml MeCN. After 30 h the precipitate was collected, washed with MeCN and diethyl ether and dried *in vacuo* to yield 0.78 g (0.89 mmol) of 1,1'-bis[3,5-bis(bromomethyl)benzyl]-4,4'-bipyridinium as the corresponding dibromide salt (93 %). 500 mg of the dibromide (0.57 mmol) dissolved in 80 ml water was precipitated by addition to 10 ml aq. solution of 10 % NH₄PF₆, collected, washed with water and dried *in vacuo* for 24 h to yield 0.3 g (0.3 mmol) of 1,1'-bis[3,5-bis(bromomethyl)benzyl]-4,4'-bipyridinium dihexafluorophosphat (53 %).

¹H-NMR (250 MHz, DMSO): 9.5 (d, ³J[H,H]= 6.8 Hz, 4 H), 8.78 (d, ³J[H,H] = 5 Hz, 4 H), 7.62 (s, 6H), 5.94 (s, 4 H), 4.69 (s, 8H).

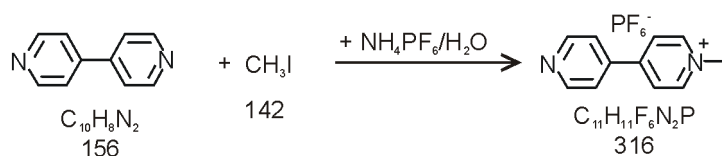
6.2.18. Synthesis of 1,1'-bis[3,5-bis(bromomethyl)phenyl]-4,4'-bipyridinium dihexafluorophosphate (18)



The synthesis was performed according to a literature procedure [146]. 1,1'-Bis[3,5-bis[hydroxymethyl]phenyl]-4,4'-bipyridinium salt (630 mg, 0.875 mmol) (also prepared according to a procedure already described, chapter 6.2.12.) was dissolved in 150 ml of HBr/acetic acid under argon and stirred for 4 d. at r.t. The reaction mixture was evaporated, and the residue was dissolved in 2 ml of water and 3 ml of a 10% aq. NH_4PF_6 solution was added. The brown precipitate was filtered, washed with water and dried in HV. The resulting brown powder was dissolved in MeNO_2 and 5 ml of 10% aq. NH_4PF_6 was added dropwise. The organic phase was filtered, and the light brown precipitate was washed with CHCl_3 , ether and water. A light brown powder was isolated and dried for 24 h in HV (0.501 mmol, 57% yield).

¹H-NMR: (250 MHz, CD_3CN): 9.20 (d, ³J[H,H] = 7.1 Hz, 4H), 8.66 (d, ³J[H,H] = 7.1Hz, 4H), 7.91 (s,2H), 7.81 (s, 4H), 4.71 (s, 8H), 4.70 (s,8H).

6.2.19. Synthesis of 1-methyl-4-pyridin-4ylpyridinium hexafluorophosphate (19)

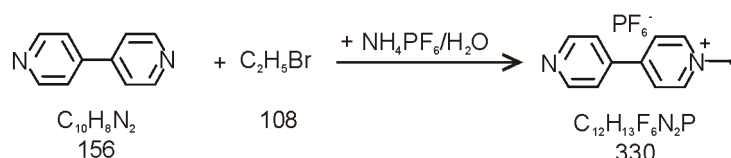


The synthesis was performed according to a literature procedure [155]. To a solution of 5 g (32 mmol) of 4,4'-bipyridyl in 20 ml of N-methyl-2-pyrrolidone (NMP), a solution of 3.42 g (24 mmol) of methyl iodide in 20 ml of NMP was added dropwise during 12 hours at 50°C. The resulting solution was stirred for another 3 hours, and then the solution was poured into 250 ml of toluene. The resulting precipitate was filtered off and washed 3 times with toluene to remove unreacted starting materials. Subsequently, the precipitate was dissolved in MeCN (600 ml), and the insoluble dimethylated by-product was filtered off. After evaporation of the solvent and drying in vacuo (r.t., 24h) 1-methyl-4,4'-bipyridinium iodide (17 mmol, 53% yield) was obtained.

1-Methyl-4,4'-bipyridinium salt (2.5 g, 8.3 mmol) was dissolved in water (20 ml) and added to 5 ml of a vigorously stirred 10% aq. NH_4PF_6 solution. The white precipitate was filtered, washed with water and dried for 24 in HV (6.1 mmol, 73%, yield).

$^1\text{H-NMR}$: (250 MHz, CD_3CN): 8.58 (d, $^3\text{J}[\text{H},\text{H}] = 6.5$ Hz, 2H), 8.23 (d, $^3\text{J}[\text{H},\text{H}] = 6.0$ Hz, 2H), 7.93 (d, $^3\text{J}[\text{H},\text{H}] = 6.0$ Hz, 2H), 7.38 (d, $^3\text{J}[\text{H},\text{H}] = 6.0$ Hz, 2H), 3.98 (s, 3H).

6.2.20. Synthesis of 1-ethyl-4-pyridin-4-ylpyridinium hexafluorophosphate (20)



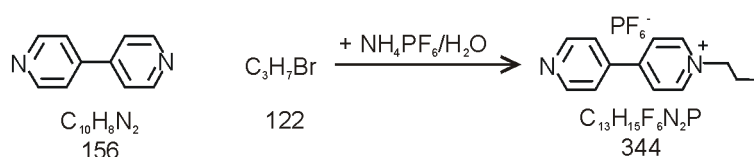
The synthesis was performed according to a literature procedure [83]. A suspension of 6 g (73.4 mmol) of 4,4'-bipyridyl with 50 g (459 mmol) of ethylbromide was stirred at 34°C for 50 h under reflux. After 30 min a brown precipitate was obtained. After 7 hours a further portion of 5 g ethylbromide in diethylether (30 ml) was added dropwise. The resulting precipitate was filtered and thoroughly washed with dry diethyl ether and toluene. The crystallization of the product proceeded slowly (48 h at 4 °C) from ethanol-ether-toluene. The resulting yellowish powder was dried for 24 h in HV (22 mmol, 30% yield).

1-Ethyl-4-pyridin-4-yl-pyridinium salt (4 g, 15 mmol) was dissolved in 80 ml of water, and 10 ml of a 10 % aq. NH_4PF_6 solution was added dropwise. The resulting solid

was filtered off, washed with cold water and dried for 24 h in HV (3.9 g 12.1 mmol, 80% yield).

¹H-NMR: (500 MHz, DMSO): 9.25 (d, ³J[H,H] = 12.5 Hz, 2H), 8.92 (d, ³J[H,H] = 4.8 Hz, 2H), 8.64 (d, ³J[H,H] = 6.5 Hz, 2H), 8.12 (d, ³J[H,H] = 4.1 Hz, 2H), 4.68 (q, ³J[H,H] = 7.3 Hz, 1H), 1.60 (t, ²J[H,H] = 7.3 Hz, 3H).

6.2.21. Synthesis of 1-propyl-4-pyridin-4-ylpyridinium hexafluorophosphate (21)

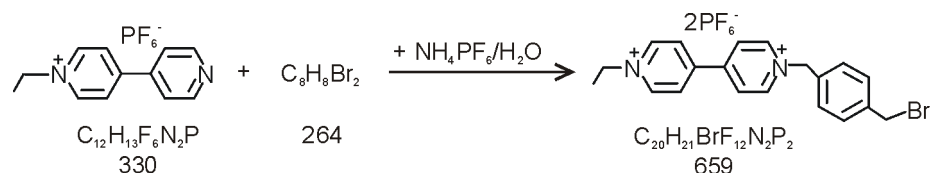


The synthesis was performed according to a literature procedure [83]. A suspension of 5 g (32 mmol) of 4,4'-bipyridyl with 100 g (82 mmol) of propylbromide was stirred at 70°C for 50 h under reflux. After 30 minutes a brown precipitate was obtained. After 7 hours a further portion of 50 g ethylbromide, dissolved in diethylether (30ml), was added dropwise. The resulting precipitate was filtered and thoroughly washed with dry diethyl ether and toluene. The crystallization of the product proceeded slowly (48 h at 4 °C) from ethanol-ether-toluene. The yellow powder was dried for 24 h in HV (mg, 15.6 mmol, 48% yield).

1-Propyl-4-pyridin-4-yl pyridinium salt (2 g, 7 mmol) was dissolved in 80 ml of water, and 10 ml of a 10% aq. NH_4PF_6 solution was added dropwise. The resulting solid was filtered off, washed with cold water and dried for 24 h in HV (1.38 g, 4.02 mmol, 57% yield).

¹H-NMR: (250 MHz, CD_3CN): 8.85 (d, ³J[H,H] = 5.0 Hz, 2H), 8.79 (d, ³J[H,H] = 7.5 Hz, 2H), 8.33 (d, ³J[H,H] = 5.0 Hz, 2H), 7.82 (d, ³J[H,H] = 5.0 Hz, 2H), 4.56 (q, ³J[H,H] = 7.3 Hz, 2H), 2.04 (q, ³J[H,H] = 15.1 Hz, 2H), 1.03 (t, ²J[H,H] = 7.3 Hz, 3H).

6.2.22. Synthesis of 1-[4-(bromomethyl)benzyl]-1'-ethyl-4,4'-bipyridinium dihexafluorophosphate (22)

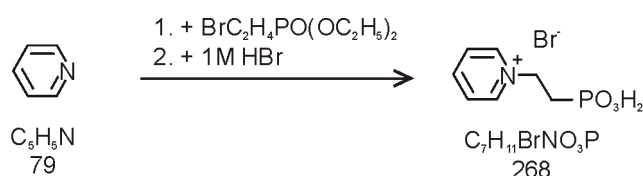


The synthesis was performed according to a literature procedure [146]. 1-Ethyl-4-pyridin-4-yl-pyridinium salt (1 g, 3.7 mmol) (also prepared according to procedure already described, chapter 6.2.20) and 2 g (7.5 mmol) of α,α' dibrom-p-xylene were dissolved in MeCN (30 ml) and stirred for 6.5 h at 70°C under reflux. From the beginning on a yellow precipitate were formed. The mixture was filtered and washed twice with MeCN (10 ml), diethylether (10 ml), and CH₂Cl₂ (5 ml). The yellow crystals of 1-[4-(bromomethyl)benzyl]-1'-ethyl-4,4'-bipyridinium salt were dried for 24h in HV (mg, 3.4 mmol, 92% yield).

1-[4-(Bromomethyl)benzyl]-1'-ethyl-4,4'-bipyridinium salt (2 g, 3 mmol) was dissolved in 80 ml of water, and 10 ml of a 10% aq. NH₄PF₆ solution was added dropwise. The solid was filtered off, washed with cold water and dried for 24h in HV (1.71g, 2.6 mmol, 86% yield).

¹H-NMR: (250 MHz, D₂O; as Br⁻ salt): 9.13 (d, ³J[H,H] = 6,7 Hz, 2H), 9.11 (d, ³J[H,H] = 6.4 Hz, 2H), 8.53 - 8.51 (m, 4H), 7.52 (d, ³J[H,H] = 8.0 Hz, 2H), 7.45 (d, ³J[H,H] = 8.0 Hz, 2H), 5.90 (s, 2H) 4.73 (q, ³J[H,H] = 7.3 Hz, 2H), 4.63 (s, 2H), 1.67 (t, ³J[H,H] = 7.3 Hz, 3H).

6.2.23. Synthesis of 1-(2-phosphonoethyl)pyridinium bromide (23)

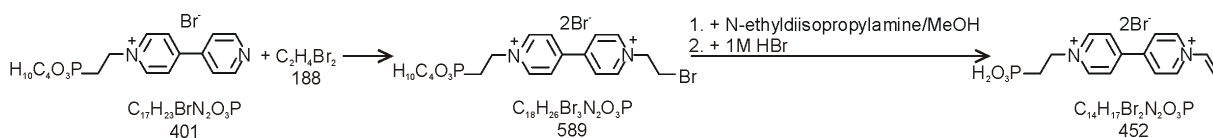


The synthesis was performed according to a literature procedure [88]. Pyridine (2 g, 25.3 mmol) was reacted with 7 g (28.6 mmol) diethyl-2-bromo-ethyl phosphonate at 50 °C for 23 h. The resulting precipitate (2 g, 25.3 mmol) was collected by filtration, washed with diethyl ether, and dried *in vacuo* at r.t. for 16 h yielding 5.6 g (17.3 mmol) of the corresponding diethyl ester as a white powder (68.3 %). The total amount of the intermediate was subjected to hydrolysis in 180 ml of 1 M HBr at 130 °C for 48 h. After evaporation of the solvent the resulting oil was dried for 48 h in *vacuo*. The crude product was dissolved in 100 ml MeOH and precipitated by addition of diethyl ether. 1-(2-Phosphonoethyl) pyridinium bromide was isolated and dried in *vacuo* to yield 3.4 g (12.7 mmol, 73.4 % yield).

MS (25 °C, API-S positive): 540.8 (100 M⁺), 265 (10).

¹H-NMR (250 MHz, D₂O): 8.83 (d, ³J[H,H] = 6.4 Hz, 2H), 8.49 (t, ³J[H,H] = 7.5 Hz, 1H), 8.01 (t, ³J[H,H] = 7.5 Hz, 2H), 4.81 - 4.73 (m, 2H), 2.43 - 2.30 (m, 2H).

6.2.24. Synthesis of 1-(2-phosphonoethyl)-1'-vinyl-4,4'-bipyridinium dibromide (24)



To a solution of 1.5 g (3.7 mmol) of 1-[2-(diethoxyphosphoryl)ethyl]-4-pyridinium bromide, dissolved in 35 ml of warm MeCN, 14.26 g (75.8 mmol) 1,2-dibromoethane was added, and the reaction mixture was stirred at 80°C for 25 h. After 3h a yellow precipitate was formed. The precipitate was filtered off and thoroughly washed with MeCN and diethyl ether. The resulting yellow powder was dried for 6h in HV (mg, 2.7 mmol, 73 % yield).

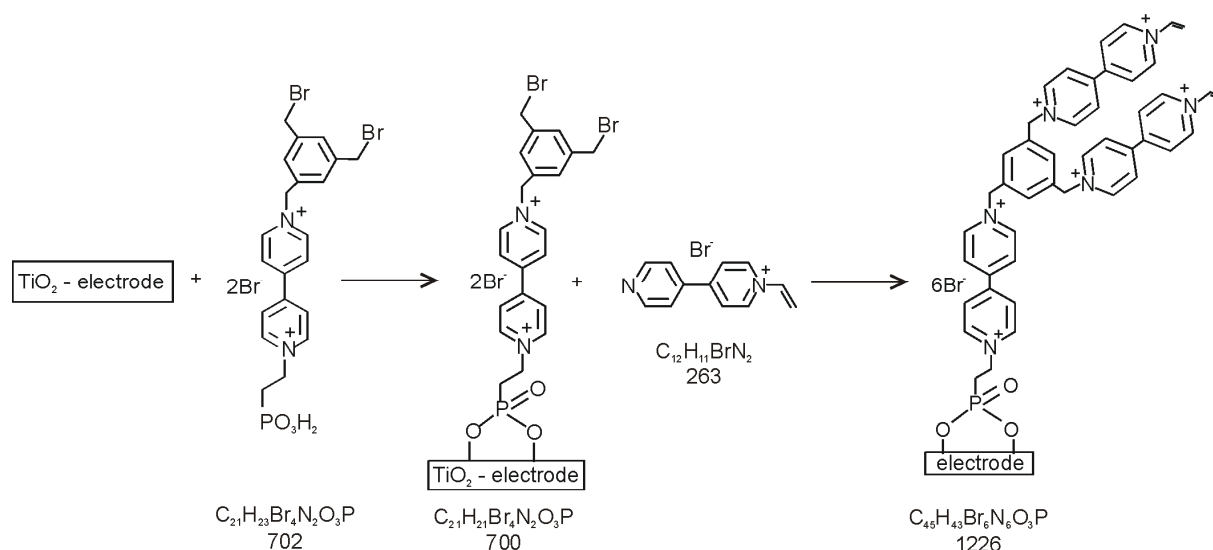
1-[2-(diethoxyphosphoryl)ethyl]-1'-(2-bromoethyl)-4,4'-bipyridinium bromide (1.6 g, 2.7 mmol) was dissolved in 170 ml of 1 M aq. HBr and heated for 72 h at 130°C

under reflux. The cold mother liquor was evaporated to dryness, and the yellow powder was isolated and dried for 36 h in HV (mg, 2.25 mmol, 83% yield).

1-(2-phosphonoethyl)-1'-(2-bromoethyl) 4,4'-bipyridinium salt (1 g, 1.8 mmol) was dissolved in 180 ml methanol, and this solution was dropped to a solution of 5g (38.7 mmol) N-ethyl-diisopropylamine in 20 ml methanol. The mixture was stirred at -10° C for 20 h. The pH value of the solution was controlled and adjusted to pH=10. The resulting solution was concentrated to about 50 ml and dropped into 250 ml ether. The resulting precipitate was filtered off and washed thoroughly with ether and dried for 24 h in HV. The crude material was purified by chromatography (Sephadex LH-20, column: 35 x 3.5 cm, MeOH as eluent) to give a slightly colored product. Most of the product polymerized, on the column as well as during the work-up).

¹H-NMR: * not yet ready

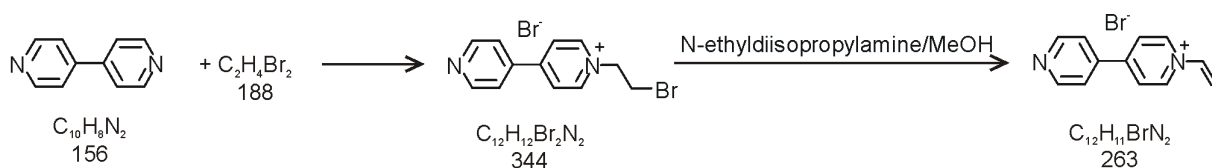
6.2.25. 'In-situ' synthesis of 1,1'-[(5-[[1'-(2-phosphonoethyl)-4,4'-bipyridinium-1-yl]methyl]-1,3-phenylene)bis(methylene)]bis(1'-vinyl-4,4'-bipyridinium) hexabromide (25)



TiO₂ plates were exposed to the anchoring electrophilic 1-[3,5-bis(bromomethyl)benzyl]-1'-(2-phosphonoethyl)-4,4'-bipyridinium dibromide (8) 1 mM in ethanol/water (1:1 vol.%) for 1h at 20°C. The plates were then treated with 4-pyridin-4-yl-1-vinylpyridinium bromide (26, 20 mM in MeCN) for 4h at 60°C, to produce the surface-confined compound 1,1'-[(5-[[1'-(2-phosphonoethyl)-4,4'-

bipyridinium-1-yl]methyl]-1,3-phenylene)bis(methylene)]bis(1'-vinyl-4,4'-bipyridinium) hexabromide (25). The surface-confined compound (25) was checked by cyclic voltammetry applying a negative electrode potential (0 to -0.8 V vs. AgCl) in MeCN/0.2 M LiClO₄ using 3 cyclic voltammetry scans (see chapter 3, figure 3.33).

6.2.26. Synthesis of 4-pyridin-4-yl-1-vinylpyridinium bromide (26)

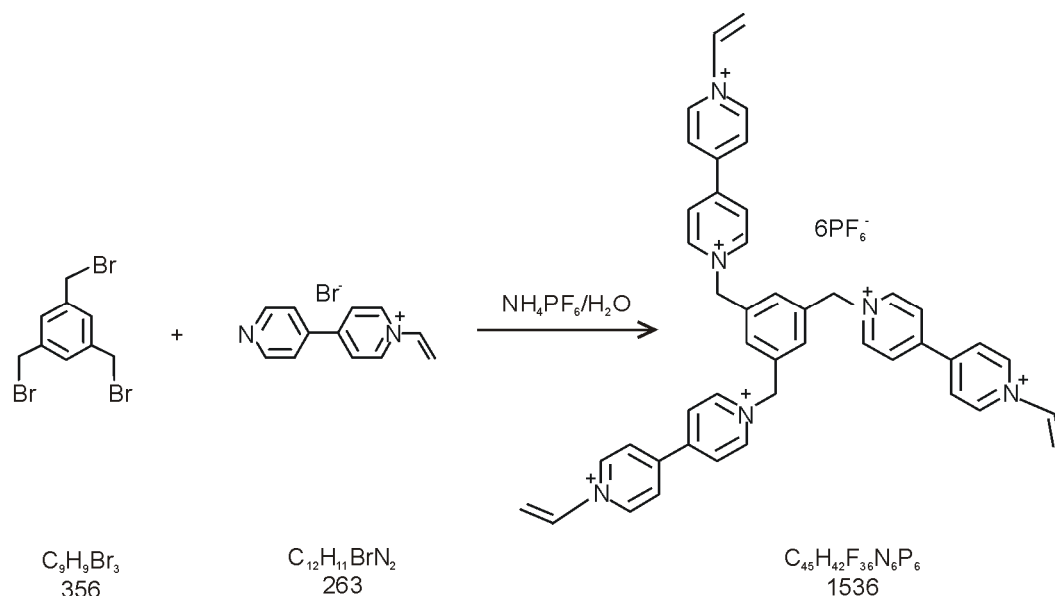


The synthesis was performed according to a literature procedure [155, 156]. A solution of 3.2 g (20.5 mmol) of 4,4'-bipyridyl in 37.6 g (200 mmol) of 1,2-dibromoethane was stirred for 6 h at 100°C. The resulting precipitate was filtered off and washed thoroughly with ether. The yellow solid was isolated and dried for 24h in HV (mg, 19.8 mmol, 97% yield).

1-Bromoethyl-4-pyridin-4-yl-pyridinium bromide (6.8 g, 19.8 mmol) was dissolved in MeOH (180 ml) and dropped to a solution of 2.5 g (19.4 mmol) of N-ethyl-diisopropylamine in MeOH (20 ml) at -10 °C. The reaction mixture was stirred at -10°C for 20h. The pH value of the solution was controlled and kept below 10. The resulting solution was concentrated to about 50 ml and dropped into 250 ml of ether. The precipitate formed was filtered off and then was dissolved in 50 ml of MeOH. The precipitation procedure was repeated once to remove N-ethyl-diisopropylamine hydrobromide salt. At last, the precipitate was filtered off, washed thoroughly with ether and dried in HV. The product was purified by chromatography (Sephadex LH-20, column: 35 x 3.5 cm, MeOH as eluent) to give a slightly colored product (3.7 g, 14.4 mmol, 73% yield).

¹H-NMR (250 MHz, D₂O): 9.00 (d, ³J[H,H] = 5.0 Hz, 2H), 8.67 (d, ³J[H,H] = 5.0 Hz, 2H), 8.37 (d, ³J[H,H] = 7.5 Hz, 2H), 7.83 (d, ³J[H,H] = 7.0 Hz, 2H), 7.46 (d,d, ³J[H] = 15 Hz, =CH=, 1H), 6.13 (d,d, ³J[H] = 15 Hz, =CH trans, 1H), 5.77 (d,d, ³J[H] = 7.5 Hz, =CH cis, 1H).

6.2.27. Synthesis of 1,1',1''-[benzene-1,3,5-triyltris(methylene)]tris(1'-vinyl 4,4'-bipyridinium) hexafluorophosphate (27)



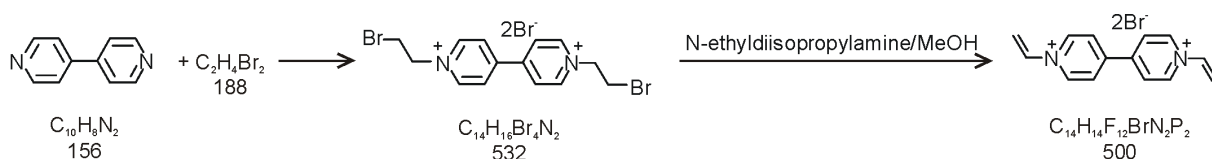
A warm solution of 220 mg (0.84 mmol) of 4-pyridin-4-yl-1-vinylpyridinium bromide in MeCN was dropped to a solution of 100 mg (0.28 mmol) of 1,3,5 tris(bromomethyl)benzene in MeCN (10 ml). The mixture was stirred for 30 h at 60°C. After approximately 3 hours a first yellow precipitate was observed. The precipitate was filtered off and washed thoroughly with MeCN and ether. The yellow solid was isolated and dried for 24 h in HV (368 mg, 0.24 mmol, 86 % yield). The product was purified by chromatography (Sephadex LH-20, column: 35 x 3.5 cm, MeOH as eluent) to give 184 mg (0.12 mmol, 50% yield) of 1,1',1''-[benzene-1,3,5-triyltris(methylene)]tris(1'-vinyl 4,4'-bipyridinium) hexabromide as a slightly yellow powder.

1,1',1''- [Benzene-1,3,5-triyltris(methylene)tris](4-pyridin-4-yl)-1-vinylpyridinium salt (184 mg, 0.12 mmol) was dissolved in 20 ml of water, and 10 ml of a 10% NH_4PF_6 solution was added dropwise. The solid was filtered off, washed with cold water and dried for 24h in HV to yield 101 mg (0.06 mmol, 21% yield) of 1,1',1''- [benzene-1,3,5-triyltris(methylene)tris](4-pyridin-4-yl)-1-vinylpyridinium hexafluorophosphate as a light yellow powder.

$^1\text{H-NMR}$ (250 MHz, CD_3CN) 9.54 (d, $^3\text{J}[\text{H},\text{H}] = 5$ Hz, 6H), 9.46 (d, $^3\text{J}[\text{H},\text{H}] = 5$ Hz, 6H), 8.87 (d, $^3\text{J}[\text{H},\text{H}] = 7.5$ Hz, 12H), 7.67 (s, 3H) 7.83 (d, $^3\text{J}[\text{H},\text{H}] = 7$ Hz, 2H), 7.46 (dd, $^3\text{J}[\text{H}] = 15$

Hz, -CH=, 1H), 6.54 (dd, $^3J[\text{H}] = 15 \text{ Hz}$, =CH trans, 3H), 6.02 (d,d, $^3J[\text{H}] = 7.5 \text{ Hz}$, =CH cis, 3H) 5.95 (s, 6H).

6.2.28. Synthesis of 1,1'-bis(vinyl)-4,4'-bipyridinium dibromide (28)

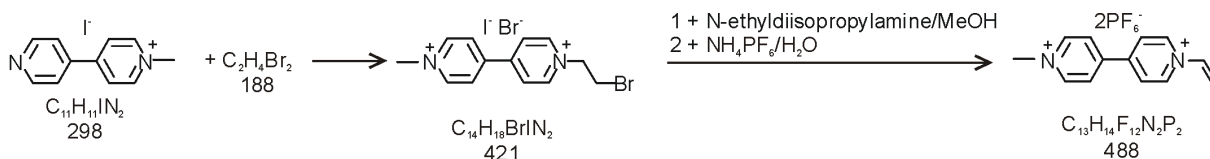


The synthesis was performed according to a literature procedure [155]. A solution of 1.6 g (10 mmol) of bipyridyl and 19 g (101 mmol) of 1,2-dibromoethane in DMF (150 ml) was stirred for 24 hours at 100°C. The resulting precipitate was filtered and washed with diethyl ether and MeCN, respectively. The precipitate was dissolved in methanol (200 ml) and filtered off. After evaporation of the mother liquor and drying for 24 h in HV, 3.7 g (7 mmol, 70% yield) of 1,1'-bis(2-bromoethyl)-4,4'-bipyridinium dibromide was obtained as yellow powder.

N-Ethyldiisopropylamine (1 g, 7.75 mmol) in methanol (5 ml) was slowly dropped into a solution of 2 g (3.7 mmol) of 1,1'-bis(2-bromoethyl)-4,4'-bipyridinium salt in 300 ml of methanol at -10 °C. The brown precipitate was filtered off, and the solution was dropped into 400 ml of diethyl ether. The resulting precipitate was filtered off and washed with diethyl ether. After drying for 24h in HV, 1 g (2 mmol, 54% yield) of crude product was obtained. The product was purified by chromatography (Sephadex LH-20, column: 35 x 3.5 cm, MeOH as eluent) to give 280 mg (0.56 mmol, 15% yield) of 1,1'-bis(vinyl)-4,4'-bipyridinium dibromide as slightly yellow powder. Most of the product polymerized on the column during the work-up).

$^1\text{H-NMR}$ (250 MHz, D_2O): 9.28 (d, $^3J[\text{H},\text{H}] = 7.0 \text{ Hz}$, 4H), 8.63 (d, $^3J[\text{H},\text{H}] = 7.0 \text{ Hz}$, 4H), 7.56 (dd, $^3J[\text{H}] = 15 \text{ Hz}$, -CH=, 2H), 6.23 (dd, $^3J[\text{H}] = 15 \text{ Hz}$, =CH trans, 2H), 5.85 (dd, $^3J[\text{H}] = 7.5\text{Hz}$, =CH cis, 2H).

6.2.29. Synthesis of 1-methyl-1'-vinyl-4,4'-bipyridinium dihexafluorophosphate (29)



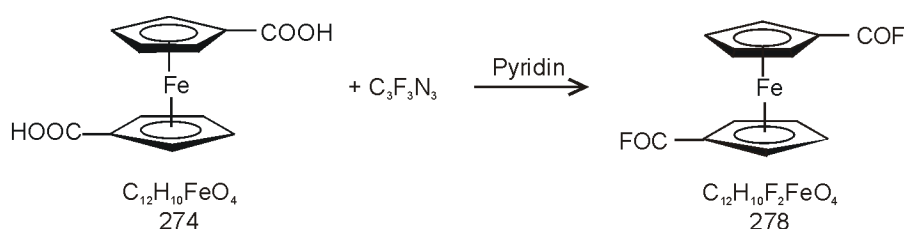
The synthesis was performed according to a literature procedure [155]. 1-Methyl-4-pyridin-4-yl-pyridinium iodide (6 g, 20 mmol) (also prepared according to procedure already described) and 40 g (95 mmol) of 1,2-dibromoethane in DMF (80 ml) was heated for 10 h at 100°C. The resulting precipitate was filtered off and washed with ether several times. After drying *in vacuo* (r.t., 24 h) 7.5 g (17.8 mmol, 89% yield) of 1-methyl-1'-(2-bromoethyl)-4,4'-bipyridinium bromodiodide was obtained.

1-Methyl-1'-(2-bromoethyl)-4,4'-bipyridinium bromodiodide (7.5 g, 17.8 mmol) was dissolved in MeOH (200 ml) and dropped slowly at -10 °C to 1.5 ml of an aq. NaOH solution (10 M). After 13 hours, the solution was adjusted to pH = 5 with 48% HBr aq. solution, and then the temperature was raised to 20°C. The solvent was evaporated, and the crude product was purified by chromatography (Sephadex LH-20, column: 35 x 3.5 cm, MeOH as eluent) to give 3.8 g (9 mmol, 50% yield) of 1-methyl-1'-vinyl-4,4'-bipyridinium salt as yellow powder.

1-Methyl-1'-vinyl-4,4'-bipyridinium salt (3.8 g, 9 mmol) was dissolved in 20 ml of water, and 10 ml of a 10% NH_4PF_6 solution was added dropwise. The solid was filtered off, washed with cold water and dried for 24 h *in HV*. 3.82 g (7.8 mmol, 44% yield) of 1-methyl-1'-vinyl-4,4'-bipyridinium hexafluorophosphate as light yellow powder was obtained.

$^1\text{H-NMR}$ (250 MHz, CD_3CN): 9.0 (d, $^3\text{J}[\text{H},\text{H}] = 7.0$ Hz, 2H), 8.89 (d, $^3\text{J}[\text{H},\text{H}] = 7.0$ Hz, 2H), 8.49 (d, $^3\text{J}[\text{H},\text{H}] = 7.0$ Hz, 2H), 8.42 (d, $^3\text{J}[\text{H},\text{H}] = 7.0$ Hz, 2H), 7.55 (dd, $^3\text{J}[\text{H}] = 15$ Hz, =CH=, 1H), 6.31 (d,d, $^3\text{J}[\text{H}] = 15$ Hz, =CH trans, 1H), 6.24 (dd, $^3\text{J}[\text{H}] = 7.5$ Hz, =CH cis, 1H), 4.43 (s, 3H).

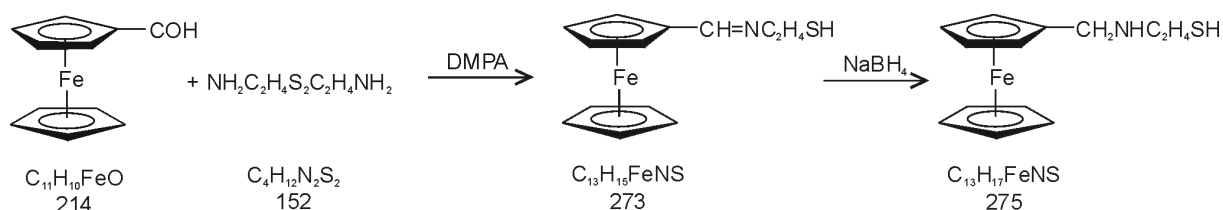
6.2.30. Synthesis of ferrocenyl-1,1'-diacid fluoride (30)



The synthesis was performed according to a literature procedure [153]. 1,1'-Ferrocene-dicarboxylic acid (0.5 g, 1.82 mmol) was dissolved in 30 ml of dry CH_2Cl_2 under argon, and 0.5 ml (6.5 mmol) of pyridine was added dropwise. The mixture was cooled to 0°C . Then, 1.3 ml (6.3 mmol) of cyanuric fluoride was added, and the mixture was vigorously stirred for 1 h. After the reaction was finished, the mixture was poured into 30 ml of ice/water. The organic phase was separated and washed twice with water (30 ml, each). The mixture was dried (CaCl_2), filtered and concentrated in *vacuo*. The product was crystallized from acetone/water. After drying for 24 h in HV, 406 mg (1.46 mmol, 80% yield) of ferrocenyl-1,1'-diacid fluoride was obtained as red-orange crystals.

$^1\text{H-NMR}$ (250 MHz, CD_3Cl): 5.0 (s, 4H), 4.73 (s, 4H).

6.2.31. Synthesis of 1-(2-mercaptoethyl)-1-(ferrocenylmethyl) amine (31)

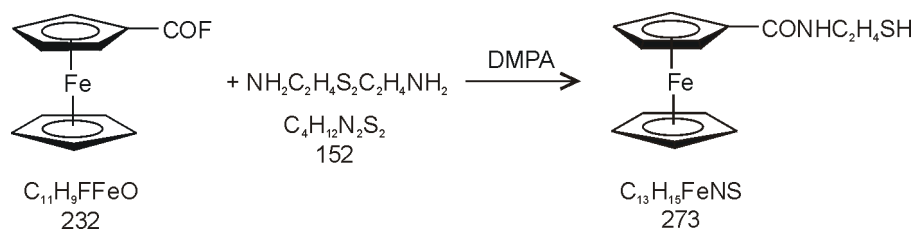


4-Dimethylaminopyridine (DMPA) (488 mg, 4 mmol) and 225 mg (1 mmol) of cystamine were dissolved in methanol (30 ml) under argon. Then, ferrocene carbaldehyde (428 mg, 2 mmol), dissolved in methanol (10 ml), was added drop wise during 1 h. The mixture was stirred for 6 hours at 80°C . The mother liquor was evaporated, and the Schiff base (red solid) was dissolved in 20 ml of ethanol to which 225 mg (5.7 mmol) of NaBH_4 were added. The mixture was heated with caution to

reflux for about 4 h, and mother liquor was then evaporated. The resulting oil was dissolved in 30 ml of petrol ether and extracted with 30 ml of water/HCl. The aqueous phase was separated, neutralized with KOH, and extracted with CH₂Cl₂. The organic layer was dried (Na₂SO₄), and the solvent was evaporated. The product was dried *in vacuo* (r.t., 48 h) to yield 264 mg (0.96 mmol, 48% yield) of N-(2-mercaptoethyl)-N-(ferrocenylmethyl) amine as a hygroscopic red oil.

¹H-NMR (250 MHz, CD₃Cl): 7.0 (s, 1H), 4.20 (s, 3H), 4.27 (s, 6H), 3.54 (s, 2H), 3.30-2.80 (brs, 4H), 1.94 (s, 1H).

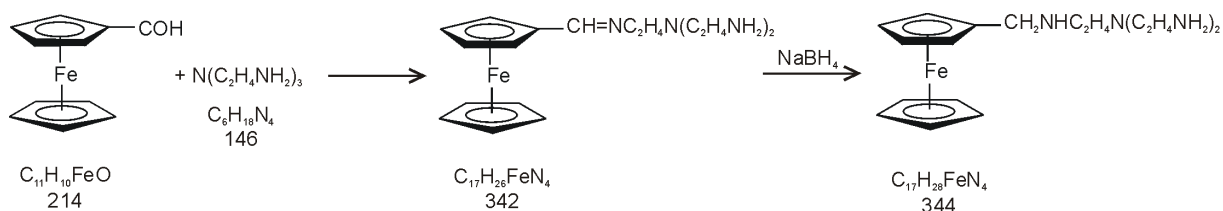
6.2.32. Synthesis of 1-(2-mercaptoethyl) ferrocene carboxamide (32)



4-Dimethylaminopyridine (DMPA) (244 mg, 2 mmol) was suspended together with 112.5 (0.5 mmol) of cystamine in CH₂Cl₂ (30 ml) under argon and heated at 40°C. Then, fluorocarbonylferrocene (232 mg, 1 mmol) - prepared according to [153] and dissolved in dry CH₂Cl₂ (10 ml) - was added drop wise during 1h. The mixture was stirred for 15 hours at 60 °C. The precipitate and the solid obtained after evaporation were dissolved in 30 ml of water/Na₂CO₃ (pH~12), and extracted with 10 ml of CH₂Cl₂. The organic layer was washed with water and dried over MgSO₄ to yield - after solvent evaporation and drying *in vacuo* (r.t., 24h) - 250mg (0.86 mmol, 86%) of N-(2-mercaptoethyl) ferrocene carboxamide as intense orange crystals.

¹H-NMR (250 MHz, CD₃Cl): 7.06 (s, 1H), 4.82 (s, 2H), 4.40 (s, 2H), 4.27 (s, 5H), 3.77 (q, ³J [H,H] = 6.1Hz, 2H), 3.02 (t, ³J[H,H] = 10.4 Hz, 2H), 1.28 (s, 1H).

6.2.33. Synthesis of 1,1'-bis(2-aminoethyl)-1-{2-[(ferrocenylmethyl)amino]ethyl} amine (33)

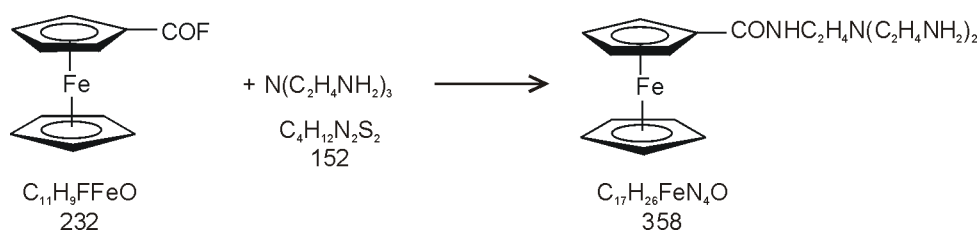


The synthesis was performed according to a literature procedure [55]. Tris(2-aminoethyl)amine (614 mg, 4 mmol) was dissolved in toluene (20 ml) under Ar, and 312 mg (1,5 mmol) of ferrocene carbaldehyde, dissolved in 10 ml of toluene, were added within 1h drop wise and reacted for 6 h at 110°C. The mother liquor was evaporated, and the Schiff base (red solid) was dissolved in ethanol (20 ml) to which 225 mg (5.7 mmol) of NaBH₄ were added. The mixture was heated with caution to reflux for about 4 hours, and the mother liquor was than evaporated. The resulting red oil was dissolved in 50 ml of petrol ether and extracted with 50 ml of water/HCl. The aqueous phase was separated, neutralized with KOH, and extracted with 70 ml of CH₂Cl₂. The organic layer was dried (Na₂SO₄). The solvent was evaporated, and the product was dried in vacuo (rt 48 h) to yield 303 mg (0.88 mmol) of N,N-bis(2-aminoethyl)-N-{2-[(ferrocenylmethyl)amino]ethyl}amine as a hygroscopic red powder in 53 % yield.

MS (25°C, API-ES Positive): 345.1 (100 M⁺),

¹H-NMR (250 MHz, CD₃Cl): 4.26 (s, 3H), 4.15 (s, 6H), 3.68 (s, 2H), 3.01-2.55 (brs. 12H), 2.19 (s, 1H), 0.90-0.87 (brs., 4H)

6.2.34. Synthesis of 1-{2-[bis(2-aminoethyl)amino]ethyl}ferrocene- carboxamide (34)



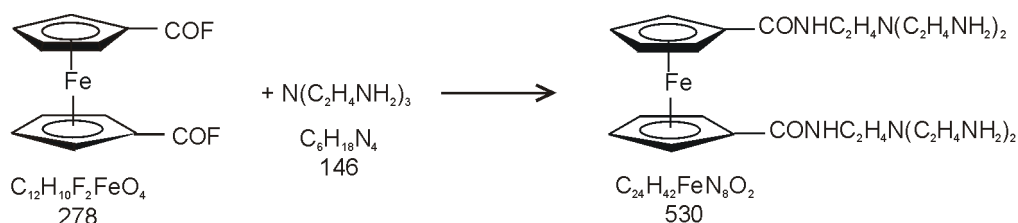
The synthesis was performed according to a literature procedure [55]. Fluorocarbonylferrocene (232 mg, 1mmol) (prepared according to the method

described to a literature[153] was reacted with 600 mg (4.1 mmol) of *tris*-N,N,N-(2-aminoethyl)amine in 10 ml of dry CH₂Cl₂, under Ar at r.t. for 5h. The reaction mixture was filtered, and the mother liquor was evaporated. The crude product was dissolved in 30 ml of water/NaCO₃ (pH~12) and extracted three times with 10 ml of CH₂Cl₂. The combined organic layers were dried over MgSO₄ *2H₂O at r.t., filtered, and the solvent was evaporated yielding 265 mg (0.73 mmol, 73% yield) of compound **4** after drying *in vacuo* (rt, 48h) as intense orange crystals.

MS (25°C, API-ES Positive): 359 (100 M⁺).

¹H-NMR (CD₃Cl): 7.06 (t, 1H), 4.76 (s, 2H), 4.33 (s, 2H), 4.21 (s, 5H), 3.49 - 3.48 (t, ³J(H,) = 7.5 Hz, 2H), 2.86 - 2.77 (m, 4H), 2.71 - 2.54 (m, 4H), 2.20 (s, 2H), 0.9 - 0.85 (t, ³J(H,) = 5.0 Hz, 4H).

6.2.35. Synthesis of 1,1'-bis{[bis(aminoethyl)amino]ethyl}ferrocene-dicarboxamide (**35**)

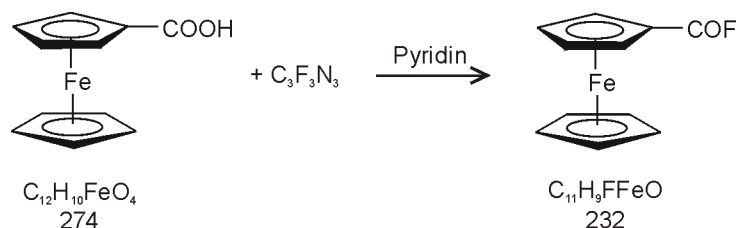


The synthesis was performed according to a literature procedure [55]. Di-fluorocarbonylferrocene (139 mg, 0.5 mmol) (prepared according to the method described in the reference [153] was reacted with 600 mg (4.1 mmol) of *tris*-N,N,N-(2-aminoethyl)amine in 10 ml of dry CH₂Cl₂ under argon at r.t. for 3h. The reaction mixture was filtered, and the mother liquor was evaporated to yield the crude product which was broken apart by ultra sound and washed several times with ether (10 ml, each). N,N'-bis{[bis(aminoethyl)amino]ethyl}ferrocene-dicarboxamide was obtained as an intense red powder (140 mg, 0.26 mmol, 52% yield) which is soluble only in acidified water.

MS (25°C, API-ES Positive mode, 50V): 531 (M^+H^+ , 25), 266.1 (M^+2H^+ , 40), 177.7 (M^+3H^+ , 25).

1H -NMR (250 MHz, D_2O+DCl): 4.37 (s, 4H), 4.34 (s, 4H), 3.06 - 3.00 (br. s, 24H).

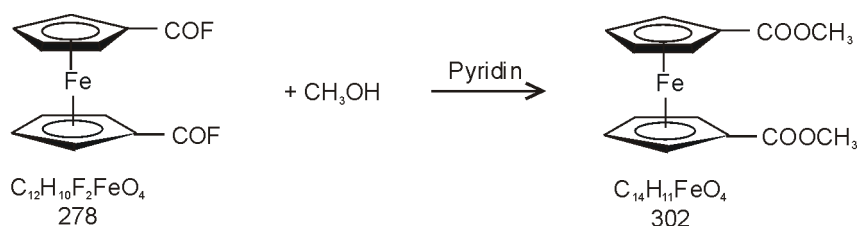
6.2.36. Synthesis of fluorocarbonylferrocene (36)



The synthesis was performed according to a literature procedure [153]. A suspension of 1 g (3.6 mmol) of ferrocenecarboxylic acid and 0.6 ml (7.2 mmol) of pyridine in dry CH_2Cl_2 (25 ml) was cooled to 0°C under argon. Cyanuric fluoride (1.2 ml, 7.2 mmol) was added, and the mixture was stirred for 1.5 h. A red precipitate was observed. The mixture was treated with ice-water, and the suspension was filtered. The organic layer was separated and washed twice with cold water (25 ml, each). The resulting solution was concentrated, and the crude product was purified by column chromatography [silica gel, column: 35 x 4 cm, solvent: hexane/EtOAc (6:1, v/v)] to give 808 mg (3.4 mmol, 94% yield) of fluorocarbonylferrocene as dark orange crystals.

1H -NMR (250 MHz, CD_3Cl): 4.85 (s, 2H), 4.58 (s, 2H), 4.31 (s, 5H).

6.2.37. Synthesis of fluorocarbonylferrocene-dimethylester (37)



The synthesis was performed according to a literature procedure [153]. A solution of 73.5 mg (0.26 mmol) of di-fluorocarbonylferrocene (prepared according to the method described in the literature [153]) in 3 ml of dry CH₂Cl₂ was added slowly to solution of methanol (0.26 mmol) containing 31.7 mg (0.26 mmol) of DMAP. The mixture was stirred at room temperature for 12 h. The mixture was filtered and washed with CH₂Cl₂. The mother liquor was evaporated and dried for 12h in HV. The fluorocarbonylferrocene was obtained as an orange powder (57 mg, 0.19 mmol, 76% yield).

¹H-NMR (250 MHz, CD₃CN): 4.69 (s, 4H), 4.68 (s, 4H), 3.68 (s, 6H).

Chapter 7

Summary

In this work a new approach for the immobilization of electroactive compounds on mesoporous electrodes is described. It consists in the formation of a self assembled monolayer on the inner walls of the mesopores (ITO, FTO, ATO, TiO₂). This layer was then cross-linked and grown towards the center of the pore using substitution, condensation or electropolymerisation reactions.

The cascade type reaction was used for three types, of applications:

- a) electrochromic film based an viologen multilayers on mesoporous TiO₂;
- b) high capacity redox active films based on ferrocene multilayers on mesoporous ATO;
- c) electrocatalytic films based on vitamin B₁₂ multilayers on mesoporous TiO₂.

Electrochromic films

Starting point of this work was a new technique for the preparation of high resolution electrochromic images which has been developed in our group. A drawback was the weak intensity and the insufficient stability of the ink-jetted electrochromic picture.

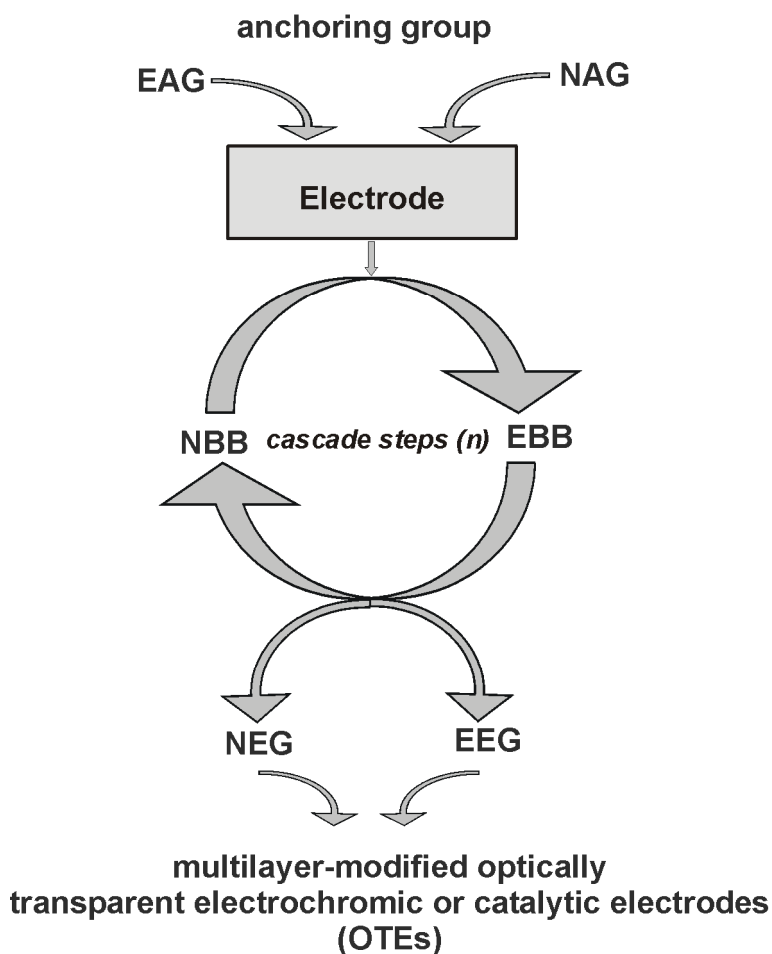
In my work I developed a cross-linking procedure that allows the preparation of stable electrochromic picture with increased contrast and durability of more than 18 months.

It involved the syntheses of on-purpose prepared molecular units with latent or fully developed electrochromic properties. The units were 4,4'-bipyridins with optional N-alkyl, N-benzyl or N-phenyl groups exhibiting nucleophilic or electrophilic character, or equipped with TiO₂ anchoring groups.

The cascade reaction yielded electrodes of different surface concentration and different degree of pimerisation.

Moreover, it was possible to optimize durability and contrast to the point of commercial requirements.

Cascade type preparation of modified electrodes



N: nucleophilic, *E*: electrophilic, *AG*: anchoring group, *BB*: building block, *EG*: end group;

The optimization of the counter electrode was achieved by a similar procedure, but using ferrocene derivatives. The charge capacities obtained from multilayer cross-linked and amplified ferrocene-on-ATO electrodes was excellent except for a greenish tint due to ferrocene in the oxidized form.

Finally the cascade type reaction sequence was applied to vitamin B₁₂ derivatives in order to prepare catalytically active TiO₂ electrodes.

Different procedures, including ester type linkage and S_N2 type N-alkylation were used for this purpose.

The B₁₂ modified electrodes showed increased stabilities, higher turn over numbers and larger turnover rates as compared to B₁₂ modified electrodes on the same support, but without cross linker.

The electrodes catalyzed efficiently the reduction of vicinal dibromides without loss of the catalyst from the support.

Zusammenfassung

In dieser Arbeit wird ein neuer Ansatz beschrieben, elektroaktive Verbindungen auf mesoporösen Elektroden zu fixieren. Dies wurde erreicht durch die Bildung eines sich selbst organisierenden Monolayers auf der Innenseite eines mesoporösen Trägers (ITO, FTO, ATO, TiO₂). Dieser Layer wurde dann vernetzt und in Richtung des Porenzentrums weiter aufgebaut durch Substitutions- Kondensations- oder Elektropolymerisations- Reaktionen.

Diese Kaskadenreaktion wurde für drei Arten von Anwendungen verwendet:

- a) elektrochrome Filme, basierend auf Viologen - Multilayern auf mesoporösem TiO₂;
- b) hoch speicherfähige redoxaktive Filme, basierend auf Ferrocen - Multilayern auf mesoporösem ATO;
- c) elektrokatalytische Filme, basierend auf B₁₂ – Multilayern auf mesoporösem TiO₂.

Elektrochrome Filme

Ausgangspunkt dieser Arbeit war eine neue Technik für die Herstellung hochaufgelöster elektrochromer Bilder, die in unserer Arbeitsgruppe entwickelt wurde. Ein bisheriger Mangel war die schwache Intensität und die unzureichende Stabilität der elektrochromen Bilder.

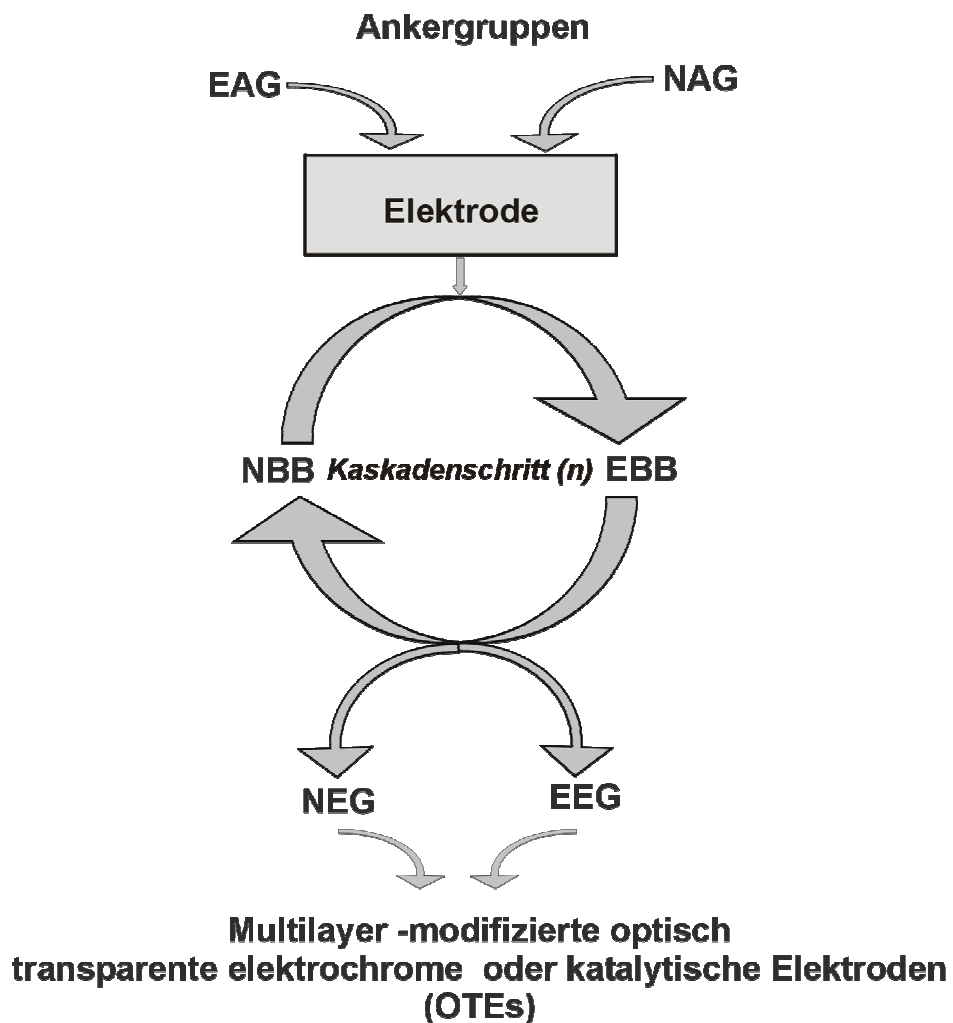
In der vorliegenden Arbeit habe ich ein Vernetzungsverfahren entwickelt, welches die Herstellung stabiler elektrochromer Bilder mit verbessertem Kontrast und einer Haltbarkeit von mehr als 18 Monaten erlaubt.

Es beinhaltet die Synthesen von molekularen Einheiten mit latent vorhandenen oder voll entwickelten elektrochromen Eigenschaften. Diese Einheiten waren 4,4'-Bipyridine, die entweder mit optionalen N-alkyl, N-benzyl oder N-phenyl Gruppen mit nukleophilem oder elektrophilen Eigenschaften oder mit TiO₂ Ankergruppen versehen waren.

Die Kaskadenreaktion ergab Elektroden mit unterschiedlichen Oberflächenkonzentrationen und unterschiedlichen Polymerisationsgraden.

Darüberhinaus gelang es, die Haltbarkeit und den Kontrast so weit zu steigern, dass sie kommerziellen Ansprüchen genügen.

Kaskadenreaktionstyp für die Vorbereitung der modifizierten Elektroden



N: nucleophilic, E: electrophilic, AG: Ankergruppen, BB: Bausteine, EG: Abschlussgruppen;

Die Optimierung der Gegenelektroden wurde durch ein ähnliches Verfahren erreicht unter Verwendung von Ferrocen-Derivaten. Die Ladungskapazitäten, die durch Multilayer Vernetzung auf ATO-Ferrocen Elektroden erhalten wurden, waren hervorragend mit Ausnahme der Tatsache dass ein schwach grüner Farbton, verursacht durch oxidiertes Ferrocen, vorhanden war.

Schließlich wurde die Kaskadenreaktion auf B₁₂ Derivate angewendet zur Herstellung von katalytisch aktiven TiO₂ Elektroden.

Verschiedene Verfahren, einschließlich Esterbindung und N-Alkylierung vom S_N2-Typ wurden für diesen Zweck verwendet.

Die mit B₁₂ modifizierten Elektroden zeigten verbesserte Stabilität, höhere „turn over“- Zahlen und größere „turn over“-Raten im Vergleich zu unvernetzten B₁₂ modifizierten Elektroden.

Die Elektroden katalysierten effizient die Reduktion von vicinalen Dibromiden ohne Ablösung des Katalysators vom Trägermaterial.

Abbreviations

SAMs	Self-assembled monolayers
LB	Langmuir-Blodgett
ATO	Antimony tin oxide
FTO	Fluoro tin oxide
ITO	Indium tin oxide
TiO ₂	Titanium dioxide
EAG	Electrophilic anchoring groups
NAG	Nucleophilic anchoring groups
EBB	Electroleophilic building blocks
NBB	Nucleophilic building blocks
EEG	Electrophilic end group
NEG	Nucleophilic end group
PB	Prussian Blue
ECD	Electrochromic devices
OTEs	Optically transparent electrode
VLSI	Very large scale integrated circuits
AR	Antireflective
VB	Valence band
CB	Conduction band
CBE	Conduction band edge
LUMO	Lowest unoccupied molecular orbitals
HOMO	Highest unoccupied molecular orbitals
EC	Electrochromic
E-	Electrode (TiO ₂ , FTO, ITO or ATO)
UV-VIS	Ultraviolet-visible spectrophotometry
CV	Cyclic voltammetry
Γ	Surface concentration
LP	Lithium perchlorate /Fluka
MeCN	Acetonitrile /Merck
PEG 200	Polyethylene glycol 200 /Fluka
TEG-DiMe	Tetraethylene glycol dimethyl ether /Fluka
EG	Ethylene glycol /Fluka
γ-BL+G	γ-Butyrolactone and glutaronitrile /Fluka

γ -BL+G	γ -Butyrolactone and 3- methoxypropionitrile /Fluka
APS	Aminopropyl triethoxy silane /Acros
Fecp	Ferrocene
TBAP	Tetrabutylammoniumhexafluorophosphate /Merck
PC	Propylencarbonate /Merck
HAc	Acetic acid /Fluka
DBEt	1,2 Dibromoethane /Fluka
DBCH	Dibromocyclohexane /Fluka
EDTA	Ethylen-diamin- tetra-acid
EtOH	Ethanol /Merck
MeOH	Methanol /Merck
HBr	Hydrobromic acid /Merck
HBr/AcOH	Hydrogen bromide /glacial acetic acid /Merck
HCl	Hydrochloric acid/Merck
EtOAc	Ethylacetate /Merck
DMPA	4-Dimethylaminopyridine /Fluka
HV	High vacuum
r.t.	Room temperature
CC1-5 and CC8-14	Commercial compounds /Fluka, Merck or Acros
CC6-7 and CC15-17	Compounds prepared by B. Steiger
0.11-0.24	Intermediary synthesis compounds
1-37	Synthesis compounds

Literature

1. Decher, G. and J.D. Hong, *Buildup of Ultrathin Multilayer Films by a Self-Assembly Process: I. Consecutive Absorption of Anionic and Cationic Bipolar Amphiphiles*. Makromolec. Chem., Macromol. Symp., 1991. **46**: p. 321-327.
2. Mao, G., et al., *Self-Assembly of Photopolymerizable Bolaform Amphiphile Mono- and Multilayers*. Langmuir, 1993. **9**: p. 3461-3470.
3. Cooper, T.M., A.L. Campbell, and R.L. Crane, *Formation of Polypeptide-Dye Multilayers by an Electrostatic Self-Assembly Technique*. Langmuir, 1995. **11**: p. 2713-2718.
4. Ariga, K., Y. Lvov, and T. Kunitake, *Assembling Alternate Dye-Polyion Molecular Films by Electrostatic Layer-by-layer Adsorption*. J.Am.Chem.Soc., 1997. **119**: p. 2224-2231.
5. Cheng, L., et al., *Electrochemical Growth and Characterization of Polyoxometalate-Containing Monolayers and Multilayers on Alkanethiol Monolayers Self-Assembled on Gold Electrodes*. Chem. Mater., 1999. **11**: p. 1465-1475.
6. Zou, B., et al., *Ex Situ SFM Study of 2-D Aggregate Geometry of Azobenzene Containing Bolaform Amphiphiles after Adsorption at the Mica/Aqueous Solution Interface*. Langmuir, 2001. **17**: p. 3682-3688.
7. Lvov, Y., et al., *Films of Manganese Oxide Nanoparticles with Polycations or Myoglobin from Alternate-Layer Adsorption*. Langmuir, 2000. **16**: p. 8850-8857.
8. Keller, S.W., et al., *Photoinduced Charge Separation in Multilayer Thin Films Grown by Sequential Polyelectrolyte Adsorption*. J.Am.Chem.Soc., 1995. **117**: p. 12879-12880.
9. Shen, J.C., J. Sun, and X. Zhang, *Polymer nanocomposite films*. Pure App. Chem., 2000. **72**: p. 147-155.
10. Watanabe, S. and S.L. Regen, *Dendrimers as Building Blocks for Multilayer Construction*. J. Am.Chem.Soc, 1994. **116**: p. 8855-8856.
11. Tsukruk, V.V., F. Rinderspacher, and V.N. Bliznyuk, *Self-Assembled Films from Dendrimers*. Langmuir, 1997. **13**: p. 2171.
12. Laurent, D. and J.B. Schlenoff, *Multilayer Assemblies of Redox Polyelectrolytes*. Langmuir, 1997. **13**: p. 1552-1557.
13. Decher, G., et al., *Nanobiocomposite Films for Biosensors: Layer-by-layer adsorbed Films of Polyelectrolytes, Proteins or DNA*. Biosens. Bioelectron., 1994. **9**: p. 677-684.
14. Elbert, D.L., C.B. Herbert, and J.A. Hubbell, *Thin Polymer Layers Formed by polyelectrolyte Multilayer Techniques on Biological Surfaces*. Langmuir, 1998. **15**: p. 5355-5367.
15. Niemeyer, C.M. and C.A. Mirkin, *Nanobiotechnology. Concepts, Applications and Perspectives*. 2004, Weinheim: WILEY-VCH. 469.
16. Lvov, Y., K. Ariga, and T. Kunitake, *Layer-by-layer Assembly of Alternate Protein/Polyion Ultrathin Films*. Chem. Lett., 1994: p. 2323-2326.
17. Lang, J. and M.H. Lin, *Layer-by-layer Assembly of DNA Films and Their Interactions with Dyes*. J.Phys.Chem. B, 1999. **103**: p. 11393-11397.
18. Brynda, E., et al., *Characterisation of Flexibility of Ultrathin Protein Films By Optical Sensing*. Langmuir, 2000. **16**: p. 4352-4357.
19. Ladam, G., et al., *Protein Adsorption Onto Auto-Assembled Polyelectrolyte Films*. Langmuir, 2001. **17**: p. 878-882.
20. Picart, C., et al., *Buildup Mechanism for Poly(L-lysine)/Hyaluronic Acid Films onto a Solid Surface*. Langmuir, 2001. **17**: p. 7414-7424.

21. Forzani, E.S., V.M. Solis, and E.J. Calvo, *Electrochemical-Behavior of Polyphenol Oxidase Immobilized in self-Assembled Structures Layer-by-layer with Cationic Polyallylamine*. Anal. Chem., 2000. **72**: p. 5300-5307.
22. Maoz, R., et al., *Self-Replicating Amphiphilic Monolayers*. Nature, 1996. **384**(6605): p. 150-153.
23. Schoen, P., et al., *Charge Propagation in 'Ion Channel Sensors' Based on Protein Modified Electrodes and Redox Marker Ions*. J. Am.Chem.Soc., 2005, in press.
24. Blodgett, K.L., *Molecular Films of Fatty Acids on Glass*. J. Am.Chem.Soc, 1934. **56**: p. 495.
25. Kuhn, H. and D. Moebius, *Systeme aus Monomolekularen Schichten-Zusammenbau und chemisches Verhalten*. Angew. Chem., 1971. **83**: p. 672-690.
26. Decher, G. and A.P. Hong, *Buildup of ultrathin Multilayer Films by Self-Assembly Process. 2. Consecutive Adsorption of Anionic and Cationic Bipolar Amphiphiles and Polyelectrolytes on Charged Surfaces*. Ber. Bunsen-Ges. Phys. Chem., 1991. **95**(11): p. 1430-1434.
27. Decher, G. and U. Sohling, *Langmuir-Blodgett Monolayer and Multilayer Assemblies of Amphiphilic Liquid-Crystalline Normal-Alkyl-4'-Normal-Alkoxybiphenyl-4-Carboxylates.1*. Ber. Bunsen-Ges. Phys. Chem., 95. **95**(11): p. 1538-1542.
28. Decher, G., et al., *Highly-Ordered Ultrathin Lc Multilayer Films on Solid Substrates*. Advanced Materials, 1991. **3**(12): p. 617-619.
29. Decher, G. and A.P. Hong, *Buildup of ultrathin Multilayer Films by Self-Assembly Process. 1. Consecutive Adsorption of Anionic and Cationic Bipolar Amphiphiles and Polyelectrolytes on Charged Surfaces*. Macromolekulare Chemie-Macromolecular Symposia, 1991. **46**: p. 321-327.
30. Shimazaki, Y., et al., *Preparation and Characterization of the Layer-by-layer Deposited Ultrathin-Film Based on the Charge-Transfer Interaction in Organic-Solvents*. Langmuir, 1998. **14**: p. 2768-2773.
31. Shimazaki, Y., et al., *Molecular.Weight Dependence of Alternate Adsorption Through Charge-Transfer Interaction*. Langmuir, 2001. **17**: p. 953-956.
32. Stockton, W.B. and M.F. Rubner, *Molecular-level Processing of Conjugated Polymers. Layer-by-layer manipulation of Polyaniline via Hydrogen-Bonding Interactions*. Macromolecules, 1997. **30**: p. 2717-2725.
33. Wang, L.Y., et al., *Multilayer Assemblies of Copolymer Psoh and PVP on the Basis of Hydrogen-Bonding*. Langmuir, 2000. **16**: p. 10490-10494.
34. Mecking, S. and R. Thomann, *Core-Shell Microspheres of a Catalyrically Active Rhodium Complex Bound to a Polyelectrolyte-Coated Latex*. Advanced Materials, 2000. **12**: p. 953.
35. Li, W.J., et al., *Fabrication of Multilayer Films Containing Horseradish-Peroxidase and Polycation Bering Os Complex by Means of electrostatic Layer-by-layer Adsorption and Its Application as a Hydrogen-Peroxide Sensor*. Anal.Chim.Acta, 2000. **418**: p. 225-232.
36. Netz, R.R. and J.F. Joanny, *Adsorption of Semiflexible Polyelectrolytes on Charged Planar Surfaces-Charge Compensation, Charge Reversal and Multilayer Formation*. Macromolecules, 1998. **32**: p. 9013-9025.
37. Lee, S.S., et al., *Layer-by-layer Deposited Multilayer Assemblies of Ionene-Type Polyelectrolytes Based on the Spin-Coating Method*. Macromolecules, 2001. **34**: p. 5358-5360.
38. Anzai, J., et al., *Layer-by-layer Construction of Thin-Films Composed of Avidin and Biotin-Labeled PolyAmine)s*. Langmuir, 1999. **15**: p. 221-226.
39. Anzai, J. and Y. Kobayashi, *Construction of Multilayer Thin-films of Enzymes by Means of Sugar-Lectin Interactions*. Langmuir, 2000. **16**: p. 2851-2856.

40. Serizawa, T., S. Hashiguchi, and M. Akashi, *Stepwise Assembly of Ultrathin Pol(Vinyl Alcohol) Films on a Gold Substrate by Repetitive Adsorption/Drying Processes*. Langmuir, 1998. **15**: p. 5363-5368.
41. Serizawa, T. and M. Akashi, *A Novel approach for Fabricating Ultrathin Polymer-Films by the Repetitive of the Adsorption Drying Processes*. J. Polym. Sci. A, 1998. **37**: p. 1903-1906.
42. Serizawa, T., et al., *Stepwise Stereocomplex Assembly of Stereoregular Poly(Methyl Methacrylate)s on a Substrate*. J. Am.Chem.Soc, 2000. **122**: p. 1891-1899.
43. Serizawa, T., et al., *Stepwise Assembly of Enantiomeric Poly(Lactide)s on Surfaces*. Macromolecules, 2001. **34**: p. 1996-2001.
44. Inchinose, I., et al., *Preparation of Cross-Linked Ultrathin Films Based on Layer-by-layer Assembly of Polymers*. Polym. J., 1999. **31**: p. 1065-1070.
45. Sun, J.Q., et al., *Covalently Attached Multilayer Assemblies by Sequential Adsorption of Polycationic Diazo-Resins and Polyanionic Poly(Acrylic-Acid)*. Langmuir, 2000. **16**: p. 4620-4624.
46. Kohli, P. and G.J. Blanchard, *Desing and Demonstration of Hybrid Multilayer Structures- Layer-by-layer Mixed Covalent and Ionic Interlayer Linking Chemitry*. Langmuir, 2000. **16**: p. 8518-8524.
47. O'Regan, B. and M. Grätzel, *A low-cost, high-efficiency sollar cell based on dye-sensitized colloidal TiO₂ films*. Nature, 1991. **353**: p. 737-739.
48. Grätzel, M., *Nanocristalline oxide films*. Analisis, 1996. **24**(6): p. M17-M17.
49. Barbe, C.J. and M. Grätzel, *Mesoporous TiO₂ Electrodes for photo-electrochemical applications*. Abstracts of Papers of the American Chemical Society, 1997. **213**: p. 316-COLL.
50. Campus, F., et al., *Electrochromic devices based on surface-modified nanocrystalline TiO₂ thin-film electrodes*. Solar Energy Materials and Solar Cells, 1999. **56**(3-4): p. 281-297.
51. Felderhoff, M., et al., *Molecular suppression of the pimerization of viologens (=4,4' -bipyridinium derivatives) attached to nanocrystalline titanium dioxide thin-film electrodes*. Helvetica Chimica Acta, 2000. **83**(1): p. 181-192.
52. Gerfin, T., M. Grätzel, and L. Walder, *Molecular Level Artificial Photosynthetic Materials*, ed. K.D. Karlin. Vol. 44. 1997: JOHN WILEY & SONS, INC.
53. Mayor, M., et al., *Hetero-Supramolecular Modification of Nanocrystalline TiO₂ Film Electrodes: Photoassisted Electrocatalysis at B12-on-TiO₂*. Chimia, 1996. **50**: p. 47-49.
54. Mayor, M., M. Grätzel, and L. Walder, *Photo-Electrosynthesis on Nanocrystalline TiO₂-Electrodes Modified with Vitamin B12*. 1998: Osnabrück.
55. Asaftei, S. and L. Walder, *Covalent layer-by-layer type modification of electrodes using ferrocene derivatives and crosslinkers*. Electrochimica Acta, 2004. **49**(26): p. 4679-4685.
56. Giraldi, T.R., et al., *Effect of thickness on the electrical an optical properties of Sb doped SnO₂ (ATO) thin films*. J. Electroceram., 2004. **13**(1-3): p. 159-165.
57. Szekely, M., et al., *Behavior of fluorid-doped tin oxide electrode: A study by quartz crystal microbalance in propylene carbonate*. J.Electroanal. Chem., 1996. **401**(1-2): p. 89-93.
58. Boroumand, F.A., P.W. Fry, and D.G. Lidzey, *Nanoscale conjugated-polymer light-emitting diodes*. Nano Letter, 2500. **5**(1): p. 67-71.
59. Lin, M.H., et al., *Preparation of a po*. J. Photochem.Photobiol. A-Chem., 2004. **164**(1-3): p. 173-177.
60. Rowley, N.M. and R.J. Mortimer, *New electrochromic materials*. Science Progress, 2002. **85**(3): p. 243-262.

61. Mortimer, R.J., *Electrochromic materials*. Chemical Society Reviews, 1997. **26**(3): p. 147-156.
62. Lammertink, R.G.H., et al., *Nanostructured thin films of organic-organometallic block copolymers: One-step lithography with poly(ferrocenylsilanes) by reactive ion etching*. Advanced Materials, 2000. **12**(2): p. 98-103.
63. Rosseinsky, D.R. and R.J. Mortimer, *Electrochromic systems and the prospects for devices*. Advanced Materials, 2001. **13**(11): p. 783-793.
64. Giacomini, C., et al., *Immobilization of beta-galactosidase from Kluyveromyces lactis on silica and agarose: comparison of different methods*. Journal of Molecular Catalysis B-Enzymatic, 1998. **4**(5-6): p. 313-327.
65. Thust, M., et al., *Enzyme immobilisation on planar and porous silicon substrates for biosensor applications*. Journal of Molecular Catalysis B-Enzymatic, 1999. **7**(1-4): p. 77-83.
66. Bonhote, P., et al., *Nanocrystalline electrochromic displays*. Displays, 1999. **20**(3): p. 137-144.
67. Liu, J.Y. and J.P. Coleman, *Nanostructured metal oxides for printed electrochromic displays*. Materials Science and Engineering a-Structural Materials Properties Microstructure and Processing, 2000. **286**(1): p. 144-148.
68. Cinnsealach, R., et al., *Coloured electrochromic windows based on nanostructured TiO₂ films modified by adsorbed redox chromophores*. Solar Energy Materials and Solar Cells, 1999. **57**(2): p. 107-125.
69. Cummins, D., et al., *Ultrafast electrochromic windows based on redox-chromophore modified nanostructured semiconducting and conducting films*. Journal of Physical Chemistry B, 2000. **104**(48): p. 11449-11459.
70. Kraus, T., *unpublished report (Balzers, Liechtenstein)*. 1953.
71. Deb, S.K., *Optical and Photoelectric Properties and Color Centres in Thin-Films of Tungsten Oxide*. Philosophical Magazine, 1973. **27**(4): p. 801-822.
72. Deb, S.K., *Novel electrophotographic system*. Appl. Opt., 1969. **suppl.3.J.**: p. 192-195.
73. Schoot, C.J., et al., *New Electrochromic Memory Display*. Appl. Phys. Lett., 1973. **23**(2): p. 64-65.
74. Lampert, C.M., *Heat Mirror Coatings for Energy Conserving Windows*. Solar Energy Materials and Solar Cells, 1981. **6**(1): p. 1-41.
75. Shu, C.F. and M.S. Wrighton, *Synthesis and Charge-Transport Properties of Polymers Derived from the Oxidation of 1-Hydroxyl-(6-(Pyrrol-1-yl)hexyl)-4,4'-bipyridinium bis(hexafluorophosphate) and Demonstration of a pH-Sensitive Microelectrochemical Transistor Derived from The Redox Properties of a Conventional Redox Centre*. J.Phys.Chem., 1988. **92**(18): p. 5221-5229.
76. Dominey, R.N., T.J. Lewis, and M.S. Wrighton, *Synthesis and Characterisation of a Benzylviologen Surface-Derivatizing Reagent- N,N'-Bis[P-(Trimethoxysilyl)benzyl]-4,4'-Bipyridinium Chloride*. J.Phys.Chem., 1983. **87**(26): p. 5345-5354.
77. Bookbinder, D.C. and M.S. Wrighton, *Electrochromic Polymers Covalently Anchored to EDlectrode Surfaces-Optical and Electrochemical Properties of a Viologen-Based Polymer*. J. Electrochem. Soc., 1983. **130**(5): p. 1080-1087.
78. Monk, P.M.S., R.J. Mortimer, and D.R. Rosseinsky, *Electrochromism. Fundamentals and Application*. 1995: VCH, Weinheim, New York, Basel, Cambridge, Tokyo. 216.
79. Bird, C.L. and A.T. Kuhn, *Electrochemistry of the Viologens*. Chemical Society Reviews, 1981. **10**(1): p. 49-82.
80. Murray, R.W., *Molecular Design of Electrode Surfaces*, ed. J.W.S. Inc. 1992, New York: John Wiley & Sons. Inc.

81. Judkuis, C.M., E.W. Bohannon, and A.K. Herbig, *Self-assembly and catalytic properties of 1,1'-bridged-2,2'-dipyridinium amphiphiles*. J.Electroanal. Chem., 1998. **451**(1-2): p. 39-47.
82. Goss, C.A., C.J. Miller, and M. Majda, *Microporous Aluminium-Oxide Films at Electrodes .5. Mechanism of the Lateral Charge Transport in Bulayer Assemblies of Electroactive Amphiphiles*. J.Phys.Chem., 1988. **92**(7): p. 1937-1942.
83. Bruinink, J., C.G.A. Kregting, and J.J. Ponjee, *Modified Viologens with Improved Electrochemical Properties for Display Applications*. Journal of the Electrochemical Society, 1977. **124**: p. 1854-11856.
84. Monk, P.M.S., C. Turner, and S.P. Akhtar, *Electrochemical behaviour of methyl viologen in a matrix of paper*. Electrochimica Acta, 1999. **44**(26): p. 4817-4826.
85. Qian, D.J., C. Nakamura, and J. Miyake, *Monolayers of a series of viologen derivatives and the electrochemical properties in Langmuir-Blodgett films*. Thin Solid Films, 2000. **374**(1): p. 125-133.
86. Amao, Y., T. Hiraishi, and I. Okura, *Preparation and characterization of water soluble viologen-linked trisulfonatophenylporphyrin (TPPSCnV)*. J.Mol. Catal.A: Chem., 1997. **126**(1): p. 13-20.
87. Amao, Y., T. Hiraishi, and I. Okura, *Photoinduced hydrogen evolution using water soluble viologen-linked trisulfonatophenylporphyrins (TPPSCnV) with hydrogenase*. J.Mol. Catal.A: Chem., 1997. **126**(1): p. 21-26.
88. Moller, M.T., et al., *Switchable Electrochromic Images based on a Combined Top-Down Bottom-up Approach*. Advanced Materials, 2004. **16**(17): p. 1558-1562.
89. Bach, U., et al., *Solid-state dye-sensitized mesoporous TiO₂ solar cells with high photon-to-electron conversion efficiencies*. Nature, 1998. **395**: p. 583-585.
90. San Vicente, G., A. Morales, and M. Gutierrez, *Preparation and characterization of sol-gel TiO₂ antireflective coatings for silicon*. Thin Solid Films, 2001. **391**(1): p. 133-137.
91. Que, W., et al., *Preparation and characterisations of SiO₂/TiO₂/ gamma-glycidoxypropyltrimethoxysilane composite materials for optical waveguides*. Appl. Phy. A-Mat. Sci. & Proces., 2001. **73**(2): p. 171-176.
92. Garcia-Canadas, J., et al., *Dynamic behavior of viologen-activated nanostructured TiO₂ correlation between kinetics of charging and coloration*. Electrochimica Acta, 2004. **49**: p. 745-752.
93. Horwitz, C.P., N.Y. Suhu, and G.C. Dailey, *Synthesis, Characterization and Electropolymerization of Ferrocene Monomers with Aniline and Phenol Substituents*. Journal of Electroanalytical Chemistry, 1992. **324**(1-2): p. 79-91.
94. Cass, A.E.G., et al., *Ferrocene-Mediated Enzyme Electrode for Amperometric Determination of Glucose*. Analytical Chemistry, 1984. **56**(4): p. 667-671.
95. Dsilva, C., et al., *Electrochemical Characterization of Polyvinylferrocene Polymers - Substituent Effects on the Redox Reaction*. Journal of Materials Chemistry, 1992. **2**(2): p. 225-230.
96. Pauson, P.L., *Ferrocene Derivatives. Part I. The Direct Synthesis of Substituted Ferrocenes*. J. Am.Chem.Soc, 1954. **76**: p. 2187-2191.
97. Goldenberg, L.M., *Electrochemical Properties of Langmuir-Blodgett-Films*. Journal of Electroanalytical Chemistry, 1994. **379**(1-2): p. 3-19.
98. Gardner, T.J., C.D. Frisbie, and M.S. Wrighton, *Systems for Orthogonal Self-Assembly of Electroactive Monolayers on Au and Ito - an Approach to Molecular Electronics*. Journal of the American Chemical Society, 1995. **117**(26): p. 6927-6933.
99. Casado, C.M., et al., *Siloxane and Organosilicon Dimers, Monomers, and Polymers with Amide-Linked Ferrocenyl Moieties - Synthesis, Characterization, and Redox Properties*. Inorganic Chemistry, 1995. **34**(7): p. 1668-1680.

100. Andrieux, C.P., et al., *Electrochemistry in Hydrophobic Nafion Gels .1. Electrochemical-Behavior of Electrodes Modified by Hydrophobic Nafion Gels Loaded with Ferrocenes*. Journal of Electroanalytical Chemistry, 1990. **296**(1): p. 117-128.
101. Zhu, Y.B. and M.O. Wolf, *Electropolymerization of oligothiénylferrocene complexes: Spectroscopic and electrochemical characterization*. Chemistry of Materials, 1999. **11**(10): p. 2995-3001.
102. Stepp, J. and J.B. Schlenoff, *Electrochromism and electrocatalysis in viologen polyelectrolyte multilayers*. Journal of the Electrochemical Society, 1997. **144**(6): p. L155-L157.
103. Hempenius, M.A., et al., *Organometallic polyelectrolytes: Synthesis, characterization and layer-by-layer deposition of cationic poly(ferrocenyl(3-ammoniumpropyl)methylsilane)*. Macromolecular Rapid Communications, 2001. **22**(1): p. 30-33.
104. Steiger, B., et al., *Charge transport effects in ferrocene-streptavidin multilayers immobilized on electrode surfaces*. Electrochimica Acta, 2003. **48**(6): p. 761-769.
105. Millward, R.C., et al., *Directed assembly of multilayers - the case of Prussian Blue*. Chemical Communications, 2001(19): p. 1994-1995.
106. Kubo, T., et al., *Current state of the art for NOC-AGC electrochromic windows for architectural and automotive applications*. Solid State Ionics, 2003. **165**(1-4): p. 209-216.
107. Hillebrandt, H., et al., *High electric resistance polymer/lipid composite films on indium-tin-oxide electrodes*. Langmuir, 1999. **15**(24): p. 8451-8459.
108. Lee, G.S., et al., *Orientation-controlled monolayer assembly of zeolite crystals on glass using terephthalaldehyde as a covalent linker*. Tetrahedron, 2000. **56**(36): p. 6965-6968.
109. Herr, B.R. and C.A. Mirkin, *Self-Assembled Monolayers of Ferrocenylazobenzenes - Monolayer Structure Vs Response*. Journal of the American Chemical Society, 1994. **116**(3): p. 1157-1158.
110. Schwartz, J., et al., *Organometallic chemistry at the interface with materials science*. Polyhedron, 2000. **19**: p. 505-507.
111. Gomez, M.E. and A.E. Kaifer, *Voltammetric Behavior of a Ferrocene Derivative - a Comparison Using Surface-Confined and Diffusion-Controlled Species*. Journal of Chemical Education, 1992. **69**(6): p. 502-505.
112. Padeste, C., A. Grubelnik, and L. Tiefenauer, *Ferrocene-avidin conjugates for bioelectrochemical applications*. Biosensors & Bioelectronics, 2000. **15**(9-10): p. 431-438.
113. Scheffold, R., *In Modern Synthetic Methodes*, ed. N. Wiley: New York. Vol. 3. 1983, New York. 355-439.
114. Lund, H. and M. Baizer, *Organic Electrochemistry*. Third Edition, ed. 1991, New York, Basel, Hong Kong: Marcel Dekker, INC. 809-875.
115. Njue, C.K. and J.F. Rusling, *Organic cyclizations in microemulsions catalyzed by a cobalt corrin-polyion-scaffold on electrodes*. Electrochemistry Communications, 2002. **4**(4): p. 340-343.
116. Murakami, Y. and Y. Hisaeda, *Hydrophobic Vitamin B12.4. Addition-Reactions of Alcohols to Olefins as catalyzed by Hydrophobic Vitamin B12 Derivatives*. Bulletin of the Chemical Society of Japan, 1985. **58**(9): p. 2652-2658.
117. Scheffold, R., et al., *Synthesis and Reactions of Porphine-Type Metal-Complexes .8. Carbon-Carbon Bond Formation Catalyzed by Vitamin-B12 and a Vitamin-B12 Model-Compound - Electrosynthesis of Bicyclic Ketones by 1,4 Addition*. Journal of the American Chemical Society, 1980. **102**(10): p. 3642-3644.

118. Ahuja, D.K., et al., *Aqueous-Phase Dechlorination of Toxic Chloroethylenes by Vitamin B12 Cobalt Center: Conventional and Polypyrrole Film-Based Electrochemical Studies*. Industrial & Engineering Chemistry Research, 2004. **43**(0888-5885): p. 1049-1055.
119. Chang, B.-V., C.-W. Chiang, and S.-Y. Yuan, *Dechlorination of pentachlorophenol in anaerobic sewage sludge*. Chemosphere, 1998. **36**(3): p. 537-545.
120. Steiger, B., A. Ruhe, and L. Walder, *Poly(Vitamin-B12)-Modified Carbon Electrodes Used as a Preconcentration-Type Sensor for Alkylating-Agents*. Analytical Chemistry, 1990. **62**(7): p. 759-766.
121. Schaller, U., et al., *Ionic Additives for Ion-Selective Electrodes Based on Electrically Charged Carriers*. Analytical Chemistry, 1994. **66**(3): p. 391-398.
122. Florido, A., S. Daunert, and L.G. Bachas, *Development of polymer membrane anion-selective electrodes based on molecular recognition principles*. Biosens. Chem. Sens., 1992. **487**: p. 175-185.
123. Ruhe, A., L. Walder, and R. Scheffold, *Modification of Carbon Electrodes by Vitamin B-12-Polymers*. Makromolekulare Chemie-Macromolecular Symposia, 1987. **8**: p. 225-233.
124. Fuchs, J., (FZKA 5816), 1-110 pp. CODEN: WBFKF5 ISSN:. Report written in German. CAN 126:148093 AN 1996:675827 CAPLUS, *Synthesis of an corrinoids and immobilization on an ion exchange film for the development of an optochemical sensor for cyanide in aqueous solutions*. Wissenschaftliche Berichte - Forschungszentrum Karlsruhe, 1996(0947-8620).
125. Ariga, K., et al., *Langmuir monolayer of organoalkoxysilane for vitamin B-12-modified electrode*. Physical Chemistry Chemical Physics, 2001. **3**(16): p. 3442-3446.
126. Shimakoshi, H., et al., *Preparation and electrochemical behaviour of hydrophobic vitamin B12 covalently immobilized onto platinum electrode*. ChemCommun., 2004: p. 50-51.
127. Ruhe, A., L. Walder, and R. Scheffold, *Surface Modification of Carbon Electrodes by Polymers Consisting of Epoxy-Resins and a Derivative of Vitamin-B12. Synthesis and Reactions of Porphinoid Metal-Complexes .17*. Helvetica Chimica Acta, 1985. **68**(5): p. 1301-1311.
128. Otten, T., et al., *Synthesis of vitamin-B-12 derivatives with an electropolymerizable side chain*. Helvetica Chimica Acta, 1998. **81**(6): p. 1117-1126.
129. Shimakoshi, H., et al., *Hydrophobic vitamin B12. Part 18. Preparation of a sol-gel modified electrode trapped with a vitamin B12 derivative and its photoelectrochemical reactivity*. Dalton Trans., 2003: p. 2308-2312.
130. Schulthess, P., et al., *A Lipophilic Derivative of Vitamin-B12 as a Selective Carrier for Anions*. Helvetica Chimica Acta, 1984. **67**(4): p. 1026-1032.
131. Mayor, M., R. Scheffold, and L. Walder, *Synthesis of vitamin B-12 derivatives with a peripheral metal binding site*. Helvetica Chimica Acta, 1997. **80**(4): p. 1183-1189.
132. Stepanek, R., *Dissertation*. 1987, ETH: Zürich.
133. Steiger, B. and L. Walder, *A Reduction Catalyst Powered by Its Own 10-Electron Battery - Synthesis and Properties of a Pentaviologen-Linked Corrinatocobalt Complex*. Helvetica Chimica Acta, 1992. **75**(1): p. 90-108.
134. Mbindyo, J.K.N. and J.F. Rusling, *Catalytic electrochemical synthesis using nanocrystalline titanium dioxide cathodes in microemulsions*. Langmuir, 1998. **14**(24): p. 7027-7033.
135. Kamogawa, H. and S. Satoh, *Organic-Solid Photochromism by Photoreduction Mechanism - Aryl Viologens Embedded in Poly(N-Vinyl-2-Pyrrolidone)*. Journal of Polymer Science Part a-Polymer Chemistry, 1988. **26**(2): p. 653-656.
136. Wolff, L., *Annalen der Chemie*. Vol. 333. 1904.

137. Marvell, E.N. and I. Shahidi, *Influence of Para Substituents on Rate of Cyclization of 5-Amilino-N-Phenyl-2,4-Pentadienylideneimine*. Journal of the American Chemical Society, 1970. **92**(19): p. 5646-&.
138. Heinen, S., W. Meyer, and L. Walder, *Charge trapping in dendrimers with a viologen skeleton and a radial redox gradient*. Journal of Electroanalytical Chemistry, 2001. **498**(1-2): p. 34-43.
139. Flückiger, B., *Molekulare Wirte mit eingebautem Redox-Signalwandler*, in *Philosophisch-naturwissenschaftliche Fakultät Bern*. 1995, Universität Bern: Bern.
140. Bergbreiter, D.E., P.L. Osburn, and Y.S. Liu, *Tridentate SCS palladium(II) complexes: New, highly stable, recyclable catalysts for the heck reaction*. Journal of the American Chemical Society, 1999. **121**(41): p. 9531-9538.
141. Behrens, C., M. Egholm, and O. Buchardt, *Selective Hydrogenolysis of Bis(Hydroxymethyl)Aromatic Compounds*. Synthesis-Stuttgart, 1992(12): p. 1235-1236.
142. Staab, H.A., et al., *Electron Donor-Acceptor Compounds, .38. Electron Donor-Acceptor [2.2]Metacyclophanes - Synthesis, Structure, and Charge-Transfer Spectra*. Chemische Berichte-Recueil, 1985. **118**(3): p. 1204-1229.
143. Heinen, S., W. Meyer, and L. Walder, *Charge Trapping in Dendrimers with a Viologen Skeletron and a Radial Redox Gradient*. J. Electrochem. Soc., 2001. **498**: p. 34-43.
144. Gromov, S.P. and N.A. Kurchavov, *Formation of 4-arylpyridines form Pyridinium Salts under the Action of Methylammonium Sulfite*. Russian Chem. Bull., 2003. **52**: p. 1606-1609.
145. Simon, M.S. and P.T. Moore, *Novel Polyviologens - Photochromic Redox Polymers with Film-Forming Properties*. Journal of Polymer Science Part a-Polymer Chemistry, 1975. **13**(1): p. 1-16.
146. Heinen, S., *Elektroaktive Dendrimere mit Viologengerüst*, in *Institut für Chemie*. 1999, Universität Osnabrück: Osnabrück.
147. Hesse, G. and F. Raemisch, *Notiz ueber das Symetrische Tris-Oxymethyl-Benzol (Mesicerin)*. Chemische Berichte-Recueil, 1954. **87**(5): p. 863-874.
148. Cochrane, W., P.L. Pauson, and T.S. Stevens, *Synthesis of Symmetrically Trisubstituted Benzene Derivatives*. Journal of the Chemical Society, C-Organic, 1968: p. 630-632.
149. Vogtle, F., M. Zuber, and Lichtent.Rg, *Simplified Technique for Synthesis of 1,3,5-Tris(Bromomethyl)Benzene*. Chemische Berichte-Recueil, 1973. **106**(2): p. 717-718.
150. Lan, A.J.Y., R.O. Heuckeroth, and P.S. Mariano, *Electron-Transfer-Induced Photocyclization Reactions of Arene Iminium Salt Systems - Effects of Cation Diradical Deprotonation and Desilylation on the Nature and Efficiencies of Reaction Pathways Followed*. J.Am. Chem. Soc., 1987. **109**(9): p. 2738-2745.
151. Iyoda, T., M.M. Matsushita, and T. Kawai, *Redox-tunable pyridinium assemblies and their interactive spin-based functions*. Pure Appl. Chem., 1999. **71**(11): p. 2079-2084.
152. Hunig, S. and W. Schenk, *2 Step Redox Systems .25. Synthesis of N,N'-Disubstituted 4,4'-Bipyridyls and 1,1',4,4'-Tetrahydro-4,4'-Bipyridylidenes*. Liebigs Annalen Der Chemie, 1979(5): p. 727-742.
153. Galow, T.H., et al., *Fluorocarbonylferrocene. A Versatile Intermediate for Ferrocene Esters and Amides*. J. Org. Chem., 1999. **64**(10): p. 3745-3746.
154. Amabilino, D.B., et al., *The Self-Assembly of Branched [N]Rotaxanes-the First Step Towards Dendritic Rotaxanes*. J. Chem. Soc.-Chem. Comm., 1995(7): p. 751-753.
155. Zhao, W., *Synthesis of Electropolymerizable Bipyridinium Salts and Aromatic Diimides Used as Electrode Modifiers*, in *Philosophische-Naturwissenschaftliche Fakultät Bern*. 1992, Universität Bern: Bern.

156. Murakami, Y., et al., *Hydrogen Source in the Photochemical Cobalt-Carbon Cleavage of Hydrophobic Vitamin-B12 Derivatives in Hydrophobic Microenvironments*. *Chem. Lett.*, 1991(6): p. 977-980.

Erklärung über die Eigenständigkeit der erbrachten wissenschaftlichen Leistung

Ich erkläre hiermit eidesstattlich, dass ich die vorliegende Arbeit ohne unzulässige Hilfe Dritter und ohne Benutzung anderer als der angegebenen Hilfsmittel angefertigt habe. Die aus anderen Quellen direkt oder indirekt übernommenen Daten und Konzepte sind unter Angabe der Quelle gekennzeichnet.

Die Arbeit wurde bisher weder im In- noch im Ausland in gleicher oder ähnlicher Form einer anderen Prüfungsbehörde vorgelegt.

Ein früherer Promotionsversuch an einer deutschen Hochschule hat nicht stattgefunden.

Osnabrück den

Simona Asaftei

CURRICULUM VITAE

Personal details

Name: Carmen Simona ASAFTEI
Date of Birth: 15 January 1968
Place of Birth: Bacau/Romania
Citizenship: Romanian
Address: Institute of Materials Science,
Department Organic Chemistry II,
University Osnabrück,
Barbarastraße 7, 49069 Osnabrück,
Germany
Phone: 0541 969-2389
Fax: 0541 969-3308
Email: sasaftei@uos.de
Web page: <http://www.chemie.uni-osnabrueck.de/oc/walder/agwalder.htm>

Education and Training:

Since 2001 PhD Study Supervisor Professor L. Walder, Department of Organic Chemistry II, University Osnabrück, Germany
Subject: 'Synthesis of redox units and modification of mesoporous surfaces by covalent cascade reactions'

1997-2001 Research activity in the catalysis group of Prof. E. Dumitriu at Technical University 'Gh. Asachi' Iasi, Romania, on the heterogenic catalysis- 'Study of the hydrolysis of the polysaccharides with immobilized enzymes'

1993-1997 Study of chemistry at the University of Bacau, Romania
Dipl. ing Food chemistry

1988-1992 Study of chemistry at the University of Bacau, Romania
Engineer Inorganic chemistry

Work experience:

- 1988-1993 technical illustration in the aeroplane construction office at the Aeronautics Group 'AEROSTAR' Bacau, Romania
- 1993-1997 chemistry engineer at the University of Bacau, Department of Chemistry and Food Chemistry
- 1997-2001 Assistant for graduate and ungraduate laboratory work, Biochemistry and Food chemistry in the Department of Chemistry and Food Chemistry, at the University of Bacau;
- 2001-2005 Research assistant in the group of Professor L. Walder, Department Organic Chemistry II, University of Osnabrück, Germany, cares for organic chemistry exercise, general chemistry practical course, organic chemistry practical course, advanced practical course in synthesis of electrochromics.
- Since 2005 Research assistant in the group of PD. Dr. Helmut Rosemeyer, Department of Organic of Chemistry I, University of Osnabrück, Germany, cares for organic chemistry exercise, organic chemistry practical course

Publications

1. Walder, L., Asaftei, S., Möller, M. (2003) Neuartige Technologie für Displays und optische Filter. Chemische Innovation an Niedersächsischen Hochschulen, Niedersächs. Min. Wissensch. und Kultur.
2. Asaftei, S., Walder, L. (2004) Covalent layer-by-layer type modification of electrodes using ferrocenes and crosslinkers, *Electrochim Acta* 49, 4679-4685
3. Möller, M., Asaftei, S., Corr, D., Ryan, M., Walder, L. (2004) Switchable Electrochromic Images Based on a Combined Top-down Bottom-up Approach, *Adv. Mat.*, Cover-Article 16, 1558-1562.

4. Schön, P., Degefa, T., Asaftei, S., Meyer, W., Walder, L., Charge Propagation in Ion Channel Sensors' Based on Protein Modified Electrodes and Redox Marker Ions, J. Am.Chem. Soc., in press, 2005
5. Asaftei, S., and Walder, L., Modification of TiO₂ – Electrodes with Cross-Linkable B₁₂ – Derivatives, submitted, 2005.

Patents

1. EP Application (2004) A Device, Pichot, F., Corr, D., McAtamney, C., O'Flaherty, A., Ryan, M., Bach. U., Campbell, C., Walder, L. Möller, M., Asaftei, S., Assignee: Ntera Ltd. Ireland.

Earlier Publications

1. Gavrilă, L., Ivascan, St., Tudorache, E., Asaftei, S., (1996) Valorificarea catalizatorilor uzati cu continut de nichel din industria amoniacului . Partea 1, Revista de Chimie, 47, 11, 1039-1045;
2. Gavrilă, L., Tudorache, E., Ivascan, St., Asaftei, S., (1997) Valorificarea catalizatorilor uzati cu continut de nichel din industria amoniacului. Partea 2. Posibilitati de obtinere a sarurilor de nichel de uz galvanotehnic: Revista de Chimie, 48, 6, 512-520;
3. A.Azzouz, D. Messad, D. Nistor, A. Zvolinschi, S. Asaftei (2003) Vapor phase aldol condensation over fully ion-exchanged montmorillonite-rich catalysts, Applied Catalysis A, 241, 1-13.

Conferences

1. Zichil, V., Udrea (Asaftei) Simona, Gavrilă, L., Schnakovszki, C., Caliman, R., The Influence of Vibrations on Engines Oil Quality, 'Motor Sympo', Slovacie Motory Pre 21, Storoicie, Slovacia, 30.05-1.06. (1995), 241-245.

2. Gavrilă L., Asaftei, S., Ivascan, St., Capitalisation possibilities of spent catalysts with low nickel content in , Volumul I, Conferința de chimie și inginerie chimică, București, 20-21- 10. (1995), 230-235.
3. Gavrilă L., Zichil, V., Asaftei, S., Fanaru, A., Schnakovszki, C., Some Considerations concerning the influence of mechanical factors on the acceleration of oxidative degradation processes of lubricating oils for thermal engines, (MOCOM-1) OPROTEH-'95 Editia I-a, Iași, 26-28 (1995), 153-157
4. Gavrilă L., Zichil, V., Asaftei, S., Fanaru, A., Schnakovszki, C., Simulated process of oils break out (II) (Correlation Between Amplitudes of Vibration Movement and Organic Acidity of Mineral Oils, ITHURS'96, Proceedings of International Conference on Intelligent Technologies in Human-related Sciences, 05-07.06. (1996) Leon, Spania, vol. II, 389-393
5. Gavrilă L., Zichil, V., Asaftei, S., Fanaru, Aspecte cinetice ale modificării acidității uleiurilor lubrifiante , ROTRIB'96, (7th International Conference of Tribology) București, 10-12.09, (1996), 206-215.
6. Miron D., Asaftei, S., Utilizarea cicloimoniurilor la obținerea heterocicurilor cu azot, Sesiunea Jubiliară 1961-1996 a Universității Bacău, Bacău, 31.10-2.11 (1996)
7. Zichil, V., Gavrilă, L., Udrea (Asaftei), S., A study of computer aid upon top engine for DI Diesel engines, CCM'98, International Conference of the Claude Bernard University of Lyon, 6-8.06 (1998), France, 9.25-9.28
8. Gavrilă, L., Zichil, V., Udrea (Asaftei), S., A mathematical model of the corrosion behaviour of an industrial urea synthesis reactor, International Congress Stainless Steel '99, Science and Market, 7-9.06 (1999), Chioggia Laguna, Italy.
9. Azzouz, A., Bilba, M., Attou, M., Zvolinschi, A., Asaftei, S., Pure SAPO, CoAPO and CoAPSO ATO-like Molecular Sieves through Optimized

Synthesis Procedures, 13th International Zeolite Conference, 04-P-09, (2001) Montpellier, France.

10. Azzouz, A., Asaftei, S., Nistor, D., Huler, R., Niquette, P., Monette, F., Messad, D., Novel Pseudo-Zeolite Structures from Clay Cross-linking Polydimethylsiloxane, 14th International Zeolite Conference, H-171-C-UNL, (2001) Montpellier, France.